



Buildings and Infrastructure Protection Series

Preventing Structures from Collapsing

to Limit Damage to Adjacent Structures and Additional
Loss of Life when Explosives Devices Impact Highly
Populated Urban Centers

BIPS 05/June 2011



**Homeland
Security**

Science and Technology

Buildings and Infrastructure Protection Series

Preventing Structures from Collapsing

to Limit Damage to Adjacent Structures and
Additional Loss of Life when Explosives Devices
Impact Highly Populated Urban Centers

BIPS 05/June 2011



**Homeland
Security**

Science and Technology

The views, opinions, findings, conclusions, or recommendations expressed in this publication are those of the authors and do not necessarily reflect the official policy or position of the Department of Homeland Security (DHS) and other federal agencies. The publication of these views by DHS does not confer any individual rights or cause of action against the United States. Users of information from this publication assume all liability from such use.

Any appearances of hyperlinks do not constitute endorsement by DHS of the website or the information, products, or services contained therein. For links outside DHS, DHS does not exercise any editorial control over the information you may find at these locations. Users must adhere to any intellectual property rights contained in this publication or in material in linked websites.



Executive Summary

This Technical Report describes Weidlinger Associates, Inc.'s Phase I effort to study the effects of Blast in Urban Environments under sponsorship of the Department of Homeland Security. This effort represents a wide ranging investigation into Urban Blast effects including (a) the influence of the presence of buildings on the blast pressures propagating from explosions located in urban settings, (b) the potential for these blast pressures to damage primary structural members of buildings, (c) the sensitivity of several common building design types to experience progressive collapse due to damage of key support members, and (d) the likelihood that blast pressures may damage building equipment needed for Emergency Evacuation, Rescue and Recovery operations.

The results and insights from this broad based investigation were integrated within a fast running software program specifically focused on the Manhattan Financial District. This tool represents a 'proof of concept' demonstration of an approach for a quick running software tool for security planning and first responders' uses.

This first phase effort lays the technical foundation and software framework for refining the approach in later phases and adapting the methodology for other critical urban centers in the United States.

Foreword and Acknowledgments

Background

Following the detonation of an improvised explosive device (IED), the blast waves will propagate away from the source in all directions. For relatively simple explosive devices the blast waves will propagate spherically, with uniform intensity as a function of distance; the pattern will be more complex for oblong explosive devices. This pattern of blast wave propagation will be disrupted by reflecting surfaces that are significantly denser than air. The first such surface is typically the ground beneath a vehicle-borne improvised explosive device (VBIED), and for these scenarios the propagation pattern is typically termed hemispherical.

The intensity of the blast loading will diminish with distance from the source of the explosion as the energy is distributed over an ever expanding shock front. However, when the shock front intersects a reflecting surface, whether it be a dense masonry façade or a glazed curtain wall, the pressure wave stagnates and is amplified. Amplifications of the peak pressures and corresponding impulse may range from a factor of 2 to a factor of 10 (or more), and the effectiveness of the reflection will depend on the intensity of the blast wave peak pressure.



**The Murrah Federal Building,
Oklahoma City 1995.**

SOURCE: FEMA 277, *THE OKLAHOMA CITY BOMBING: IMPROVING BUILDING PERFORMANCE THROUGH MULTI-HAZARD MITIGATION*



Following the detonation of an improvised explosive device (IED), the blast waves will propagate away from the source in all directions.

Simplified algorithms, based on empirical data, are available for the effects of explosions in open fields, and the effects of reflections have been incorporated for simple conditions. Ray tracing methods have been developed for detonations relative to more complex geometries of reflecting surfaces; however, these methods require considerable judgment to determine the appropriate number of rays that produce an accurate loading. Computational fluid dynamics (CFD) methods provide the most comprehensive and most accurate solution; however, these analytical methods are very time consuming to apply to large problems.

Predicting the propagation of blast waves within dense urban environments presents a difficult challenge. Simplified methods may be quick but do not accurately represent the complex pattern of shadow and focus zones resulting from multiple reflections; detailed methods require weeks to calculate. The UrbanBlast Tool (UBT) resolves this conflict by storing the results of a suite of detailed CFD analyses for a specified streetscape and accessing these results quickly to evaluate the blast loads for specific blast scenarios.

Predicting the propagation of blast waves within dense urban environments presents a difficult challenge.

A means of interpolation between stored results was developed to handle scenarios that do not conform to the actual magnitudes of explosives used in the CFD calculations. In addition to accurately calculating the blast loads resulting from a detonation within the complex streetscape, the UBT uses the

calculated blast loads to determine the likely performance of representative windows, representative ground floor column performance in response to the calculated blast loads, and the performance of representative equipment that is critical to the Emergency Evaluation, Rescue and Recovery (EERR) following an explosion. The evaluation of representative building components will assist first responders and designers in quickly evaluating the hazards to buildings within the region.

Additional studies considered the effects of overcast skies and the likelihood of progressive collapse of three different types of building frames following the removal of first floor columns.

Future revisions to the software will incorporate more detailed evaluation of the potential for progressive collapse and the import of building specific information to supplement the response characteristics of representative building components.

Organization and Content

This report investigates a wide range of topics that contribute to an improved understanding of blast effects in urban settings and the potential for vehicle-borne explosive threats to damage structures or compromise critical equipment needed for emergency evacuation and rescue response. The results of these investigations contributed to the development of the UrbanBlast Tool, a fast running software tool that provides high-fidelity assessments of blast pressures generated within specific urban areas and provides guidance to security planners and first responders to assess the extent of damage caused by explosive threats.



This report investigates a wide range of topics that contribute to an improved understanding of blast effects in urban settings and the potential for vehicle-borne explosive threats to damage structures or compromise critical equipment needed for emergency evacuation and rescue response.

The information is arranged in sections in the following order:

- Chapter 1: Project Overview
- Chapter 2: High-Fidelity Simulation Software
- Chapter 3: Structural Column Damage Modeling Studies
- Chapter 4: Progressive Collapse Modeling Studies
- Chapter 5: Environmental Influences: Effect of Overcast Sky
- Chapter 6: Emergency Evaluation, Rescue and Recovery (EERR) Equipment Fragilities
- Chapter 7: UrbanBlast Tool
- Chapter 8: Guidelines on How to Apply the UBT to Protect Structures to Resist IED Attacks
- Chapter 9: References

Appendices

- Appendix A: Acronyms
- Appendix B: Glossary
- Appendix C: Methodologies Used in Developing the UrbanBlast Tool for NYC Financial District

Acknowledgments

This publication has been produced by the Department of Homeland Security (DHS), Science and Technology (S&T) Directorate, Infrastructure Protection and Disaster Management Division (IDD). It will be revised periodically, and comments and feedback to improve future editions are welcome. Please send comments and feedback to bips@dhs.gov.

Project Officer

Milagros Kennett, Architect/Program Manager, Infrastructure Protection and Disaster Management Division, Science and Technology Directorate, U.S. Department of Homeland Security

Authors

Robert Smilowitz, Weidlinger Associates, Inc.

Mohammed Ettouney, Weidlinger Associates, Inc.

Darren Tennant, Weidlinger Associates, Inc.

David Vaughan, Weidlinger Associates, Inc.

Eric Hansen, Weidlinger Associates, Inc.

Shawn Ozuna, Weidlinger Associates, Inc.

Adam Hapij, Weidlinger Associates, Inc.

Paul Hassig, Weidlinger Associates, Inc.

Reza Salari, Weidlinger Associates, Inc.

Nanne Davis Eliot, National Institute of Building Sciences

Adam Hutter, Department of Homeland Security, Science and Technology Directorate

Graphic Designer

Wanda L. Rizer, Design4Impact

Learn More:

<http://www.dhs.gov/files/programs/high-performance-integrated-design-program.shtm>

<http://www.dhs.gov/files/programs/scitech-bips-tools.shtm>

Table of Contents

| | |
|---|-----|
| Executive Summary | i |
| Foreword and Acknowledgments | iii |
| Background | iii |
| Organization and Content | v |
| Acknowledgments | vi |
| Project Officer..... | vi |
| Authors | vi |
| Graphic Designer..... | vi |
| Table of Contents | vii |
| List of Figures..... | xii |
| List of Tables | xx |
| 1 Project Overview | 1-1 |
| 2 High-Fidelity Simulation Software | 2-1 |
| 2.1 NLFlex Computational Structural Dynamics Software | 2-2 |
| 2.2 MAZ Computational Fluid Dynamics Software..... | 2-2 |
| 3 Structural Column Damage Modeling Studies | 3-1 |
| 3.1 Threat Environment..... | 3-1 |
| 3.2 Airblast Calculations..... | 3-3 |
| 3.3 Column Descriptions..... | 3-5 |
| 3.4 Column Vulnerability Calculations..... | 3-7 |

| | | |
|-----------|--|------------|
| 3.5 | Analysis Results | 3-10 |
| 3.5.1 | Airblast | 3-10 |
| 3.5.2 | Reinforced Concrete Columns..... | 3-12 |
| 3.5.3 | Steel Columns..... | 3-14 |
| 3.6 | Summary | 3-15 |
| 4 | Progressive Collapse Modeling Studies..... | 4-1 |
| 4.1 | Design of Steel and Concrete Buildings..... | 4-2 |
| 4.1.1 | Steel Moment Frame Building | 4-3 |
| 4.1.2 | Concrete Moment Frame Building | 4-4 |
| 4.1.3 | Concrete Flat Slab Building..... | 4-6 |
| 4.2 | Progressive Collapse Study of Steel Moment Frame Structures..... | 4-7 |
| 4.2.1 | Corner Column Removal..... | 4-11 |
| 4.2.2 | Removal of Two Columns | 4-17 |
| 4.2.3 | Summary of Results and Findings | 4-19 |
| 4.3 | Progressive Collapse Study of Reinforced Concrete Structures..... | 4-19 |
| 4.3.1 | Moment Frames with Joist Slabs | 4-20 |
| 4.3.1.1 | Joist Slab System with 32 ft Bay Size | 4-20 |
| 4.3.1.1.1 | Single Column Removal | 4-22 |
| 4.3.1.1.2 | Two Columns Removal | 4-26 |
| 4.3.1.2 | Joist Slab System with 25 ft Bay Size | 4-32 |
| 4.3.1.2.1 | Single Column Removal | 4-32 |
| 4.3.1.2.2 | Two Columns Removal | 4-32 |
| 4.3.2 | Flat Slabs with Drop Panels..... | 4-37 |
| 4.3.2.1 | Single Column Removal | 4-38 |
| 4.3.2.2 | Two Columns Removal | 4-38 |
| 4.3.3 | Summary of Results and Findings | 4-45 |
| 5 | Environmental Influences: Effect of Overcast Sky | 5-1 |
| 5.1 | Overview..... | 5-1 |
| 5.2 | Overcast Sky Simulation Studies..... | 5-3 |

| | | |
|----------|--|------|
| 6 | Emergency Evacuation, Rescue and Recovery Equipment Fragilities | 6-1 |
| 6.1 | Background..... | 6-1 |
| 6.1.1 | Overview of EERR Systems..... | 6-1 |
| 6.1.2 | Available Equipment and System Fragility Data in Response to Blast Loading | 6-2 |
| 6.1.3 | Portability of Available Equipment Fragility Data to Commercial EERR Equipment | 6-3 |
| 6.2 | Methodology | 6-4 |
| 6.2.1 | Identifying Representative Details..... | 6-6 |
| 6.2.2 | Identifying Critical Vulnerabilities of Equipment and Determining Prevailing Damage Mechanism to Airblast..... | 6-6 |
| 6.2.3 | Determining Discrete Limit States | 6-7 |
| 6.3 | Determination of Performance of Equipment in Response to Airblast..... | 6-7 |
| 6.3.1 | Egress Stair Enclosures..... | 6-7 |
| 6.3.2 | Stair Pressurization Systems | 6-10 |
| 6.3.3 | Fire Doors | 6-11 |
| 6.3.4 | Elevator Used During Emergencies | 6-12 |
| 6.3.5 | Emergency Communication/Fire Alarm..... | 6-13 |
| 6.3.6 | Emergency Lighting..... | 6-15 |
| 6.3.7 | Air Ducts | 6-16 |
| 6.3.8 | Conduit Chases..... | 6-17 |
| 6.3.9 | Emergency Generators..... | 6-19 |
| 6.3.10 | Fire/Smoke Detection System..... | 6-20 |
| 6.3.11 | Sprinkler System..... | 6-21 |
| 6.4 | Validation of Methodology of Determining Limit States..... | 6-24 |
| 6.5 | Generation of 3D Fragility Curves | 6-26 |
| 6.6 | Data Incorporated in the UrbanBlast Tool..... | 6-28 |
| 6.7 | Conclusions and Recommendations | 6-28 |

| | | |
|-----------|--|------|
| 7 | UrbanBlast Tool | 7-1 |
| 7.1 | Software Goals..... | 7-1 |
| 7.2 | Computing Environment Requirements | 7-2 |
| 7.2.1 | Software Environment | 7-2 |
| 7.2.2 | Hardware Environment | 7-3 |
| 7.3 | UrbanBlast Software Development..... | 7-3 |
| 7.3.1 | Software Architecture..... | 7-3 |
| 7.4 | Software Assumptions..... | 7-4 |
| 7.4.1 | Language | 7-4 |
| 7.4.2 | Systems and Units..... | 7-4 |
| 7.4.2.1 | Coordinate System | 7-5 |
| 7.4.2.2 | System of Units..... | 7-5 |
| 7.5 | UrbanBlast Model for Manhattan Financial District..... | 7-5 |
| 7.6 | UrbanBlast Database of Airblast Solutions..... | 7-6 |
| 7.7 | UrbanBlast Software | 7-6 |
| 7.7.1 | Defining Explosive Threats..... | 7-6 |
| 7.7.2 | Results Display Functions..... | 7-9 |
| 7.7.2.1 | Airblast Results | 7-10 |
| 7.7.2.1.1 | Airblast Evaluation Approach | 7-10 |
| 7.7.2.2 | Window Damage Results | 7-16 |
| 7.7.2.2.1 | Window Damage Evaluation Approach | 7-16 |
| 7.7.2.3 | Column Damage Results | 7-17 |
| 7.7.2.3.1 | Column Damage Evaluation Approach | 7-17 |
| 7.7.2.4 | EERR Damage Results | 7-18 |
| 7.7.2.4.1 | EERR Damage Evaluation Approach | 7-19 |
| 7.7.2.5 | Saving an Image of UrbanBlast Results | 7-20 |
| 7.7.3 | Viewing the Model | 7-20 |
| 7.7.3.1 | Mouse Manipulation of the Scene | 7-20 |
| 7.7.3.2 | Controls Toolbar for Viewing the Model.... | 7-21 |
| 7.7.3.3 | Controlling which Buildings are Displayed in the Scene | 7-22 |

| | | |
|-------------------|--|------------|
| 7.8 | Initial Release of UrbanBlast | 7-23 |
| 7.8.1 | Installation of the Software | 7-23 |
| 7.8.2 | Software Registration | 7-23 |
| 8 | Guidelines on How to Apply the UBT to Protect Structures to Resist IED Attacks | 8-1 |
| 9 | References | 9-1 |
| Appendices | | |
| A | Acronyms | A-1 |
| B | Glossary | B-1 |
| C | Methodologies Used in Developing the UrbanBlast Tool for NYC Financial District | C-1 |
| C.1 | Overview | C-1 |
| C.2 | Weidlinger Associates' Background | C-2 |
| C.3 | Development of Fast Running Assessment Tool for Blast in Urban Environments | C-3 |
| C.3.1 | WAI Experience Developing Fast Running Engineering Models | C-4 |
| C.4 | High Fidelity Physics Based Modeling | C-5 |
| C.4.1 | The MAZ Software for CFD Simulations | C-6 |
| C.4.2 | Verification and Validation of the MAZ CFD Code | C-7 |
| C.4.2.1 | U.S. Army Corps of Engineers – Bridge Project | C-8 |
| C.4.2.2 | TSWG/EMRTC Steel and Concrete Column Tests | C-8 |
| C.4.2.3 | Curtain Wall Test | C-10 |
| C.4.2.4 | TSWG/EMRTC CORESlab Loading Dock Tool Development | C-10 |
| C.4.2.5 | TSWG/EMRTC Urban Canyon Testing | C-12 |
| C.4.3 | The NLFlex Software for Structural Response Simulations | C-13 |
| C.4.4 | Validation of the NLFlex Software for Structural Response Simulations | C-14 |

| | | |
|---------|---|------|
| C.4.4.1 | Hard Target Defeat..... | C-14 |
| C.4.4.2 | Blast Response of Conventional Structures | C-15 |
| C.4.4.3 | ACEC Grand Conceptor Award | C-15 |
| C.4.4.4 | Progressive Collapse | C-17 |
| C.5 | References..... | C-17 |

List of Figures

Chapter 3

| | | |
|------------|--|------|
| Figure 1: | Two-lane street blast environment..... | 3-2 |
| Figure 2: | Four-lane street blast environment..... | 3-2 |
| Figure 3: | Schematic of urban blast computational environment | 3-3 |
| Figure 4: | Example of two-lane environment computational grid..... | 3-3 |
| Figure 5: | Example of four-lane environment computational grid..... | 3-4 |
| Figure 6: | Concrete column descriptions | 3-6 |
| Figure 7: | Steel column descriptions..... | 3-6 |
| Figure 8: | Concrete model unconfined compression response | 3-7 |
| Figure 9: | Concrete model stress path | 3-8 |
| Figure 10: | A572 grade 50 steel model uniaxial tension response | 3-8 |
| Figure 11: | A615 grade 60 steel model uniaxial tension response | 3-9 |
| Figure 12: | A615 grade 40 steel model uniaxial tension response | 3-9 |
| Figure 13: | Peak pressure [ksi] comparisons: MAZ urban canyon calculation (left side) vs. simple Airblast tool equivalent (right side), 30,000lb charge..... | 3-11 |

| | | |
|------------|---|------|
| Figure 14: | Peak pressure [ksi] comparisons: MAZ urban canyon (left) calculation vs. MAZ flat plane (right), both using 30,000lb rectangular charge shape | 3-12 |
| Figure 15: | Pressure [ksi] and impulse [psi-sec] difference between MAZ urban canyon (left) and flat plane (right), both using 30,000lb rectangular charges | 3-12 |
| Figure 16: | Column type C2, 4,000lb at 16ft..... | 3-13 |
| Figure 17: | Column type C4, 4,000lb at 16ft..... | 3-13 |
| Figure 18: | Column type S1, strong axis, 4,000lb at 16ft..... | 3-15 |
| Figure 19: | Column type S4, strong axis, 4,000lb at 16ft..... | 3-15 |

Chapter 4

| | | |
|------------|--|------|
| Figure 20: | Steel frame building (view from above)..... | 4-4 |
| Figure 21: | Concrete moment frame building with joist slabs (view from below) | 4-5 |
| Figure 22: | Reinforced concrete flat slab building (view from below) | 4-7 |
| Figure 23: | NLFlex model, steel building with perimeter moment frames (decks not shown)..... | 4-8 |
| Figure 24: | Plan view of moment connection designations | 4-8 |
| Figure 25: | Flex model connections..... | 4-9 |
| Figure 26: | Flex model connections (continued) | 4-9 |
| Figure 27: | View of floor and roof decks (concrete not shown) | 4-10 |
| Figure 28: | View of corner column and beams..... | 4-10 |
| Figure 29: | View of floor beams and girders..... | 4-11 |
| Figure 30: | View of corner framing, and roof framing | 4-11 |
| Figure 31: | Vertical displacement and velocity under GSA load combination | 4-12 |
| Figure 32: | Vertical displacement and velocity under UFC load combination..... | 4-13 |
| Figure 33: | Comparison of vertical response between GSA and UFC load combinations..... | 4-13 |

TABLE OF CONTENTS

Figure 34: Maximum vertical displacement (in), GSA load combination 4-14

Figure 35: Maximum vertical displacement (in), UFC load combination 4-14

Figure 36: Concrete damage, GSA load combination 4-15

Figure 37: Concrete damage, UFC load combination 4-15

Figure 38: Steel strains, GSA load combination 4-16

Figure 39: Steel strains, UFC load combination 4-16

Figure 40: Vertical displacement and velocity, two columns removed 4-17

Figure 41: Partial view of maximum vertical displacement (in), two columns removed 4-18

Figure 42: Partial view of concrete damage, two columns removed 4-18

Figure 43: Partial view of steel strains, two columns removed 4-19

Figure 44: NLFlex model, reinforced concrete moment frame with joist slab, top view 4-21

Figure 45: Flex model, reinforced concrete moment frame with joist slab, bottom view 4-21

Figure 46: Vertical velocity, column C1 removal under different live loads 4-23

Figure 47: Vertical displacement, column C1 removal under different live loads 4-23

Figure 48: Vertical displacement (in), column C1 removal, 100% live load, top view 4-24

Figure 49: Vertical displacement (in), column C1 removal, 100% live load, bottom view 4-24

Figure 50: Concrete damage, column C1 removal, 100% live load, top view 4-25

Figure 51: Concrete damage, column C1 removal, 100% live load, bottom view 4-25

Figure 52: Vertical velocity, column C1 removal, 100% live load 4-26

Figure 53: Vertical displacement, column C1 removal, 100% live load 4-26

| | | |
|-------------|--|------|
| Figure 54: | Vertical displacement (in), C1-C2 columns removal under 100% live load | 4-28 |
| Figure 55: | Vertical displacement (in), C1-C3 columns removal under 100% live load | 4-28 |
| Figure 56 : | Vertical velocity, removal of columns C1-C2 vs. C1-C3..... | 4-29 |
| Figure 57: | Vertical displacement, removal of columns C1-C2 vs. C1-C3..... | 4-29 |
| Figure 58: | Vertical velocity, C1-C2 columns removal under different live loads..... | 4-30 |
| Figure 59: | Vertical displacement, C1-C2 columns removal under different live loads | 4-30 |
| Figure 60 : | Concrete damage, removal of C1-C2 columns, 100% live load, top view..... | 4-31 |
| Figure 61: | Concrete damage, removal of C1-C2 columns, 100% live load, bottom view | 4-31 |
| Figure 62: | Vertical velocity, column C1 removal, 100% live load..... | 4-33 |
| Figure 63: | Vertical displacement, column C1 removal, 100% live load..... | 4-33 |
| Figure 64: | Vertical displacement (in), column C1 removal, 100% live load | 4-34 |
| Figure 65: | Concrete damage, column C1 removal, 100% live load..... | 4-34 |
| Figure 66: | Vertical velocity, two columns removal, 100% live load..... | 4-35 |
| Figure 67: | Vertical displacement, two columns removal, 100% live load..... | 4-35 |
| Figure 68: | Vertical displacement (in), two columns removal, 100% live load, top view | 4-36 |
| Figure 69: | Vertical displacement (in), two columns removal, 100% live load, bottom view..... | 4-36 |
| Figure 70: | Concrete damage, two columns removal, 100% live load, top view | 4-37 |
| Figure 71: | Concrete damage, two columns removal, 100% live load, bottom view | 4-37 |

TABLE OF CONTENTS

Figure 72: NLFlex Model - flat slab with drop panels,
top view 4-39

Figure 73: NLFlex Model - flat slab with drop panels,
bottom view..... 4-39

Figure 74: Vertical velocity, column C1 removal,
25% live load..... 4-40

Figure 75: Vertical displacement, column C1 removal,
25% live load..... 4-40

Figure 76: Vertical displacement (in), column C1
removal, 25% live load, top view 4-41

Figure 77: Vertical displacement (in), column C1
removal, 25% live load, bottom view..... 4-41

Figure 78: Concrete damage, column C1 removal, 25%
live load, top view 4-42

Figure 79: Concrete damage, column C1 removal, 25%
live load, bottom view..... 4-42

Figure 80: Vertical velocity, two columns removal,
25% live load..... 4-43

Figure 81: Vertical displacement, two columns removal,
25% live load..... 4-43

Figure 82: Vertical displacement (in), two columns
removal, 25% live load, top view 4-44

Figure 83: Vertical displacement (in), two columns
removal, 25% live load, bottom view..... 4-44

Figure 84: Vertical displacement (in), two columns
removal, 25% live load, top view 4-45

Figure 85: Vertical displacement (in), two columns
removal, 25% live load, bottom view..... 4-45

Chapter 5

Figure 86: Vertical sound speed profiles illustrating
effects on acoustic propagation..... 5-2

Figure 87: Comparison of Overcast Sky temperature
profile (blue) with U.S. Standard
Atmosphere (red) 5-3

Figure 88: Comparison of calculated maximum overpressure for two different atmosphere profiles 5 seconds after detonation of 30,000 lb at Location A 5-5

Figure 89: Comparison of calculated maximum overpressure for two different atmosphere profiles 5 seconds after detonation of 1,000 lb at Location A..... 5-6

Figure 90: Comparison of calculated maximum overpressure for two different atmosphere profiles 5 seconds after detonation for 30,000 lb at Location B 5-7

Figure 91: Comparison of calculated maximum overpressure for two different atmosphere profiles 5 seconds after detonation for 1,000 lb at Location B 5-8

Figure 92: Increase in maximum overpressure at 5 sec between Standard and Overcast Sky Atmosphere Models for 30,000 lb at Location A..... 5-9

Figure 93: Increase in maximum overpressure at 5 sec between Standard and Overcast Sky Atmosphere Models for 1,000 lb at Location A..... 5-10

Figure 94: Increase in maximum overpressure at 5 sec between Standard and Overcast Sky Atmosphere Models for 30,000 lb at Location B..... 5-11

Figure 95: Increase in maximum overpressure at 5 sec between Standard and Overcast Sky Atmosphere Models for 1,000 lb at Location B..... 5-12

Chapter 6

Figure 96: Typical 2D fragility curves 6-5

Figure 97: Basic methodology for developing EERR equipment response to airblast pressures..... 6-5

Figure 98: Example of egress stairwell 6-8

Figure 99: Example of stair pressurization fans used in office buildings 6-10

Figure 100: Example of fire door in commercial building..... 6-11

TABLE OF CONTENTS

Figure 101: Example of elevator doors installed in a commercial building 6-12

Figure 102: Example of fire alarm control panel in commercial building 6-13

Figure 103: Example of emergency lighting system in commercial building 6-15

Figure 104: Example of a stud wall system commonly used to construct chases..... 6-17

Figure 105: Example of a generator found in a commercial building 6-19

Figure 106: Example of fire detection device in a commercial building 6-21

Figure 107: Example of fire sprinkler system installed in a commercial office building 6-22

Figure 108: Schematic of sprinkler pipe supported by hanger rods..... 6-22

Figure 109: Fragility surface for representative EERR system..... 6-27

Chapter 7

Figure 110: Start-up screen for UrbanBlast–Manhattan Financial District..... 7-1

Figure 111: Primary software components 7-4

Figure 112: Cartesian coordinate system for UrbanBlast 7-5

Figure 113: Buildings contained within the Manhattan Financial District model..... 7-5

Figure 114: UrbanBlast software for Manhattan Financial District.... 7-7

Figure 115: Selectable threat locations (shown in yellow) 7-7

Figure 116: Select the threat location by clicking on one of the yellow Threat Location Points; the selected location is colored magenta 7-8

Figure 117: Computed results are presented in the display window..... 7-9

Figure 118: User can select seventeen different types of results for display..... 7-10

Figure 119: Comparison of approximated values of peak pressure and peak impulse from UrbanBlast with high-fidelity MAZ CFD calculated results 7-11

Figure 120: Comparison of approximated values of peak pressure and peak impulse from UrbanBlast with high-fidelity MAZ CFD calculated results 7-12

Figure 121: Comparison of approximated values of peak pressure and peak impulse from UrbanBlast with high-fidelity MAZ CFD calculated results 7-13

Figure 122: Comparison of approximated values of peak pressure and peak impulse from UrbanBlast with high-fidelity MAZ CFD calculated results 7-14

Figure 123: Comparison of approximated values of peak pressure and peak impulse from UrbanBlast with high-fidelity MAZ CFD calculated results 7-15

Figure 124: Example of window breakage and window hazard distribution in urban setting 7-16

Figure 125: Example of steel column failure display 7-18

Figure 126: Example of EERR equipment damage display: emergency lighting 7-19

Figure 127: Rotated and zoomed image of the model 7-21

Figure 128: Display control toolbar..... 7-21

Figure 129: Close-in view of the blast pressure provided by UBT 7-22

Figure 130: Building display toolbar 7-22

Figure 131: Specific buildings can be elected for display 7-22

Appendix C

Figure 132: Pressure comparison between MAZ and SHAMRC..... C-8

Figure 133: Impulse comparison between MAZ and SHAMRC..... C-9

Figure 134: Comparison of measured and calculated airblast C-9

Figure 135: Comparison of measured and predicted blast pressures..... C-10

Figure 136a: Loading dock test structure..... C-11

Figure 136b: Propagating Airblast pressures explosive test simulation from MAZ..... C-11

Figure 137: Comparison of measured and predicted pressure time history for loading dock test C-11

Figure 138: Comparison of measured and predicted impulse time history for loading dock test C-12

Figure 139: Comparison with measured and predicted blast pressures..... C-12

Figure 140: Comparison with measured and predicted blast pressures..... C-13

Figure 141: Comparison of experimental and computed response for internal wall..... C-14

Figure 142: Photos of CTS1 test vs. pretest NLFlex simulation results..... C-15

Figure 143: ACEC Grand Conceptor Award to WAI C-16

Figure 144. Comparison of progressive collapse analysis with test..... C-17

List of Tables

Chapter 4

Table 1: Summary of progressive collapse analyses for 32 ft moment frame..... 4-47

Table 2: Summary of progressive collapse analyses for 25 ft moment frame..... 4-47

Table 3: Summary of progressive collapse analyses for 25 ft flat slab building..... 4-47

Chapter 6

Table 4: Wall performance levels considered in determining fragility data 6-9

Table 5: Limit states of the stair pressurization system unit..... 6-11

Table 6: Limit states of representative fire door 6-12

Table 7: Limit states of representative elevator door system..... 6-13

Table 8: Limit states of representative fire alarm control panel 6-14

Table 9: Limit state of representative fluorescent light bulbs 6-16

Table 10: Representative air duct dimension, thickness 6-16

Table 11: Limit states of representative air duct system 6-17

Table 12: Wall performance levels considered in determining fragility data 6-18

Table 13: Limit states of representative emergency generator..... 6-20

Table 14: Limit states of representative smoke detection system 6-21

Table 15: Representative sprinkler pipe size and weight 6-23

Table 16: Limit states of representative fire sprinkler system 6-23

Table 17: Summary of validation of methodology..... 6-26

Chapter 7

Table 18: Window damage criteria 7-16

Project Overview

Weidlinger Associates, Inc. (WAI) has completed the initial phase effort of the Department of Homeland Security (DHS), Science and Technology (S&T) Directorate project, “Preventing Structures from Collapsing to Limit Damage to Adjacent Structures and Additional Loss of Life when Explosives Devices Impact Highly Populated Urban Centers.” The stated objective of this effort is:

To conduct research to reduce substantial damage to buildings located in large urban centers as a result of improvised explosive device (IED) attacks.

The effort had several key areas of investigation. One area of focus was the study of the blast response of columns under urban blast loading scenarios and the evaluation of new methods to mitigate the potential for large scale structural failure and collapse in response to extreme loading conditions associated with IED explosive attacks. New methods under consideration in the blast design community include the Indirect Design Approach, Alternate Path Approach, Specific Local Resistance Approach, and methodologies developed by the General Services Administration (GSA), the Department of Defense (DOD), the United Kingdom, and others. In this effort, WAI looked at the effects of Unified Facilities Criteria (UFC) 4-023-03 *Design of Buildings to Resist Progressive Collapse* criteria for three types of construction: concrete moment frame, steel moment frame, and concrete flat slab buildings. WAI developed detailed structural models and investigated

their behavior when subjected to the loss of one or more support columns. The responses of generic and upgraded designs were investigated to determine the influence of the UFC design techniques on the post-damaged response of the structures.

Another main area of investigation was the determination of airblast pressure levels in an urban setting and the influence of the presence of buildings on the pressure and impulse levels that result from explosions. It is important to quantify accurately the airblast environment resulting from the detonation of an IED in an urban setting to evaluate the performance of structures in response to these loads. WAI evaluated the structural loads that result from IED charges detonated in a selected urban location (i.e. the Manhattan Financial District). Variations in charge size and location were considered for this urban setting. The results of these calculations were incorporated within an UrbanBlast Tool (UBT), which will support activities of Federal, State, and local agencies and organizations responsible for designing and/or protecting urban centers. This information may be used by security planners and first responders to more fully understand the threats posed by explosive devices detonated in urban settings and to aid in developing effective strategies for minimizing blast damage effects in urban centers.

WAI also studied Emergency Evacuation, Rescue and Recovery (EERR) systems and developed fragility information to determine the likelihood of damage as a result of an IED attack. Airblast loads that impact system and structural response of critical systems were investigated to quantify the blast pressure range within which the blast environment would be great enough to compromise the functionality of the equipment following an explosive event.

The primary deliverables for this effort are this final report and the fast running airblast and structural damage assessment tool, herein termed: UrbanBlast – Manhattan Financial District.



The UrbanBlast Tool (UBT) developed by the U.S. Department of Homeland Security, Science and Technology Directorate, Infrastructure Protection and Disaster Management Division, is a fast running airblast and structural damage assessment tool for the urban location.

The tool uses an easy to use graphical user interface that accesses the airblast data generated from high-fidelity computational fluid dynamics analyses and uses compiled P-I diagrams relating structural and equipment damage to airblast loads at various ranges from the detonation.

High-Fidelity Simulation Software

Urban environments provide a complicated setting for determining the airblast loads that result from explosive detonations and the structural damage they may produce. Tall buildings divert and channel airblast resulting in significant enhancement of loads at range from the detonation. Buildings reflect pressures to increase loading at some locations and shield other areas thus mitigating the loads. The pressure loads acting on a building can damage key structural members and potentially cause a progressive collapse of the damaged structure. Even when primary structural components are not damaged, window breakage and/or damage to key emergency equipment can lead to significant human injury and potentially loss of life.

Urban environments provide a complicated setting for determining the airblast loads that result from explosive detonations and the structural damage they may produce.

High-fidelity physics-based (HFPB) simulation models are required to accurately address the challenges of defining airblast behavior and structural response in urban settings. The complex airblast interaction with buildings, streets, and alleyways is best predicted using high-fidelity computational fluid dynamics (CFD) simulations. In the current project, multiphase adaptive zoning (MAZ) and NLFlex software provide the high-fidelity modeling component of all the simulation studies performed. Appendix C briefly describes these software programs and validation for the areas of application considered below.

In this effort, the MAZ CFD software was used to simulate blast pressure propagation in urban environments. MAZ has a long track record of accurate simulation of airblast pressures, and its capabilities for airblast modeling are continually being advanced. Additionally, the NLFlex software was used to compute the structural response of buildings subjected to blast and fragment loads and other extreme events. NLFlex has over 20 years of application to modeling structural response to nuclear, terrorist, and conventional weapons effects. The software is also a leader in the field of simulating progressive collapse of blast damaged buildings.

2.1 NLFlex Computational Structural Dynamics Software

NLFlex [2] is an explicit, nonlinear, large deformation transient analysis finite element software for the analysis of structures subjected to airblast, fragment, impact, and ground shock loadings. NLFlex software has been used to support a wide range of DOD and other United States Government organizations including the Defense Threat Reduction Agency (DTRA), the U.S. Air Force, the U.S. Army, and the

Central Intelligence Agency (CIA). NLFlex has a library of finite elements and constitutive models that are tailored to the solution of large, transient nonlinear structural blast response problems through failure. The primary emphasis of the software is dynamic analysis, but static solution options are also available for combined gravitational, impact, and blast loading of buildings. Theoretically sound constitutive models for ductile and brittle materials and for pressure dependent and rate sensitive materials have been developed during the past 30 years [References 3 through 8] and are

available so that buildings, building components, hardened structures, and equipment that are constructed from metals, masonry, ceramics, fiber reinforced composites, rock, and reinforced concrete are readily analyzed through failure.

2.2 MAZ Computational Fluid Dynamics Software

MAZ¹ is a three-dimensional (3D) CFD program that solves the Reynolds-averaged, unsteady Navier-Stokes equations. It employs a second-order accurate linearized Riemann scheme for the two-dimensional (2D)/3D Euler equations with the total variation

¹ MAZ is currently being used by WAI for predictions of environments produced by terrorist attacks using explosives.



NLFlex is an explicit, nonlinear, large deformation transient analysis finite element

software for the analysis of structures subjected to airblast, fragment, impact, and ground shock loadings.

decreasing (TVD) flux limiting method of Harten [10]. A general finite-volume formulation is implemented to accommodate the underlying grid methodology, which includes adaptive zoning (AZ) and Arbitrary Lagrangian-Eulerian (ALE) grid motion and geometries. AZ of individual cells (3D hexahedrals, 2D quadrilaterals) allows spatial resolution to be concentrated automatically where numerical detail is most needed. ALE enables the tracking of a moving physical interface between different types of materials as well as defining the boundaries of arbitrarily-shaped physical elements. All grid/variable data is stored in memory within an unstructured topology, which lends itself to efficient use of vectorizing central processing unit (CPU) architectures. WAI implemented symmetric multi-processing (SMP) directives in MAZ in order to take advantage of the multiple CPU/multiple core processors available in today's computers.

WAI has applied MAZ to a wide range of airblast applications including blast in urban environments and internal detonations and uses this software extensively for generating high-fidelity blast pressure loads for computing the response of structural models.²



equations.

MAZ is a 3D CFD program that solves the Reynolds-averaged, unsteady Navier-Stokes

2 The primary funding for the original MAZ software development came from DTRA.

Structural Column Damage Modeling Studies

The performance of both steel and concrete columns was investigated in response to loading environments that are representative of those that would be experienced in IED attacks in urban settings.

3.1 Threat Environment

The setting for these column vulnerability studies is a dense urban environment. In such an environment, the conditions exist to both reflect the airblast pressures off of the surrounding structures and funnel the blast wave down the street. As such, column vulnerability is not only limited to the column directly opposite the explosion but also potentially extends downrange as the blast wave funnels down the urban canyon environment.

Two geometries are considered in this study to evaluate the potential of urban environments to increase the effects of airblast on surrounding structures: a two-lane street and a four-lane street configuration. Figures 1 and 2 illustrate both configurations. Two threat locations are considered for the two-lane environment, and four threat locations are considered for the four-lane environment.

Figure 1:
Two-lane street blast environment

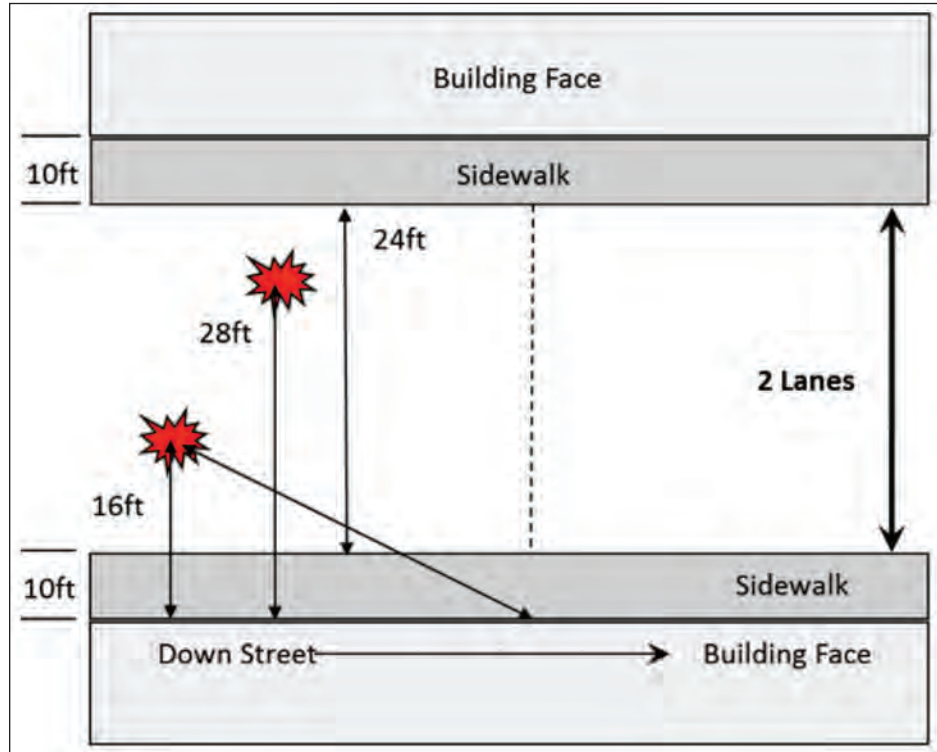
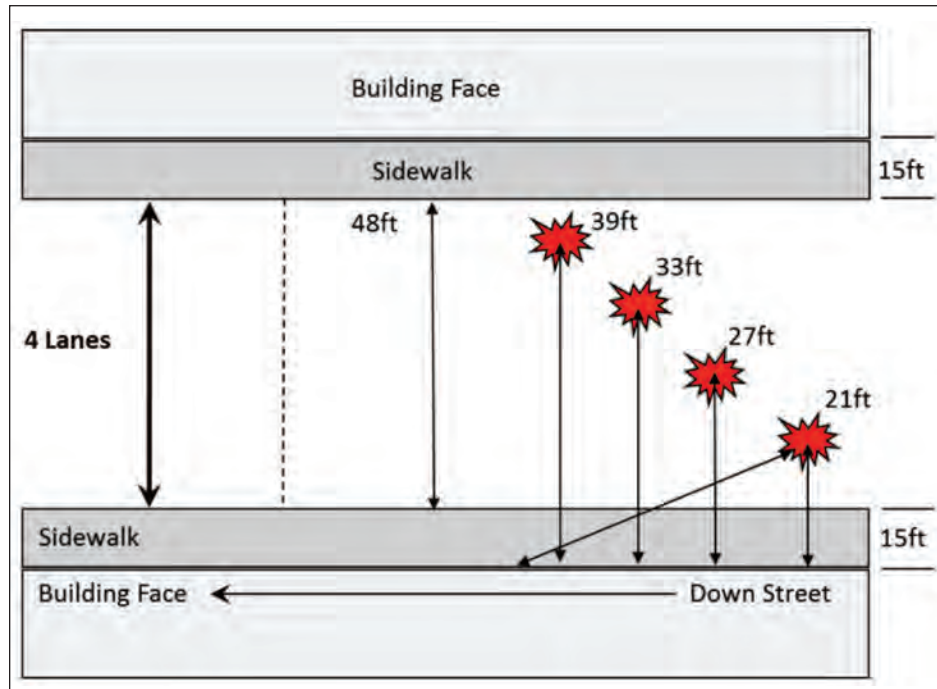


Figure 2:
Four-lane street blast environment



3.2 Airblast Calculations

Airblast calculations for the urban environments are performed with the MAZ CFD software. The computational grids form the urban canyon blast environment, as shown in Figure 3, and extend 100 ft from the center of blast (COB). Figures 4 and 5 show examples of the computational grids for the two-lane and four-lane configurations (opposite street-side boundaries are removed for clarity).

Airblast calculations for the urban environments are performed with the MAZ CFD software.

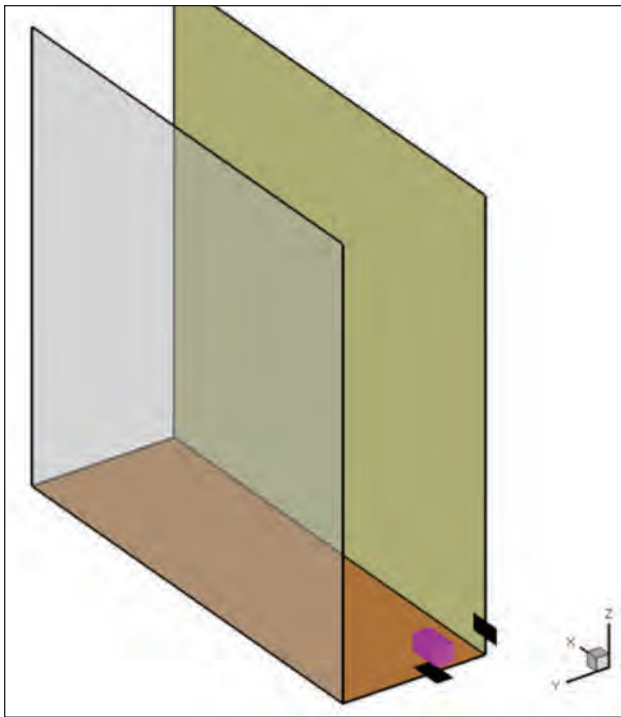


Figure 3: Schematic of urban blast computational environment

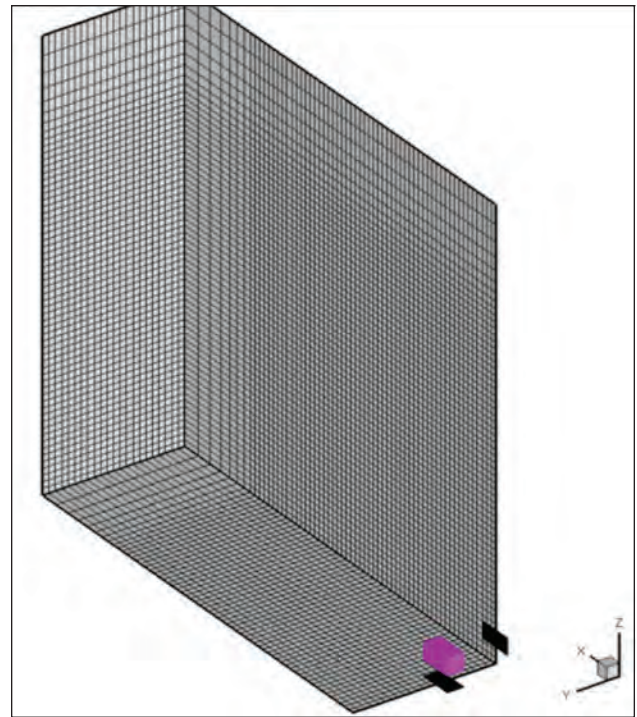
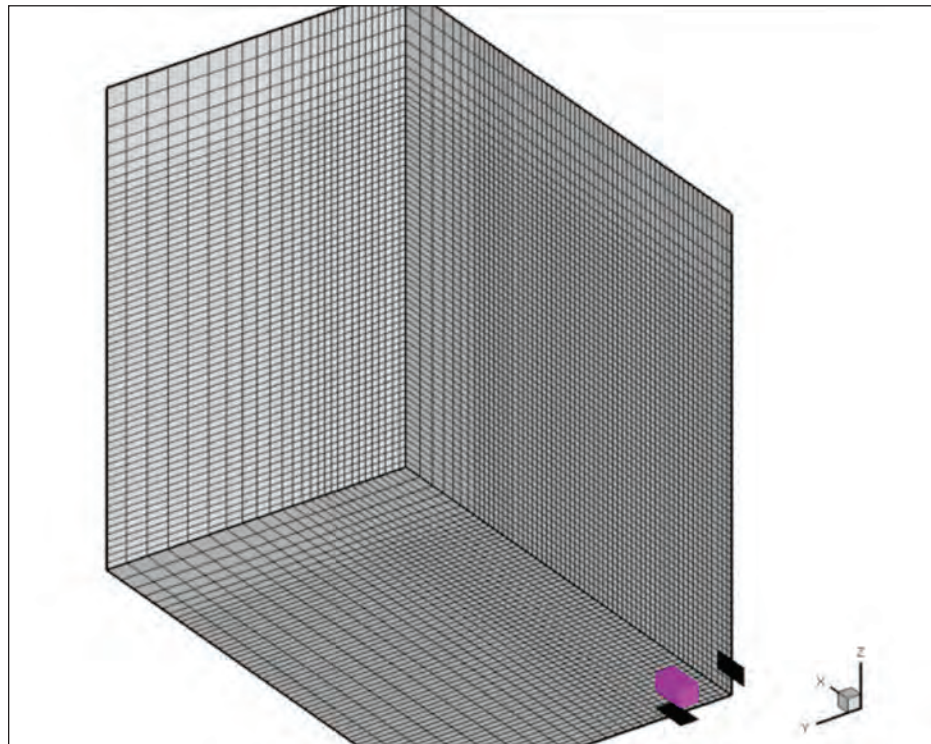


Figure 4: Example of two-lane environment computational grid

Figure 5:
Example of four-lane
environment computational
grid



Five charge weights, representative of explosive devices that could be delivered by small to very large vehicles, are considered in these calculations: 500lbs, 1,000lbs, 4,000lbs, 10,000lbs, and 30,000lbs [trinitrotoluene (TNT)-equivalent] of explosive. Charge shape can have a significant effect on structural response, so these calculations assume a 2 (long) x 1 (wide) x 1 (high) charge shape, a fair assumption for vehicle-borne devices and usually more damaging than the more common spherical or hemispherical shapes assumed by simple airblast tools. The 500lb and 1,000lb devices assume 36 in. from the roadway to the bottom of charge, the 4,000lb device assumes 48 in., and the 10,000lb and 30,000lb devices assume 60 in. These heights are representative values based on the sizes of the vehicle required to carry the threats.

Five charge weights, representative of explosive devices that could be delivered by small to very large vehicles, are considered in these calculations: 500lbs, 1,000lbs, 4,000lbs, 10,000lbs, and 30,000lbs (TNT-equivalent) of explosive.

A total of 17 analyses were performed for the two-lane environment with the 2x1x1 charge shape and listed charge weights. Twenty analyses were performed for the four-lane environment. Additional analyses were performed using a single flat wall (non-urban environment) as the target and using a hemispherical shaped charge to investigate the changes in airblast response due to these variables.

3.3 Column Descriptions

A seemingly infinite number of columns can be envisioned for buildings, dictated for example by column demand, structural system requirements, available space, and building architecture. However, a small set of columns representative of typical columns found in mid- and high-rise office buildings can be defined, and this was done for the single-column vulnerability study performed here for both reinforced concrete and steel moment framed structures.

Guidelines for the design of structural concrete structures in the U.S. are defined by the American Concrete Institute (ACI) *Building Code Requirements for Structural Concrete* (ACI 318-05) and *Commentary* (ACI 318R-05). ACI 318 dictates, among its many guidelines, the minimum area of longitudinal steel rebars (primary steel) required in columns and the amount of lateral ties (secondary steel) to provide lateral stability for the primary steel. ACI 318 guidelines are followed by the eight representative columns used in this study. The columns have square cross-sections, typical of the majority of reinforced concrete construction. Reinforcement ratios (the ratio of longitudinal reinforcement to gross concrete area) for all designs are between 1.5% and 2.5%, which satisfy the ACI 318 minimum reinforcement ratio of 1.0% and recommended maximum of 4.0% for lap-spliced columns. Size, number, and geometry of secondary steel follow guidelines dictated by ACI 318. Columns have 14 ft clear heights, typical of ground floor office space, with moment continuity assumed at both column ends. Detailed descriptions of the reinforced concrete columns used in this study are shown in Figure 6.



Guidelines for the design of structural concrete structures in the U.S. are defined by the American Concrete Institute *Building Code Requirements for Structural Concrete* (ACI 318-05) and *Commentary* (ACI 318R-05).

The majority of steel framed structures use rolled steel shapes for both axial and flexural members. Geometries of these rolled shapes are dictated by the American Institute of Steel Construction (AISC), whose building code for steel construction is defined in its *Steel Construction Manual (13th Edition)*. Typical steel framed structures rely on nominally 14 in. deep sections (W14 sections) for columns with a primarily axial demand. This study chose five W14 columns with increasing axial capacity as representative steel columns, summarized in Figure 7. All columns have 14 ft clear heights, typical of ground floor office space, with moment continuity assumed at both column ends.

Figure 6:
Concrete column descriptions

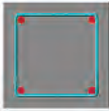
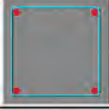
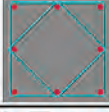
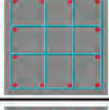
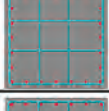
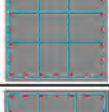
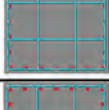






| Column Type | Column Size | Primary Steel | Secondary Steel | |
|-------------|-------------|---------------|-----------------|---|
| C1 | 14"x14" | (4) No. 8 | No. 3 @ 12" |  |
| C2 | 18"x18" | (4) No. 10 | No. 3 @ 12" |  |
| C3 | 24"x24" | (8) No. 10 | No. 4 @ 12" |  |
| C4 | 27"x27" | (12) No. 10 | No. 4 @ 12" |  |
| C5 | 36"x36" | (24) No. 8 | No. 4 @ 12" |  |
| C6 | 44"x44" | (24) No. 10 | No. 6 @ 12" |  |
| C7 | 48"x48" | (44) No. 8 | No. 6 @ 12" |  |
| C8 | 48"x48" | (72) No. 8 | No. 6 @ 12" |  |

Figure 7:
Steel column descriptions

| Column Type | Column Size | Steel Area [in ²] | |
|-------------|-------------|-------------------------------|--|
| S1 | W14x82 | 24.0 |  |
| S2 | W14x176 | 51.8 |  |
| S3 | W14x257 | 75.6 |  |
| S4 | W14x342 | 101.0 |  |
| S5 | W14x500 | 147.0 |  |

3.4 Column Vulnerability Calculations

Structural response calculations were performed with NLFlex. Concrete is modeled using hexahedral continuum elements with single-point integration, with the constitutive formulation provided by WAI's SFT1 concrete model, a three-invariant plasticity-based material model with rate dependency and softening. Concrete uniaxial compression strength is assumed to be 5 ksi. Primary reinforcing steel in the concrete columns is explicitly modeled using one-dimensional (1D) flexural elements, and secondary reinforcing steel uses 1D axial elements. The w-sections in the steel column study are composed of 2D shell elements. All steel elements use a plasticity-based piecewise linear material formulation with rate dependency and softening. Primary reinforcing steel is assumed to be A615³ grade 60 steel, secondary reinforcing steel is A615 grade 40 steel, and the w-section columns are assumed to be A562 grade 50 steel. Examples of the material model responses are shown in Figures 8 through 12.

All structural response calculations were performed with NLFlex.

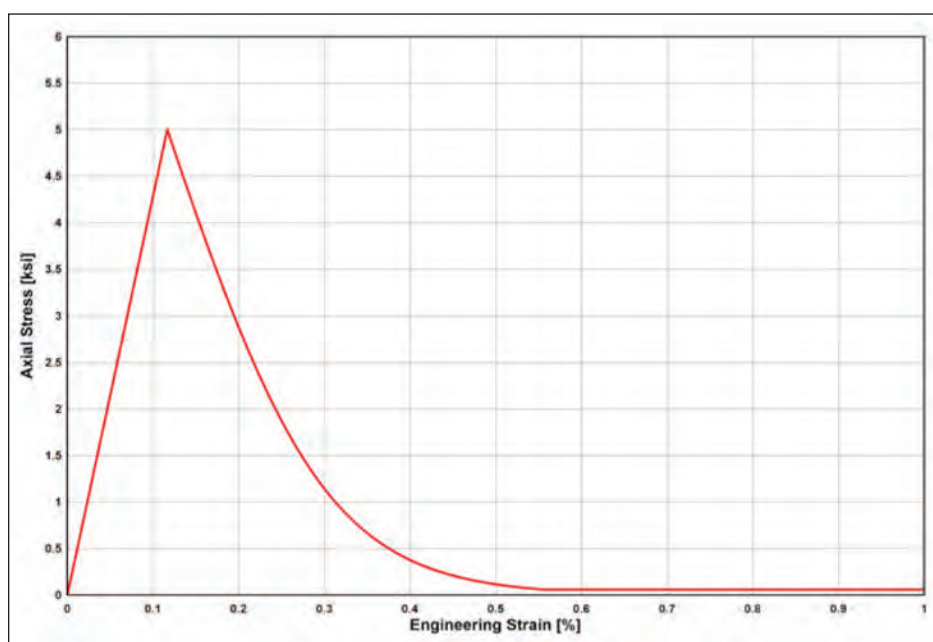


Figure 8:
Concrete model unconfined
compression response

3 A615 is a standard specification for deformed and plain carbon-steel bars for concrete reinforcement.

Figure 9:
Concrete model stress path

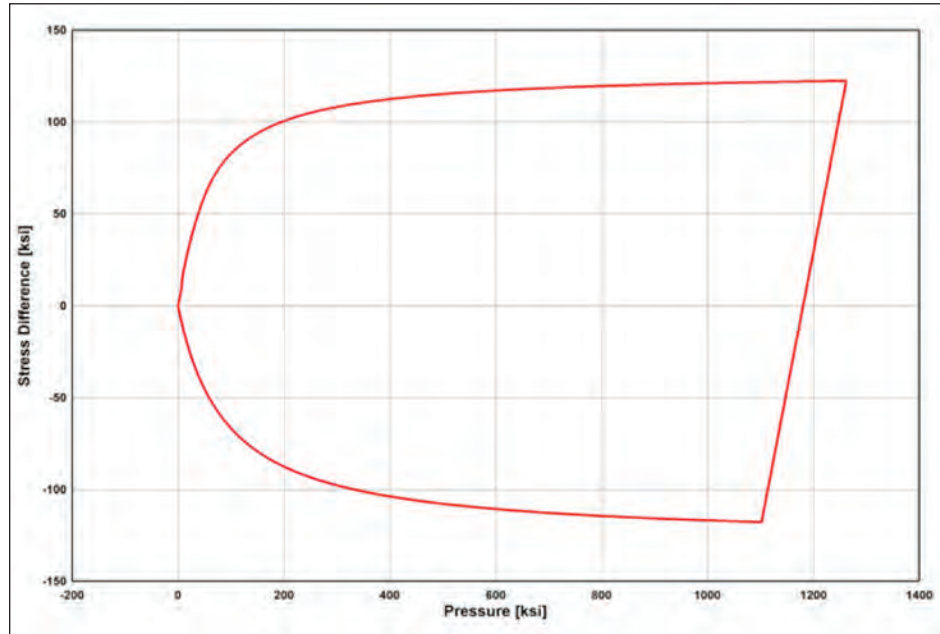
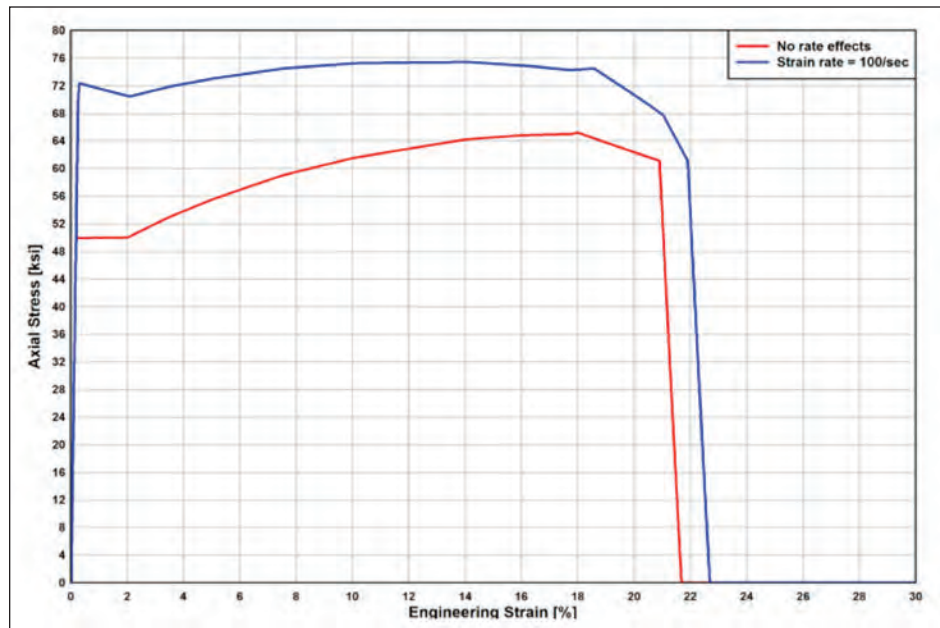


Figure 10:
A572 grade 50 steel model
uniaxial tension response



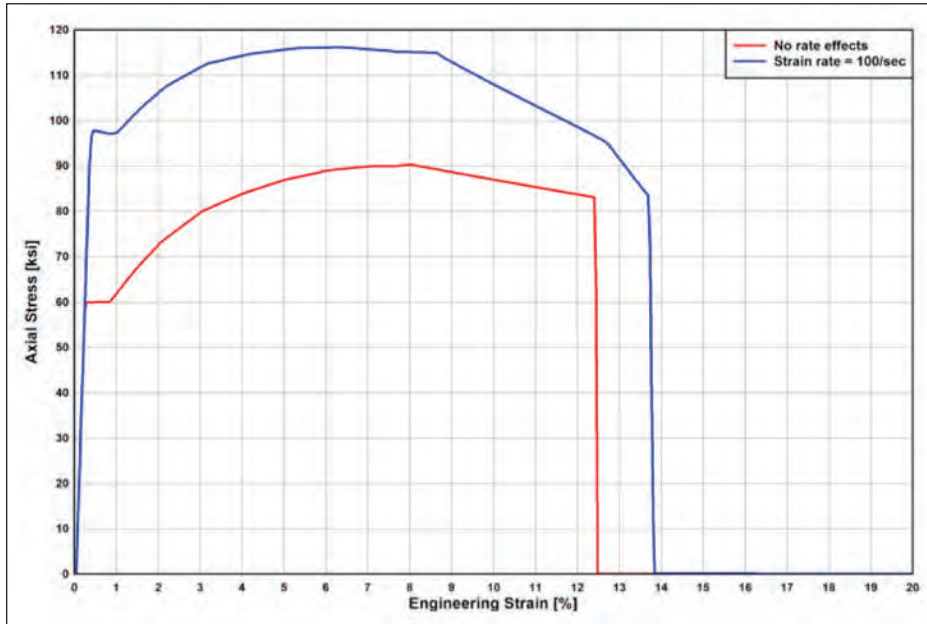


Figure 11:
A615 grade 60 steel model
uniaxial tension response

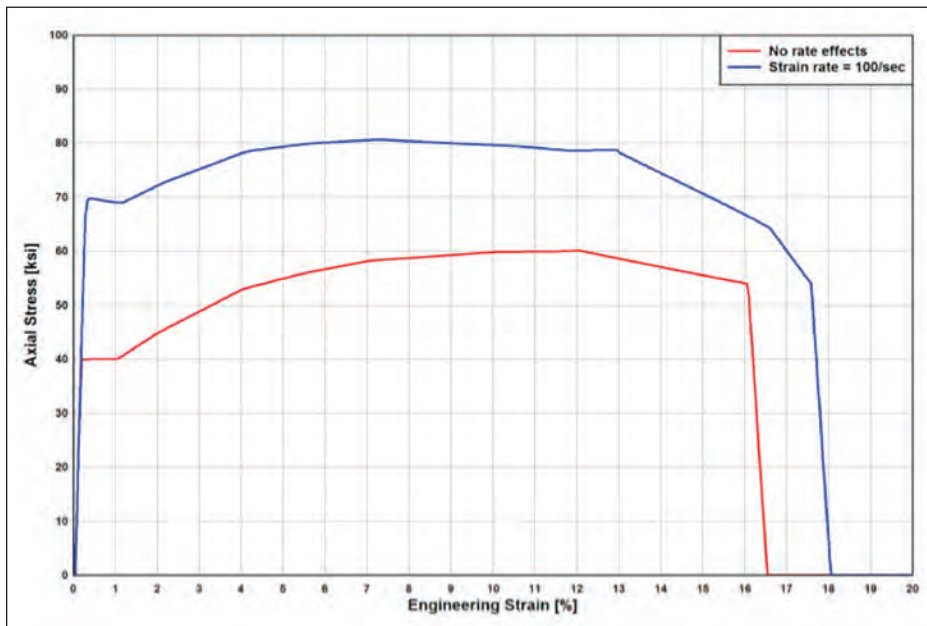


Figure 12:
A615 grade 40 steel model
uniaxial tension response

Five column locations are considered with respect to the center of blast (COB):

1. Column centered directly opposite the COB
2. Column centered down street 5 ft from the COB
3. Column centered down street 10 ft from the COB
4. Column centered down street 15 ft from the COB
5. Column centered down street 20 ft from the COB

The goal of this column study is to evaluate column vulnerability to airblast, where vulnerability (column damage) is related to a column's lateral deformation under direct blast loading. It has been previously found that a column's axial load does not significantly affect the column's peak lateral deformation during the blast loading phase. For multi-story structures, the time required for the structure to begin moving downwards after a column is damaged is typically much greater than the time it takes for the direct blast loading to damage the column. So, secondary effects like P-Delta⁴, driven by column axial demand and which may contribute to structural collapse when the structure responds, do not affect the column's lateral deformation response during the blast phase. As this study is focused on single columns and not assessing the structural response of building assemblies, column axial load is not considered.

A total of 1120 analyses were performed for the concrete column vulnerability investigation, and 1500 analyses were performed for the steel columns. The steel column cases include both strong axis and weak axis bending configurations.

3.5 Analysis Results

3.5.1 Airblast

As mentioned, simplified blast tools typically do not consider actual charge shapes when reporting blast pressures, instead assuming either a spherical or hemispherical charge shape. The effect of this simplification is illustrated in Figure 13, which compares peak pressure distributions.

Simplified blast tools typically do not consider actual charge shapes when reporting blast pressures, instead assuming either a spherical or hemispherical charge shape.

A much larger concentration of high pressures is seen at the blast location in the MAZ calculation than from the simplified tool, and higher pressures also extend down-range. The higher pressures in the immediate vicinity of the COB will be more damaging to the target structure, and the increased extent down-street of high pressures could extend the range of damage away from the COB.

The effect of the urban canyon itself is more subtle, at least in the near vicinity to the charge. Figure 14 shows the peak pressure contours for the MAZ urban canyon calculation (left side) versus the MAZ flat plane calculation (right side) for the 30,000lb at 16 ft case. Differences between

⁴ P-Delta is the secondary effect on shears and moments of structural members due to the action of the vertical loads induced by horizontal displacement of the structure resulting from various loading conditions. The secondary shears and moments produced by the P-Delta effect contribute to the destabilization of the structure.

the two calculations are more apparent when the pressure and impulse difference contours are investigated (see Figure 15). The pressure difference (left side) shows only localized minor differences within a range of about 90 ft vertically and laterally from COB. Any peak pressure differences within this range are on the order of 100 psi or less. The difference is clearer however when looking at peak impulse difference (right side). No difference is observed within a 60 ft radius from COB. The impulse differences become more pronounced outside of this range, with the urban canyon calculation delivering more impulse outside of 60 ft than the flat plane. This shows that there is a measurable effect of pressure reflections down the urban canyon, and these effects become increasingly evident down-street from the COB. While this may not have a large affect on primary structural elements, such as building columns at such a range due to the small magnitudes of total impulse down-street, it will certainly have an effect on façade response, which can be critical to the vulnerability of building inhabitants even 100 ft or farther from COB.

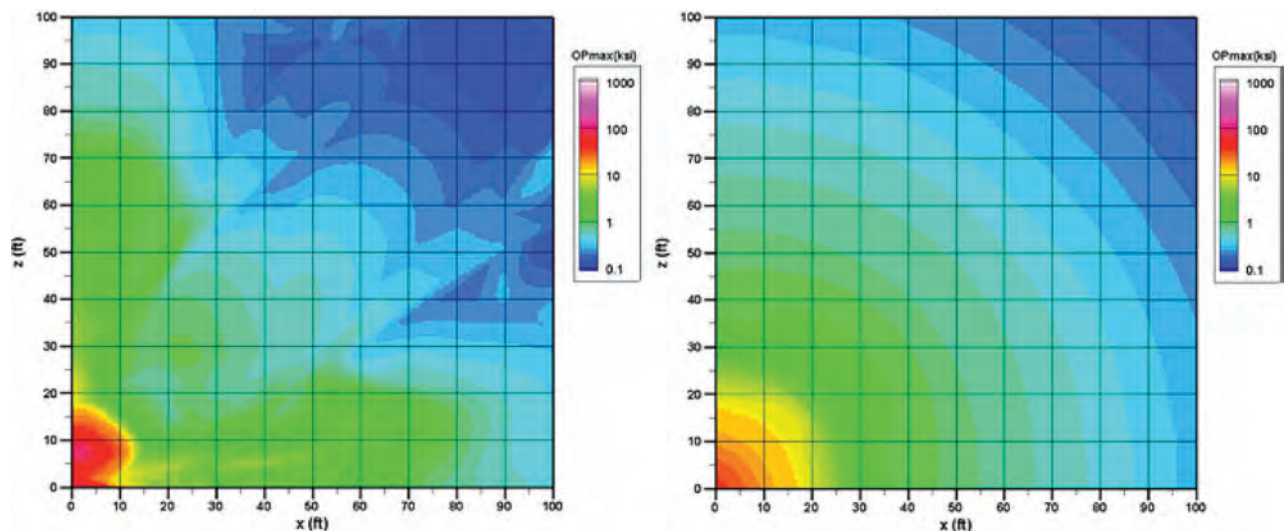


Figure 13:
Peak pressure [ksi] comparisons: MAZ urban canyon calculation (left side) vs. simple Airblast tool equivalent (right side), 30,000lb charge

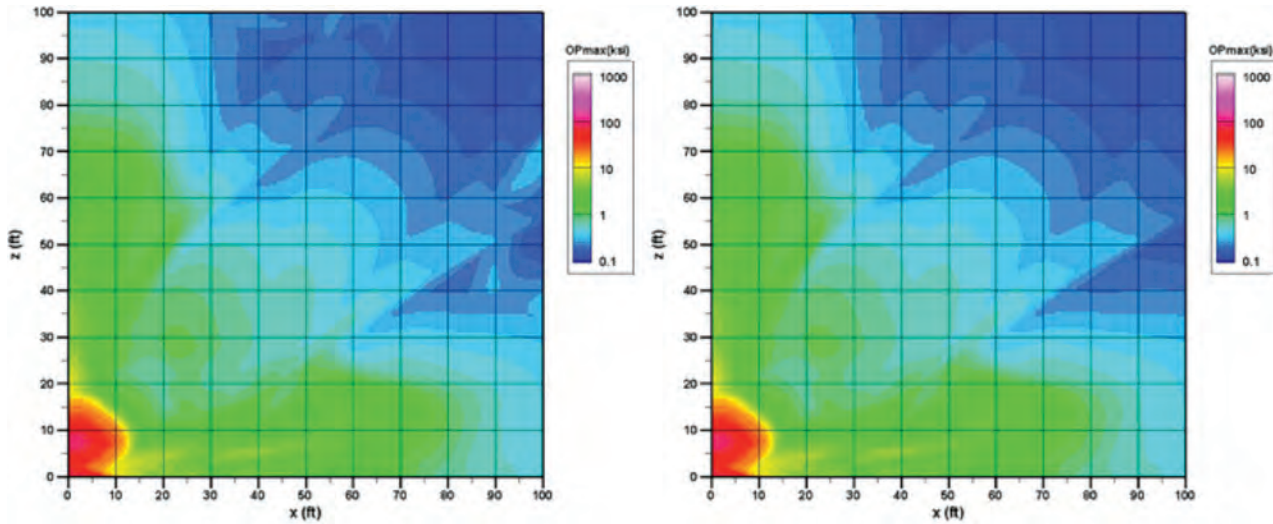


Figure 14:
Peak pressure [ksi] comparisons: MAZ urban canyon (left) calculation vs. MAZ flat plane (right), both using 30,000lb rectangular charge shape

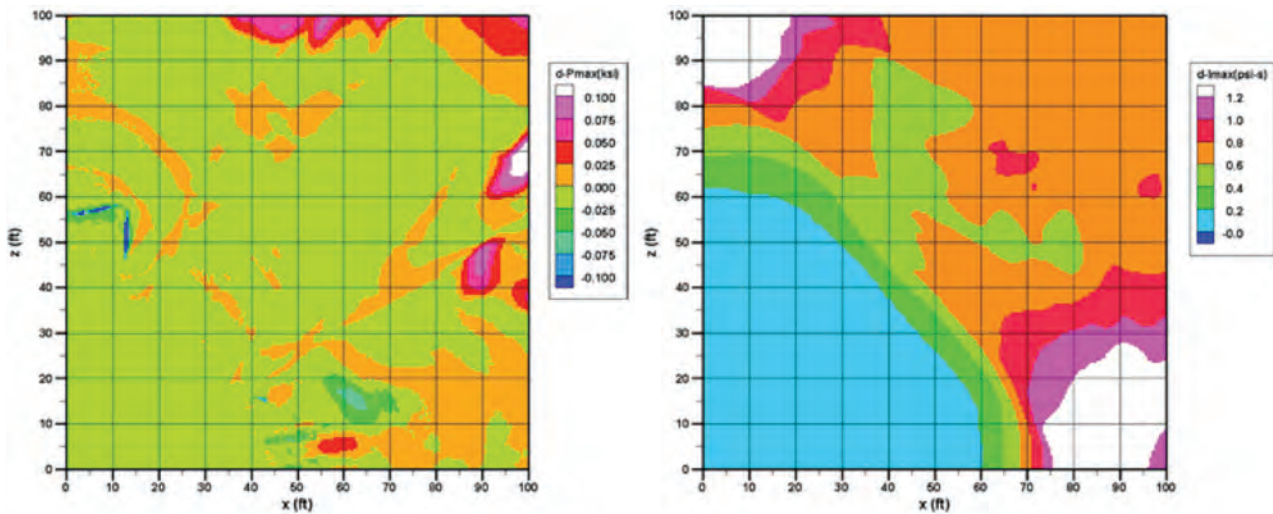


Figure 15:
Pressure [ksi] and impulse [psi-sec] difference between MAZ urban canyon (left) and flat plane (right), both using 30,000lb rectangular charges

3.5.2 Reinforced Concrete Columns

As shown in the previous section, the urban canyon has little effect on the peak pressure and total impulse within about a 60 ft radius down-street from the blast, so the shape of the urban landscape itself does not appear to play a role in the response of structural columns, at least for

the two-lane and four-lane geometries investigated in this study. But what is of great interest are the responses of the down-street columns to the blasts, regardless of urban landscape.

Figures 16 and 17 illustrate the concern regarding column design and vulnerability to multiple failures. The threat in both cases is 4,000 lb at 16 ft, the closer of the two-lane street threats. The columns are spaced at 5 ft on center down-street from the COB. Column type C2, an 18"x18" column, is failed at 0 ft and 5 ft down-street from the COB. A peak rotation limit of 3.5 degrees is one measure of unacceptable column damage as defined by the U.S. Army Corps of Engineers (USACE) Protective Design Center (PDC). When this criteria is applied, the results show that all five columns exceed that limit and are considered to fail because the peak rotation of the column located 20 ft down-street is over 5 degrees.

When the column strength is increased to the C4 design, the overall vulnerability is decreased. The columns directly opposite the COB and 5 ft down-street still fail, but the remaining columns down-street do not fail outright. When the 3.5 degree rotation limit is enforced, the columns 15 ft and 20 ft down-street survive. The column 10 ft down-street has a peak rotation of just over 4 degrees, so while it fails the peak rotation limitation, it will continue to carry much or all of its axial demand post-event.

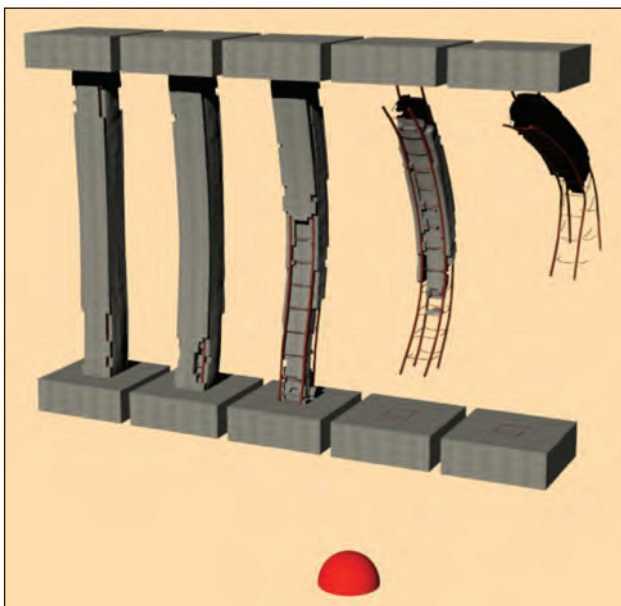


Figure 16: Column type C2, 4,000lb at 16ft

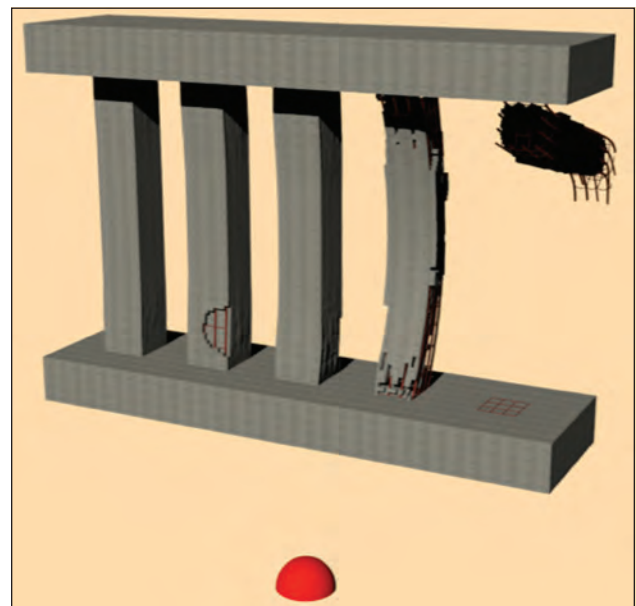


Figure 17: Column type C4, 4,000lb at 16ft



Concrete column failure is defined as peak column rotations greater than 3.5 degrees.

The closest safe distances from the COB for the eight different column designs were calculated using the two-lane and four-lane configurations. Column failure is defined as peak column rotations greater than 3.5 degrees.

The majority of the results follow the obvious trend that increasing standoff leads to greater survivability of the columns closer to the COB. At a 21 ft standoff, this column design must be 10 ft down-street from the COB to survive. But at 27 ft and 33 ft standoffs, the column only needs to be 5 ft down-street, and at a 39 ft standoff the target column directly opposite the COB survives.

There is an exception to this response, and it occurs in the largest columns, C6 – C8, with the largest threat sizes at greatest standoff. At a 21 ft standoff, the column 20 ft down-street survives the 30,000lb blast effects. This same column survives the 10,000lb blast at only 15 ft down-street. However, at larger standoffs the column 20 ft down-street fails vs. the 30,000lb threat, and at 39 ft the safe distance for the 10,000lb threat increases from 15 ft to 20 ft. These responses appear to be due to the changes in the angle of incidence between the shaped charge and the loaded column face. At smaller standoffs, the incidence angles between the charge and the column faces down-street are small, and these columns receive more of a glancing blow than a direct hit.

3.5.3 Steel Columns

The steel columns follow a similar response pattern to the concrete columns. Increasing standoff and column size both increase the survivability of columns opposite the threats and down-street from the threats. Figures 18 and 19 show examples of the steel column responses for the

The steel columns follow a similar response pattern to the concrete columns. Increasing standoff and column size both increase the survivability of columns opposite the threats and down-street from the threats.

two-lane 4,000lb threat at 16 ft for column types S1 (W14x82) and S4 (W14x342). The USACE PDC sets a rotation limit of 2.35 degrees for a low level of protection for exterior steel columns. With this limit, the safe radius for column type S1 is 15 ft for the 4,000lb at 16 ft threat, while the radius reduces to 10 ft for column type S4.

The closest safe distances from the COB for the five different column sections were calculated using the two-lane and four-lane configurations. Both strong axis and weak axis bending directions are included. Column failure is defined as peak column rotations greater than 2.35 degrees.

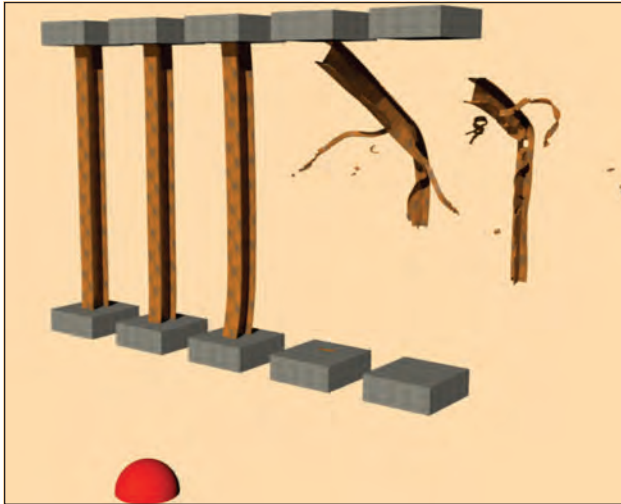


Figure 18: Column type S1, strong axis, 4,000lb at 16 ft

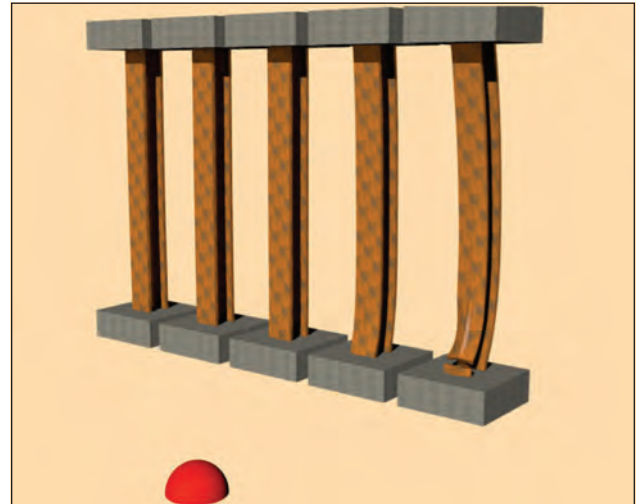


Figure 19: Column type S4, strong axis, 4,000lb at 16 ft

3.6 Summary

A suite of airblast and structural response calculations were performed to assess the effect of urban environments on airblast severity and propagation and its corresponding effect on the response of reinforced concrete and steel columns. Representative geometries for two-lane and four-lane urban streets were modeled with MAZ, a computational fluid dynamics code specializing in explosives calculations. Five different charge sizes were considered to cover a range of vehicle sizes, and multiple standoffs were used for the two street environments. Key findings of this airblast study are:

- Detailed airblast calculations that include accurate modeling of the charge shape give higher peak pressure profiles both opposite the COB and down-street from the threat, compared to simplified blast tools that typically assume either a spherical or hemispherical charge shape.
- Modeling an urban environment in the airblast calculations does result in increased pressure and impulse due to pressure reflections propagating down the urban canyon, but the differences are only apparent at distances downrange from the COB.
- Because the pressure and impulse changes due to the urban environment take place only down-range from the COB where pressure

Airblast and structural response calculations were performed to assess the effect of urban environments on airblast severity and propagation and its corresponding effect on the response of reinforced concrete and steel columns.

and impulse is greatly decreased, the urban environment itself is unlikely to significantly change the response of ground level structural columns.

- The pressure and impulse changes due to the urban environment are significant enough away from the COB to possibly affect façade response, which is important to building inhabitant vulnerability.

The airblast pressure loads were applied to reinforced concrete and steel columns that are representative of typical columns used in urban structures. Columns were placed directly opposite the COB and also at distances 5 ft, 10 ft, 15 ft, and 20 ft down-street from the COB. The analysis results provide a large database of column responses to the various threat sizes and standoffs. For a given column design and threat size/location, the radius from COB to the nearest safe column can be determined.

Progressive Collapse Modeling Studies

The progressive collapse of blast damaged buildings can result in significantly greater loss of life than would be caused by the direct blast pressures themselves. There are ongoing efforts to develop improved design methods that increase the ability of buildings to resist progressive failure in the event of structural damage from blast effects.

WAI has developed extensive capabilities for simulating progressive collapse phenomenology for blast damaged structures. As part of the current effort, WAI investigated several different buildings designed using different construction methods. The NLFlex software was used to assess the potential for urban blast damage producing partial or total progressive collapse for these types of structures.

WAI designed several different types of steel frame and reinforced concrete buildings for this study. Two designs for each building type were produced:

1. A standard design based on traditional building codes used in the U.S.
2. An upgraded design using the UFC criteria for resisting progressive collapse.

Models of the different building designs were constructed, and the NLFlex software was used to simulate their response when one or more of a building's critical support columns were damaged.

High-fidelity simulations of progressive collapse are computationally intensive, potentially requiring months of computer time to compute the response of a single building to a specific damage state. Five-story buildings were investigated in the current study, because they provide a structure large enough to represent the complex interactions that govern progressive collapse without being so large that they became impractical to analyze in the time frame of the project.

High-fidelity simulations of progressive collapse are computationally intensive, potentially requiring months of computer time to compute the response of a single building to a specific damage state.

Both in-house computational resources and DOD High Performance Computing (HPC) resources were used for this computational effort. Access to HPC resources were contributed by both DTRA and the USACE Engineer Research and Development Center (ERDC). Although the HPC resources became available fairly late in the effort, they were

critical to completing the sets of computations presented below.

The suites of simulations performed provide useful insights into progressive collapse behavior for the types of buildings considered and provide a good basis for defining follow-on studies to address questions remaining after the current effort.

4.1 Design of Steel and Concrete Buildings

Three major types of building structural systems were designed:

1. Steel moment frame
2. Concrete moment frame using the joist slab variation
3. Concrete flat slab

All structural systems were designed using the following parameters:

- Designs based on International Building Code (IBC) 2006 using loads derived per American Society of Civil Engineers (ASCE) 7-05 requirements, based on a New York City location.
- Design load criteria.
 - Wind: 120 mph basic wind speed, Exposure B
 - Seismic parameters: $S_s = .362$, $S_1 = .06997$, $T_L = 6$ sec, Site class C
 - Snow load: 21 psf
 - Floor live load: 100 psf

- ❑ Roof live load: 30 psf
- ❑ Self-weight plus superimposed dead load
- ❑ Cladding for all systems is assumed to run along the perimeter of each floor and consists of glazing and precast concrete panels. The glazing⁵ is assumed to be an IGU with a makeup of 3/8" HS, 1" air gap, 1" TT.
- Building Geometry.
 - ❑ Classified as Regular, both in plan and elevation
 - ❑ 4 bays x 5 bays in plan
 - ❑ 5 stories
- Progressive Collapse hardening.
 - ❑ Progressive Collapse Design requirements for Occupancy Category II per Draft UFC 4-023-03, dated 1 October 2008 (steel frame and 25 ft bay concrete moment frame) or dated 14 July 2009 (flat slab and 32 ft bay concrete moment frame) [11] (Note that the UFC was finalized and officially adopted on 27 January 2010.)
 - ❑ Option 1: Tie Force and Enhanced Local Resistance of corner and penultimate columns
- All concrete sections are designed in accordance with ACI 318-05.
 - ❑ $f'_c = 4,000$ psi
 - ❑ $f_y = 60$ ksi
- For design purposes, all structural systems assumed pinned column to foundation connections.

4.1.1 Steel Moment Frame Building

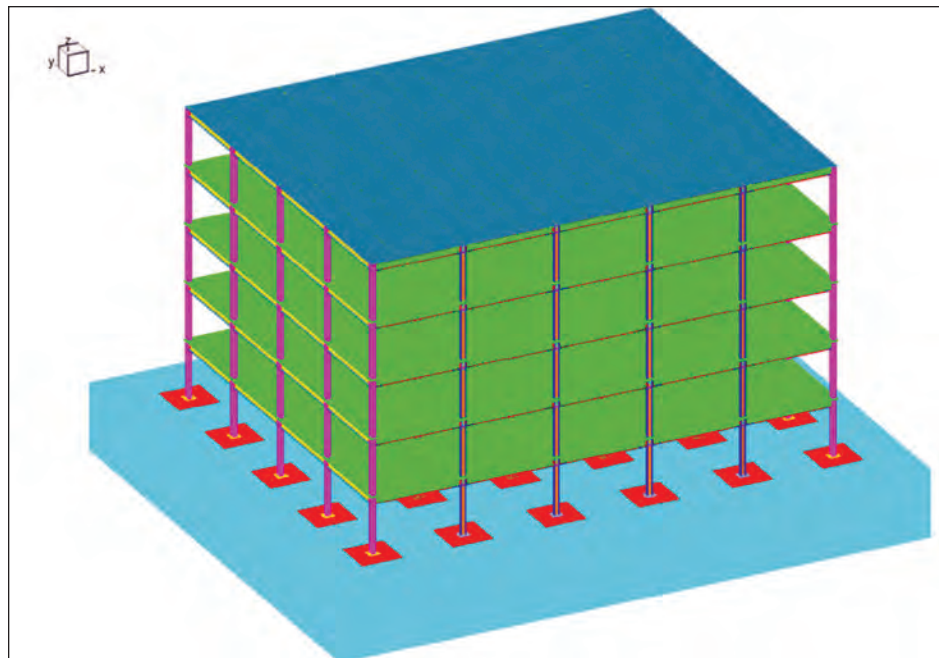
The steel frame building design developed for this effort is shown in Figure 20. The steel frame for this type of building provides support for the gravity loads and resistance to lateral loads simultaneously. For design purposes, this structural system is classified as a steel intermediate moment frame (IMF). The moment frames run in each perpendicular direction, along the building perimeter. This structural system was designed using STAAD-Pro structural design software.

⁵ Glazing types used in the models for calculation are: insulated glazing unit (IGU), heat strengthened glass (HS), and thermally tempered glass (TT).

Details specific to the design are:

- 25 ft bay spacing each way
- 14'- 8" between stories
- All gravity frame connections are assumed pinned
- All steel shapes use A992 steel, $F_y = 50$ ksi
- All floor slabs are poured concrete on a metal deck and function as rigid diaphragms
 - Floor decks are 2" deep, 22 gauge cold formed steel sections
 - Total slab depth is 5" (3" above top of deck)
- Floor slabs are supported by floor joists made composite with the concrete deck using shear studs
- The roof deck functions as a flexible diaphragm
 - 1.5" deep, 18 gauge metal deck

Figure 20:
Steel frame building (view
from above)



4.1.2 Concrete Moment Frame Building

Concrete frames support the gravity loads and provide resistance to lateral loads simultaneously. The concrete moment frame design developed for this effort is shown in Figure 21. For design purposes, this structural system is classified as concrete intermediate moment frames (IMF).

The moment frames in the long direction run along the building's exterior gridlines. Frames in the short direction run along all major gridlines. Floor beams (or joists) span the frames in the short direction to support the floor slab. Similar to the steel moment frame system, story height is 14'- 8" for all stories. STAAD-Pro was also used in the design of this system.

Two separate designs were performed for this structure type, one with 25 ft bays in both directions, and the other with 32 ft bays in both directions.

Details specific to the design with 25 ft bay spacing are as follows:

- Floor slab is 5" thick
- Floor beams are tapered, pan-formed concrete joists 8" wide at the bottom by 15" deep (not including slab depth), set at 8'- 4" on center
- Moment frame girders are 18" wide by 24" deep (not including slab)
- All columns are 27"x27"

Details specific to the design with 32 ft bay spacing:

- Floor slab is 5-1/2" thick
- Floor beams are concrete joists 10" wide by 18" deep (not including slab depth), set at 10'-8" on center
- Moment frame girders are 18" wide by 26" deep (not including slab)
- All columns are 26"x26"

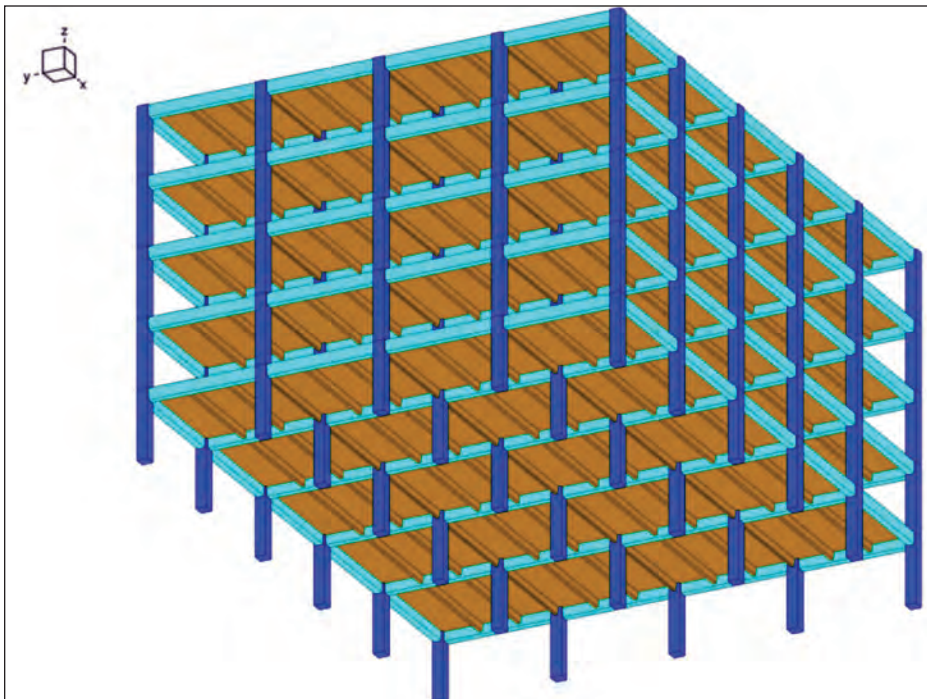


Figure 21:
Concrete moment frame
building with joist slabs (view
from below)

4.1.3 Concrete Flat Slab Building

Reinforced concrete flat slab buildings use a structural system consisting of concrete columns directly supporting the floor slab. When drop panels are used at the columns to resist punching shear, the system is referred to as a flat slab, as opposed to a flat plate where drop panels are not used. Gravity loads are supported by two-way action of the slab and then transferred to the columns. For detailing purposes, the slab is divided into column strips and middle strips, and reinforcement is specified by the number of bars within the strips. Column strips are the widths of slab along the column gridlines, having an effective width equal to half the bay length. Middle strips are the slab strips bounded by the column strips. The lateral load-resisting system can be designed a variety of ways. For this project, the lateral load-resisting system uses moment frame action where the moment frame consists of the columns and the slab. The slab spanning the columns acts as a thin, wide beam. The concrete moment frame design developed for this effort is shown in Figure 22. This particular structural system was designed using E-TABS. The slabs were designed using SAFE.

Details specific to this design are:

- 25 ft bay spacing in each perpendicular direction.
- 1st story is a 15' tall story, all other stories are 12'
- Slab reinforcement is the same in both directions
- Exterior columns are 22"x22"
- Interior columns are 24"x24"
- Slab and drop panel thicknesses (in addition to slab):
 - Stories 1 through 4
 - 12" slab
 - Exterior columns: 8" drop panels
 - Interior columns: 4-1/4" drop panels
 - Roof
 - 9-1/2" slab
 - Exterior columns: 6-1/4" drop panels
 - Interior columns: 4-1/4" drop panels

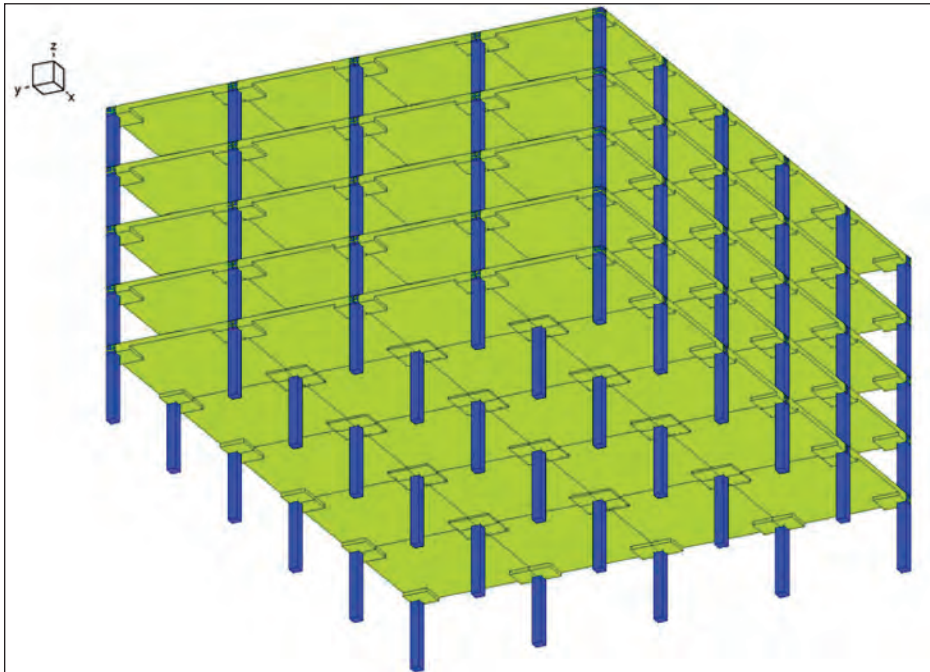


Figure 22:
Reinforced concrete flat slab
building (view from below)

4.2 Progressive Collapse Study of Steel Moment Frame Structures

A progressive collapse analysis was performed to study the performance of a steel perimeter moment frame structure under the loss of one exterior column. The building has five bays in the long direction, four bays in the short direction and five stories. The floor systems consist of steel wide flange beams and a composite steel deck with concrete topping. The roof consists of a metal deck supported by open web steel joists. Structural design of each building is presented in the preceding section. Figure 23 shows the NLFlex model of the entire steel building. All members, floors, foundation, and connections were modeled explicitly. Cladding was not modeled, but a uniform cladding load was applied to all perimeter beams. Figure 24 shows a plan view of the moment connection designations, while Figures 25 and 26 show the actual NLFlex modeling of the connections. Figure 27 shows a view of the floor and roof deck in the NLFlex model. Figure 28 shows a view of the corner column and beams framing into it. Figure 29 shows a view of the floor beams and associated connections. Figure 30 shows two miscellaneous views.

All progressive collapse analyses were performed in two consecutive phases: a static phase under the dead load (or percentage of the dead load) and a percentage of the live load followed by a dynamic phase that

includes initial damage in the structure. The scenario considered for the initial damage is removal of the first floor corner column. Two load combinations were considered. The first one, as specified by the GSA, is 100% of the entire dead load plus 25% of the live load. The second load combination, as specified by the UFC, is 120% of the entire dead load plus 50% of the live load.

Figure 23:
NLFlex model, steel building
with perimeter moment frames
(decks not shown)

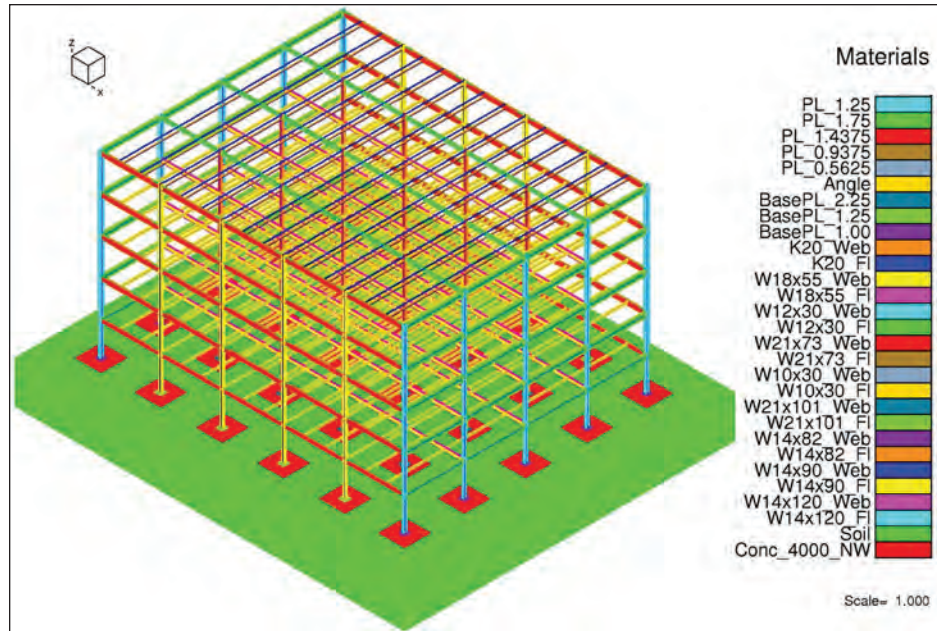
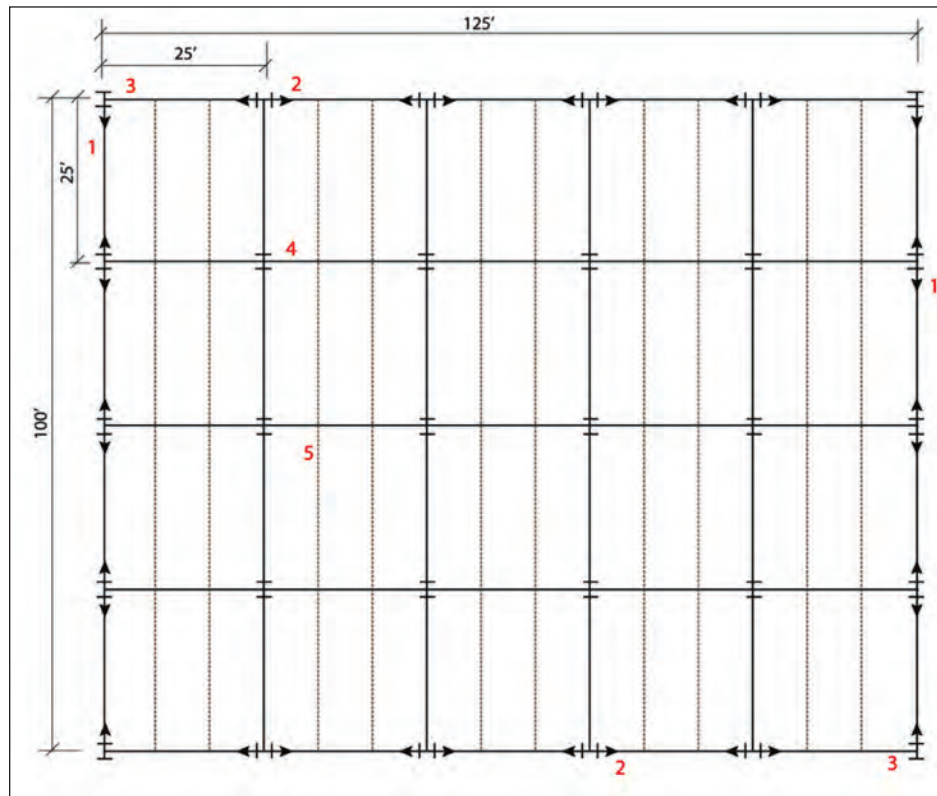


Figure 24:
Plan view of moment
connection designations



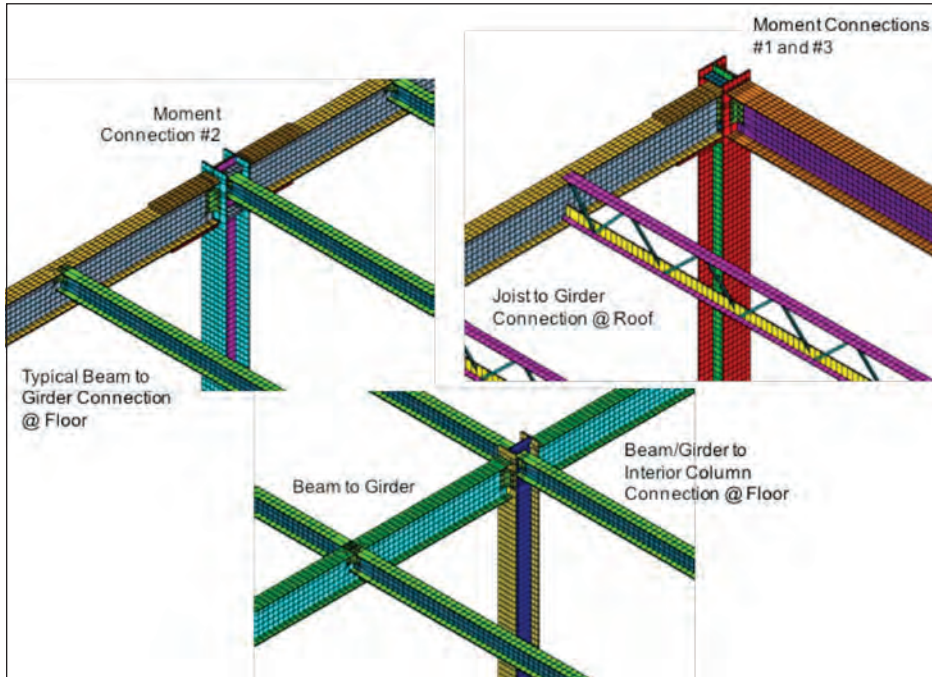


Figure 25:
Flex model connections

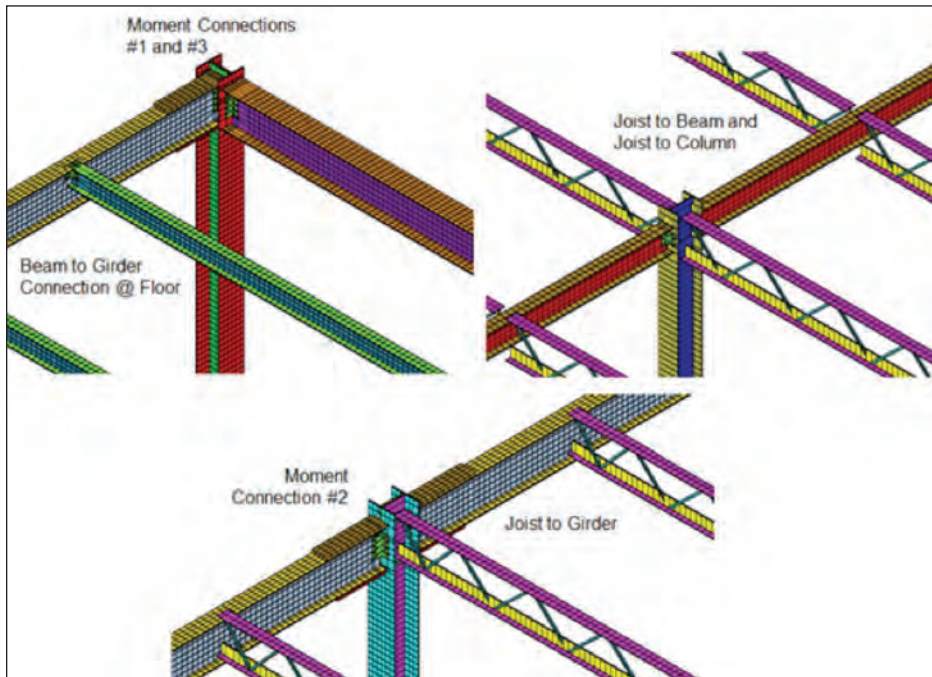


Figure 26:
Flex model connections
(continued)

Figure 27:
View of floor and roof decks
(concrete not shown)

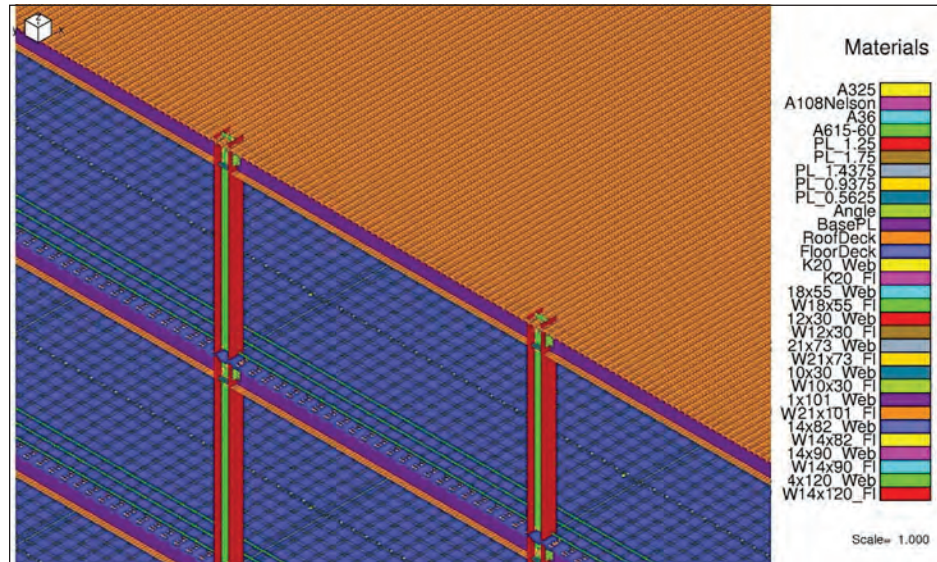
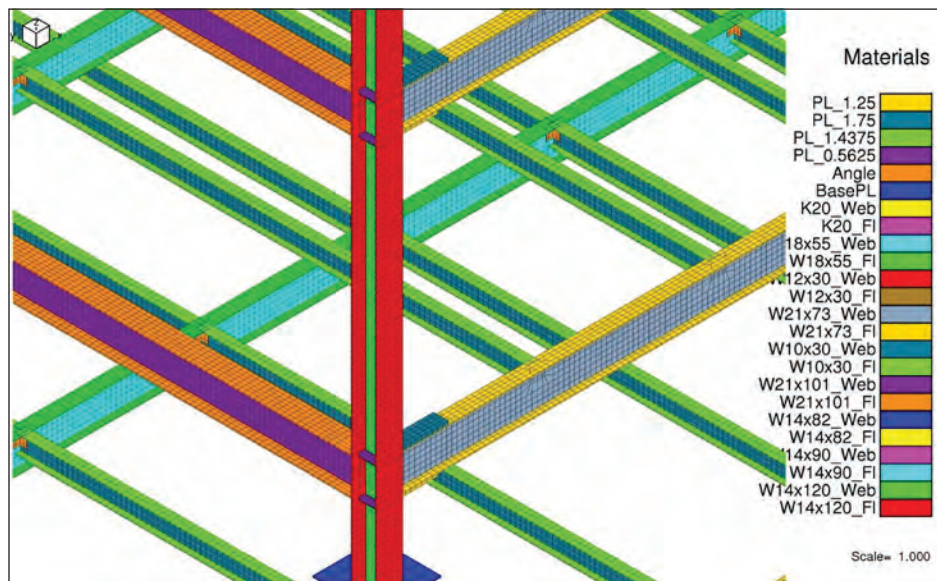


Figure 28:
View of corner column and
beams



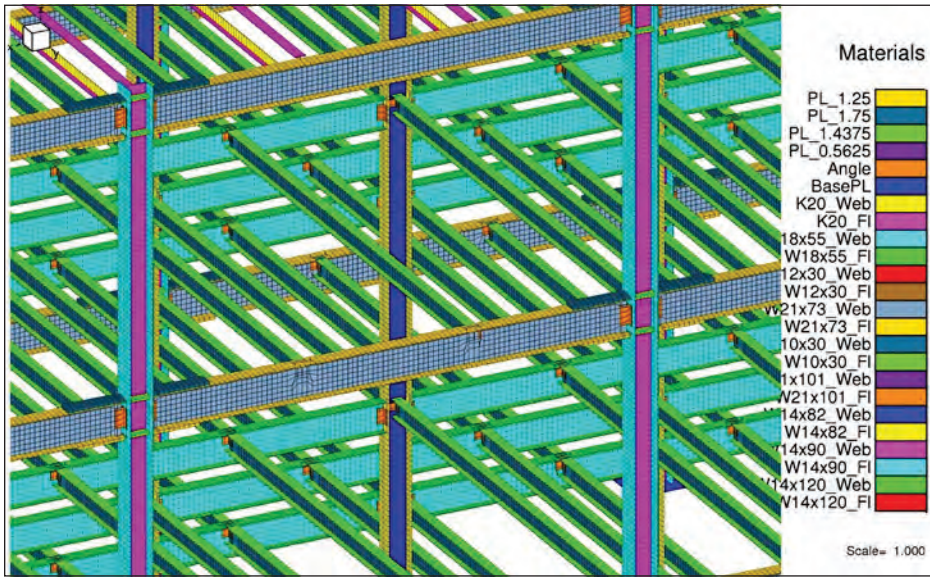


Figure 29:
View of floor beams and
girders

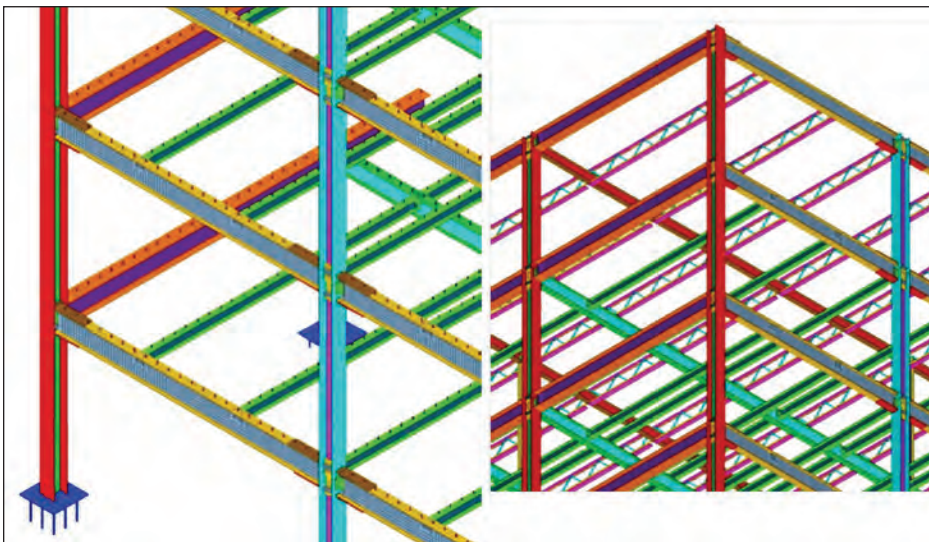


Figure 30:
View of corner framing, and
roof framing

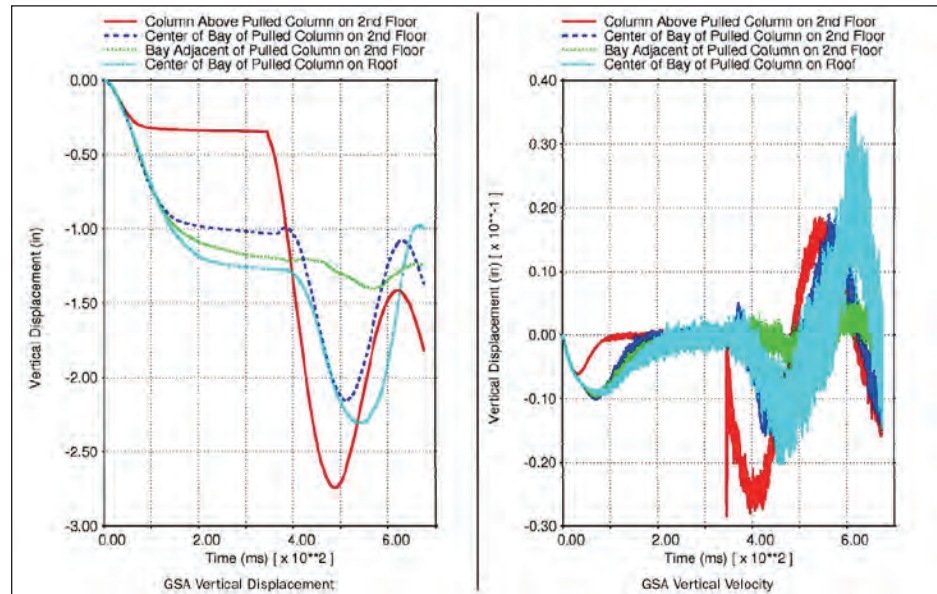
4.2.1 Corner Column Removal

The progressive collapse analysis of the steel building is performed under the corner column removal. Analyses are performed under both the GSA and UFC load combinations. Displacements and velocities at different locations of beams, columns, and slabs are recorded to monitor the behavior of the structure. Figures 46 and 47 show the time histories of the vertical displacement and velocity at locations above the removed column for the GSA and UFC load combinations, respectively. Figure 48 shows a comparison of response between the two load combinations. As shown in these figures, upon removal of the corner column the floors above this column experience a relatively small

plastic deformation even under the highest live load level. As such, removal of the corner column does not trigger a disproportionate collapse of the building under the two load combinations examined.

The snapshot of the maximum vertical displacements under the GSA and UFC load combinations, are shown in Figures 34 and 35, respectively. Figures 36 and 37 show snapshots of the concrete damage at the end of analysis under the two load combinations. Also, Figures 38 and 39 show snapshots of the strains in the steel under the two load combinations. As shown in the figures, steel strains and concrete damage are mainly limited to the members and slabs on floor levels directly above the removed column, which is consistent with the displacements levels observed after the column removal.

Figure 31:
Vertical displacement and velocity under GSA load combination



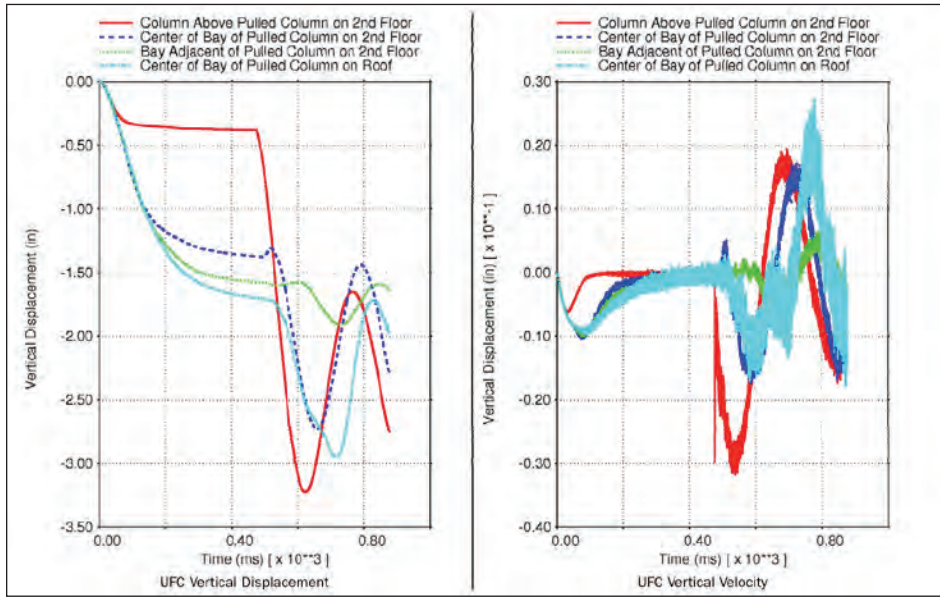


Figure 32:
Vertical displacement and velocity under UFC load combination

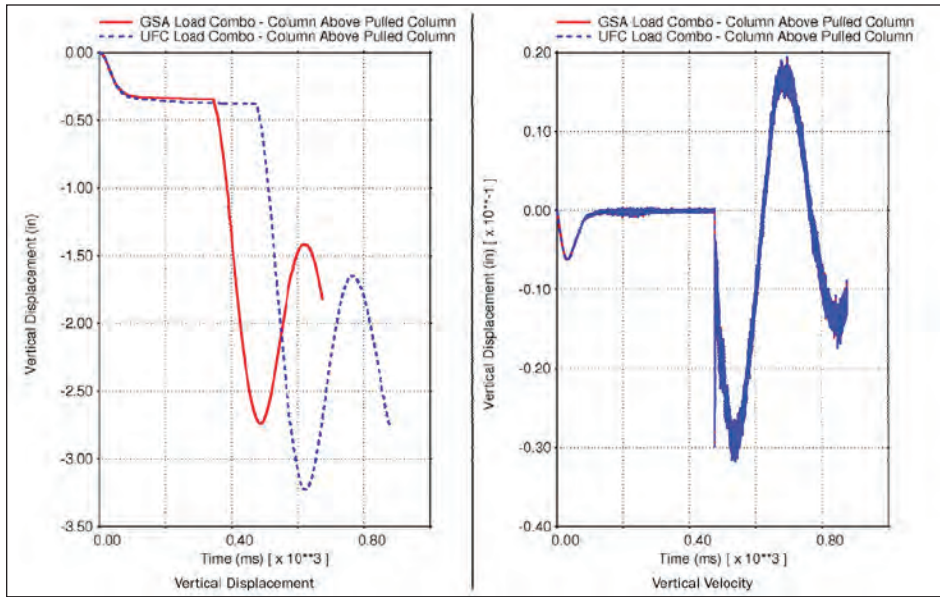


Figure 33:
Comparison of vertical response between GSA and UFC load combinations

Figure 34:
Maximum vertical displacement
(in), GSA load combination

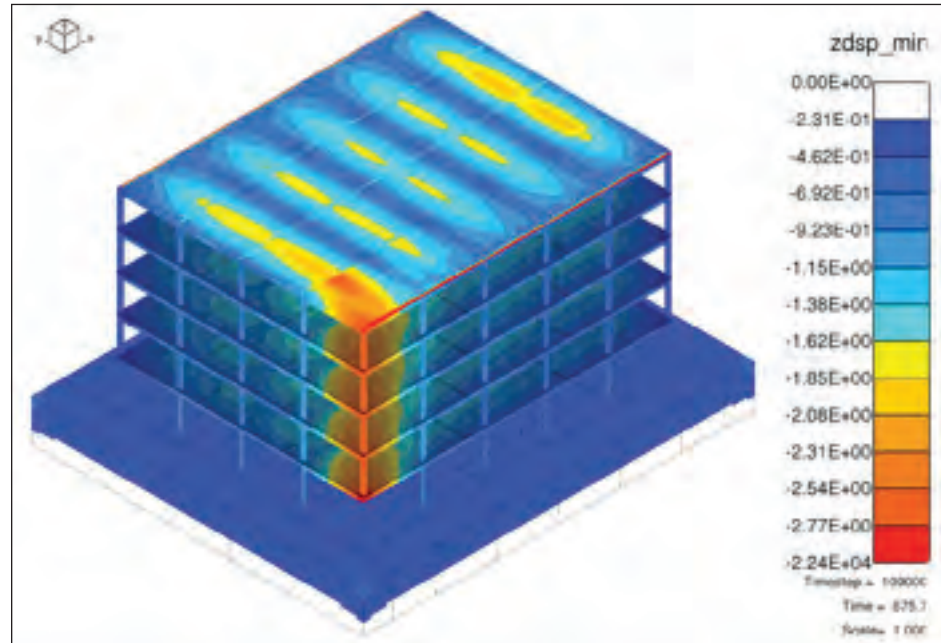
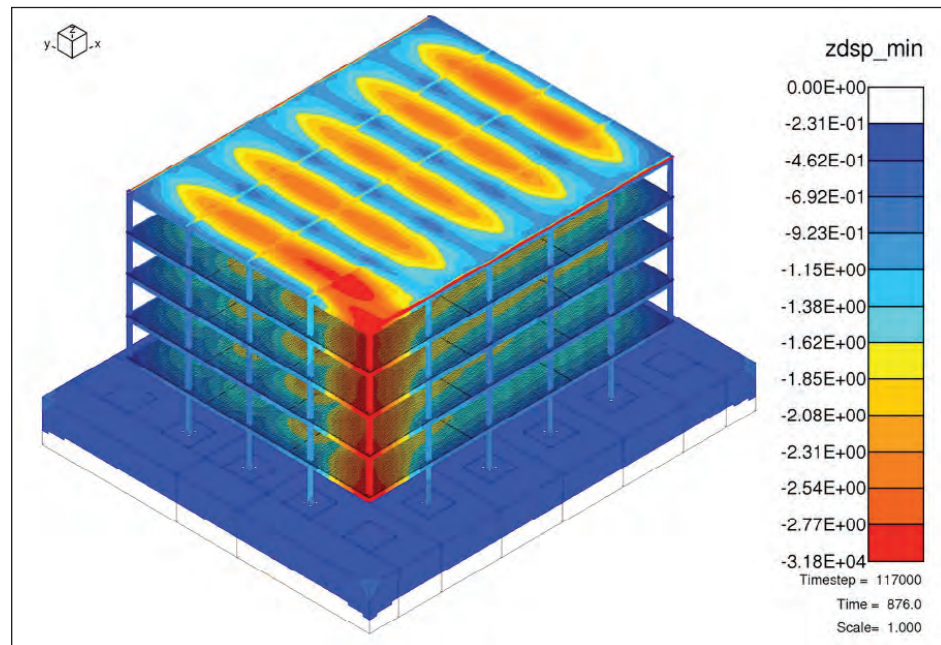


Figure 35:
Maximum vertical displacement
(in), UFC load combination



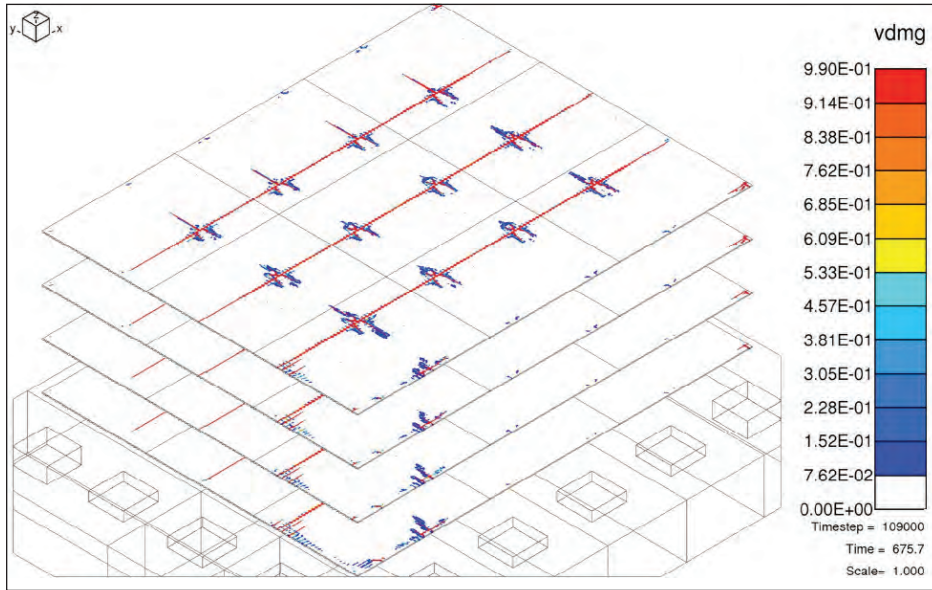


Figure 36:
Concrete damage, GSA load combination

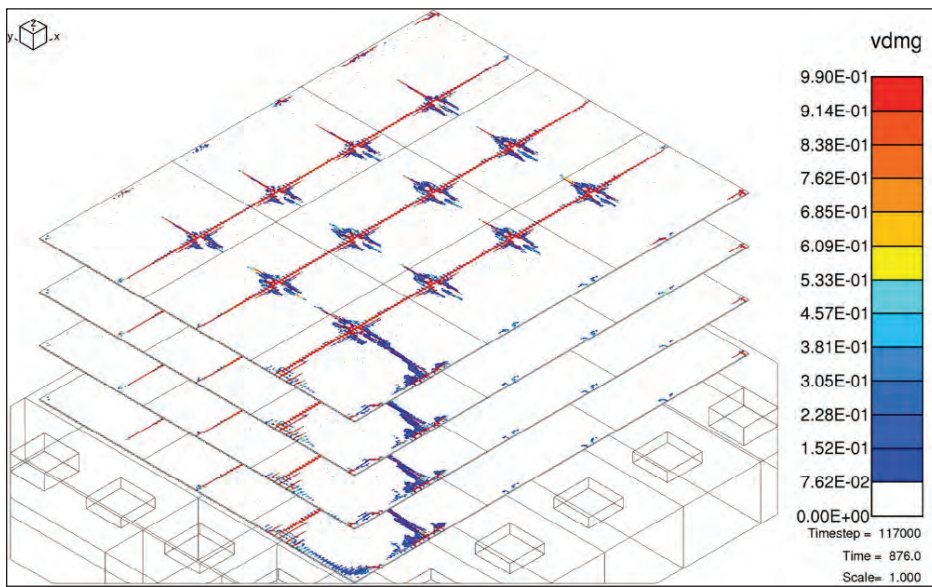


Figure 37:
Concrete damage, UFC load combination

Figure 38:
Steel strains, GSA load
combination

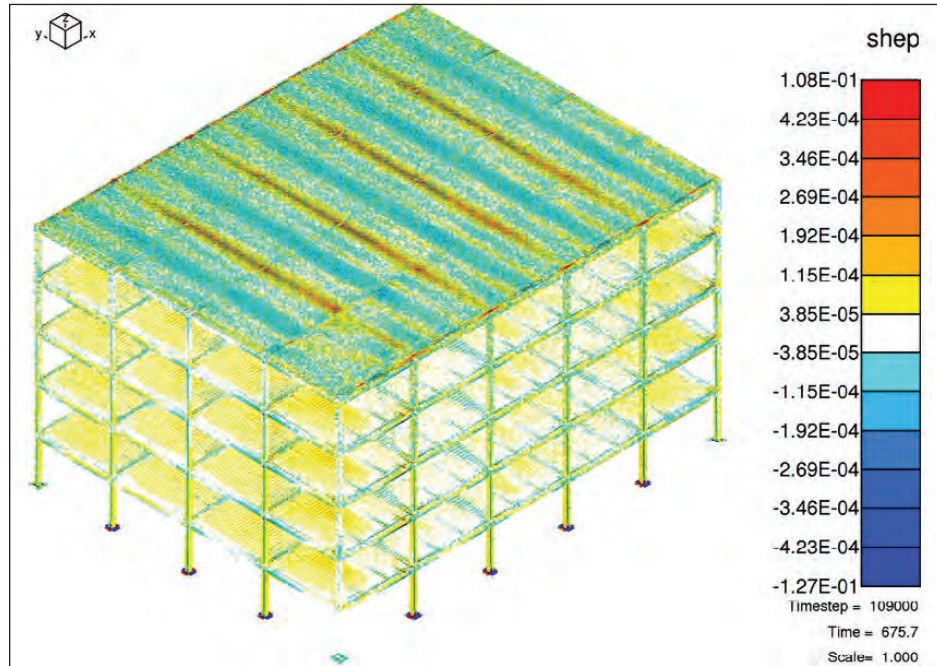
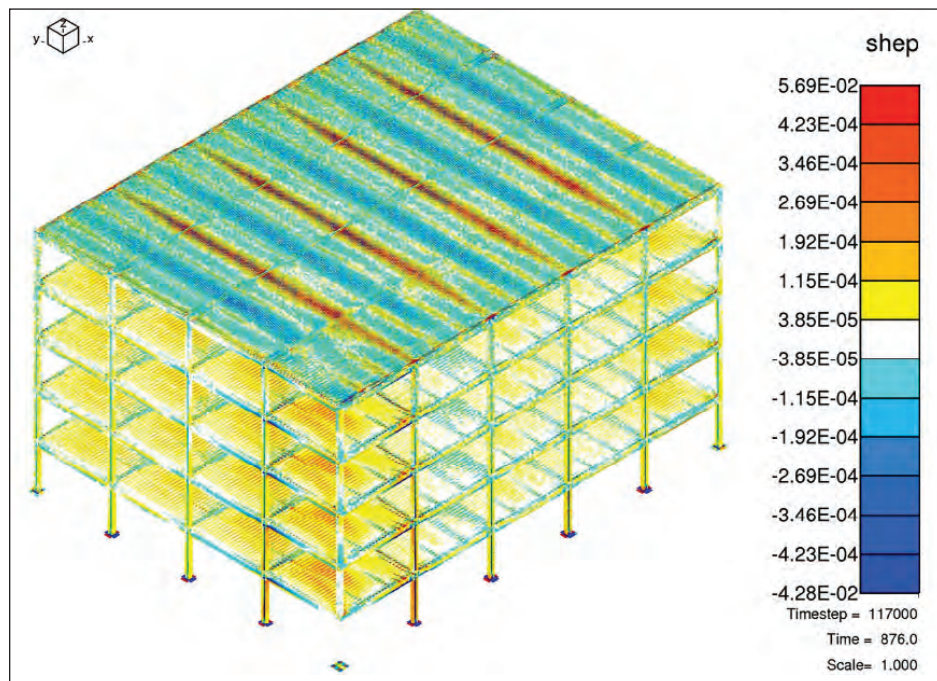


Figure 39:
Steel strains, UFC load
combination



4.2.2 Removal of Two Columns

In addition to removing one corner column, the progressive collapse analysis of the steel building is performed with the penultimate column and the corner column simultaneously removed. The analysis is performed using the standard GSA load combination. As before, displacements and velocities at different locations of beams, columns, and slabs are recorded to monitor the behavior of the structure. Figure 40 shows the time histories of the vertical displacement and velocity at locations above the removed column. As shown in this figure, upon removal of the corner and adjacent columns, the floors and columns above experience a large deformation, but start to rebound. As such, removal of the corner and penultimate columns does not trigger a disproportionate collapse of the building.

The snapshot of the maximum vertical displacements for a portion of the building is shown in Figure 41. Figure 42 shows the snapshot of the concrete damage at the end of analysis, and Figure 43 shows the snapshot of the strain in the steel. As shown in these figures, steel strains and concrete damage are mainly limited to the members and slabs on floor levels directly above the removed column, which is consistent with the displacements levels observed after the column removal.

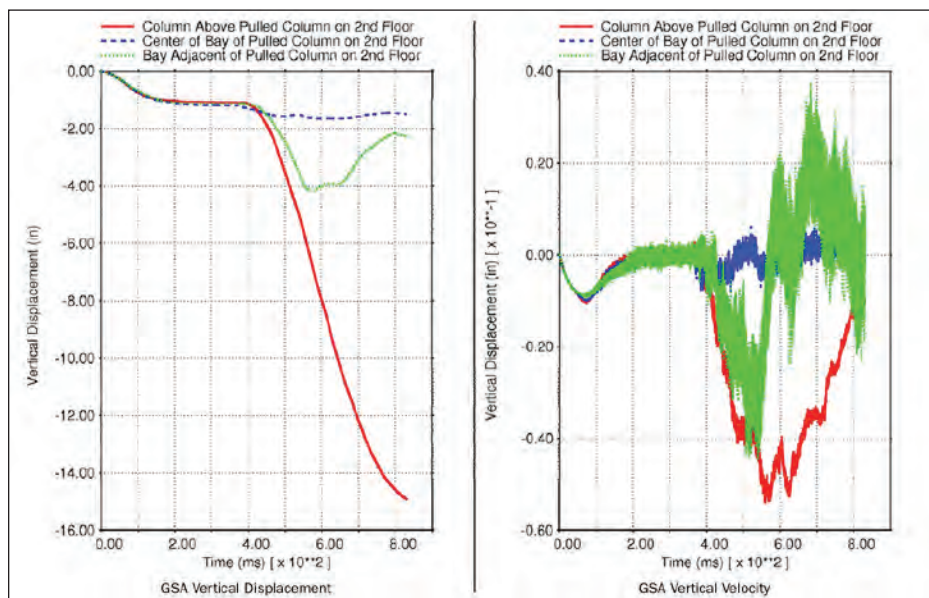


Figure 40:
Vertical displacement and
velocity, two columns removed

Figure 41:
Partial view of maximum vertical displacement (in), two columns removed

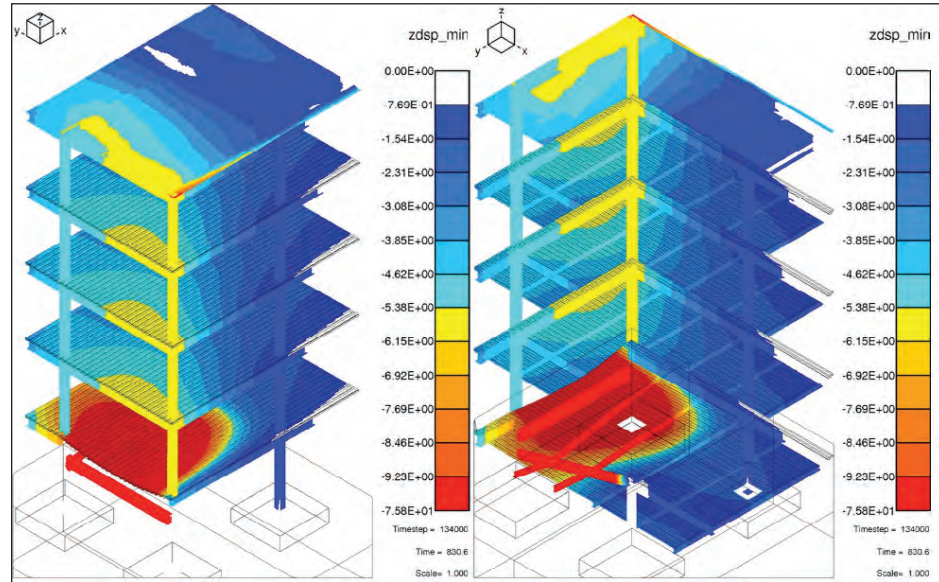
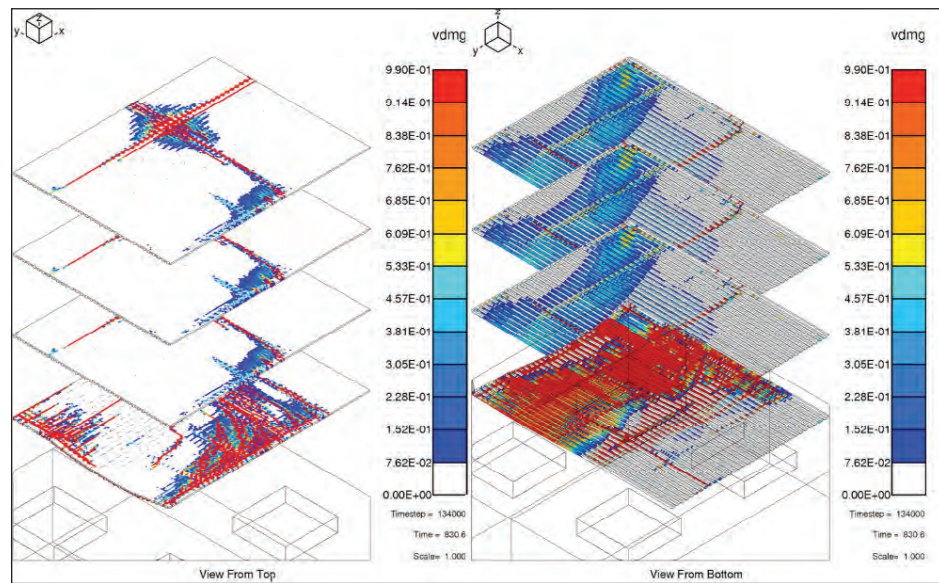


Figure 42:
Partial view of concrete damage, two columns removed



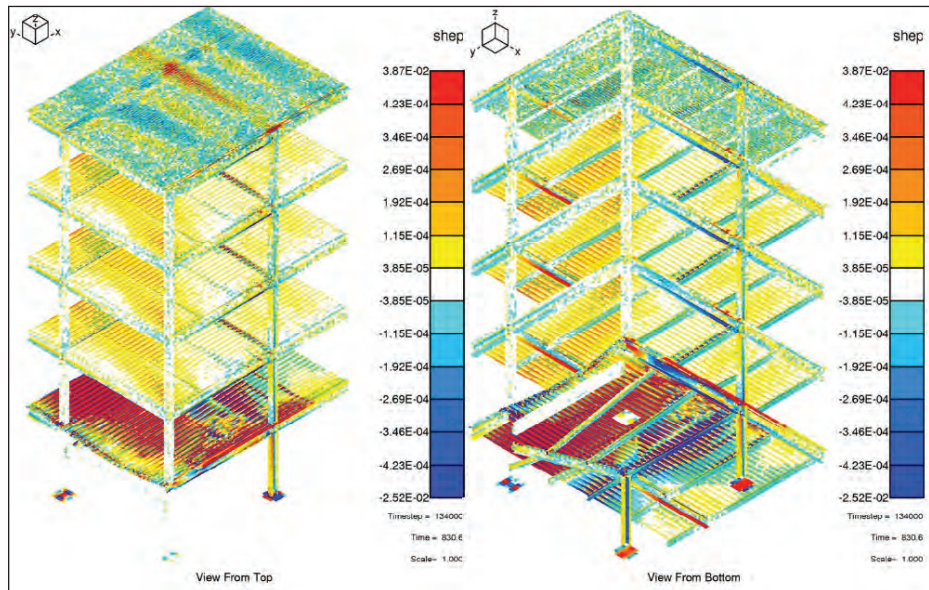


Figure 43:
Partial view of steel strains,
two columns removed

4.2.3 Summary of Results and Findings

A summary of progressive collapse analyses performed under this study for steel moment frame buildings is presented here. Two column removal scenarios were analyzed: a single corner column removal or a corner column and penultimate column removed simultaneously. When a single corner column is removed, no failure was observed in any component of the structure. When a corner column and penultimate column were removed simultaneously, some beams directly supported by the removed columns failed. Regardless of this local beam failure, no progression of collapse was seen.

4.3 Progressive Collapse Study of Reinforced Concrete Structures

A series of progressive collapse analyses were also performed to study the performance of reinforced concrete structures under the loss of one or two exterior columns. This study is focused on concrete buildings with two different types of floor systems. The first system consists of reinforced concrete moment frames in one direction and one-way joist slab floors in the other direction (normal to the moment frames). The floor design also includes spandrel beams around the building in all floor levels. The second system consists of flat slab floors with drop panels and no spandrel beams. Each building has five bays in the long direction, four bays in the short direction, and five stories.

The structural design of each building, as presented in the preceding section, consists of a baseline design and an enhanced design. The baseline design is developed to resist only the conventional loads on the structure including the seismic and wind loads, while the enhanced design is developed to meet the progressive collapse design requirements of UFC as well. [11] Comparison of performance of baseline and enhanced designs in progressive collapse can provide useful information on the effectiveness of the UFC design.

All progressive collapse analyses were performed in two consecutive phases: a static phase under the dead load and a percentage of the live load followed by a dynamic phase that includes initial damage in the structure. Two scenarios are considered for the initial damage: (a) removal of the first floor corner column and (b) simultaneous removal of the first floor corner and penultimate columns. Results of progressive collapse analyses for each building type are presented and discussed in the following.

4.3.1 Moment Frames with Joist Slabs

For the purpose of this study, two moment frame systems with different bay sizes of 25 ft and 32 ft are considered. Although this level of bay size variation provides some useful information for progressive collapse study, more extensive analyses with more bay size variations would contribute to investigation of the response sensitivity to the bay size variations.

4.3.1.1 Joist Slab System with 32 ft Bay Size

Figures 44 and 45 show the top and bottom views of the NLFlex model of the reinforced concrete moment frame system with one-way joist slab floors and 32 ft bay size, respectively. To reduce the size of the model and the run time, only the first two and a half bays of the building are modeled in each direction. In addition to the fixities at buildings base, appropriate boundary conditions are provided on all floor levels to maintain structural continuity and compatibility conditions at border lines where the modeled structure meets the rest of the structure. Three columns identified as C1, C2, and C3 in Figure 44 are selected as target initiator components whose failure may trigger the propagation of failure to the surrounding structure.

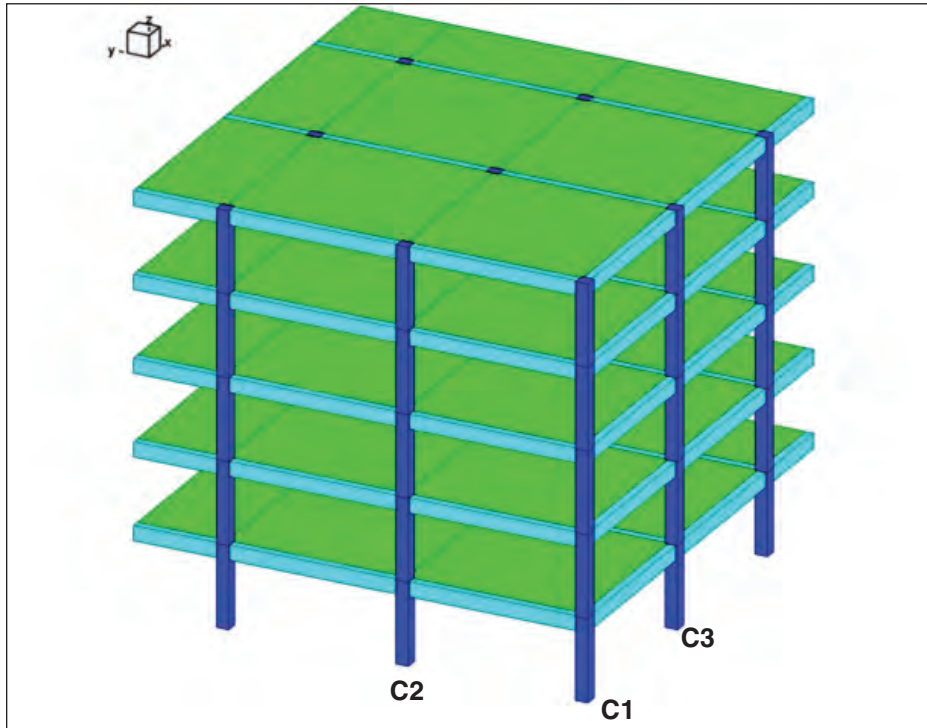


Figure 44:
NLFlex model, reinforced
concrete moment frame with
joist slab, top view

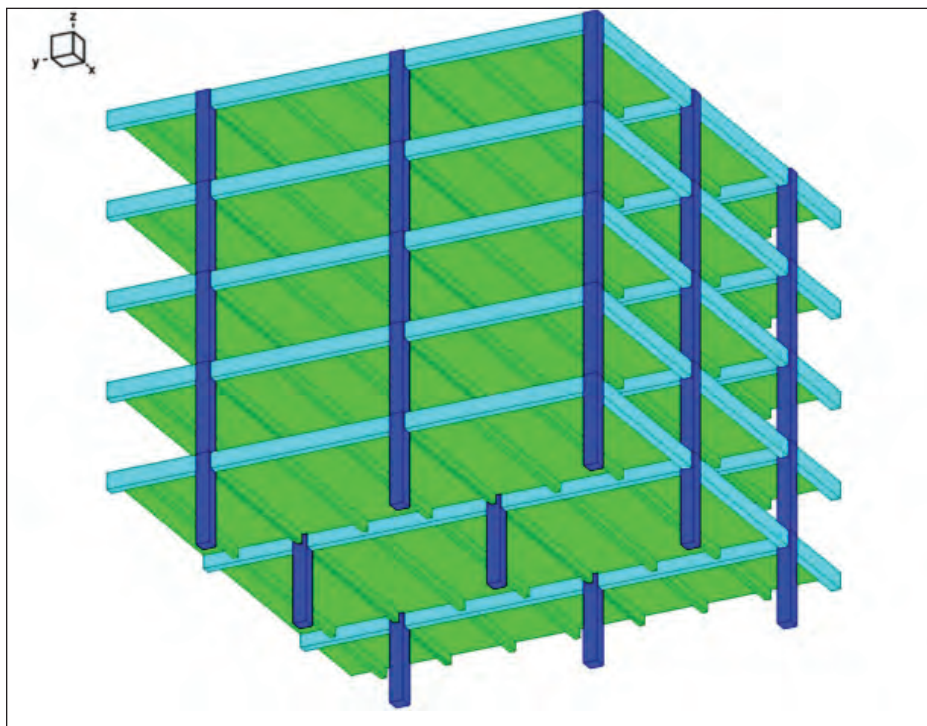


Figure 45:
Flex model, reinforced concrete
moment frame with joist slab,
bottom view

4.3.1.1.1 Single Column Removal

The first set of progressive collapse analyses of the enhanced moment frame structure is performed assuming the removal of the corner column (column C1). Analyses are performed under 25%, 50%, 75%, and 100% of the live load intensity. Velocities and displacements at different locations of all beams, columns, and slabs are recorded to monitor the behavior of the structure. Figures 46 and 47 show the time histories of the vertical velocity and vertical displacement of the top of the building at a location above the removed column for all live load levels, respectively. As shown in these figures, upon removal of the corner column C1 the floors above this column experience a relatively small plastic deformation even under the highest live load level. As such, removal of column C1 does not trigger a disproportionate collapse of the building under any percentage of the live load.

The top and bottom view snapshots of the vertical displacements of the structure at the end of analysis under the 100% live load are shown in Figures 48 and 49, respectively. Also Figures 50 and 51 show the top and bottom view snapshots of the concrete damage at the end of analysis under the 100% live load. As shown in the figures, concrete damage is mainly limited to the beams and slabs on floor levels directly above the removed column, which is consistent with the displacement magnitudes observed after the column removal.

To investigate the effectiveness of the UFC design criteria, the baseline design of the building is also analyzed under the column C1 removal scenario. Figures 52 and 53 compare the time histories of the vertical velocity and vertical displacement of the baseline and enhanced designs at the top of the building at a location directly above the removed column, respectively, under the 100% live load. According to these results, the baseline design experiences only a slightly larger displacement than the enhanced design when column C1 is removed. Therefore, removal of the corner column in the baseline design does not trigger a progressive collapse.

The small difference observed in the responses of the baseline design and the enhanced design is discussed in the following. In general, the enhanced design requires some additional rebar in the form of internal tie (longitudinal and transverse) and peripheral tie on each floor, vertical tie for each column, and additional stirrups for the corner and penultimate perimeter columns at the first floor above grade to enhance their local resistance. In the current building, the enhanced design did not require any additional rebar to provide the required longitudinal and transverse tie resistance. As the progressive collapse design can

take advantage of the existing reinforcement in the structure, the slab rebar in the baseline design was adequate to act as longitudinal and transverse ties. As such, the only additional rebar for floor enhancement is the peripheral tie parallel to the floor edges (3 #8 for 1st to 4th floors and 3 #7 for the roof). This additional rebar slightly reduces the floor deflections of the enhanced design versus the baseline design under the single column removal scenario. Column enhancement does not make a difference in the current mode of deformation.

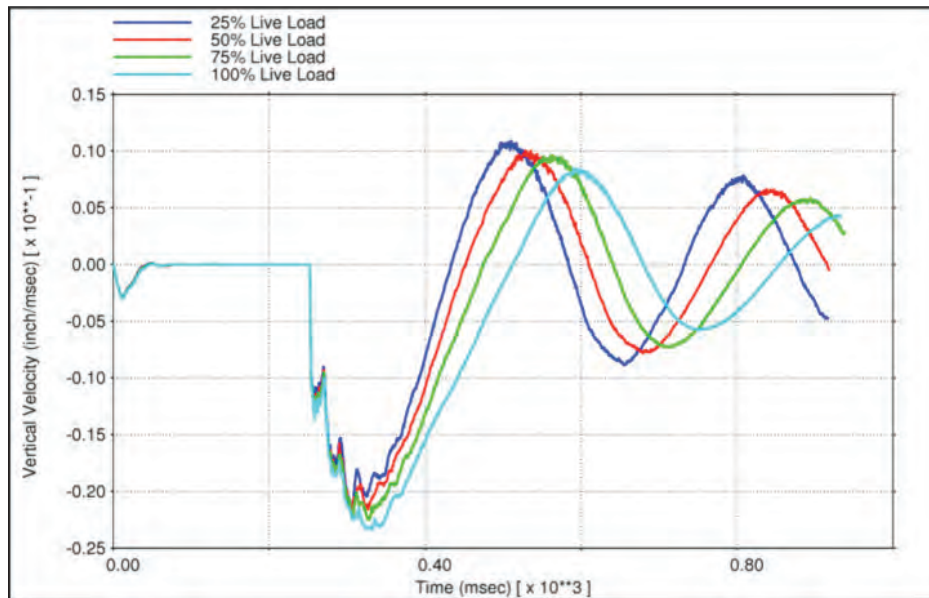


Figure 46:
Vertical velocity, column C1
removal under different live
loads

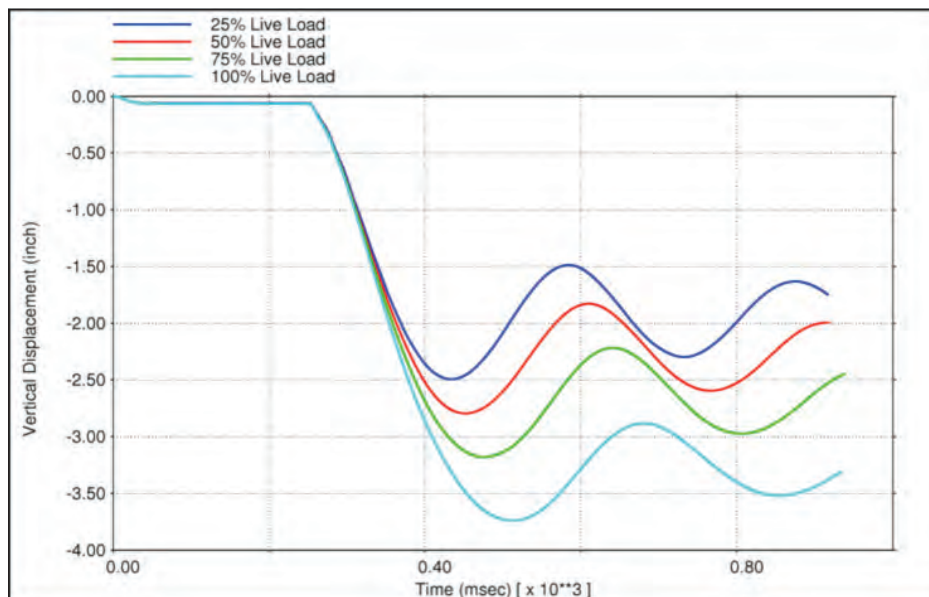


Figure 47:
Vertical displacement, column
C1 removal under different live
loads

Figure 48:
Vertical displacement (in),
column C1 removal, 100% live
load, top view

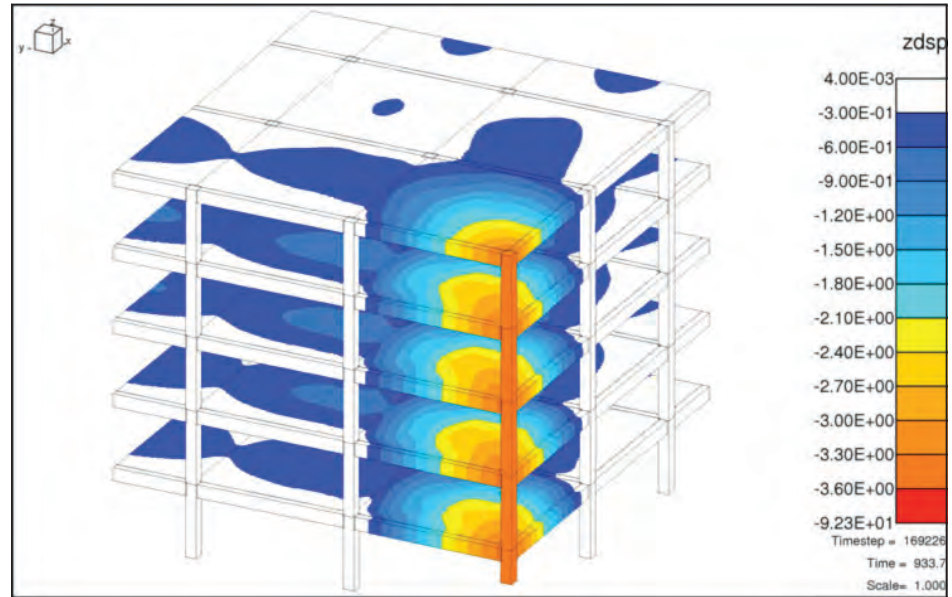
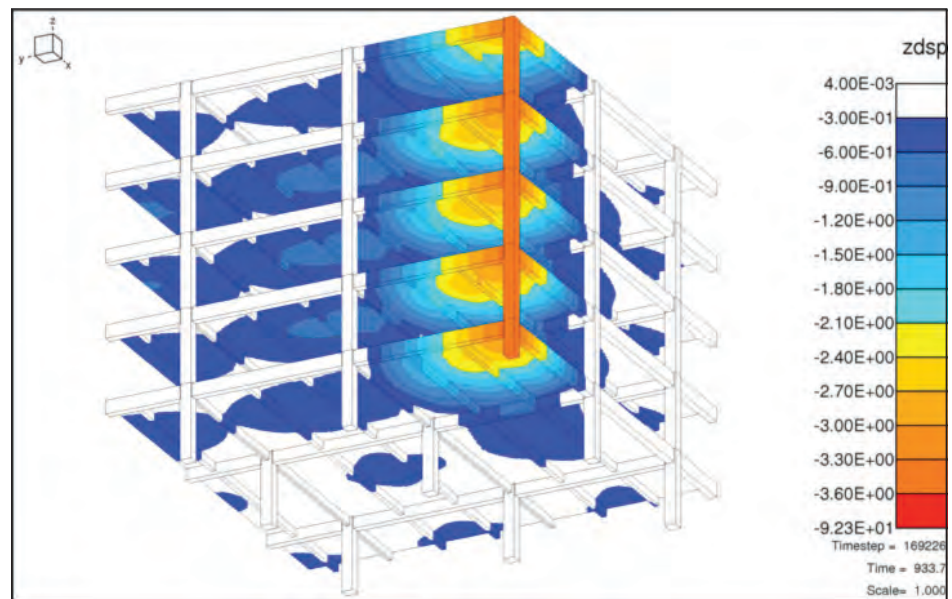


Figure 49:
Vertical displacement (in),
column C1 removal, 100% live
load, bottom view



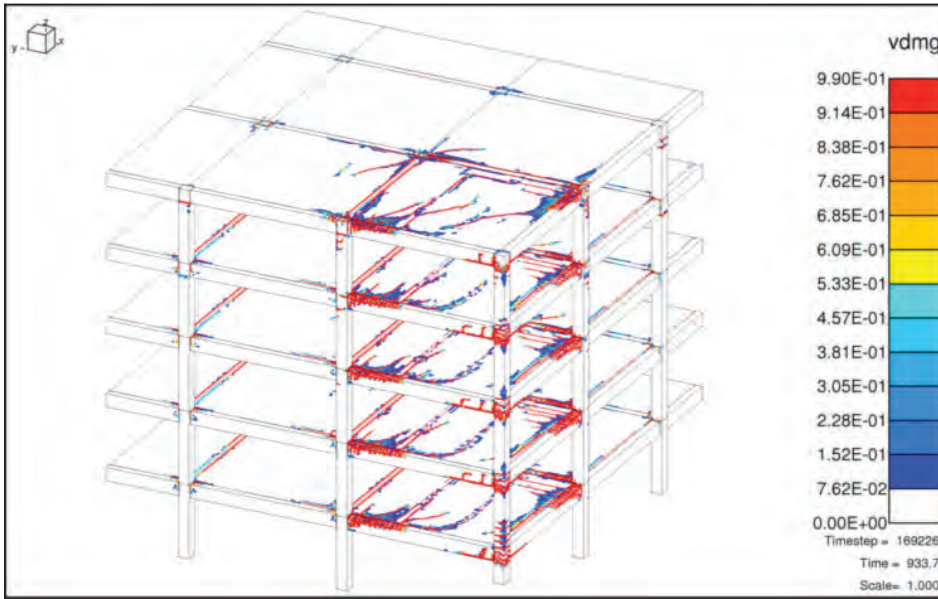


Figure 50:
Concrete damage, column C1
removal, 100% live load, top
view

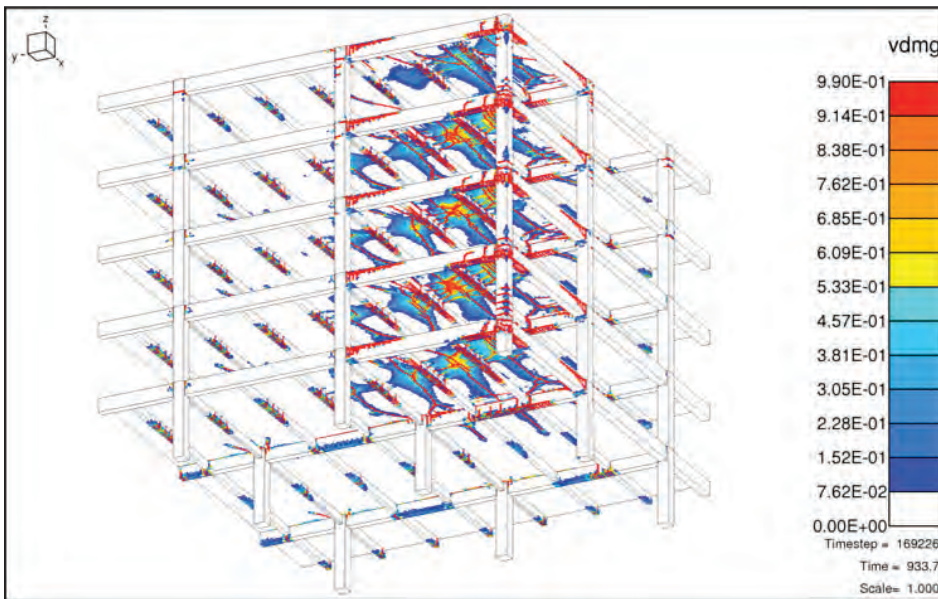


Figure 51:
Concrete damage, column
C1 removal, 100% live load,
bottom view

Figure 52:
Vertical velocity, column C1
removal, 100% live load

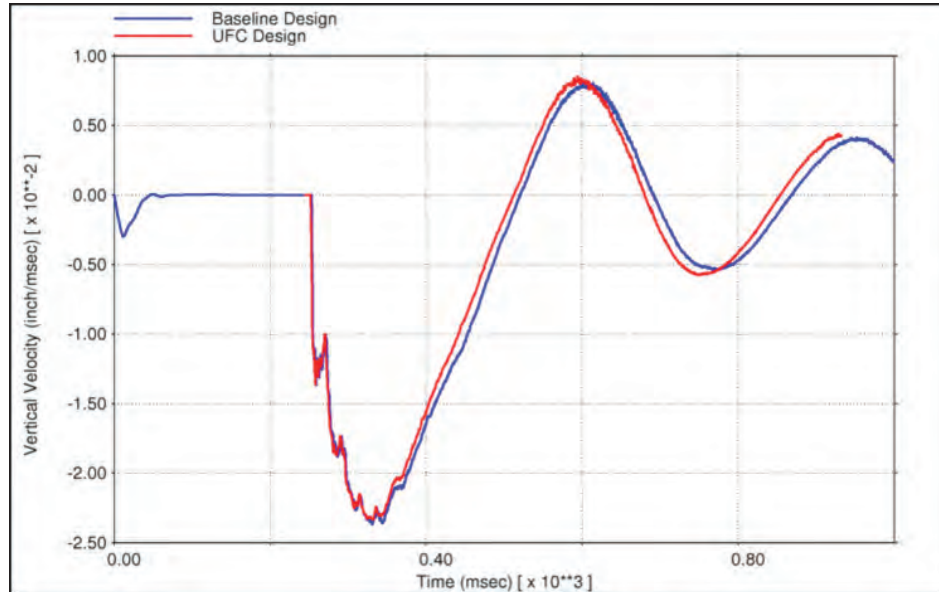
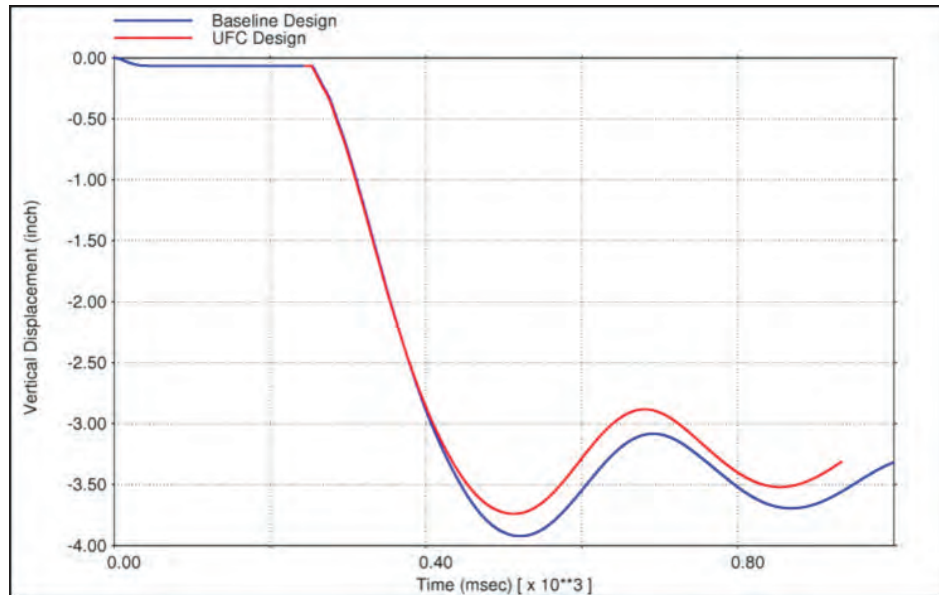


Figure 53:
Vertical displacement, column
C1 removal, 100% live load



4.3.1.1.2 Two Columns Removal

The reinforced concrete moment frame with one-way joist slab floor system does not have a symmetric design. As such, simultaneous removal of columns C1 and C2 may result in a different response than the simultaneous removal of columns C1 and C3. To determine which column removal scenario is more critical, both scenarios are investigated under 100% live load. Figure 54 shows a snapshot of the vertical displacements of the enhanced moment frame structure under simultaneous removal of columns C1 and C2. Similarly, Figure 55 provides a snapshot of the vertical displacements of the structure

under simultaneous removal of columns C1 and C3. The time histories of vertical velocity and vertical displacement at the top of the building at a location above the column C1 are presented in Figures 56 and 57, respectively. Although both scenarios have resulted in large floor deflections and slab failure above the removed columns, the simultaneous removal of columns C1 and C2 is slightly more critical than the simultaneous removal of columns C1 and C3. Therefore, all progressive collapse studies of moment frame with joist slab floors under two columns removal scenario are performed by removing columns C1 and C2.

Progressive collapse analyses of the enhanced moment frame structure under C1-C2 columns removal are performed for 25%, 50%, 75%, and 100% live loads. Figures 58 and 59 show the time histories of the vertical velocity and vertical displacement of the top of the building at the location above the corner column for all live load levels. Figures 60 and 61 show the concrete damage at the end of analysis under 100% live load. As shown in these figures, simultaneous removal of columns C1 and C2 results in failure of slabs and spandrel beams on all floors above the removed columns even under the smallest live load level considered in this study. Simultaneous removal of columns C1 and C2, however, does not lead to the horizontal propagation of damage to adjacent columns and bays. This indicates that the columns adjacent to the removed columns are strong enough to carry the additional loads originally transferred by the columns C1 and C2 under the 100% live load.

Similar behavior was observed for the baseline design. Slabs and spandrel beams on all floors above the removed columns failed even under the smallest live load level. This behavior was expected, as all floors above the removed columns of the enhanced design also failed under the lowest live load. No horizontal propagation of damage to adjacent columns and bays was observed for the baseline design even under the highest live load level. In general, no significant improvement was observed in the performance of the enhanced design compared to the baseline design.

Figure 54:
Vertical displacement (in),
C1-C2 columns removal under
100% live load

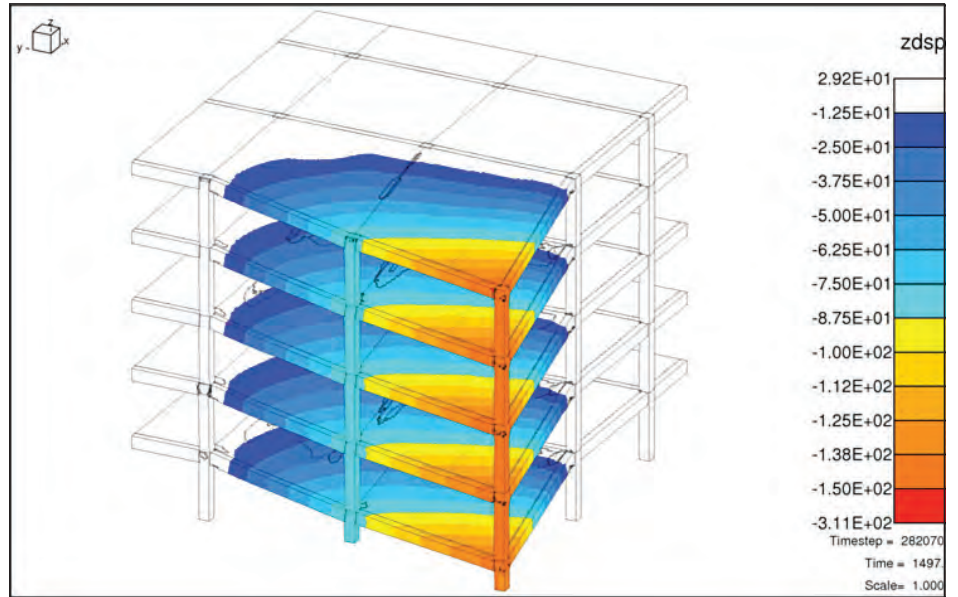
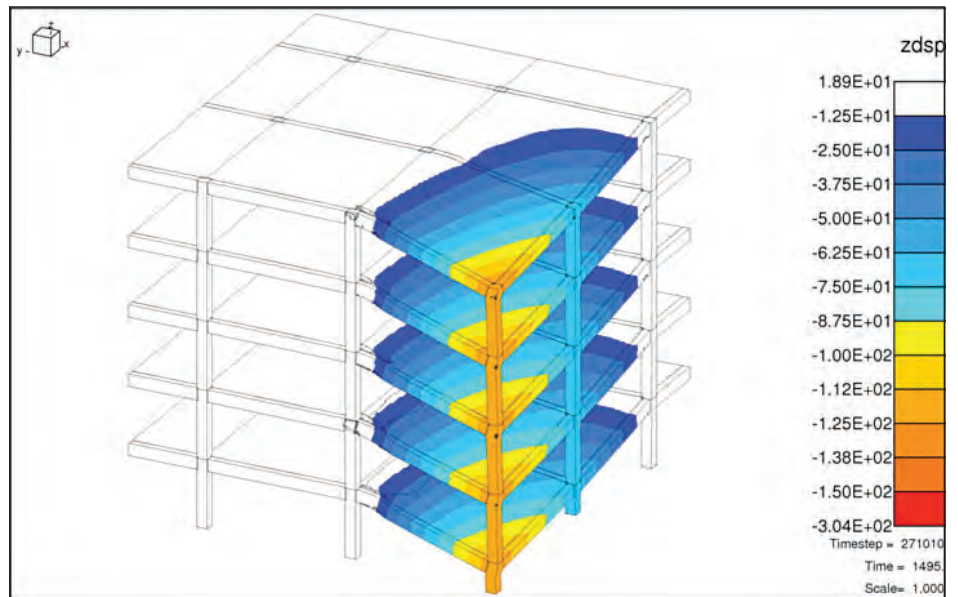


Figure 55:
Vertical displacement (in),
C1-C3 columns removal under
100% live load



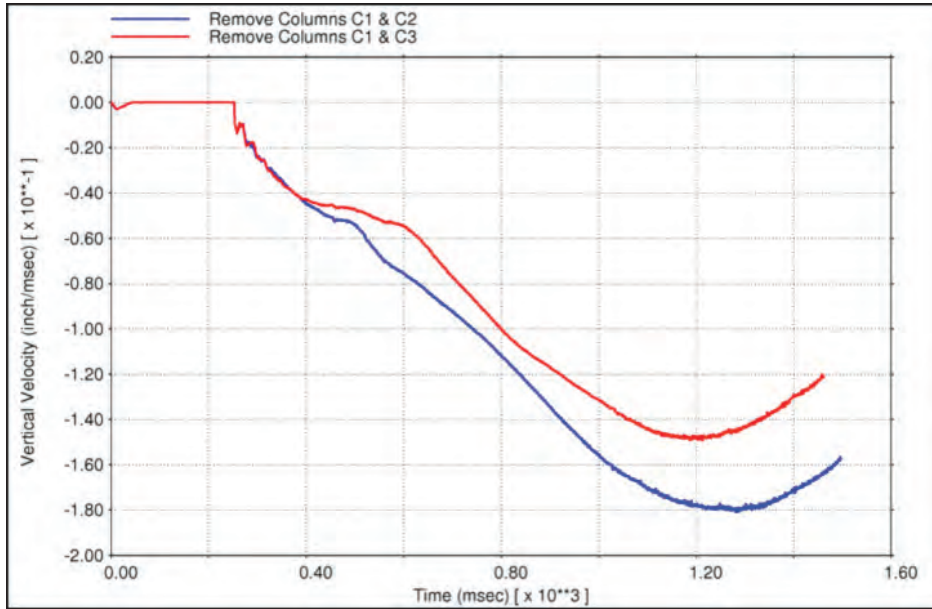


Figure 56 :
Vertical velocity, removal of
columns C1-C2 vs. C1-C3

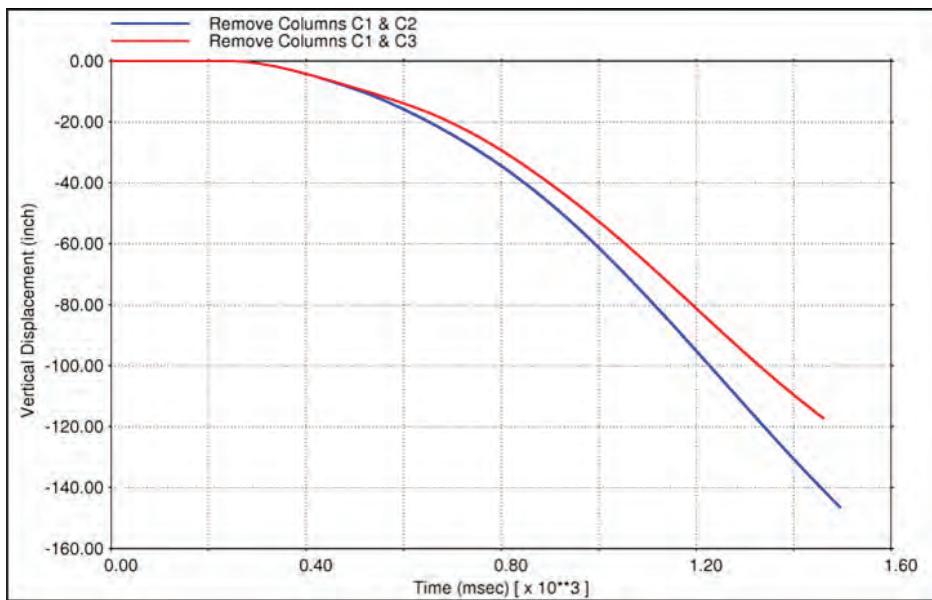


Figure 57:
Vertical displacement, removal
of columns C1-C2 vs. C1-C3

Figure 58:
Vertical velocity, C1-C2 columns
removal under different live
loads

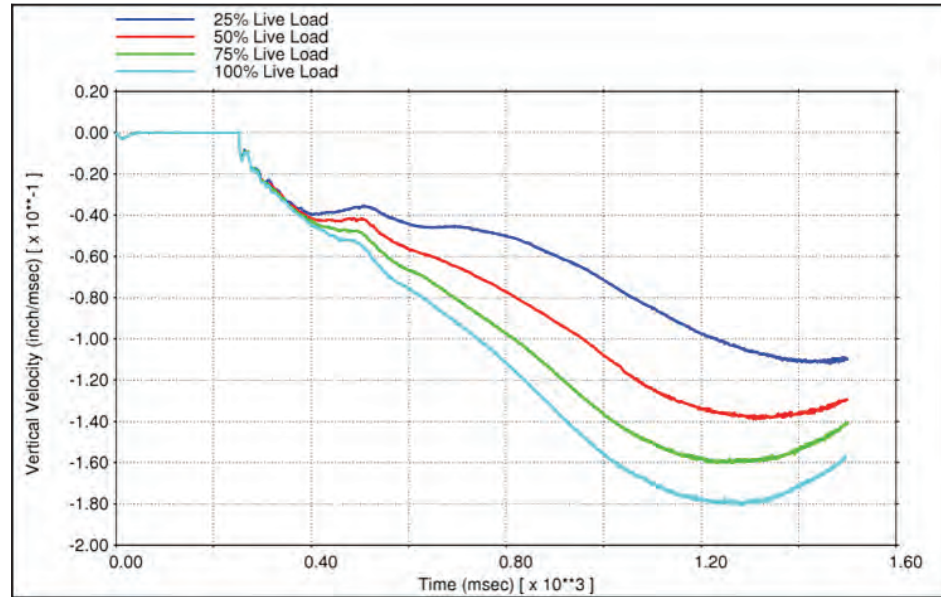
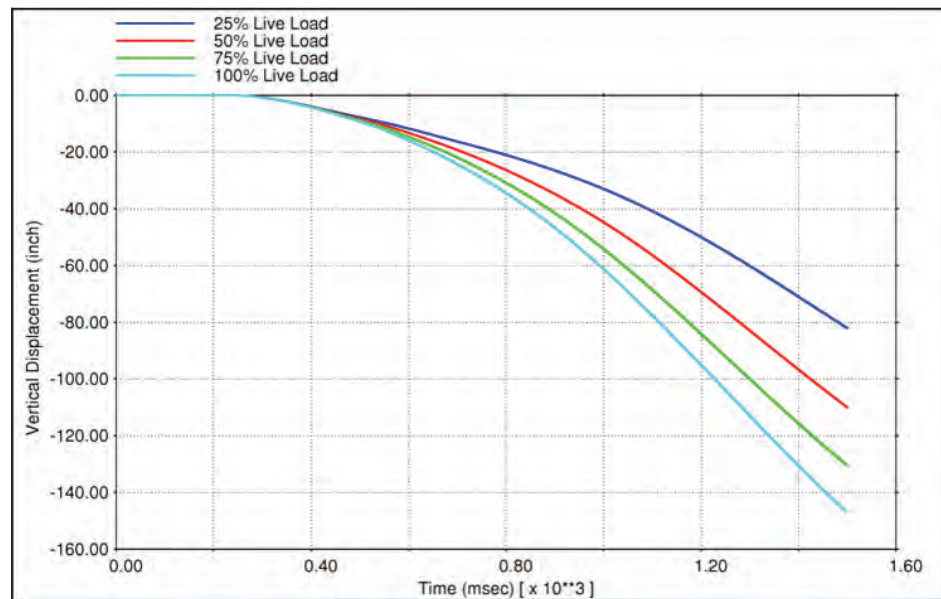


Figure 59:
Vertical displacement, C1-
C2 columns removal under
different live loads



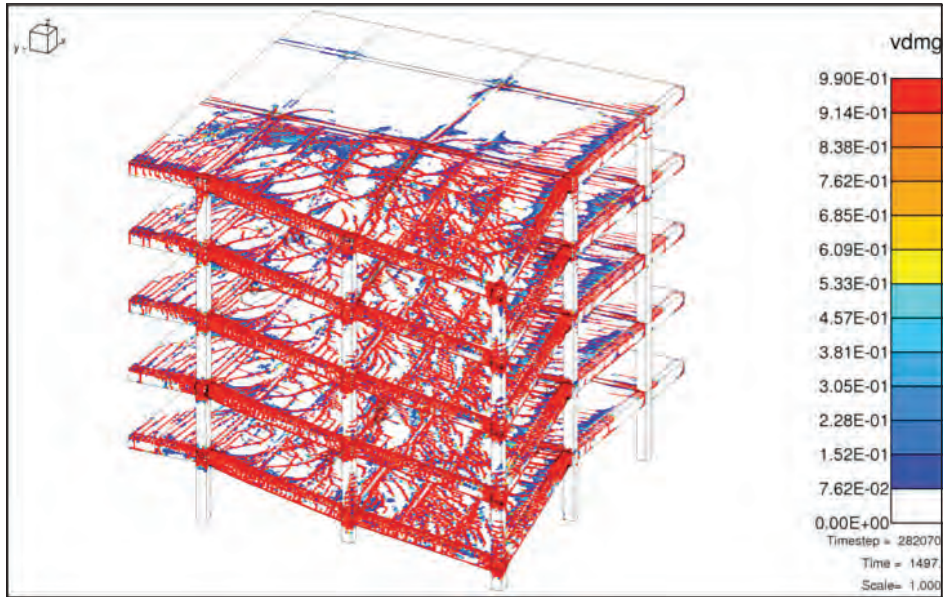


Figure 60 :
Concrete damage, removal of
C1-C2 columns, 100% live load,
top view

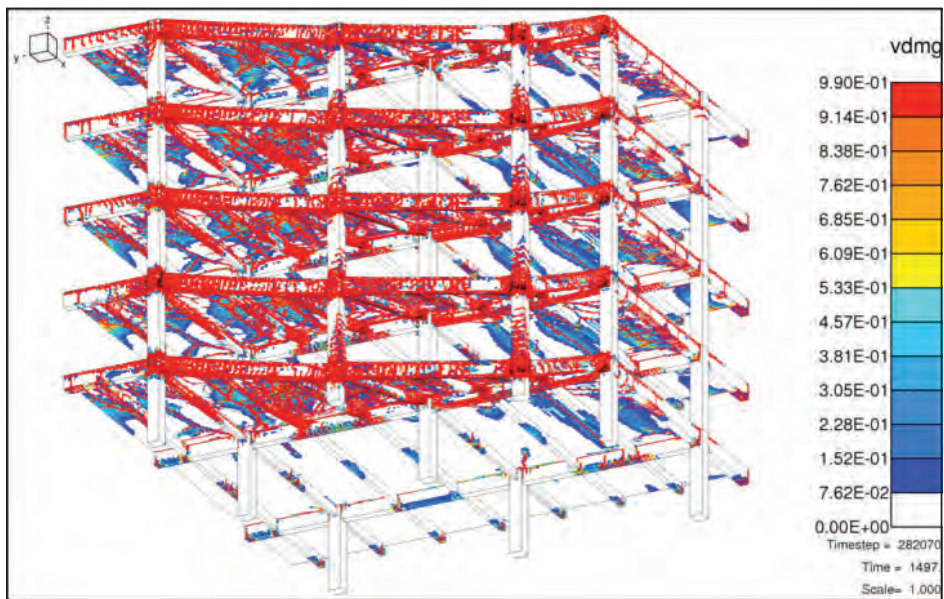


Figure 61:
Concrete damage, removal of
C1-C2 columns, 100% live load,
bottom view

4.3.1.2 Joist Slab System with 25 ft Bay Size

The NLFlex model of the reinforced concrete moment frame with 25 ft bay size resembles the NLFlex model of the one with 32 ft bay size and therefore is not shown here. Only the first two and a half bays of the building were modeled in each direction. Progressive collapse analyses were performed under the column C1 removal, as well as the simultaneous removal of columns C1 and C2.

4.3.1.2.1 Single Column Removal

Progressive collapse analyses of the baseline and the enhanced moment frame structure with 25 ft bay size under the corner column removal showed no disproportionate collapse of the structure under any of the live load levels. A comparison of the baseline and enhanced designs performances under 100% live load is shown in Figures 62 and 63, which provide the time histories of the vertical velocity and vertical displacement at the top of the building at a location directly above the removed column, respectively.

Figure 64 shows a top view snapshot of the vertical displacements of the enhanced design at the end of analysis under the 100% live load. A top view snapshot of the concrete damage of the enhanced structure at the end of analysis under the 100% live load is shown in Figure 65. As shown in the figure, concrete damage is mainly limited to the end sections of beams and slabs on floor levels directly above the removed column.

4.3.1.2.2 Two Columns Removal

Progressive collapse studies of moment frame under two columns removal scenario were performed by removing columns C1 and C2. The enhanced design failed only under the 100% live load, while the baseline design failed under 75% and 100% live loads. Failure in all cases was limited to the slabs and beams directly supported by the removed columns and on all of the above floors. Columns adjacent to the removed columns were capable of carrying the additional loads originally transferred by the removed columns. As such, no horizontal propagation of damage was observed.

Figures 66 and 67 represent a comparison of the baseline and enhanced designs under two columns removal scenario and 100% live load in terms of the vertical velocity and vertical displacement time histories of the top of the building at the location above the corner column. Figures 68 and 69 show the top and bottom view snapshots of displacements at the end of analysis under 100% live load. The top

and bottom views of concrete damage, at the end of analysis under 100% live load, are presented in Figures 70 and 71. Extensive concrete damage can be observed in all slabs and spandrel beams above the removed columns.

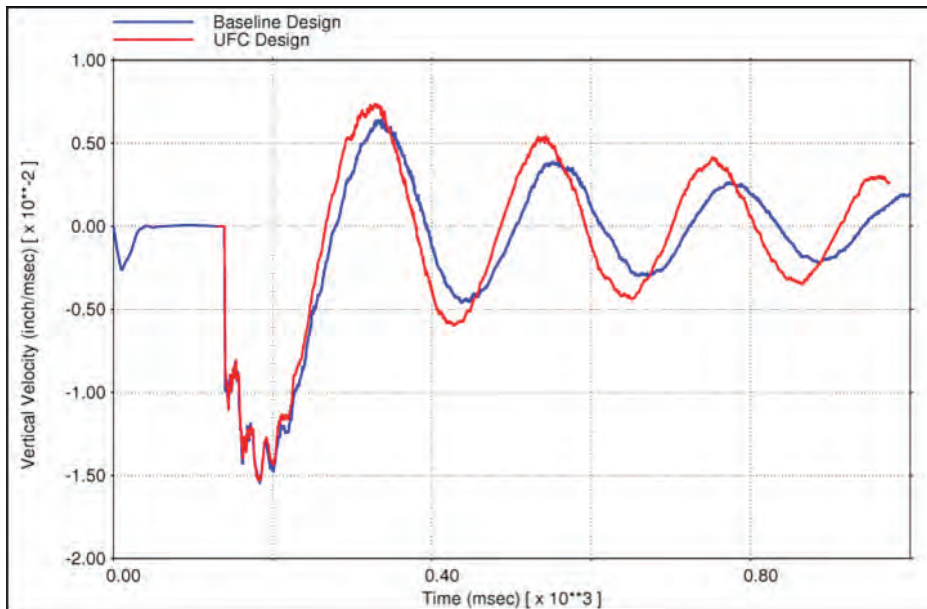


Figure 62:
Vertical velocity, column C1
removal, 100% live load

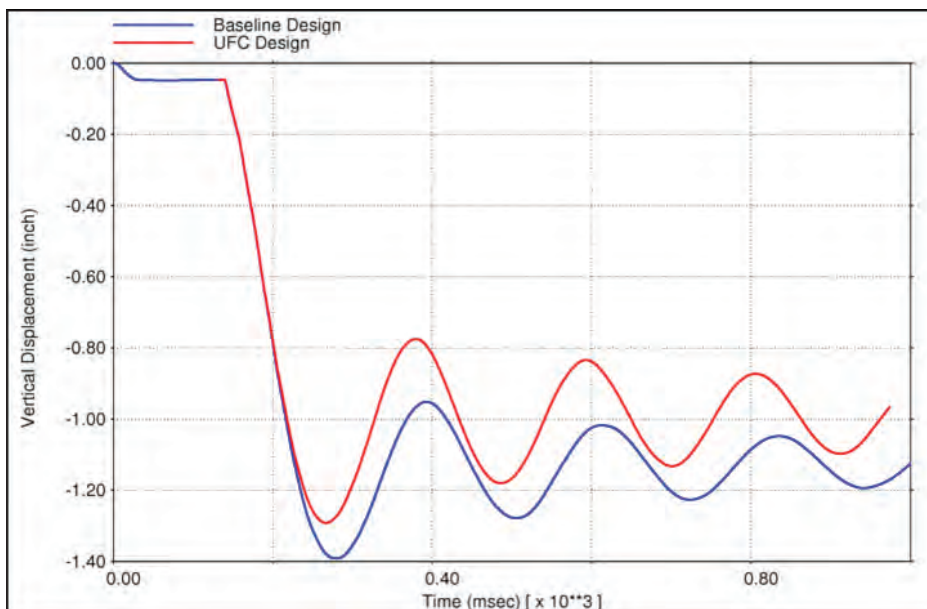


Figure 63:
Vertical displacement, column
C1 removal, 100% live load

Figure 64:
Vertical displacement (in),
column C1 removal, 100% live
load

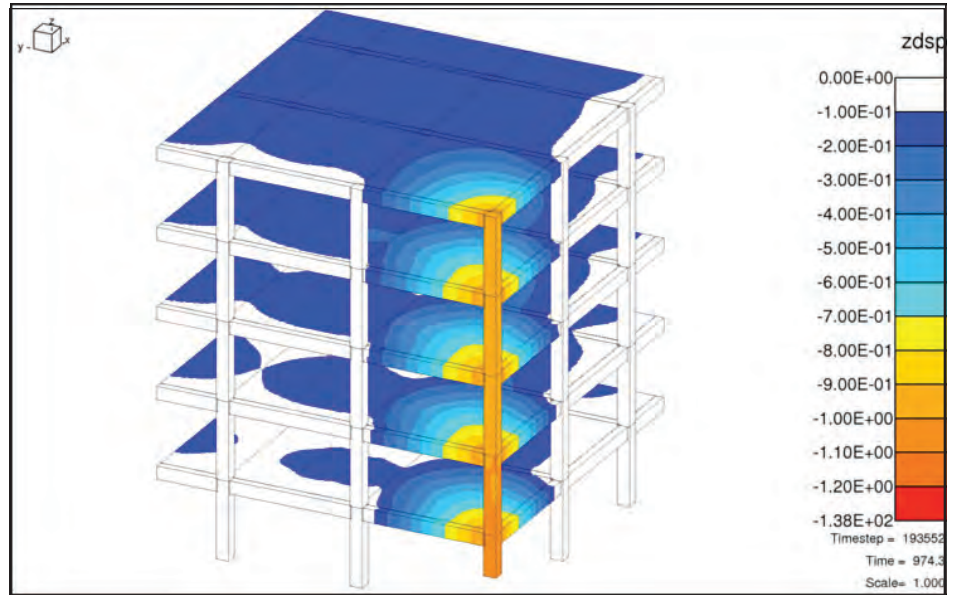
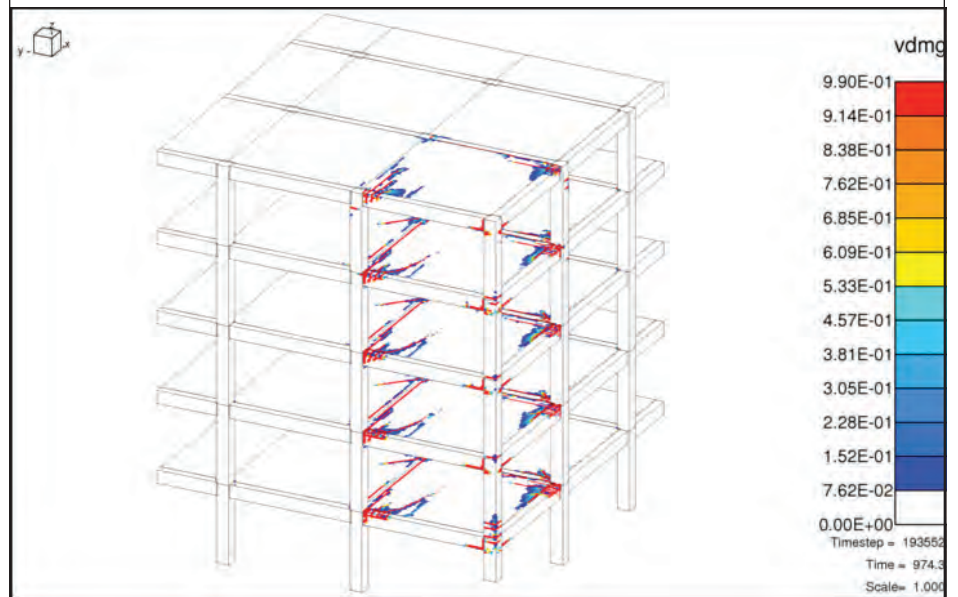


Figure 65:
Concrete damage, column C1
removal, 100% live load



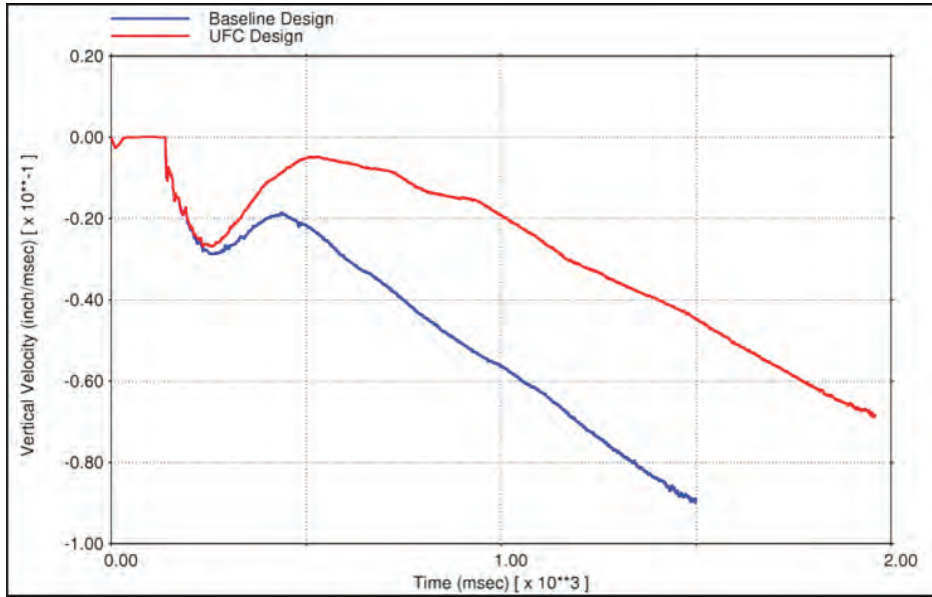


Figure 66:
Vertical velocity, two columns removal, 100% live load

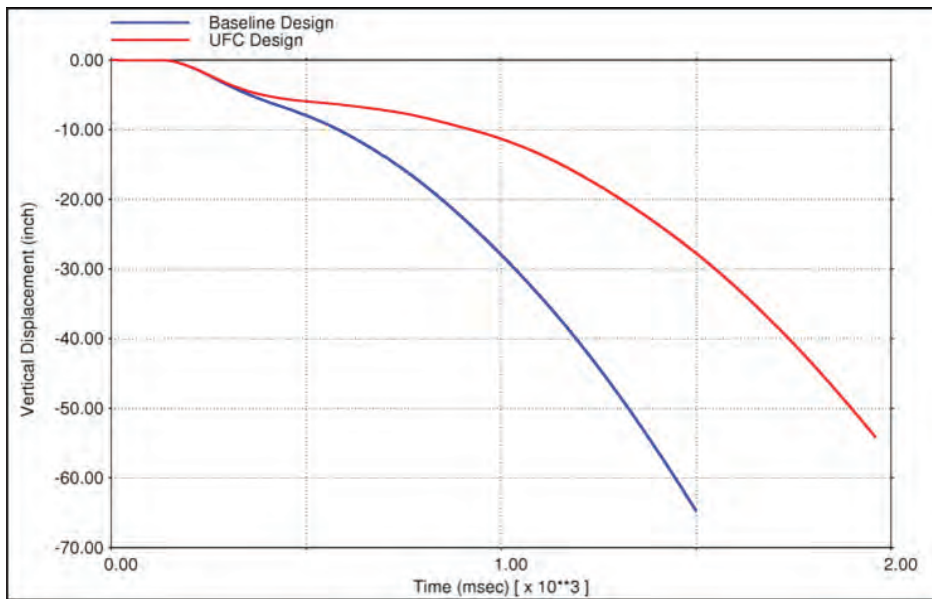


Figure 67:
Vertical displacement, two columns removal, 100% live load

Figure 68:
Vertical displacement (in), two
columns removal, 100% live
load, top view

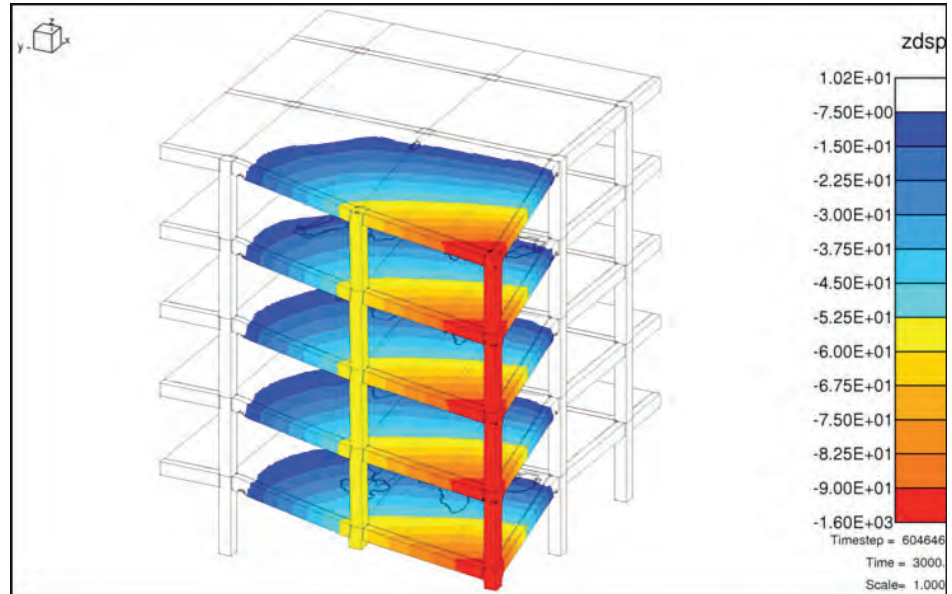
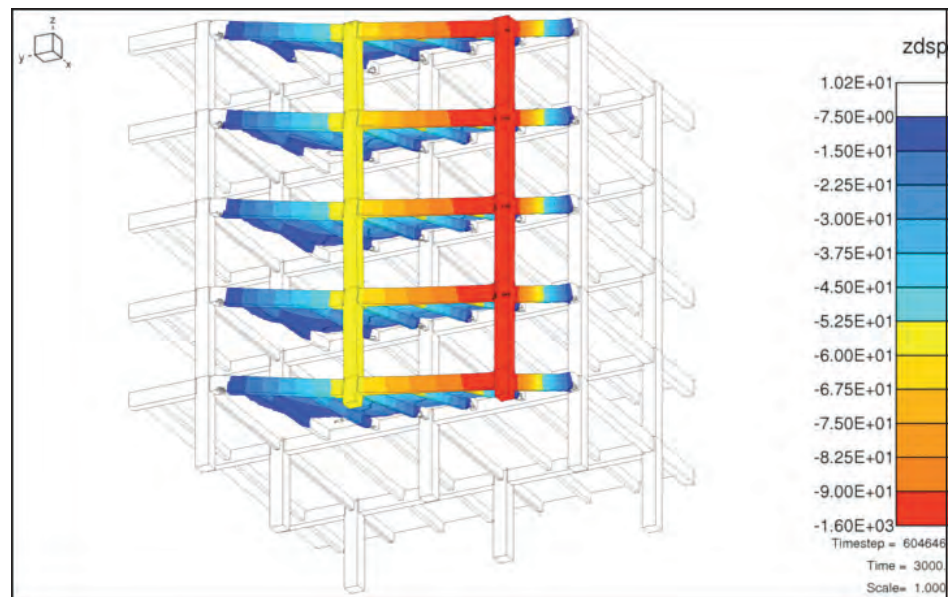


Figure 69:
Vertical displacement (in), two
columns removal, 100% live
load, bottom view



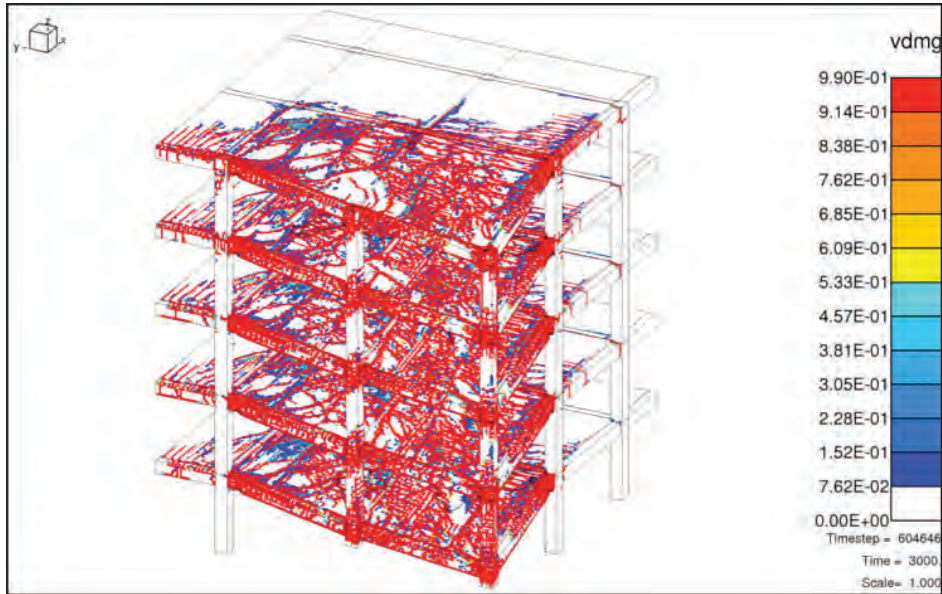


Figure 70:
Concrete damage, two columns
removal, 100% live load, top
view

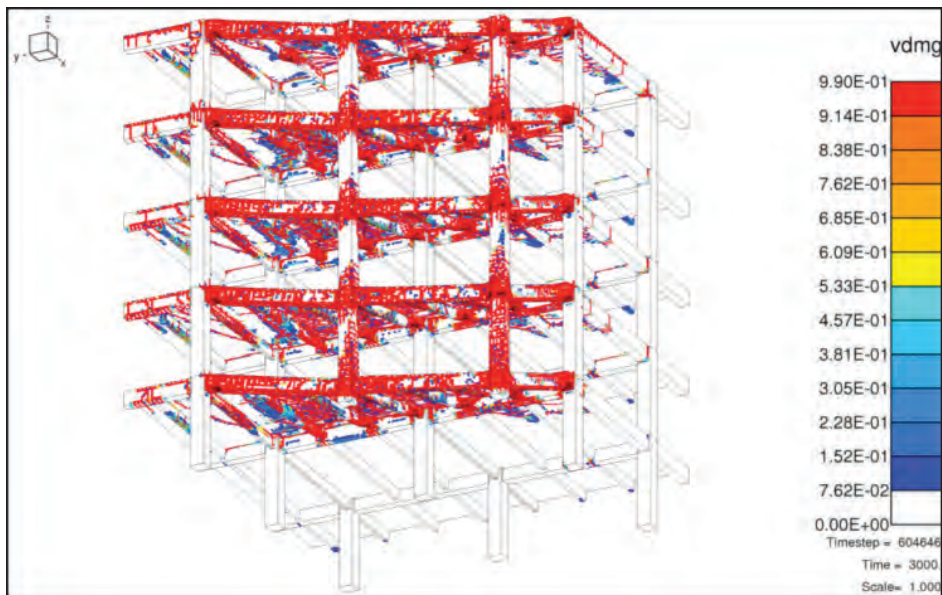


Figure 71:
Concrete damage, two columns
removal, 100% live load,
bottom view

4.3.2 Flat Slabs with Drop Panels

Figures 72 and 73 show the top and bottom views of the NLFlex model of the reinforced concrete building with flat slabs and drop panels. One building geometry with 25 ft bay size is considered. To reduce the size of the model, only the first two and a half bays of the building are modeled in each direction. Appropriate boundary conditions are provided on all floor levels to maintain structural continuity and

compatibility conditions at border lines where the modeled structure meets the rest of the structure. Progressive collapse analyses were performed under the column C1 removal, as well as the simultaneous removal of columns C1 and C2.

4.3.2.1 Single Column Removal

Progressive collapse analyses of both baseline and enhanced designs of the flat slab building under the corner column removal showed slab failure under any of live load levels. This indicates that the flat slab building is very susceptible to column removal. The drop panels did not prevent slabs from failing, as failure was mainly due to the low bending capacity of the flat slabs under the cantilever action.

Results of progressive collapse analysis of enhanced building under single column removal and 25% live load, which is the lowest live load level considered in this study, are presented in Figures 74 through 79. Figures 74 and 75 show the time histories of the vertical velocity and vertical displacement at the top of the enhanced building, respectively, at a location directly above the removed column. The top and bottom view snapshots of the vertical displacements of the building at the end of analysis are presented in Figures 76 and 77. Finally, the top and bottom view snapshots of the concrete damage are shown in Figures 78 and 79. The poor performance of the flat slab system under the lowest live load level and the high level of concrete damage in the slabs above the removed column are shown in the figures.

4.3.2.2 Two Columns Removal

Based on flat slab failure under single column removal and the lowest live load level, one can conclude that two columns removal will at least lead to failure of slabs above the removed columns. However, a series of progressive collapse studies under two columns removal were performed to investigate possibility of horizontal propagation of collapse.

Figures 80 through 85 show the results of progressive collapse analysis of enhanced building under the removal of C1 and C2 columns and 25% live load. Although concrete damage is very extensive, it is mainly limited to the slabs above the removed columns. Similar behavior was also observed under higher live load levels. Progressive collapse analysis of flat slab building under 100% live load where columns experience the highest loads also showed no column failure and hence no horizontal propagation of collapse.

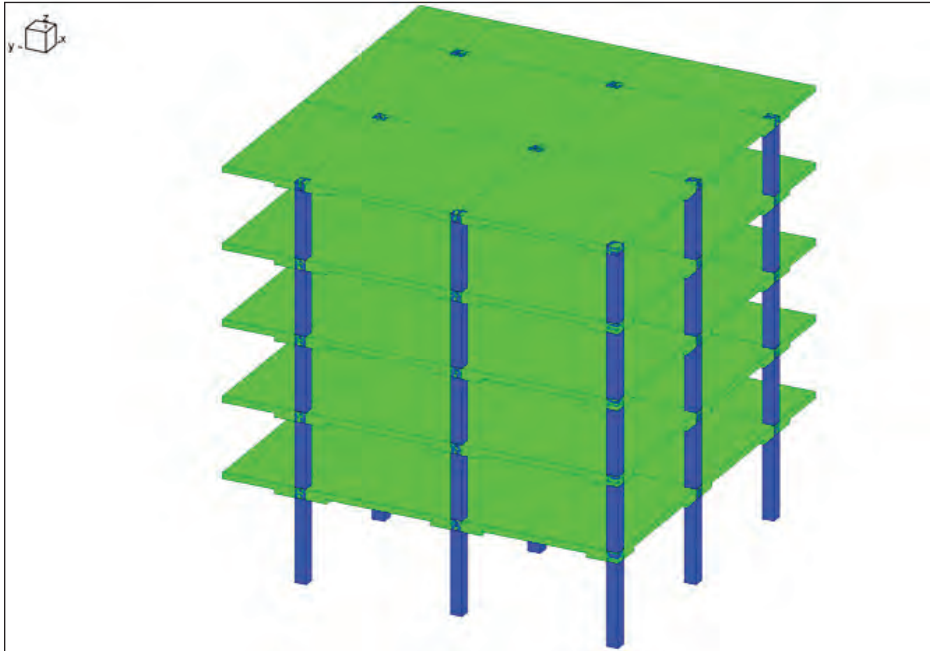


Figure 72:
NLFlex Model - flat slab with
drop panels, top view

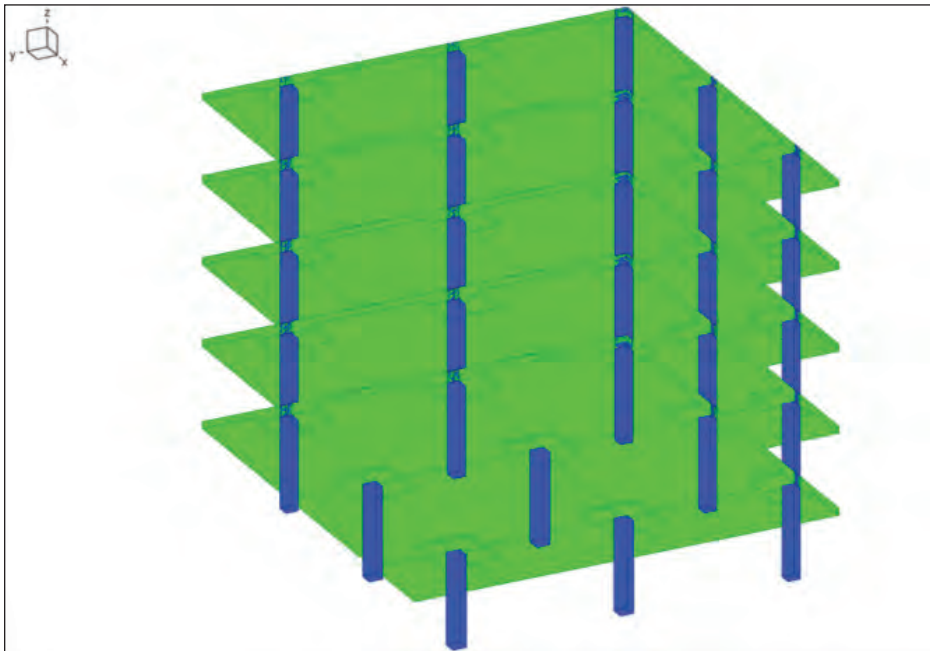


Figure 73:
NLFlex Model - flat slab with
drop panels, bottom view

Figure 74:
Vertical velocity, column C1
removal, 25% live load

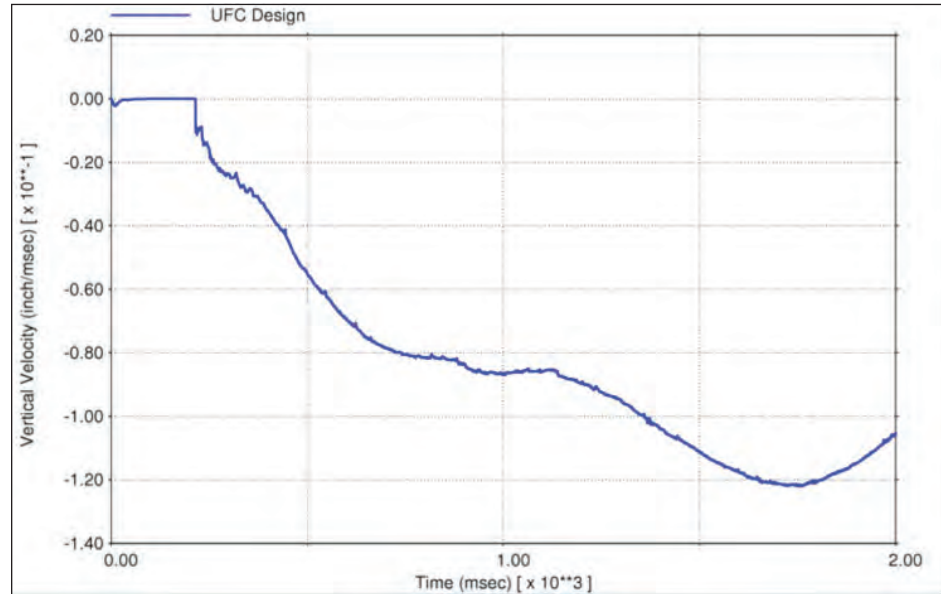
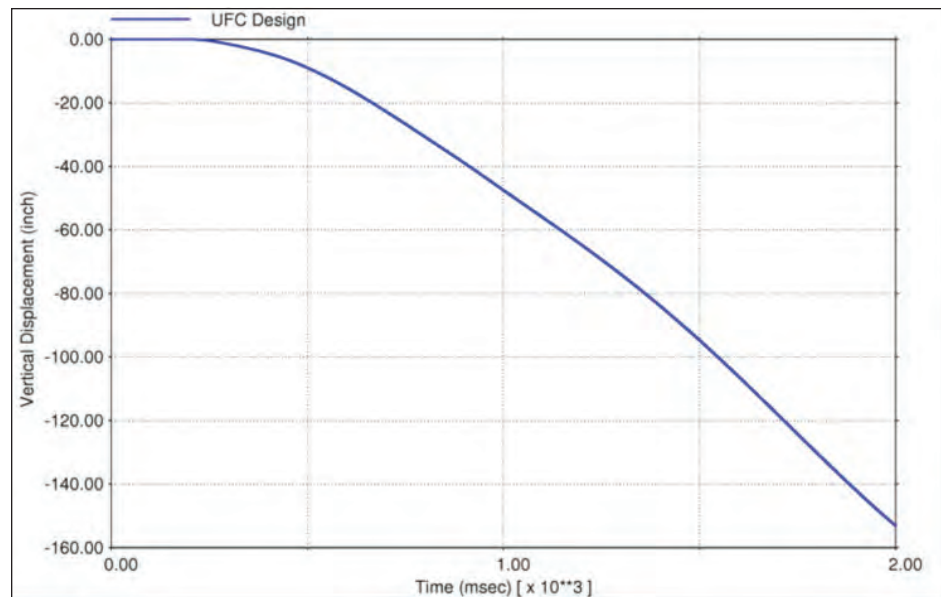


Figure 75:
Vertical displacement, column
C1 removal, 25% live load



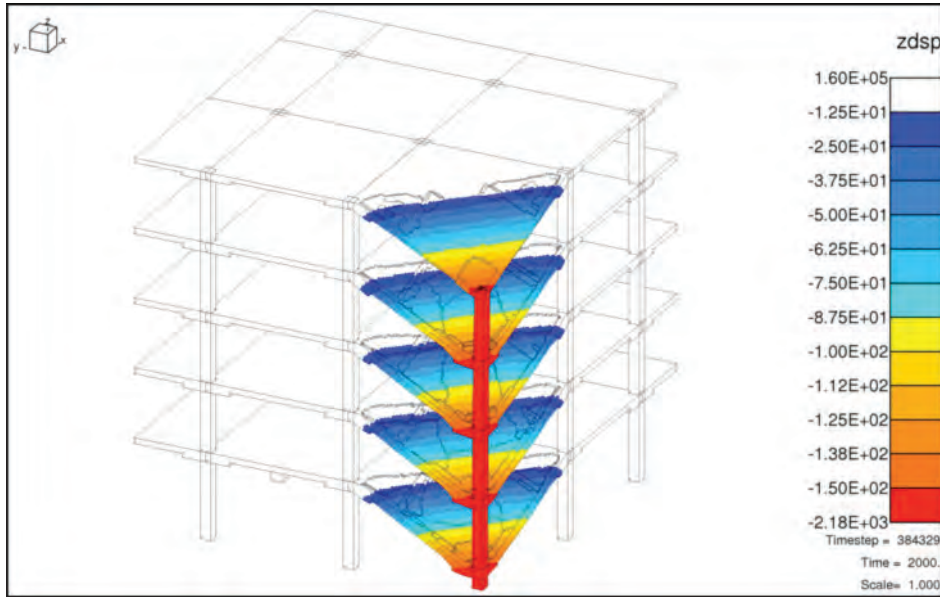


Figure 76:
Vertical displacement (in),
column C1 removal, 25% live
load, top view

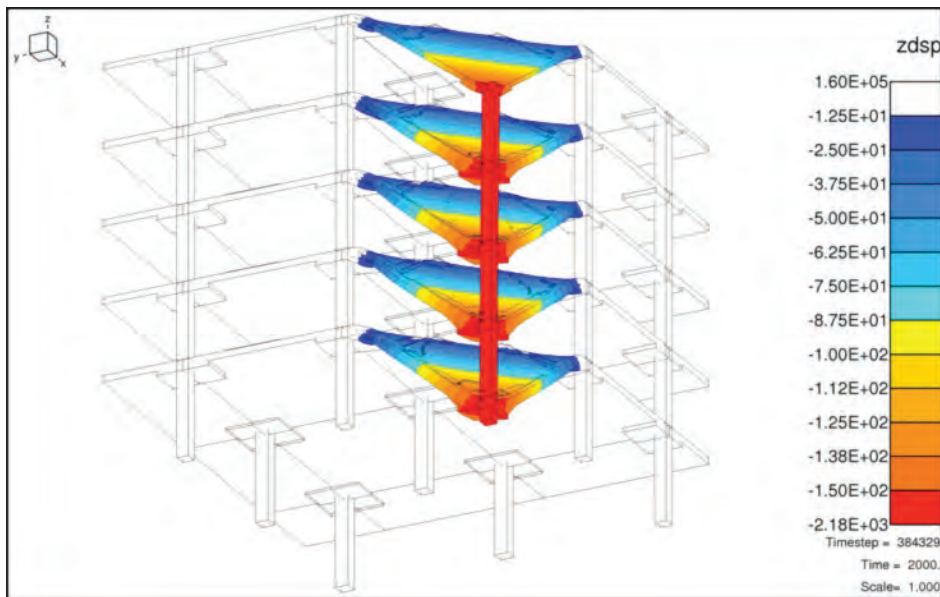


Figure 77:
Vertical displacement (in),
column C1 removal, 25% live
load, bottom view

Figure 78:
Concrete damage, column C1
removal, 25% live load, top
view

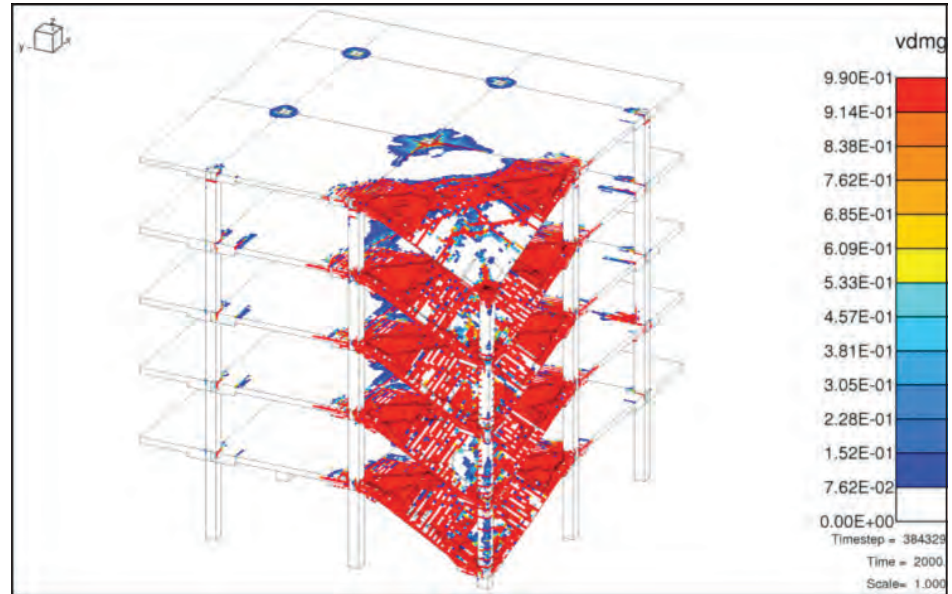
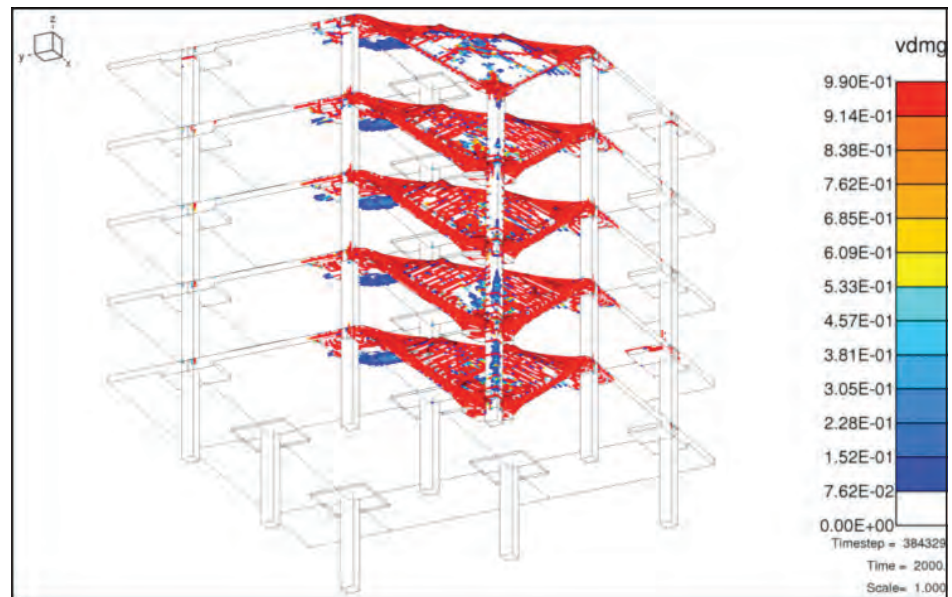


Figure 79:
Concrete damage, column
C1 removal, 25% live load,
bottom view



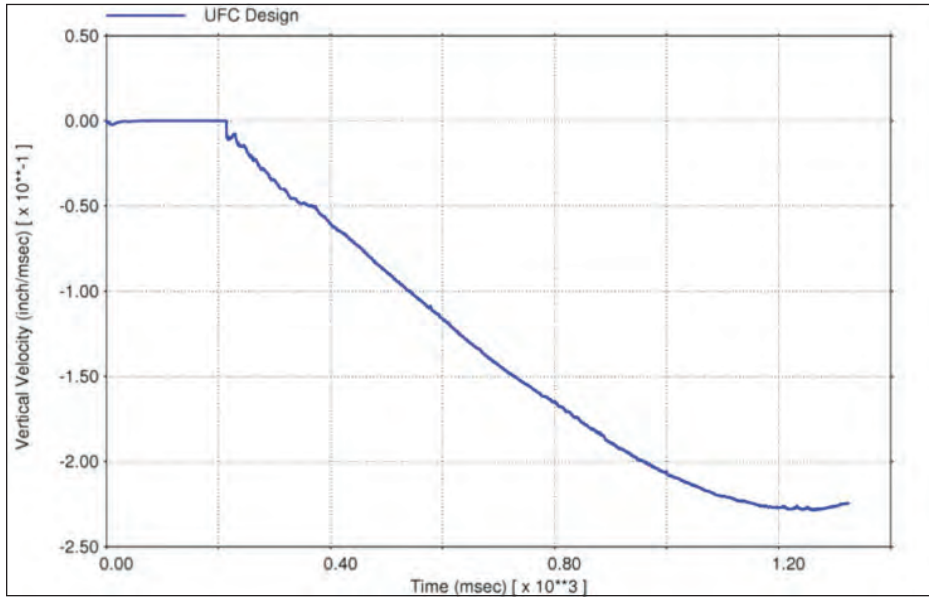


Figure 80:
Vertical velocity, two columns
removal, 25% live load

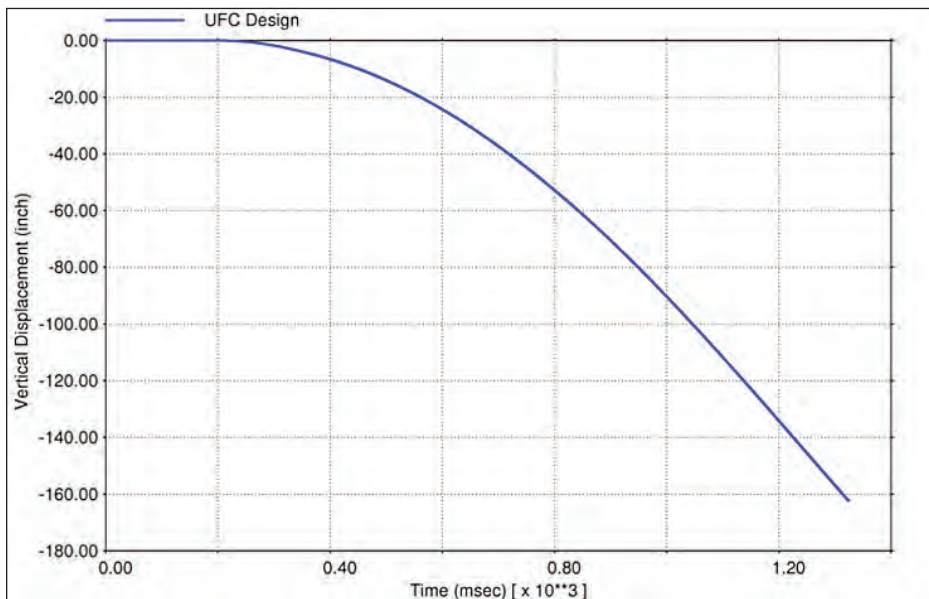


Figure 81:
Vertical displacement, two
columns removal, 25% live
load

Figure 82:
Vertical displacement (in), two
columns removal, 25% live
load, top view

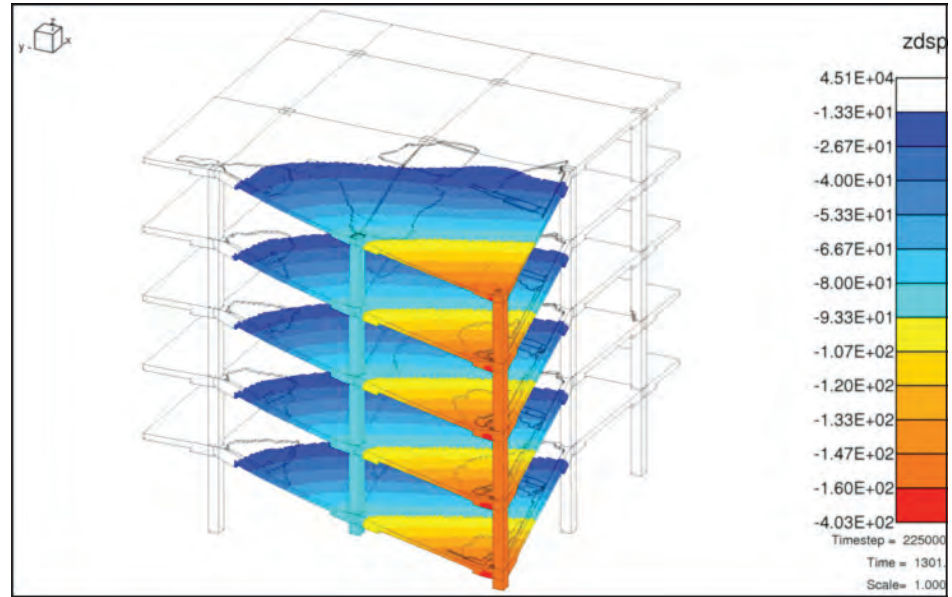
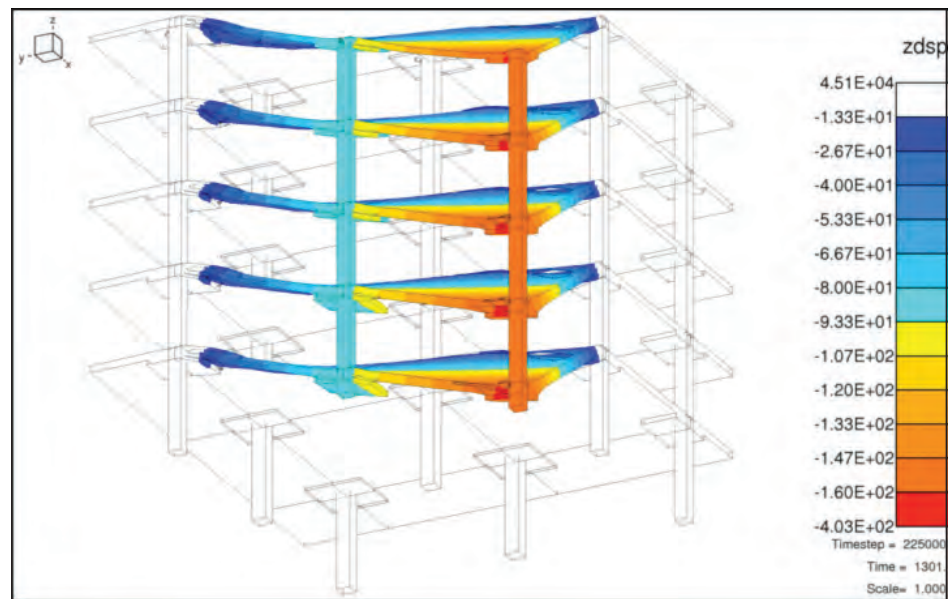


Figure 83:
Vertical displacement (in), two
columns removal, 25% live
load, bottom view



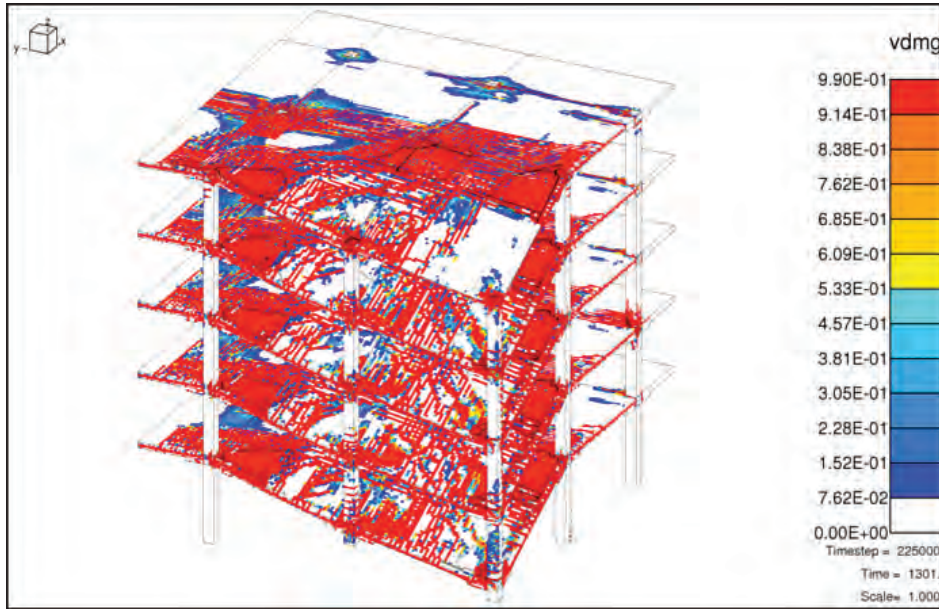


Figure 84:
Vertical displacement (in), two
columns removal, 25% live
load, top view

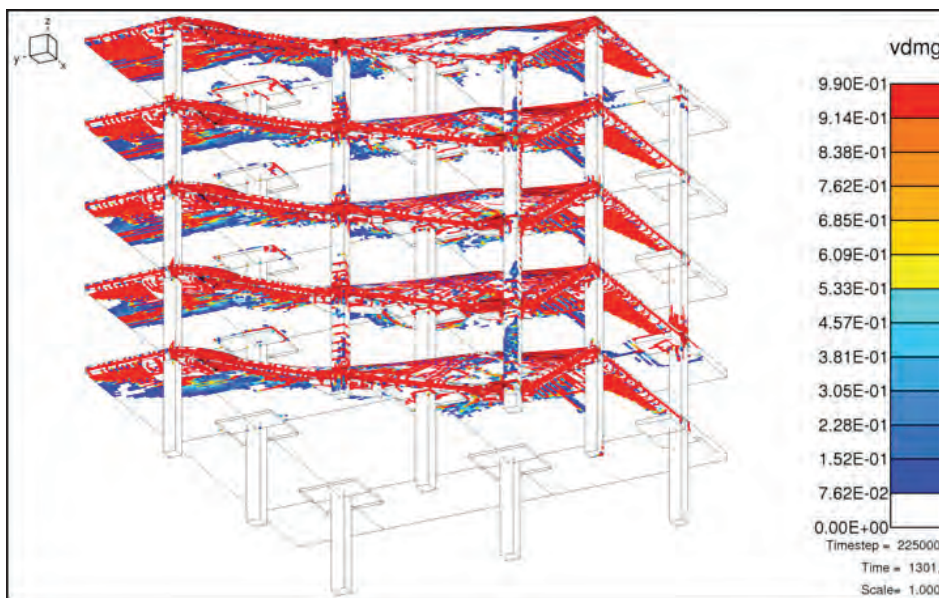


Figure 85:
Vertical displacement (in), two
columns removal, 25% live
load, bottom view

4.3.3 Summary of Results and Findings

A summary of progressive collapse analyses performed under this study for reinforced concrete moment frame buildings with one-way joist slabs and for buildings with flat slabs and drop panels is presented in Table 1, Table 2, and Table 3. In general, two distinct behaviors were observed under the column removal scenarios. Either no failure

(N) was observed in any component of the structure, or all slabs and beams directly supported by the removed columns and on the above floors failed (F). These two behaviors are denoted by letters N and F in the tables, respectively.

The high-fidelity models used for these analyses are computationally intensive. Consequently, only a portion of the structure was modeled for these analyses and the amount of simulated response time was on the order of one to three seconds in order to assess whether the structure would experience a collapse. These calculations were not run out to reach the final state of the collapsed debris because of the large run times required.

A summary of other observations specific to a certain, or all, reinforced concrete buildings considered in this study is presented in the following. One should notice that these observations are only based on the limited number of reinforced concrete buildings that were specifically designed for the purpose of this study. Any definitive conclusions about these observations will require more analyses on a larger variety of reinforced concrete building types and designs.

1. Flat slabs are susceptible to progressive collapse and should be detailed to provide redundant load redistribution capacity. [14]
2. Joist slabs with relatively small bay size (< 25 ft) perform well under relatively high percentage of the total live load for both single and two columns removal scenarios.
3. Joist slabs with relatively large bay size (> 32 ft) perform well under high percentage of the total live load for single column removal. [15]
4. Compared to the baseline design of the buildings considered in this study, the UFC design slightly improved the behavior of slabs under column removal scenarios. [16]
5. In all baseline and enhanced building designs analyzed in this study, columns adjacent to the removed columns were capable of carrying the additional loads originally transferred by the removed columns. As such, no column failure and horizontal propagation of damage was observed in any of the analyses, and the damage was mainly limited to the slabs and beams directly above the removed columns.

Table 1: Summary of progressive collapse analyses for 32 ft moment frame

| Column(s) Removed | Design | Percent Live Load | | | |
|----------------------|----------|-------------------|----------|----------|----------|
| | | 25 | 50 | 75 | 100 |
| C1 | Enhanced | N | N | N | N |
| | Baseline | N | N | N | N |
| C1-C2 | Enhanced | F | F | F | F |
| | Baseline | F | F | F | F |

Table 2: Summary of progressive collapse analyses for 25 ft moment frame

| Column(s) Removed | Design | Percent Live Load | | | |
|----------------------|----------|-------------------|----|----------|----------|
| | | 25 | 50 | 75 | 100 |
| C1 | Enhanced | N | N | N | N |
| | Baseline | N | N | N | N |
| C1-C2 | Enhanced | N | N | N | F |
| | Baseline | N | N | F | F |

Table 3: Summary of progressive collapse analyses for 25 ft flat slab building

| Column(s) Removed | Design | Percent Live Load | | | |
|----------------------|----------|-------------------|----------|----------|----------|
| | | 25 | 50 | 75 | 100 |
| C1 | Enhanced | F | F | F | F |
| | Baseline | F | F | F | F |
| C1-C2 | Enhanced | F | F | F | F |
| | Baseline | F | F | F | F |

Key

N = No Failure, F = Failure

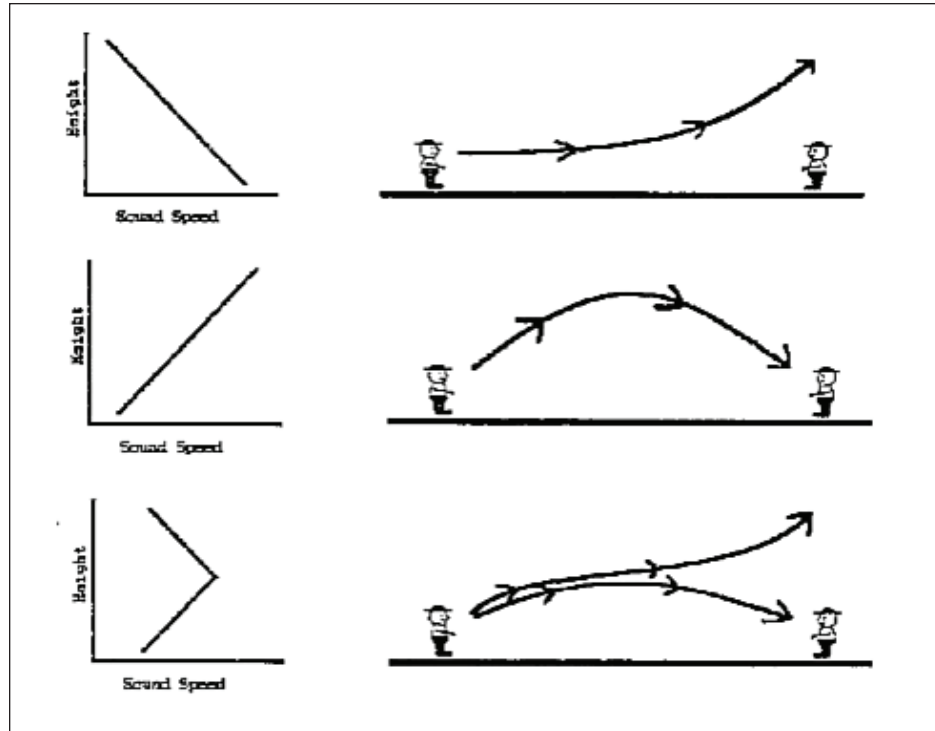
Environmental Influences: Effect of Overcast Sky

5.1 Overview

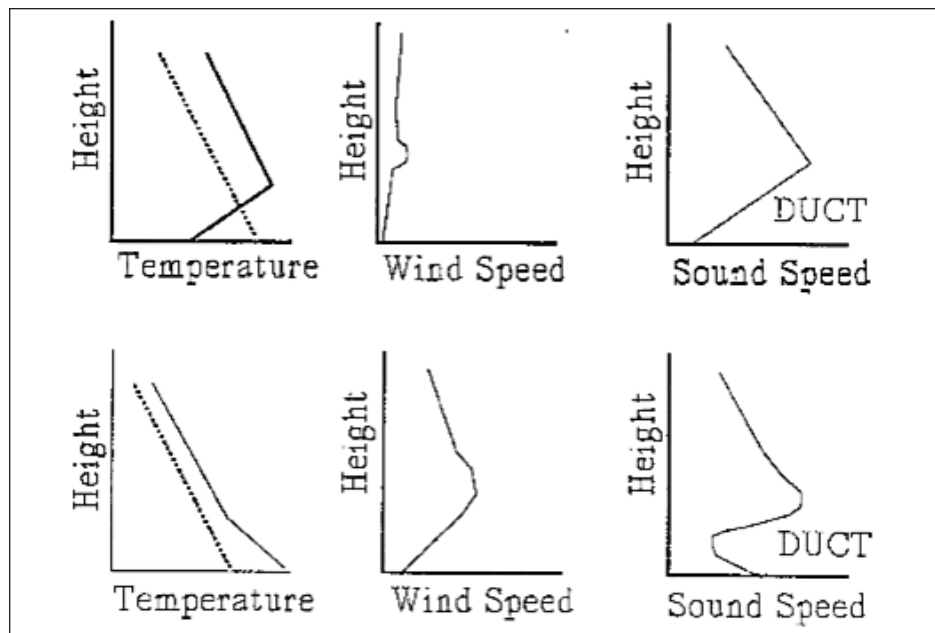
Temperature and wind are the most important characteristics of the atmosphere which may affect airblast. Primarily they can influence the airblast shock and sound speeds, however slightly [12, 13]. For near-field distances, while the airblast is still propagating as a shock wave, warmer ambient temperatures can result in a slightly earlier shock arrival (order of msec) without changing its strength. For far-field distances, after the airblast shock has transitioned to an acoustic (or sound) wave, the vertical profile of air temperature or wind can refract the propagating wave to either enhance or weaken its strength. This is illustrated in Figure 86 [Figures taken from Reference 13].

For the airblast calculations comprising the data for the UrbanBlast Tool discussed later in this report, the ambient environment is modeled with the U.S. Standard Atmosphere [14]. For altitudes below 11 km, its vertical temperature structure is represented by a constant lapse rate of -6.5 K/km, starting with a temperature of 288 K and pressure of 14.7 psi at the surface. The maximum horizontal extent of the computational domain is roughly 1.2 km in the N-S and E-W directions. For a nominal sound speed of 343 m/s, it takes 3.5 sec for an acoustic signal to travel this distance. All airblast calculations were carried out to 5 sec, which is more than enough time to model the transit of the airblast across the grid from any of the potential charge locations.

Figure 86:
Vertical sound speed profiles
illustrating effects on acoustic
propagation



(a) Sound speed profiles and their effects on acoustic propagation [13]



(b) Wind and temperature profiles that result in sound ducts [13]

5.2 Overcast Sky Simulation Studies

Given the geographic extent of the airblast calculations, an important issue to understand is how sensitive are the calculated results to different atmospheric conditions. For example, how would an overcast sky atmospheric condition influence the airblast?

To answer this question, selected airblast calculations were performed which incorporated a vertical temperature profile representative of overcast sky conditions. This profile was measured at the Brookhaven National Laboratory while a marine stratus layer propagated northward over Long Island, N.Y. on the night of 11 May 2005 [15]. It is compared with the U.S. Standard Atmosphere in Figure 87.

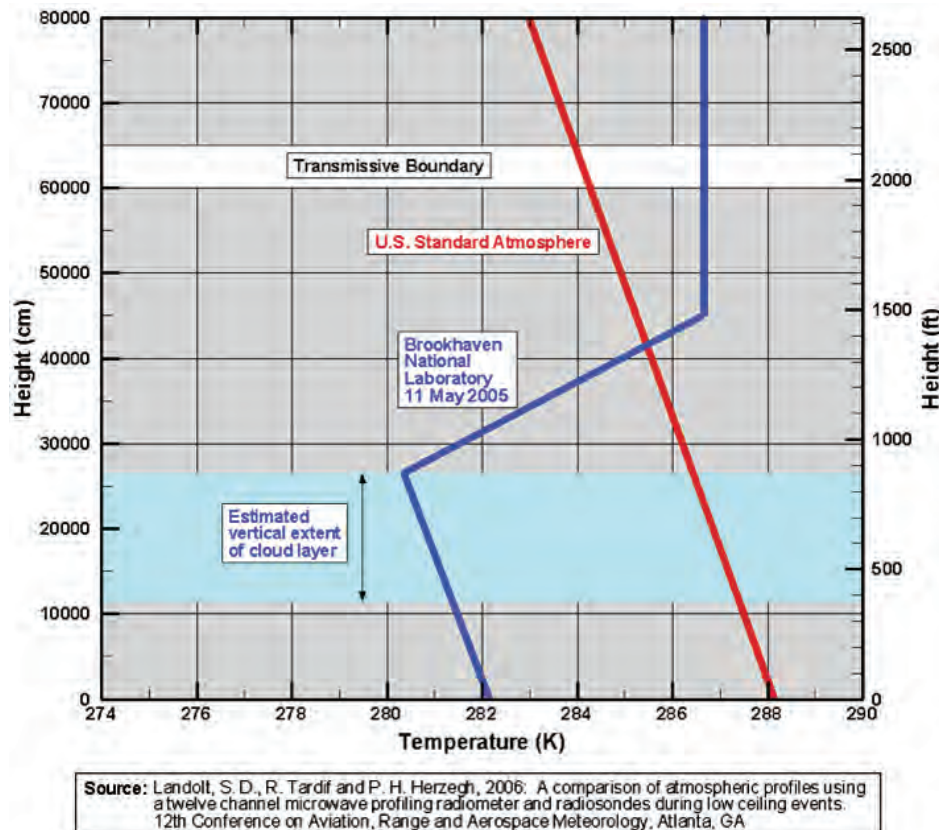


Figure 87:
Comparison of Overcast Sky
temperature profile (blue)
with U.S. Standard Atmosphere
(red)

Two different locations (Locations A and B) within a typical urban setting (i.e., Manhattan Financial District) were selected, and the peak pressure distribution that results from detonating a 1,000lb and 30,000lb explosive charge were computed. The results were computed with both the Standard Atmosphere Model and the Overcast Skies Atmosphere Model. The influence of overcast sky atmospheric conditions can be quantified by comparing the peak pressure fields produced throughout the urban setting for the two different atmosphere models. The results for these eight simulations are presented in Figures 88 through 91. When visually comparing the maximum overpressures at a simulation time of 5 sec, the results are virtually indistinguishable.

The effect of an overcast sky has negligible effect on the maximum overpressures produced in the computational domain for the charge sizes considered.

To fully quantify the difference in the peak pressure fields, the peak pressure field for the Overcast Sky case was subtracted from the same set of results for the Standard Atmosphere case for the two threat weights and two threat locations. This difference is plotted at each grid location for the urban setting for each case considered, and the results are presented in Figures 92 through 95. The upper half of each figure shows how the overcast sky increases the maximum overpressure at each location. The magnitudes are no more than 0.02 psi for the 30,000lb charge size, half that for the 1,000lb charge. These increases are plotted as a percentage on the lower half of each figure. As expected, the largest percentage changes are farthest away from the charge, with magnitudes of, at most, 15-20% for maximum overpressures of less than 0.2 psi.

The effect of an overcast sky, it was concluded, has negligible effect on the maximum overpressures produced in the computational domain for the charge sizes considered.

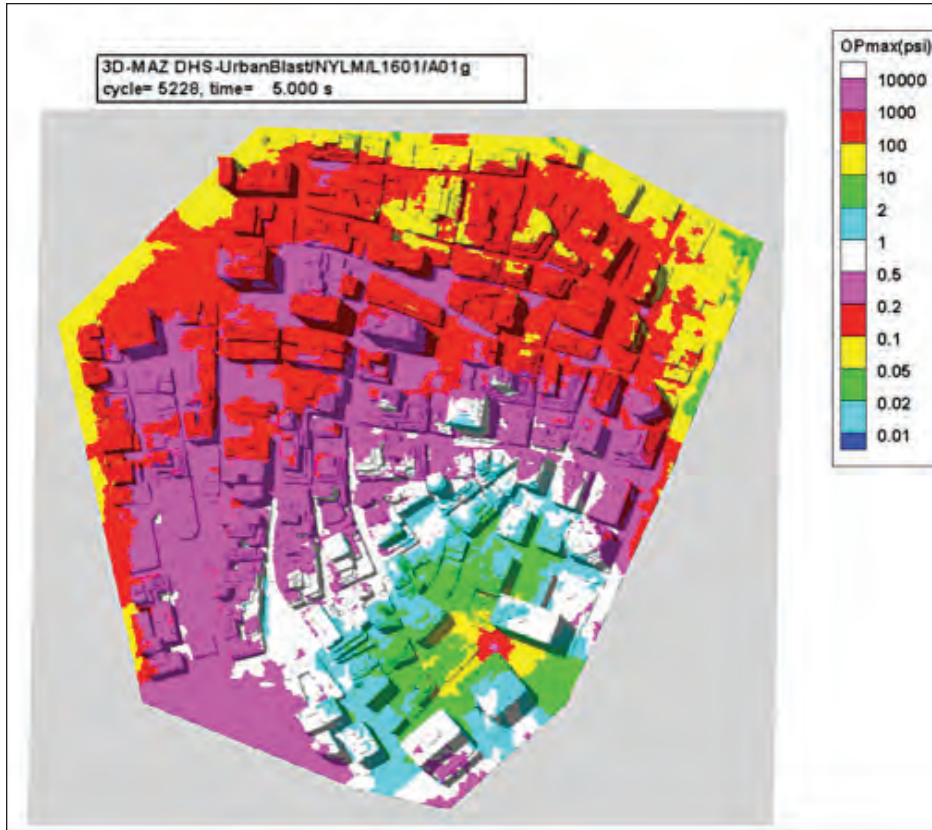
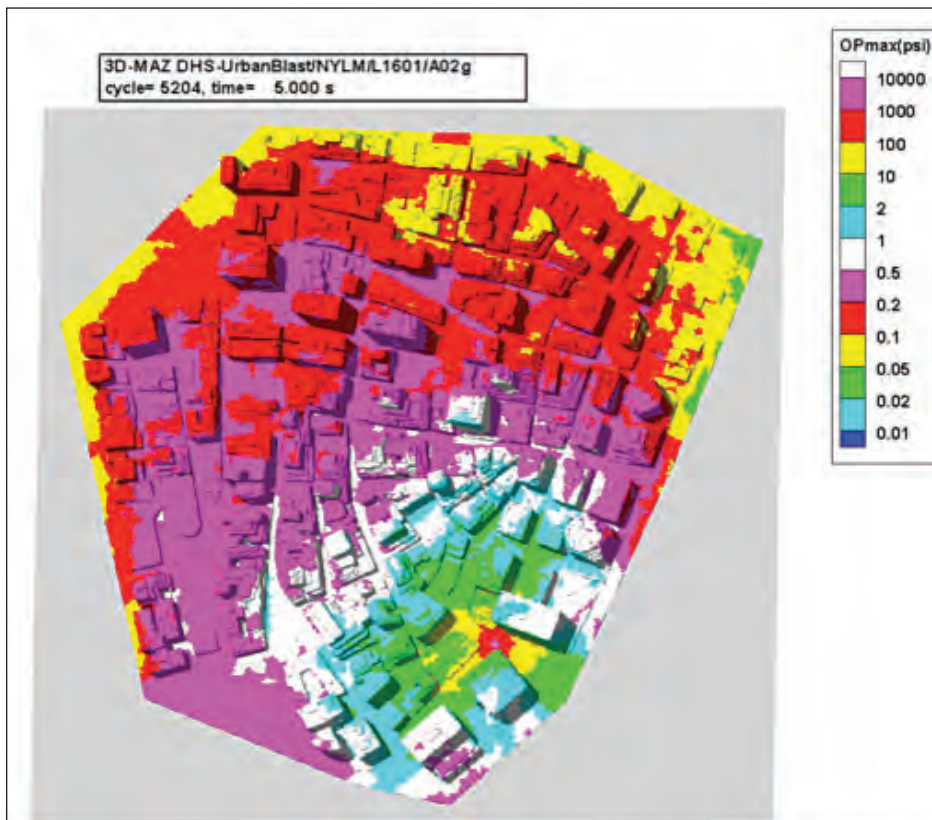


Figure 88:
Comparison of calculated maximum overpressure for two different atmosphere profiles 5 seconds after detonation of 30,000 lb at Location A

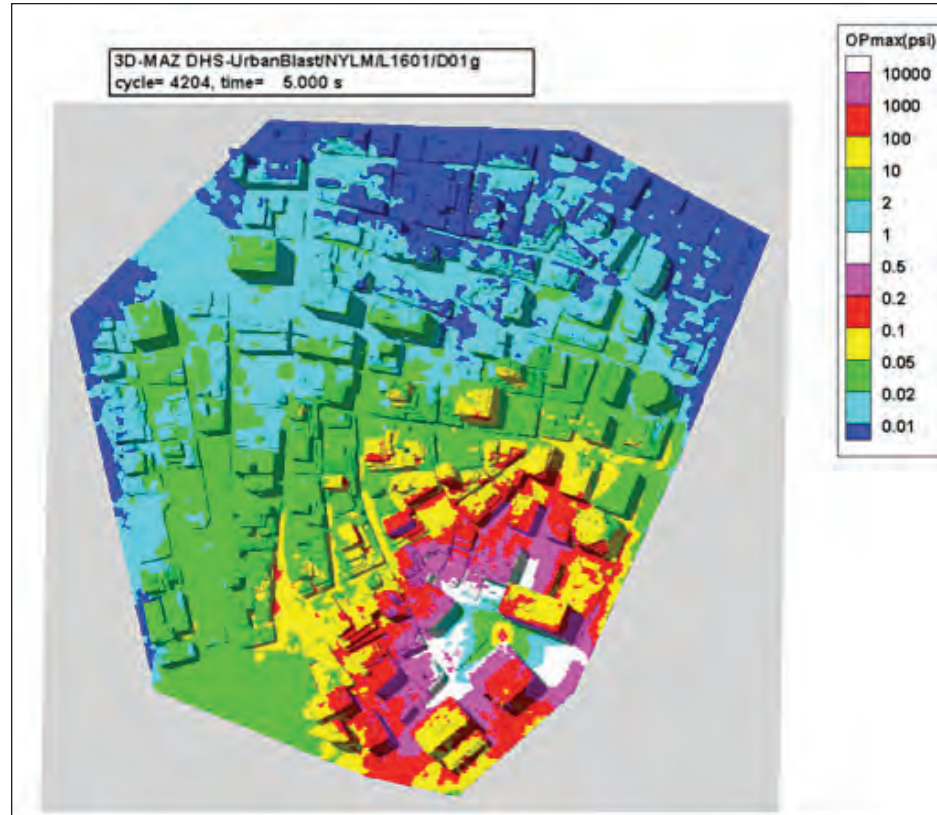
(a) Results for standard atmosphere



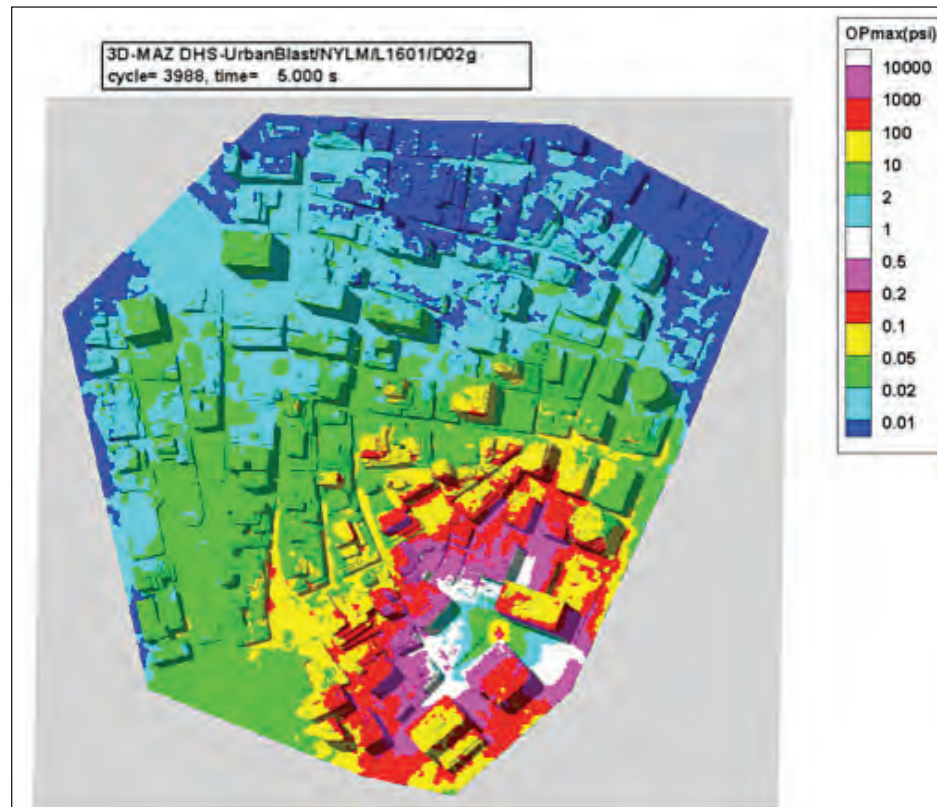
(b) Results for overcast sky atmosphere

Figure 89:
Comparison of calculated
maximum overpressure for two
different atmosphere profiles
5 seconds after detonation of
1,000 lb at Location A

(a) Results for standard
atmosphere



(b) Results for overcast sky
atmosphere



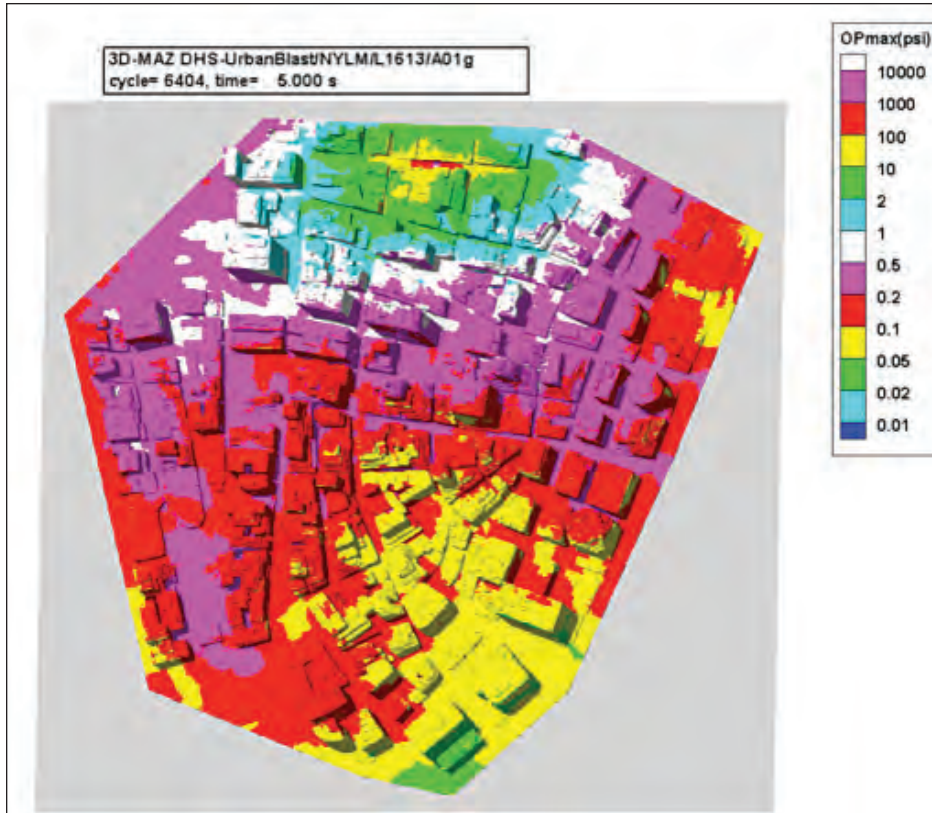
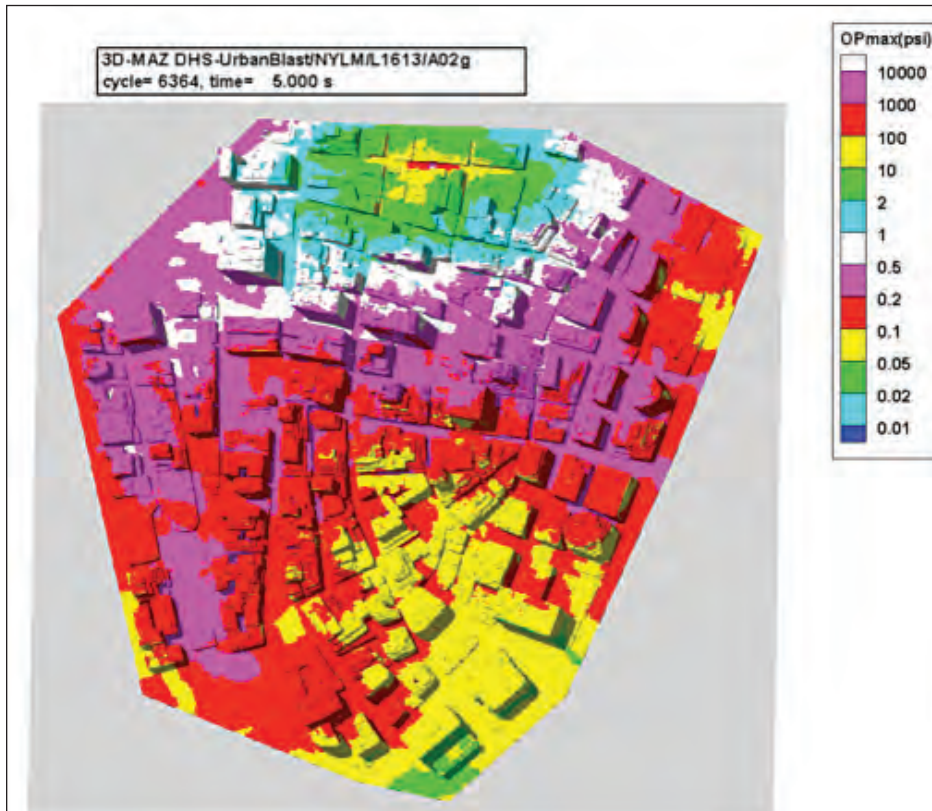


Figure 90:
Comparison of calculated
maximum overpressure for two
different atmosphere profiles
5 seconds after detonation for
30,000 lb at Location B

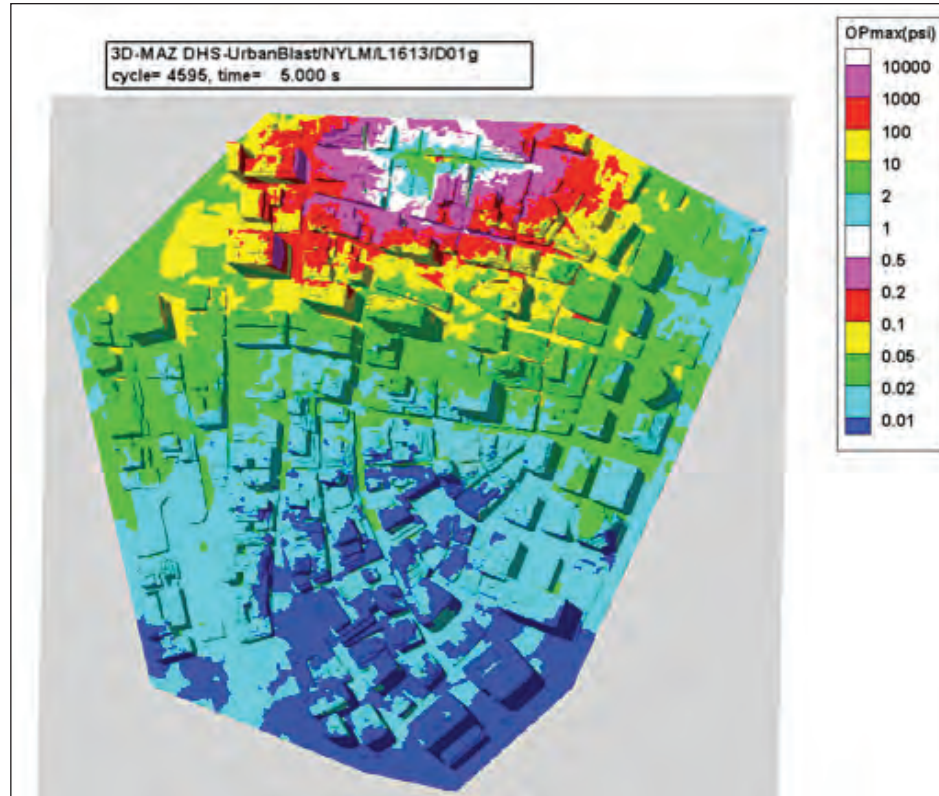
(a) Results for standard
atmosphere



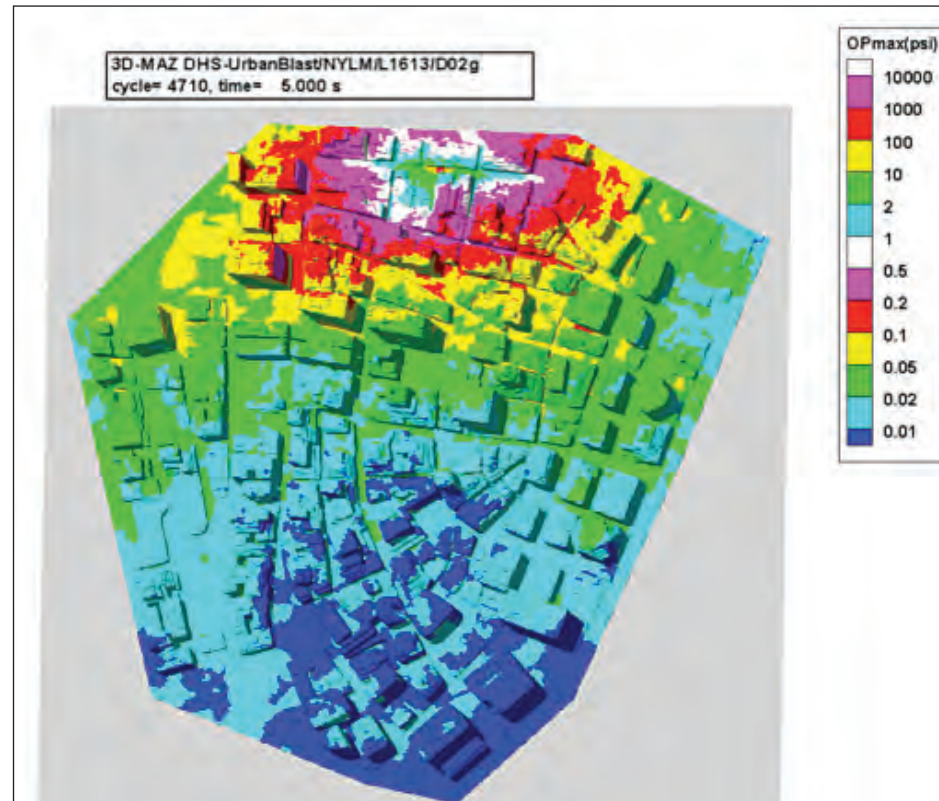
(b) Results for overcast sky
atmosphere

Figure 91:
Comparison of calculated
maximum overpressure for two
different atmosphere profiles
5 seconds after detonation for
1,000 lb at Location B

(a) Results for standard
atmosphere



(b) Results for overcast sky
atmosphere



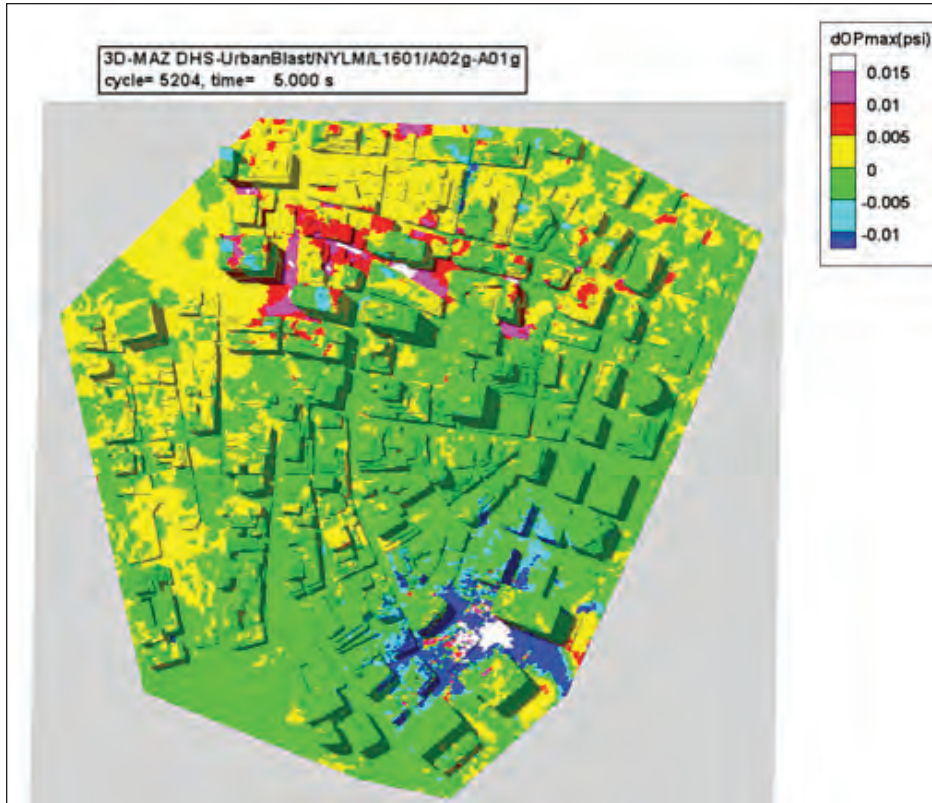
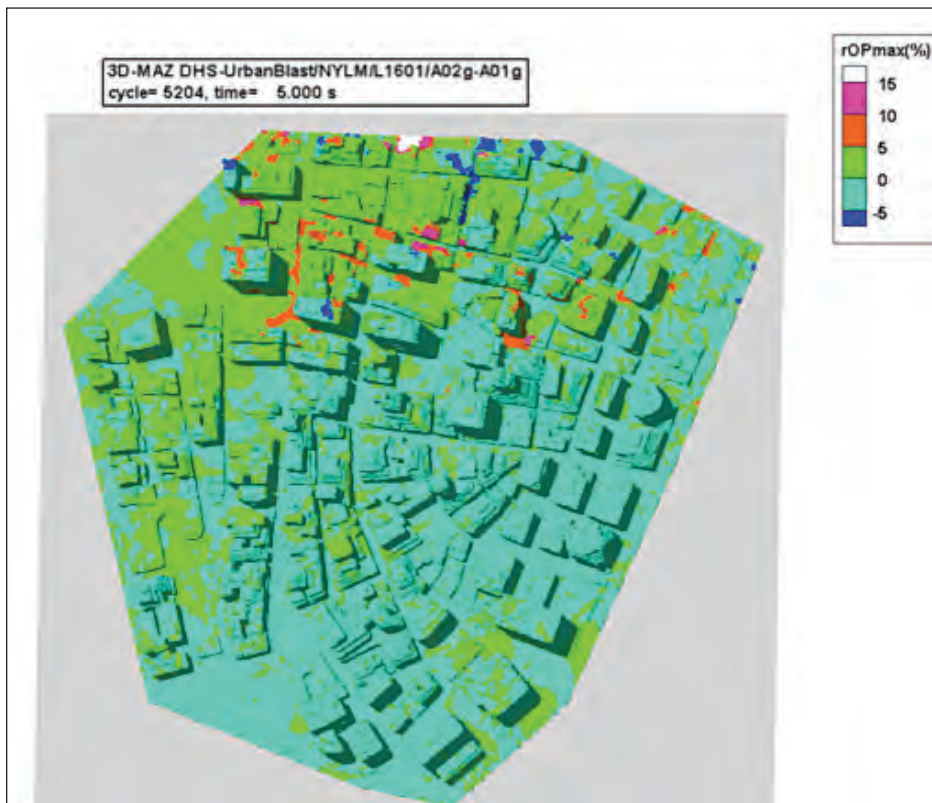


Figure 92:
Increase in maximum
overpressure at 5 sec between
Standard and Overcast Sky
Atmosphere Models for 30,000
lb at Location A

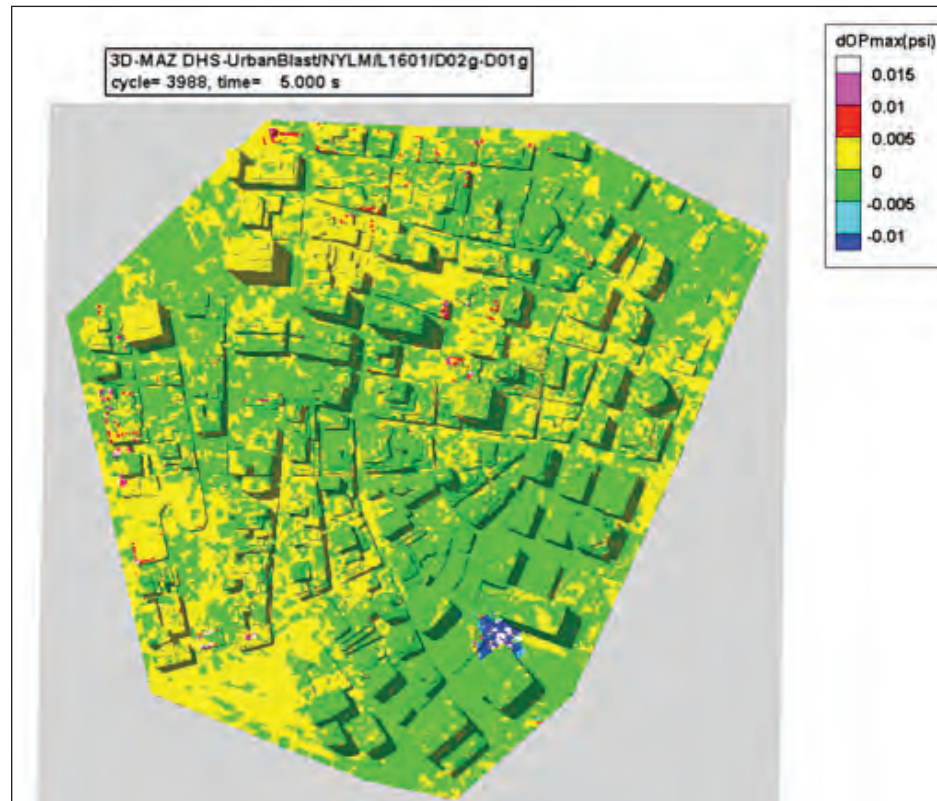
(a) Change in pressure (psi)



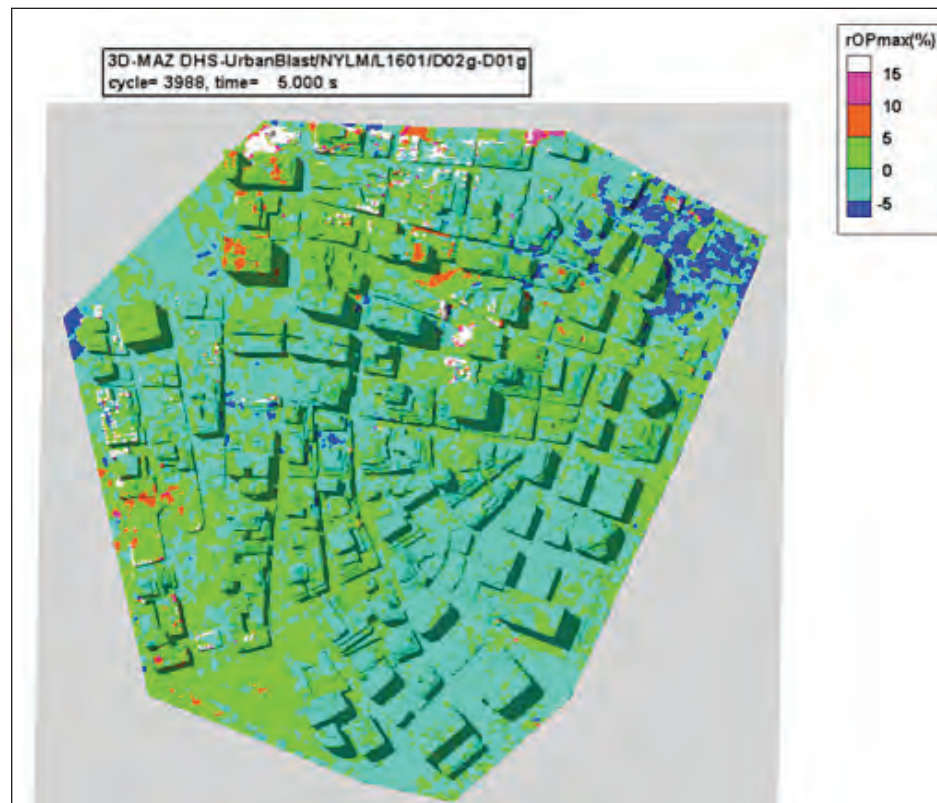
(b) Change in pressure (%)

Figure 93:
Increase in maximum
overpressure at 5 sec between
Standard and Overcast Sky
Atmosphere Models for 1,000
lb at Location A

(a) Change in pressure (psi)



(b) Change in pressure (%)



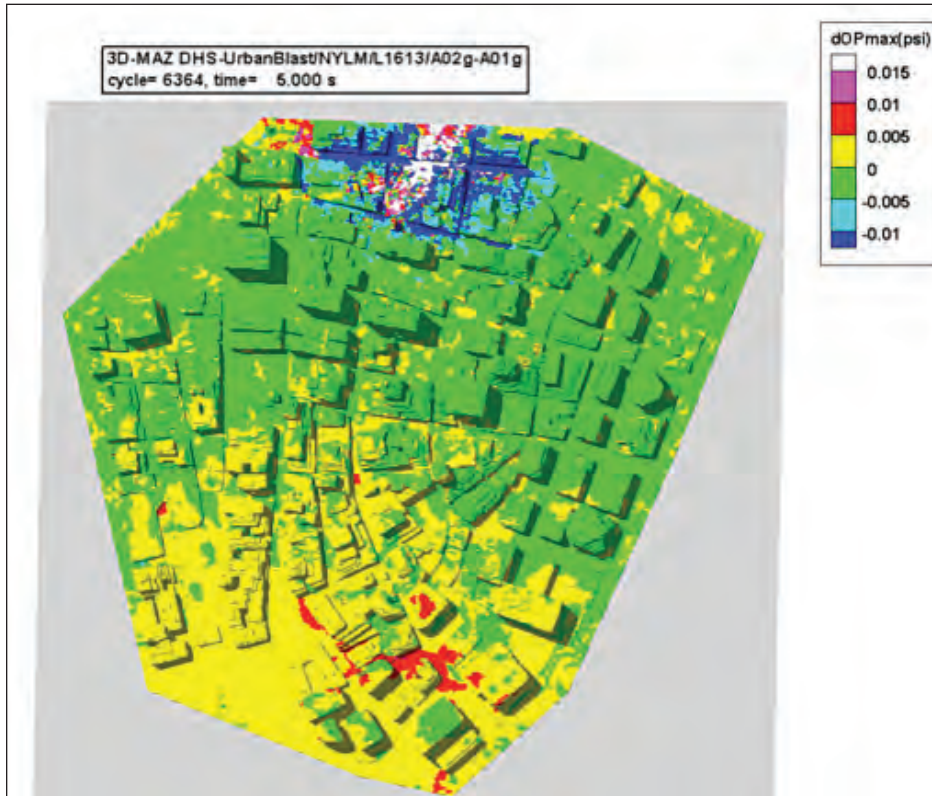
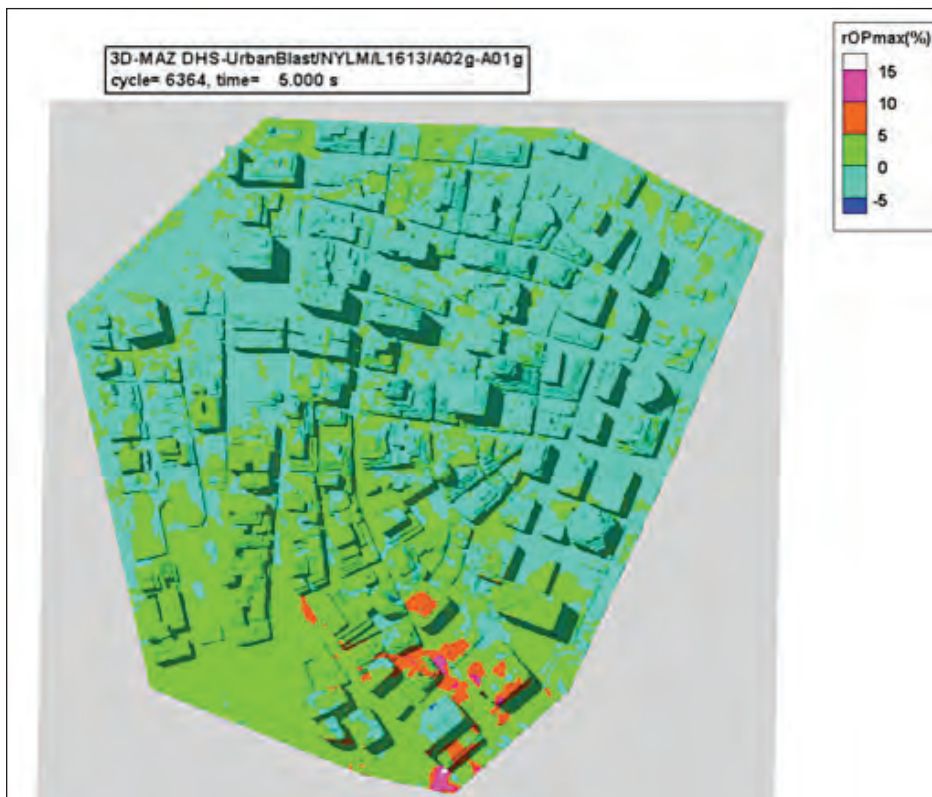


Figure 94:
Increase in maximum
overpressure at 5 sec between
Standard and Overcast Sky
Atmosphere Models for 30,000
lb at Location B

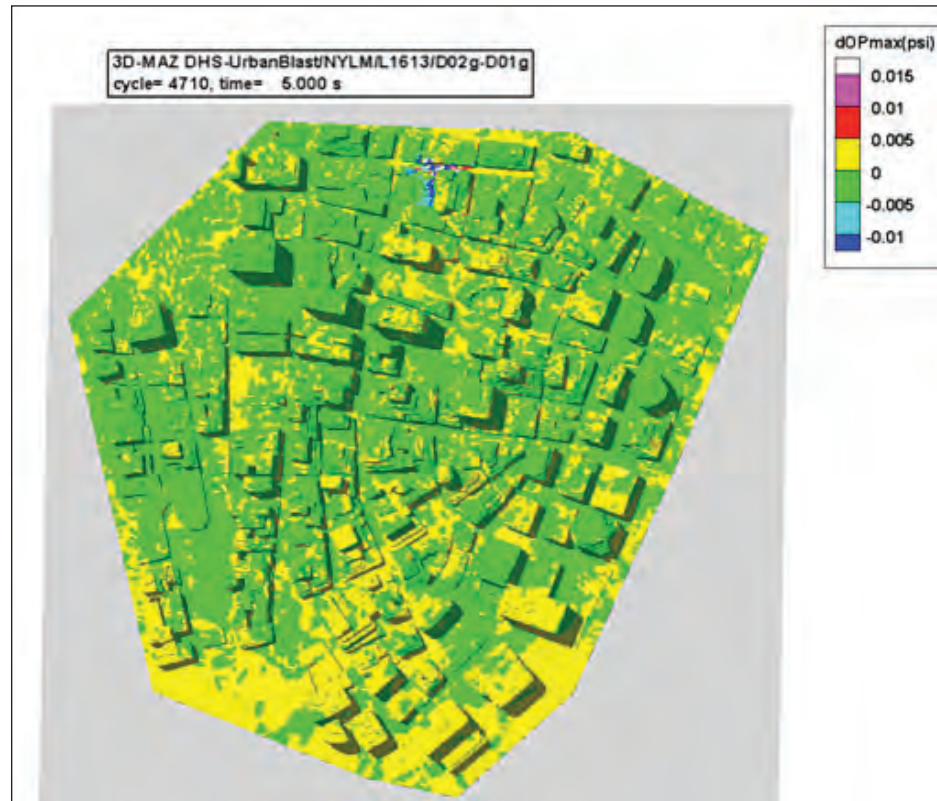
(a) Change in pressure (psi)



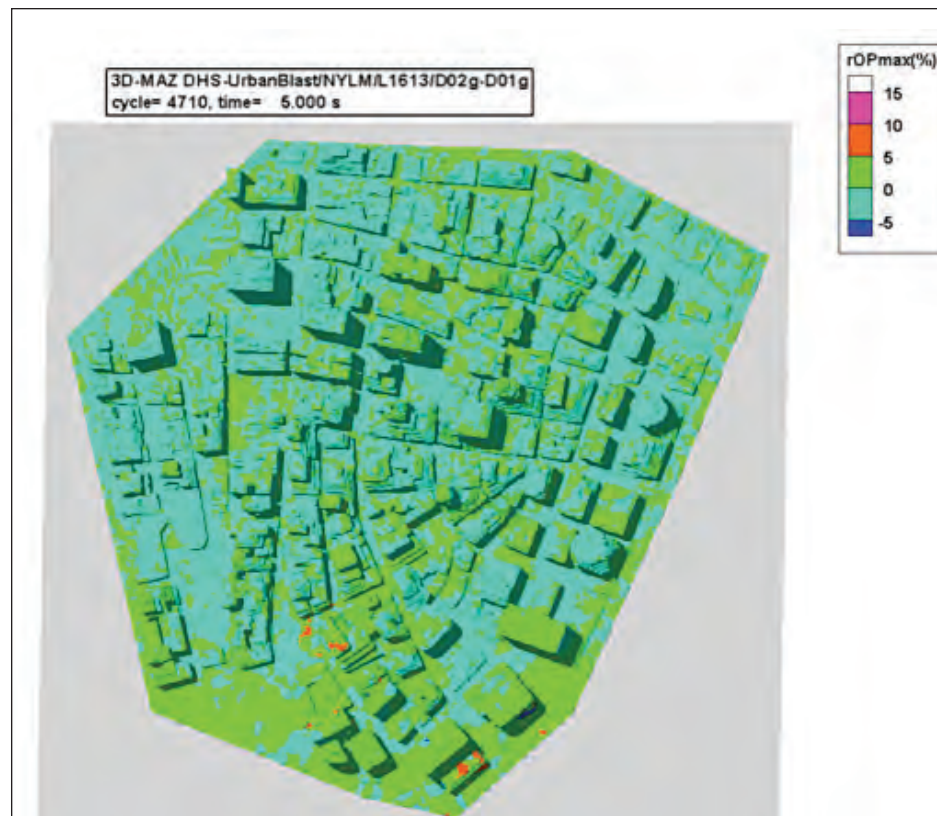
(b) Change in pressure (%)

Figure 95:
Increase in maximum
overpressure at 5 sec between
Standard and Overcast Sky
Atmosphere Models for 1,000
lb at Location B

(a) Change in pressure (psi)



(b) Change in pressure (%)



6

Emergency Evacuation, Rescue and Recovery Equipment Fragilities

The UrbanBlast Tool (UBT) determines the likelihood of damage to Emergency Evacuation, Rescue and Recovery (EERR) systems in response to detonations in urban streetscapes. The EERR assessment component of the UBT software provides first responders guidance on performance of EERR systems in different buildings in response to airblast. The description provided herein summarizes the methodology, the ultimate capacities of equipment items/systems to airblast, validation of computed capacities, generation of fragility curves, and implementation of the data into the software.

6.1 Background

6.1.1 Overview of EERR Systems

Numerous systems and architectural building design features play critical roles in meeting the EERR requirements of a building. The EERR assessment module was designed to provide guidance to first responders, allowing them to make informed decisions regarding their rescue and recovery missions. This module evaluates the likely survival of critical life-safety equipment that supports EERR systems.

A comprehensive array of EERR systems was evaluated including:

1. Egress stair enclosures
2. Stair pressurization systems
3. Fire doors
4. Elevator used during emergencies
5. Emergency communication/fire alarm
6. Emergency lighting
7. Air ducts
8. Conduit chases
9. Emergency generators
10. Fire/Smoke detection systems
11. Sprinkler pipe systems

In evaluating the likely performance of these systems, first responders can make prompt strategic decisions affecting local and regional rescue missions. Note that the methodology is applicable to any other EERR system. As such, adding other systems or equipment to the above list is fairly straight forward and methodical effort.

6.1.2 Available Equipment and System Fragility Data in Response to Blast Loading

An extensive search of archives and repositories of EERR systems subjected to blast loading was conducted. The search resulted in the following two classes of data:

- Fragility data for hardened military grade equipment in response to blast [41]
- Equipment fragility and response data to nuclear blast loading [41]

Equipment fragility data has been developed for some military hardware and equipment. For example, Naval Surface Warfare Center, Dahlgren Division, developed fragility data for command, control, communications, and intelligence (C3I) equipment [41]. Additionally, the Defense Threat Reduction Agency (DTRA) developed pressure fragility definitions for probability of kill of military grade equipment in conjunction with their Munitions Effects Assessment software [18]. Additional references are included in Chapter 9, References [16, 17, 19-40, 42-45].

Equipment fragility data for airblast, reported in the various sources, was generally developed using one of the following methodologies:

- Motion fragility data
- Fragility data developed from nuclear airblast

In all the above referenced cases, the methodologies were straightforward and were premised on an idealization consistent with equipment installed in military facilities or on naval platforms. The methodology for developing equipment fragility data in response to airblast from motion fragility data inherently assumes the equipment is a rigid body that is resiliently mounted. The methodology for developing equipment fragility data in response to nuclear airblast uses fragility data developed from failure of equipment to long-duration impulsive loading and extrapolates the data for short duration. Both methods provide some estimate of the response of military-grade equipment to airblast. Consequently, it was decided that the available methods are not consistent with the current problem definition: conventional EERR systems' response to IED-generated airblast. In addition, several of the considered EERR systems were not considered by other referenced methodologies. A new approach is developed for the purpose of the current work.

6.1.3 Portability of Available Equipment Fragility Data to Commercial EERR Equipment

The methodology using motion fragility data summarized in Section 6.1.2 could be easily implemented to the DHS effort; however, the approach idealizes the equipment as a resiliently mounted rigid body. In the case of commercially available equipment and systems in office buildings in an urban environment, equipment may not be resiliently mounted, unless equipment isolation systems are provided to mitigate equipment-generated vibrations.

The available data and capabilities for assessing the response of metal stud wall and masonry wall systems to airblast was found to be acceptable and appropriate to be used in the Phase 1 UBT.

With regard to the response of specific equipment to airblast, the adaptation/porting of available equipment fragility data to commercial EERR equipment was found to be plausible. However, there are distinct differences between systems participating in the EERR objectives of a building and hardened equipment used to support critical systems used in military applications. For example, fragility data or failure thresholds for several systems (such as emergency lighting or elevator used during emergency systems) were not found.

Since military-grade (i.e., hardened) equipment has significantly greater resilience, the vulnerability of commercial, non-hardened, EERR equipment had to be determined using a different approach.

6.2 Methodology

To determine fragility of specific classes of EERR equipment in response to airblast, a methodology was developed and tailored to determine the fragility of commercial equipment used in the support of critical EERR functions of office buildings in an urban environment. The methodology consists of the following key steps:

- Identification of details that are representative of equipment items found in office buildings, built within the last 50-75 years, and are currently being used within the A/E community.
- Identification of critical vulnerabilities for each equipment item to airblast.
- Determine the mechanism, whose deformation can be used as a gauge of the equipment's performance.
- Representative upper and lower ranges of the mechanism(s) are accommodated, when applicable.
- Develop representative single degree of freedom (SDOF) system for above mechanism(s).
- Assign reasonable uncertainties (coefficients of variation (CV)) to the properties of the SDOF system. These CVs are used to determine the probabilistic features in equipment fragility. Figure 96 shows a typical example of 2D fragility that relates a given loading hazard to probabilities of occurrence of different limit states. Note that the objective of this effort was to generate 3D equipment fragility that relate blast pressure, blast impulse to probabilities of occurrence of different limit states.
- Determine discrete limit states (i.e., capacities at specific levels of performance).
- Determine equipment fragilities, using SDOF, CV, and limit states.
- The mechanisms and limit states are validated against commonly used seismic mechanisms and limit states for different equipment, whenever appropriate.

This methodology is summarized in Figure 97.

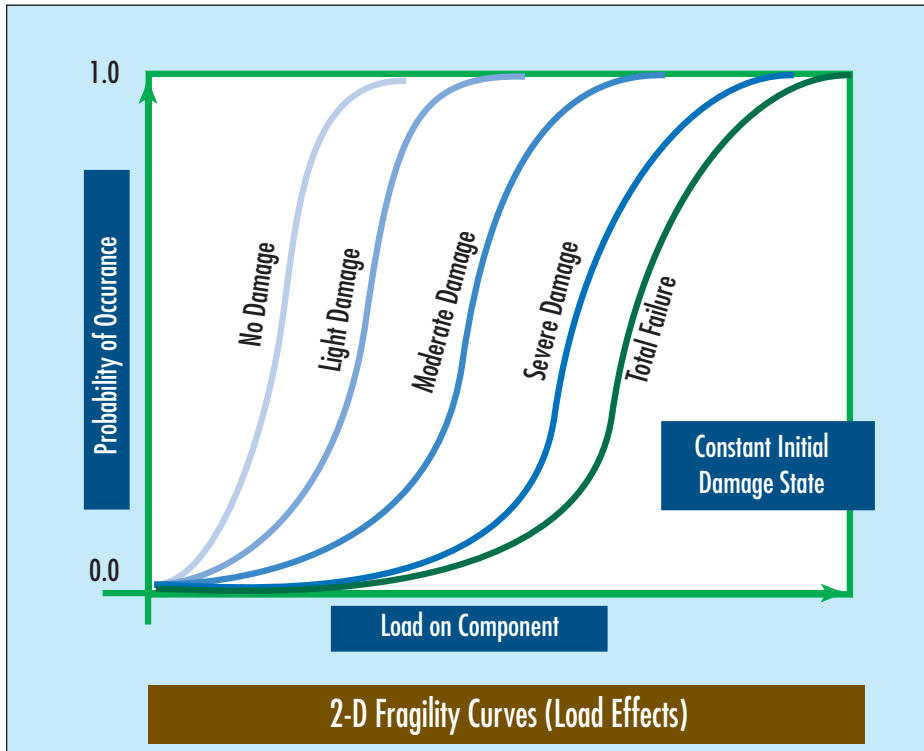


Figure 96:
Typical 2D fragility curves

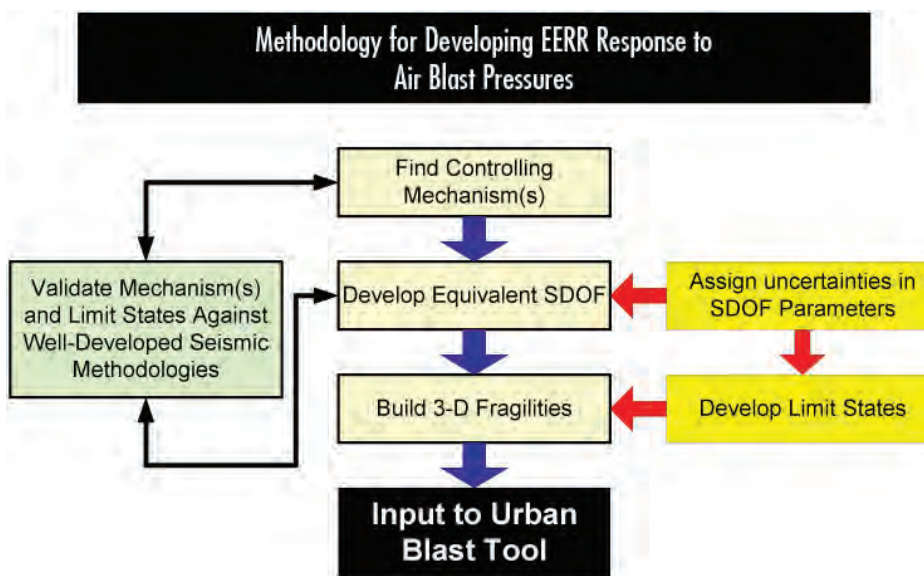


Figure 97:
Basic methodology for
developing EERR equipment
response to airblast pressures

The methodology for determining the fragility of commercial grade EERR equipment and systems to airblast was followed for all items, with the exception of the steel stud wall and masonry unit systems. The methodology inherently accounts for various uncertainties, such as:

- The specific type of equipment items; for example, air-cooled vs. water-cooled generator.

- The specific size of the equipment; for example, 0.75", 1.5", or 3.0" sprinkler pipe.
- The specific design details of the equipment components:
 - Stiffness, for example, 14 gauge plate vs. 18 gauge plate housing for fire alarm control panel.
 - Strength, for example, 36 ksi vs. 50 ksi steel strength for pipe hanger system.

6.2.1 Identifying Representative Details

A comprehensive review of information, identified as representative of typical details for a specific class of equipment items, was obtained from sources such as:

- Personal communication with practicing professionals: mechanical, electrical, plumbing, fire/life-safety engineers, and architects.
- Pamphlets and brochures provided by specific equipment manufacturers.
- Vendor and manufacturer data posted online.

In one instance, a complete set of drawings for a commercial elevator door operator and associated systems was located and verified as representative by industry professionals. As another example, the representative details and dimensions for fire alarm control panels were obtained after reviewing numerous specifications for fire alarm control panels provided by vendors.

A thorough review of the compiled information allowed the prevailing details, or details most representative of equipment types likely to have been installed in urban commercial office buildings constructed in the last 50 years, to be identified.

6.2.2 Identifying Critical Vulnerabilities of Equipment and Determining Prevailing Damage Mechanism to Airblast

The compiled raw data for the representative details for the specific classes of equipment was carefully reviewed. Damage mechanisms were identified for specific equipment components, and their relative strengths to overpressures were compared in order to identify the critical vulnerability that would be the first to affect the continued operation of the specific equipment item. The review of component vulnerability was supplemented by input from practicing industry professionals.

Following this approach, the critical vulnerability for each representative equipment item that could be used to assess the equipment system's performance to airblast was identified. A good example of the identification of critical vulnerabilities can be seen in the failure of the emergency communication system. After reviewing the vulnerability of a typical fire alarm loop, vulnerability of discrete units (horns and strobes), and the vulnerability of a fire alarm control panel, the critical vulnerability of this system was found to be the disabling of the fire alarm control panel, which is typically located in the ground floor lobby.

6.2.3 Determining Discrete Limit States

Once the prevailing damage mechanism was identified for the critical vulnerability of an equipment item, discrete limit states were determined. These limit states are:

1. Onset of damage: Pristine condition.
2. Intermediate damage states: These limit states are equipment-dependent. For brittle equipment, there are no intermediate limit states. For ductile equipment, there can be one or more intermediate limit states.
3. Failure state.

Determining limit states involved identifying a specific extent of stress, deformation, or strain that the critical component can sustain in response to a specific magnitude of blast loading before exceeding a specified performance level.

6.3 Determination of Performance of Equipment in Response to Airblast

The methodology for all EERR equipment items reviewed was described in Section 3. Following is a summary of the critical review of the different systems studied over the course of this effort.

6.3.1 Egress Stair Enclosures

Stairway enclosures serve as a means of egress from the facility in the event of an emergency and serve a critical function in EERR objectives for first responders. Two representative classes of stairway enclosure systems were considered in this effort:

- Stud wall systems
- Concrete masonry unit (CMU) wall system



Figure 98:
Example of egress stairwell

SOURCE: WEIDLINGER
ASSOCIATES, INC.

Stud wall systems are commonly used for egress stair enclosures in modern construction; however, buildings constructed more than 20 years ago are likely to use CMU wall systems for stairway enclosure. An example of an emergency egress stairway is shown in Figure 98.

The responses of stud wall and CMU wall systems to airblast have been studied by various government organizations. The U. S. Army Corps of Engineers has developed a fast running tool, Component Explosive Damage Assessment Workbook (CEDAW), that is based on their Protective Design Center's Facility and Component Explosive Damage Assessment Program (FACEDAP), supplemented by test data in a way that SDOF techniques can be used to consider response modes of tension membrane and arching. CEDAW can be used to assess the response of metal stud wall systems, unreinforced and reinforced masonry wall systems, reinforced concrete wall systems, and others. CEDAW produces the pressure-impulse (P-I) diagrams for

a specific component by unscaling dimensionless P-I relationships for each component. The P-I curves are produced by applying the Kingery-Bulmarsh relationships for HE explosives in a hemispherical surface burst configuration. [43]

Stud wall and CMU wall systems were analyzed to determine their lower bound resistance to blast pressures. Table 4 summarizes the different performance levels considered for each enclosure wall system. The levels of performance of the walls systems are comparable to level of protection descriptions provided in Protective Design Center, PDC-TR 06-08 Rev 1, *Single Degree of Freedom Structural Response Limits for Antiterrorism Design* [44].

Table 4: Wall performance levels considered in determining fragility data

| Level of Wall Performance | Description of Wall Damage |
|---------------------------|--|
| Superficial Damage | Wall has no visible permanent damage. |
| Moderate Damage | Wall has some permanent deflection. It is generally repairable, if necessary, although replacement may be more economical and aesthetic. |
| Heavy Damage | Wall has not failed, but it has significant permanent deflection causing irreparable damage. |
| Hazardous Failure | Wall has failed, and debris velocities range from insignificant to very significant. |

For the initial release of the UBT software, bounds to the performance of the egress stair enclosure were provided by using two performance levels: superficial damage was used as a measure of the *onset of damage* and heavy damage was used as a measure of the *failure* of the stairway enclosure system.

To reflect the variation in construction of non-load bearing CMU walls found in common building design, four CMU wall conditions were considered:

- Case A: 8" CMU wall, unreinforced, 12 ft high
- Case B: 8" CMU wall, unreinforced, 20 ft high
- Case C: 8" CMU wall, grouted reinforced, 12 ft high
- Case D: 8" CMU wall, grouted reinforced, 20 ft high

Of these four systems, Case A was identified as the most likely condition to exist in buildings spanning 50+ years of construction. The analysis of the CMU wall systems assumed the following conditions:

- Simply supported boundary conditions for lateral loading
- Compressive strength of CMU and grout is 1,800 psi
- Every other cell is grouted
- CMU reinforced with #6 bars (60ksi) placed every 16" on center

With the identified details of the prevailing system, pressure-impulse curves for specific limit states were obtained using the CEDAW utility [43].

6.3.2 Stair Pressurization Systems

Stair pressurization systems serve a critical function in EERR objectives of a facility by providing an egress stair with fresh air, smoke extraction, and preparing the stairwell as exit way in emergency situations for occupants as well as emergency rescue teams [49]. Stair pressurization is a fairly recent system to be implemented in support of EERR objectives; therefore, only information for recently manufactured units served as the basis for this review.

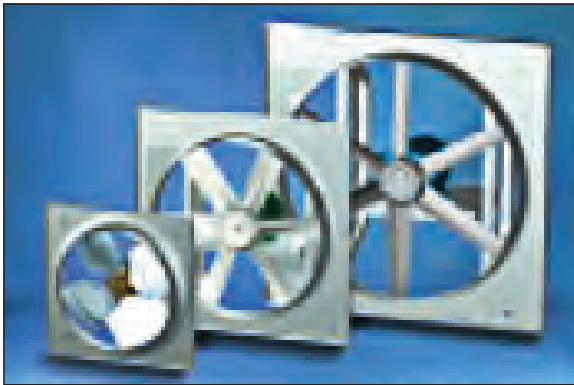


Figure 99:
Example of stair pressurization fans used in office buildings

SOURCE: FEMA

A typical stair pressurization system consists of an air supply and air release unit, a fan box made from galvanized metal sheet with insulation, as shown in Figure 99. Typically, air supply units are distributed evenly over the height of a stairwell system, where the maximum distance between air supply units does not exceed three stories.

Stair pressurization units vary in size and weight. Correspondingly, the blades of the fan and the hub are available in different sizes and shapes.

Bending of the aluminum blades was identified as the dominant damage mechanism that would precipitate the deactivation of the stair pressurization system. Stair pressurization systems were analyzed to determine their lower bound resistance to impulsive pressure loads.

Two representative stair pressurization system unit types were studied to span the range of capacities of available systems:

- Case A: 4,000 CFM unit
- Case B: 64,000 CFM unit

The analysis of the stair pressurization system unit assumed that the aluminum blade is cantilevered from the hub. Considering the wide variety of blade shapes, a rectangular shape of blade was assumed, with the blade material likely being aluminum with yield strength of 13.8 ksi. The most vulnerable blade cross section adjacent to the blade-hub connection is a rectangular solid cross section with:

- Case A: thickness $t = 0.157$ " (4 mm), width 3.5", and length 7"
- Case B: thickness $t = 0.315$ " (8 mm), width 7.8", and length 15.7"

The limit states for representative stair pressurization units with smaller blades (lower bound) and larger blades (upper bound) were determined, based on the damage mechanism associated with the bending of the fan blades. Table 5 lists the blast pressure on the blades for the different limit states.

Table 5: Limit states of the stair pressurization system unit

| Level of Performance | Blast Pressures (psi) | |
|----------------------|-----------------------|--------|
| | Case A | Case B |
| Onset of Damage | 2.3 | 1.85 |
| Failure | 3.49 | 2.77 |

6.3.3 Fire Doors

Areas of a building may be separated into fire compartments. These compartments are linked by fire doors of specific fire rating. Fire doors serve a critical function in EERR objectives of a facility that establishes compartmentalization, as well as access to emergency egress corridors for both building occupants and emergency evacuation teams.

A typical fire door opens in only one direction, restrained by a set of hinges and a latch, see Figure 100. In the opposite direction, the door bears on the door jamb on three sides. Combined bending and shear failure of the latch was identified as the dominant damage mechanism that would precipitate the deactivation of the fire door.

Fire doors were evaluated in this effort with the following representative details:

- Door geometry: 3.3 ft width, 7.2 ft height
- The latch cross section: 0.39" x 0.5"
- Steel latch material: 36 ksi yield strength
- Effective door weight: 350 lbs



Figure 100:
Example of fire door in
commercial building

SOURCE: UNITED STATES OFFICE
OF COMPLIANCE SAFETY AND
HEALTH

The limit states for a representative fire door was determined, based on the damage mechanism associated with the bending and shear of the door latch. Table 6 lists the computed blast pressure on the representative fire door for the different limit states.

Table 6: Limit states of representative fire door

| Level of Performance | Blast Pressures (psi) |
|----------------------|-----------------------|
| Onset of Damage | 1.17 |
| Failure | 1.76 |

6.3.4 Elevator Used During Emergencies

In emergency conditions, existing elevator systems within a building may be used by emergency response teams for EERR purposes. Conventional elevator systems in commercial buildings consist of a cab with doors that are actuated by a door operator, located above or below the door mechanism. Typical elevator systems are powered by electric motors with either a cable/counterweight system or a piston actuated by hydraulic fluid.



Entry to an elevator cab from any floor requires that two sets of parallel doors open:

- Elevator doors at a particular level that grant access to the hoistway (Figure 101).
- Elevator cab doors that grant access to the cab itself.

Opening an elevator door requires the movement of several door components. The failure of any one of these components will restrict access to the elevator cab. When a dynamic pressure impinges on the elevator doors, the lateral load engages the door hanger, which hangs from a door roller that runs on a track. When the attachment between the door hanger and the track is in any way disrupted, the elevator door will fail to open.

Figure 101:
Example of elevator doors installed in a commercial building

SOURCE: WEIDLINGER ASSOCIATES, INC.

The lateral deformations of the up-thrust roller against the track walls are the most likely damage failure mechanism that will precipitate the failure of the elevator. When sustaining significant deformations, the track will restrict the door hanger movement and the ability to open the elevator door.

Elevator doors were evaluated in this effort with the following representative details:

- Two doors: each 2 ft width, 7 ft height
- Track plating thickness: 1/8"
- Steel track material: 36 ksi yield strength

The limit states for a representative elevator were determined, based on the damage mechanism associated with the bending of the elevator door rail. Table 7 lists the computed blast pressures on the representative elevator doors for the different limit states.

Table 7: Limit states of representative elevator door system

| Level of Performance | Blast Pressures (psi) |
|----------------------|-----------------------|
| Onset of Damage | 2.1 |
| Failure | 3.3 |

6.3.5 Emergency Communication/Fire Alarm

The fire alarm system is a critical component of the EERR objectives of a commercial office building in an urban environment. It is used to alert the building occupants of the need to evacuate in case of a fire or other emergency. Fire alarm systems consist of a fire alarm control panel interconnected with devices (i.e., horns and strobes) via a fire alarm loop extending over the entire building.

The fire alarm control panel is a critical component of the electrically powered fire alarm system. Typically, the panel, as illustrated in Figure 102, is located at the ground floor lobby of a building inside a multipurpose cabinet adjacent to the fire command station. This cabinet commonly houses other systems, such as a fan control panel used to regulate smoke



Figure 102:
Example of fire alarm control panel in commercial building

SOURCE: WEIDLINGER ASSOCIATES, INC.

purge and smoke exhaust fans. Cabinet containing the fire alarm control panel will weigh approximately 500 lb for small office buildings and approximately 1,000 lb for large office buildings. Much of the weight of these fire control panels consists of the co-located battery backup.

The fire command station communicates with the occupants of a building via horns and strobes in the event of an emergency. The devices are located on every floor in numerous locations and communicate with occupants through audible and visual means. Because multiple devices are located on each floor, damage to any one of the devices has only a regional impact. The vulnerability of these devices will most likely depend on the performance of the non-structural system on which they typically are mounted (i.e., stud wall system or CMU wall).

The failure of the fire alarm control panel in the lobby of the building was considered the dominant damage mechanism that would precipitate the failure of the fire alarm system. Several failure mechanisms of the fire alarm control panel were analyzed to determine their lower bound resistance to impulsive pressure loads.

The localized failure of the fire alarm control panel was attributed to the deformations (in bending) of the sheet metal housing of the cabinet containing the fire alarm system that would inhibit access the controls. The analysis of the fire alarm control panel assumed the following conditions [17]:

- Simply supported boundary conditions for lateral loading
- Sheet metal housing: 18 gauge
- A36 steel with an ultimate capacity of 58 ksi
- Panel walls sized at 18" x 48"

The limit states for a representative fire alarm control panel were determined, based on the damage mechanism associated with the bending of the sheet metal housing. Table 8 lists the computed blast pressure on the representative fire alarm control panel for the different limit states.

Table 8: Limit states of representative fire alarm control panel

| Level of Performance | Blast Pressures (psi) |
|----------------------|-----------------------|
| Onset of Damage | 0.34 |
| Failure | 0.54 |

6.3.6 Emergency Lighting

Emergency lighting is a battery-backed lighting system that is activated automatically when a building experiences a power outage. Emergency lighting serves a critical function in EERR objectives of a facility, serving both the occupants exiting the building as well as emergency rescue teams entering into a building during an emergency. Additionally, emergency lighting serves a critical role in offering increased visibility in cases of fire with accumulated smoke conditions.

An emergency lighting system, most commonly used in office buildings, consists of the existing lighting infrastructure, as opposed to a regionally independent emergency lighting device, as shown in Figure 103. Emergency lighting would be activated with the loss of power, either via emergency power or a regional battery backup for the lighting device. Lighting fixtures commonly used in industry use fluorescent light bulbs, with a cylindrical annealed glass bulb.



Figure 103:
Example of emergency lighting system in commercial building

SOURCE: WEIDLINGER ASSOCIATES, INC.

The cracking of the glass bulb was considered the dominant damage mechanism that would precipitate the failure of the emergency lighting system. Several emergency lighting systems were analyzed to determine their lower bound resistance to impulsive pressure loads.

To reflect the variation in existing lighting infrastructure found in common building design, two types of fluorescent light bulbs were considered:

- Case A: 48" fluorescent light bulb
- Case B: 96" fluorescent light bulb

Although both systems were considered, the 48" bulb was identified as representative of most installed configurations.

The capacity of fluorescent light bulbs was determined on the basis of a glass bulb failing as a result of cracking. The critical damage mechanism of the glass bulb was assumed to be bending. The analysis of the fluorescent light bulbs assumed the following conditions:

- Simply supported boundary conditions for lateral loading
- Outer diameter of bulb: 1.0"
- Bulb thickness: 0.0295" (0.75mm)
- Tensile capacity of annealed glass: 12,300 psi (assuming a probability of 500 breaks per thousand)

- Bulbs are not pressurized
- Elasticity: perfectly brittle glass material (i.e. no ductility)

The value corresponding to fluorescent light bulb failure is summarized in Table 9. Note that the limiting value is consistent with the minimum impulse value at specified level of performance.

Table 9: Limit state of representative fluorescent light bulbs

| Level of Performance | Blast Pressures (psi) |
|----------------------|-----------------------|
| Failure | 0.91 |

6.3.7 Air Ducts

Ducts are key elements in delivering and removing air in the heating, ventilation, and air conditioning (HVAC) of a building. Air ducts, a term that encompasses supply air, return air, and exhaust air, serve in the overall ventilation of the designed public space. Given the role the ducts serve in the condition of the air occupants breathe, the air duct system serves a critical function in EERR objectives of a facility.

Ducts are key elements in delivering and removing air in the heating, ventilation, and air conditioning (HVAC) of a building

Generally, air ducts are attached to the overhead slab structure, most commonly with trapeze support systems or brackets. The ducts are typically fabricated out of 36 ksi sheet metal (steel). The limiting sizes of air ducts are provided in Table 10:

Table 10: Representative air duct dimension, thickness

| Duct Class | Width [inch] | Height [inch] | Sheet Metal Thickness [inch] |
|------------|--------------|---------------|------------------------------|
| Small | 8.0 | 8.0 | 3.937E-3 |
| Large | 124.0 | 124.0 | 4.92E-3 |

Because air ducts are typically reinforced from the exterior, to sustain the pressurization of air inside the duct itself, the bending of the steel brackets, was identified as the dominant damage mechanism that would precipitate the deactivation of the air duct system. Analyses were performed for air ducts of various sizes to determine their lower bound resistance to blast pressure loads.

Table 11 summarizes the blast pressure at which the different limit states occur.

Table 11: Limit states of representative air duct system

| Level of Performance | Small Exposure (psi) | Large Exposure (psi) |
|----------------------|----------------------|----------------------|
| Onset of Damage | 0.18 | 0.012 |
| Failure | 0.27 | 0.017 |

6.3.8 Conduit Chases

Chases are defined as confined spaces dedicated to enclosing pipes (sometimes referred to as pipe chase) and other conduits as they interconnect two adjacent spaces. Conduit chases are found behind walls or in spaces not immediately accessible and out of view of the occupants. These conduit chases commonly enclose critical utilities and services supporting the EERR objectives of a facility.

In commercial office buildings, conduit chases are commonly constructed using a stud wall system with gypsum board. The wall system spans between floors, braced at both top and bottom. An example of a stud wall system is illustrated in Figure 104.

These wall systems were analyzed to determine their lower bound resistance to blast pressures. Table 12 summarizes the different performance levels considered for each enclosure wall system. The levels of performance of the walls systems are comparable to level of protection descriptions used in CEDAW [43].



Figure 104:
Example of a stud wall system commonly used to construct chases

SOURCE: WEIDLINGER ASSOCIATES, INC.

Table 12: Wall performance levels considered in determining fragility data

| Level of Wall Performance | Description of Wall Damage |
|---------------------------|---|
| Superficial Damage | Wall has no visible permanent damage |
| Moderate Damage | Wall has some permanent deflection. It is generally repairable, if necessary, although replacement may be more economical and aesthetic |
| Heavy Damage | Wall has not failed, but it has significant permanent deflection causing it to be unreparable |
| Hazardous Failure | Wall has failed and debris velocities range from insignificant to very significant |

For the initial release of the software, bounds to the performance of the chase wall enclosure was provided by only using two of the performance levels: superficial damage was used as a measure of the onset of damage and heavy damage was used as a measure of the failure of the chase enclosure system.

To reflect the variation in stud wall construction found in common building design, four stud wall conditions were considered:

- Case A: 12 gauge 12 ft high stud wall system
- Case B: 16 gauge 12 ft high stud wall system
- Case C: 12 gauge 20 ft high stud wall system
- Case D: 16 gauge 20 ft high stud wall system

The analysis of the stud wall systems assumed the following conditions:

- Simply supported boundary conditions for lateral loading
- 6" studs spaced 16" on center
- A572 steel for studs
- ½" gypsum wallboard

A commonly found stud wall configuration that would likely serve as the walls of a conduit chase is Case B: 16 gauge 6" studs, 12 ft high. With the identified details of the prevailing system, pressure-impulse curves for specific limit states were obtained using the CEDAW utility [43].

6.3.9 Emergency Generators

Emergency generators provide electricity to a building in case of a power outage. Emergency generators serve a critical function in EERR objectives of a facility by providing a backup source of power to critical equipment and systems during interruption of the electric utility service.



Figure 105:
Example of a generator found
in a commercial building

SOURCE: FEMA

Emergency generators in commercial buildings are commonly installed either at the ground floor, building mid-height (at a mechanical level with louvered openings), or at the top level of a building. An example of a commercial grade generator is shown in Figure 105. Generators can be either air cooled or water cooled. A common emergency generator system in urban settings is cooled with water delivered via hoses with clamped connections.

Damage to the water cooling pipe, which acts as a cantilever connected to the housing of the emergency generator, due to excessive bending was identified as the dominant damage mechanism that would precipitate the shutdown of the emergency generator system; the failure of the cooling pipe would quickly result in the overheating of the generator. Commercial emergency generators, commonly found in residential buildings, were analyzed to determine their lower bound resistance to blast loads. Generators found in office buildings were analyzed to provide a basis for comparison. The representative residential and office building generator system were identified as a 45kW unit and 100kW unit engine, respectively.

The analysis of the emergency generator systems assumed the following representative details:

- 2,100 lb weight of generator system
- Clamped boundary condition of the water cooling pipe
- Pipe size: 3.5" O.D., 3.3" I.D.
- Pipe length: 5 ft
- Pipe material: A36 steel

The generator set in the residential building was assumed to weigh 2,100 lbs.

The limit states of the representative emergency generator were determined. Table 13 summarizes the blast pressures at which these limit states occur.

Table 13: Limit states of representative emergency generator [34]

| Level of Performance | Blast Pressures (psi) |
|----------------------|-----------------------|
| Onset of Damage | 6.57 |
| Failure | 8.35 |

6.3.10 Fire/Smoke Detection System

Fire and smoke detection systems consist of devices that detect fire and smoke and are connected to the fire alarm system. Fire and/or smoke detectors serve a critical function in EERR objectives of a facility by detecting fire and/or smoke at an early stage and helping to localize the fire event and notify building occupants.

A representative fire/smoke detection system was identified to consist of the pipe system and the laser detector with the following representative details:

- Pipe diameter (1.0") and thickness (0.174")
- Pipe is suspended from ceiling slab system at a 5' spacing
- The pipe material is plastic
- Pipe weight is 0.168lb/ft

For fire/smoke detection system (an example of a detection device is shown in Figure 106), whether suspended from a ceiling slab or affixed to a wall system, the prevailing damage mechanism would be damage sustained by the stud wall system on which the fire/smoke detection system would be mounted.

The analysis of the stud wall system assumed the following conditions:

- Simply supported boundary conditions for lateral loading
- 6" studs spaced 16" on center
- A572 steel for studs
- ½" gypsum wallboard

A commonly found stud wall configuration that would likely serve as the walls of a conduit chase is 16 gauge 6" studs, 12ft high.[35] With the identified details of the prevailing system, pressure-impulse curves for specific limit states were obtained using the CEDAW utility. WAI generated pressure-impulse curves for the enclosures using the CEDAW utility [43], and this information is summarized in Table 14.

Table 14: Limit states of representative smoke detection system

| Level of Performance | Blast Pressures (psi) |
|----------------------|-----------------------|
| Onset of Damage | 6.57 |
| Failure | 8.35 |

6.3.11 Sprinkler System

Sprinkler systems [38] offer fire protection for corridors, elevator lobbies, and storage areas. Sprinklers reduce the amount of smoke generated during a fire, as well as the rate of burning. Sprinklers limit the expansion of fire and, therefore, serve a critical function in EERR objectives of a facility. An example of a fire sprinkler main is illustrated in Figure 107. Figure 108 shows a schematic of a sprinkler pipe supported by hanger rods.

Fire sprinkler system pipes are commonly suspended below the ceiling slab at every building floor with clevis-type hanger rod systems. The sprinkler pipes are typically fabricated out of steel, light wall steel, copper, chlorinated polyvinyl chloride (CPVC), or polybutylene (PB); Table 15 provides typical dimensions [46].



Figure 106:
Example of fire detection device in a commercial building

SOURCE: OSHA

Figure 107:
Example of fire sprinkler
system installed in a
commercial office building

SOURCE: U.S. OFFICE OF
 COMPLIANCE SAFETY AND
 HEALTH



Figure 108:
Schematic of sprinkler pipe
supported by hanger rods

SOURCE: WEIDLINGER
 ASSOCIATES, INC.

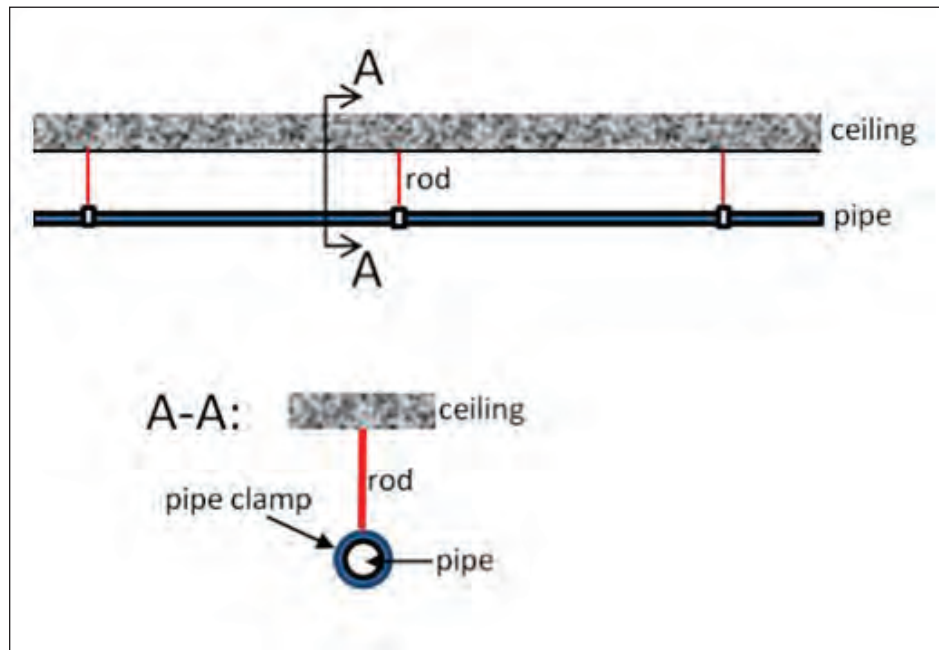


Table 15: Representative sprinkler pipe size and weight

| Nominal Size [in] | Steel Pipe[kg/m] | Typical Lightwall Steel[kg/m] | Copper [kg/m] | CPVC [kg/m] | PB [kg/m] |
|-------------------|------------------|-------------------------------|---------------|-------------|-----------|
| 0.75 | N/A | N/A | 0.49 | 0.25 | 0.13 |
| 1.0 | 2.5 | 1.82 | 0.68 | 0.39 | 0.20 |
| 1.25 | 3.38 | 2.35 | 1.01 | 0.62 | 0.31 |
| 1.5 | 4.05 | 2.8 | 1.40 | 0.82 | 0.43 |
| 2.0 | 5.43 | 3.75 | 2.17 | 1.28 | 0.73 |
| 2.5 | 8.62 | 6.07 | 3.02 | 1.87 | N/A |
| 3.0 | 11.3 | 7.46 | 3.99 | 2.78 | N/A |

The analysis of the fire sprinkler system assumed the following conditions:

- Sprinkler pipe is a continuous beam supported by the hanger rods at a 6 ft spacing
- Rod diameter is 3/8"
- Rod is clamped at the ceiling slab; length of hanger rod is 10"
- A36 steel for the rods

The dominant damage mechanism for the sprinkler pipe system is the bending of the steel hanger rods which support the sprinkler line. Damage to the hanger rod will lead to excessive deformation of the sprinkler line, likely causing a failure of the sprinkler line. Analyses have been performed with fire sprinkler systems of various sizes to determine their lower bound resistance to blast loading.

The limit states of the representative sprinkler pipe system were determined. Table 16 summarizes the blast pressures at which these limit states occur.

Table 16: Limit states of representative fire sprinkler system

| Level of Performance | Blast Pressures (psi) |
|----------------------|-----------------------|
| Onset of Damage | 0.11 |
| Failure | 0.19 |

6.4 Validation of Methodology of Determining Limit States

The methodology of determining critical damage mechanism affecting the performance of representative EERR systems was validated in order to demonstrate it accurately identified the damage mechanisms that lead to disabling of the equipment. The equipment items included in the validation effort were those for which pressure-impulse data was not obtained using the CEDAW utility. (The CEDAW utility has been validated elsewhere.)

Following the 2006 International Building Code (IBC), ASCE 7-10 was used to compute the seismic design forces for equipment items, as nonstructural components. The seismic design requirements for nonstructural components (consistent with the representative systems in this effort) are listed in CEDAW Chapter 13 as:

 Equation

$$F_p = \frac{0.4a_p S_{DS} W_p}{\left(\frac{R_p}{I_p}\right)} \left(1 + 2\frac{z}{h}\right)$$

Where:

F_p is the horizontal seismic design force

a_p is the amplification factor related to the response of a system or component as affected by the type of seismic attachment

S_{DS} is the spectral response acceleration parameter at short periods

W_p is the component operating weight

z is the height in structure of point of attachment of component with respect to the base

h is the average roof height of structure with respect to the base

R_p is the component response modification factor

I_p is the component importance factor

Taking into account different component amplification factors, response modification factors, and component importance factors for each class of equipment/system, a representative seismic design force was computed. The weight of the entire equipment item was used in this evaluation.

Because seismic design forces are designed to preclude failure, a damage factor (ξ) was used to obtain the seismic failure force, which would lead to disabling or failing of the specific EERR system:

$$F_{p\xi} = F_p * \xi$$

A damage factor (ξ) of 1.5 was used, based on commonly used safety factors found in structural design codes. (See, for example, ATC-3)[21].

The enhanced seismic design force ($F_{p\xi}$) was compared against blast forces on equipment components for limit states corresponding to *failure*. The pressures computed at specific limit states were integrated over the exposed surface area of the specific component to obtain an effective blast force that could be compared against the enhanced seismic design force. Because both seismic forces of the above equations and the computed blast pressures were computed for an equivalent static system, the comparison against the enhanced seismic design force was considered valid.

The comparison of the two quantities was used as an effective means of validating the methodology for determining the critical damage mechanism affecting the performance of the representative EERR systems. When the two computed forces were deemed comparable, the damage mechanism and characterization of EERR equipment performance was considered validated.

All EERR systems for which pressure-impulse data was not available were successfully validated. Table 17 summarizes the ratios of the integrated blast pressures and the enhanced seismic design forces for all EERR system considered in this effort. In numerous instances more than one system was considered, so as to assess the range of likely equipment items that might be found in commercial building in an urban environment. In cases where more than one system was evaluated, the average ratio was reported. This approach is consistent with the practice used in seismic designs of EERR equipment and was deemed adequate, given the resolution of the current project.



Table 17: Summary of validation of methodology

| Evaluated EERR Equipment/System | Average Comparative Ratio |
|------------------------------------|---------------------------|
| Egress Stair Enclosures | N/A ⁶ |
| Stair Pressurization Systems | 1.7 |
| Fire Doors | N/A ⁷ |
| Elevator Used During Emergencys | 0.9 |
| Emergency Communication/Fire Alarm | 0.8 |
| Emergency Lighting | 1.4 |
| Air Ducts | 2.5 |
| Conduit Chases | N/A ⁸ |
| Emergency Generators | 0.6 |
| Fire/Smoke Detection Systems | N/A ⁹ |
| Sprinkler Pipe System | 0.8 |

The comparative ratios reported in Table 17 indicate that the identified damage mechanisms are reasonable to implement in the performance assessment of the EERR systems to airblast.

6.5 Generation of 3D Fragility Curves

With damage mechanisms validated, dynamic nonlinear single degree of system (SDOF) models were developed for each of the critical components governing the performance of the EERR equipment. Using the SDOF analyzer, pressure-impulse (P-I) curves were obtained for each limit state of each EERR equipment item and system. Where possible, the blast loading precipitating a specific limit state for a given equipment item was compared to fragility data for hardened equipment used to support critical systems in military applications.

⁶ Method validated in Reference 28

⁷ Seismic mechanism is different from Airblast mechanism, as such direct comparison is not valid.

⁸ Method validated in Reference 28

⁹ Method validated in Reference 28

For ductile systems, a displacement ductility of 1.0 was identified as an *onset of damage*, a ductility of 6.0 was considered *medium level of damage*, and a ductility of 12.0 was considered as *failure*. For brittle modes of failure, *onset of damage* and *failure* were both identified as a ductility of 1.0. P-I curves were developed for each of the considered limit states.

Fragility is defined as the probability that a particular level of equipment damage would occur in response to a given blast demand, expressed as peak pressure and impulse. Since the probability of damage is a function of both peak pressure and impulse, it is displayed graphically as 3D fragility surface. The 3D fragility surfaces were computed by modeling the eleven EERR systems as probabilistic single degree of freedom (SDOF) systems, with the equipment properties represented as random variables. Different combinations of peak pressure and impulse were applied to the probabilistic SDOF models and the calculated random responses (displacements and or internal forces) were used to develop the 3D fragility surface plots.

Fragility is defined as the probability that a particular level of equipment damage would occur in response to a given blast demand, expressed as peak pressure and impulse.

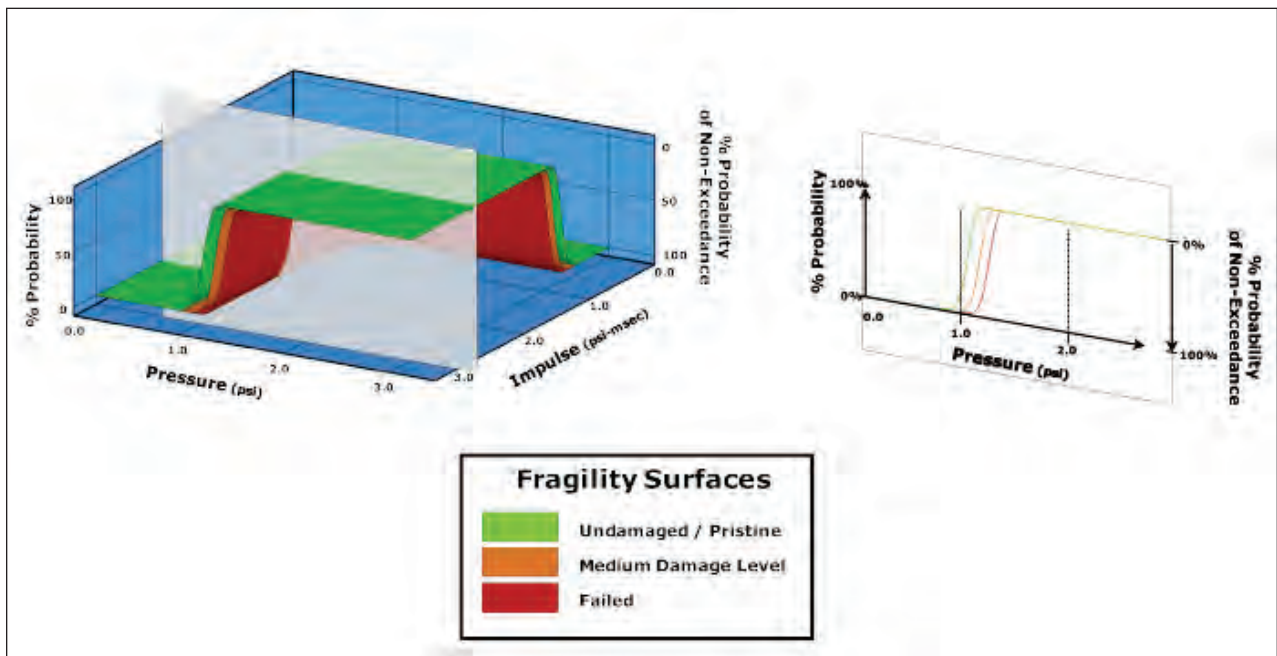


Figure 109: Fragility surface for representative EERR system

6.6 Data Incorporated in the UrbanBlast Tool

The initial release of the urban blast software includes a simplified representation of the fragility data. Two representative limit states were implemented in the software to assess the performance of the EERR systems to the location-specific, threat-specific blast scenarios:

- **Onset of damage:** The limit state obtained by taking the 15% probability of non-exceedance for the undamaged/pristine fragility surface.
- **Failure:** The limit state obtained by taking the 85% probability of non-exceedance for the failed fragility surface.

6.7 Conclusions and Recommendations

The EERR assessment component of the software provides first responders guidance on performance of EERR systems in different buildings in response to airblast. The assessment capabilities contained in the software were validated against data consistent with the 2006 IBC and ASCE 7-10. Additional validation of the fragility levels for several of these commercial systems via testing in actual blast environments would be desirable. The EERR blast assessment capabilities implemented in this software offer an effective means of identifying overall performance of specific systems in a commercial building located in an urban setting.

Future enhancements to the tool could include the following features:

- Processing of fragility surfaces to obtain a comprehensive assessment of the probability of attaining a specific limit state.
- Assessment of equipment performance in multiple locations within a building.

The EERR blast assessment capabilities implemented in this software offer an effective means of identifying overall performance of specific systems in a commercial building located in an urban setting.

UrbanBlast Tool

This section describes the methodology and key functionalities of the fast running UrbanBlast Tool (UBT) developed by WAI in the current phase of the project. The UBT, also referred to as UrbanBlast, is a site specific software program customized for each individual urban setting. The Manhattan Financial District (MFD) was chosen as a relevant urban site to demonstrate the UBT methodology; therefore, the software will be referred to as the UrbanBlast-MFD module as shown in Figure 110. The same approach can be used in future efforts to develop custom modules for other major urban centers in the U.S.



7.1 Software Goals

The UBT provides the security design community and first responders with more complete information on the threats posed by explosive devices detonated in urban settings, with the goal of supporting development of effective strategies for minimizing blast damage effects in urban centers. UBT accurately characterizes the complex pressure loading on buildings from an explosive event based on the charge size and its location within the city. The effects of the urban terrain (such as, building locations and street layouts) are included in the results. UBT, or UrbanBlast, is an effective tool for domestic counterterrorism

Figure 110:
Start-up screen for
UrbanBlast– Manhattan
Financial District

planning and will support activities of Federal, State, and local agencies and organizations responsible for designing and/or protecting urban centers.

The UrbanBlast software includes a graphical user interface (GUI) specifically designed to make the software an easy-to-use program for non-technical users. The user need only select the threat location within the urban scene and define the weight of the explosive. The results are then calculated in a few seconds and presented in an easily manipulated 3D display of the city section of interest. The GUI allows non-technical users to display important results in a form that is easy to visualize and interpret.



The UrbanBlast software includes a graphical user interface (GUI) specifically designed to make the software an easy-to-use program for non-technical users.

Fast running tools must balance the demands for simulation accuracy with speed of simulation. The UBT is designed to provide an effective engineering solution to the questions of how the propagation of blast pressures is affected by the presence of the urban landscape and how this translates into an

assessment of potential damage to buildings in the vicinity of the blast. The types of damage that are currently evaluated by the tool include direct blast damage to structural columns, window breakage, and potential damage to the equipment that relates to the emergency evacuation, rescue and recovery (EERR) mission.

7.2 Computing Environment Requirements

Computing environments are constantly evolving. Proper design and implementation of the software maximizes its ability to take advantage of improved hardware and software environments in the future. The target computing environment for UrbanBlast is described here.

7.2.1 Software Environment

The UrbanBlast software was designed to run on computers using Microsoft Windows[®] operating systems. Both 32-bit and 64-bit Windows operating systems, commonly found on desktop central processing unit (CPU) and laptop computers, are supported. Supporting both types of operating systems allows the software to be compliant with the increasing shift from 32-bit to 64-bit computing. UBT was tested on Windows XP, Windows Vista, and Windows 7 operating systems, covering the range of environments that are operational today.

7.2.2 Hardware Environment

The minimum hardware configuration for running UBT is a single core 32-bit CPU with 1 gigabyte of RAM. Hard disk capacity should be at least 100 gigabytes. A specialized graphics card is not required to visualize the model and simulation results; although, mouse manipulation of the 3D model will be less responsive when using computers with low end graphics capability. Most computers on the market exceed this base specification by a significant margin.

7.3 UrbanBlast Software Development

The GUI and graphical display of the model/results are important components of the UrbanBlast software. Qt,¹⁰ a widely used commercial software development environment, was used to create the GUI for UrbanBlast. Qt is a powerful development framework that allows support for cross-platform applications.

Display of the actual urban cityscape model and the airblast solution is provided by using OpenGL graphics, a commonly used graphics display protocol, in conjunction with the Visualization Toolkit (VTK), often used for display of technical data. Interactive graphic display functions are provided so that model orientation is easily controlled through mouse clicks and movement. Additionally, groups of buildings can easily be selected using the mouse for close-up visual inspection.

7.3.1 Software Architecture

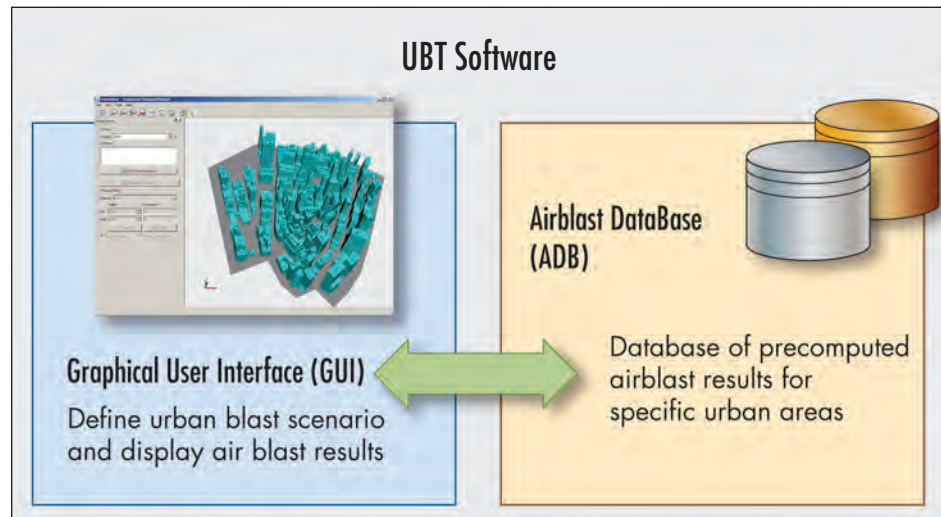
The UrbanBlast software was developed using a modular approach that provides an extensible framework for upgrading the tool in the future for other cities and additional analysis and display functions. The software is composed of two main components as shown in Figure 111.

The UrbanBlast software is composed of two main components, the Graphical User Interface (GUI) and the AirblastDataBase (ADB).

1. The **Graphical User Interface (GUI)** provides users with tools for defining the explosive threat's size and location within the urban setting and computing/displaying the blast results.
2. The **Airblast DataBase (ADB)** contains the HFPB airblast results for a large number of threat locations and yield combinations for the specific urban site of interest.

¹⁰ <http://www.qtsoftware.com>

Figure 111:
Primary software components



The GUI component of UrbanBlast was written in the C++ programming language. The Qt development environment was used to create the various display screens, menus, and dialogue boxes required by the program. This GUI provides preprocessing functions to define and visualize the urban blast scenario of interest and post-processing functions to allow the user rapid visualization of the airblast assessment results.

Combined, the GUI and database allow rapid engineering assessments of important aspects of blast damage caused by detonation of a high explosive device within the city. The spatial distribution of peak pressure and impulse caused by the explosion, as well as assessments of damage to critical structural components, are computed by the tool in only a few seconds on common desktop computers.

7.4 Software Assumptions

7.4.1 Language

UrbanBlast uses the English language for all its GUI and display options.

7.4.2 Systems and Units

UrbanBlast assumes a standard coordinate system for the model geometry and a consistent system of units for representing model data and computed airblast results.

7.4.2.1 Coordinate System

A Cartesian Right-Hand Rule coordinate system is used to define and orient the model of the cityscape geometry. The Z-axis defines the vertical direction as shown in Figure 112 and the X- and Y-axes define the horizontal plane for the urban setting. A reference ground plane is located at a coordinate of $Z = 0.0$, and upwards is in the positive direction.

7.4.2.2 System of Units

UrbanBlast uses English units, the most commonly used in the U.S. The display of peak pressure fields is shown in pounds per square inch (psi) and the display of peak impulse fields is presented in units of psi-seconds (psi-s).

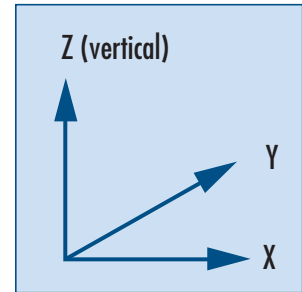


Figure 112:
Cartesian coordinate system
for UrbanBlast

7.5 UrbanBlast Model for Manhattan Financial District

A computer-aided design (CAD) database providing the geometry for buildings in the MFD was acquired from Fugro EarthData, Inc. The database incorporates all the important geometric details of the buildings in the area of Manhattan shown in Figure 113. This CAD data was used to construct both the MAZ CFD models used to compute the airblast solution for explosions occurring on city streets and also to provide the display geometry for the UBT.

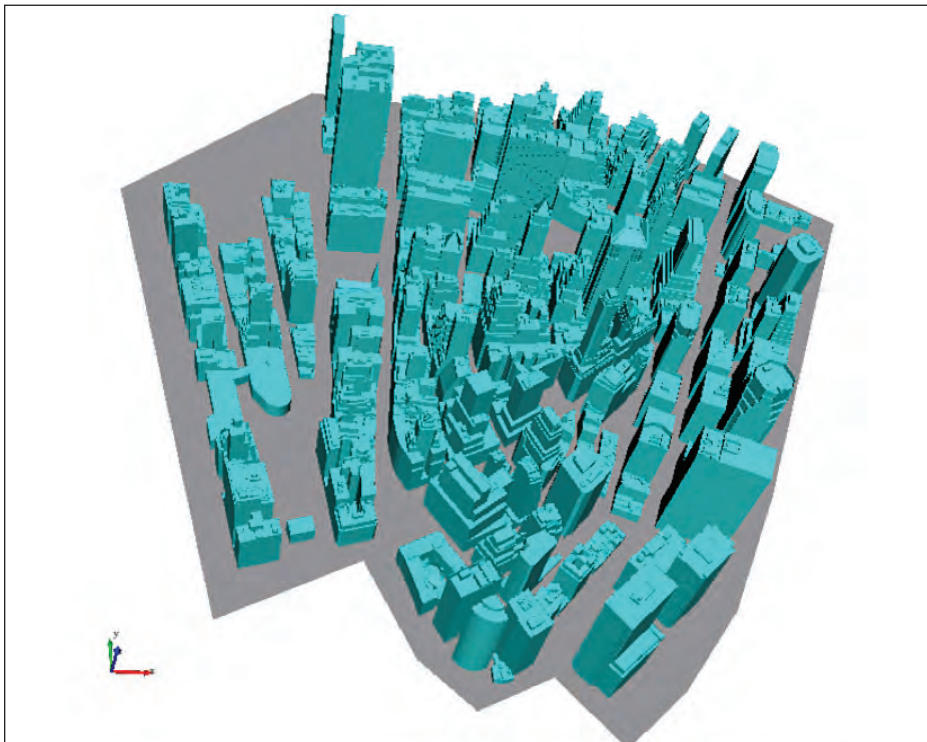


Figure 113:
Buildings contained within the
Manhattan Financial District
model

7.6 UrbanBlast Database of Airblast Solutions

The geometry of the MFD was used to construct an accurate MAZ model for computing the airblast propagation from an explosion. This model was used to compute the blast response at 291 pre-defined locations on streets within the city. These numerous locations allow placing the explosive threat at street intersections and midway between intersections throughout the urban area of interest. At each location selected, an airblast simulation was performed for an explosive yield of 1,000 lb and 30,000 lb of TNT.

The peak pressure and impulse results from these airblast simulations were stored in a database for use by the fast running UBT. This database is used by UrbanBlast to evaluate the airblast results for the user specified threat weight.

7.7 UrbanBlast Software

Figure 114 provides a screen shot from the UrbanBlast software. The 3D geometry of the city area of interest is shown in the main viewing pane of the application. The user has interactive mouse control of the city geometry and can easily rotate and zoom in and out of the model to facilitate visualization of the results.

At the upper left side of the screen, the user has controls to define both the location and weight of the explosive threat. The controls for selecting the specific type of information to display, for example, the Threat Effect, are located beneath the left hand side threat definition section of the tool.

7.7.1 Defining Explosive Threats

An explosive threat within an urban setting is fully characterized by the weight of the explosive and its physical location. The UBT provides the user with a number of selectable threat locations as shown in Figure 115. These locations are displayed when the Set Threat Location button is active. The weight of the explosive can be entered by the user in the upper left side of the GUI screen. The weight of the explosive must be defined in the range of 500 lb to 30,000 lb of TNT equivalent.

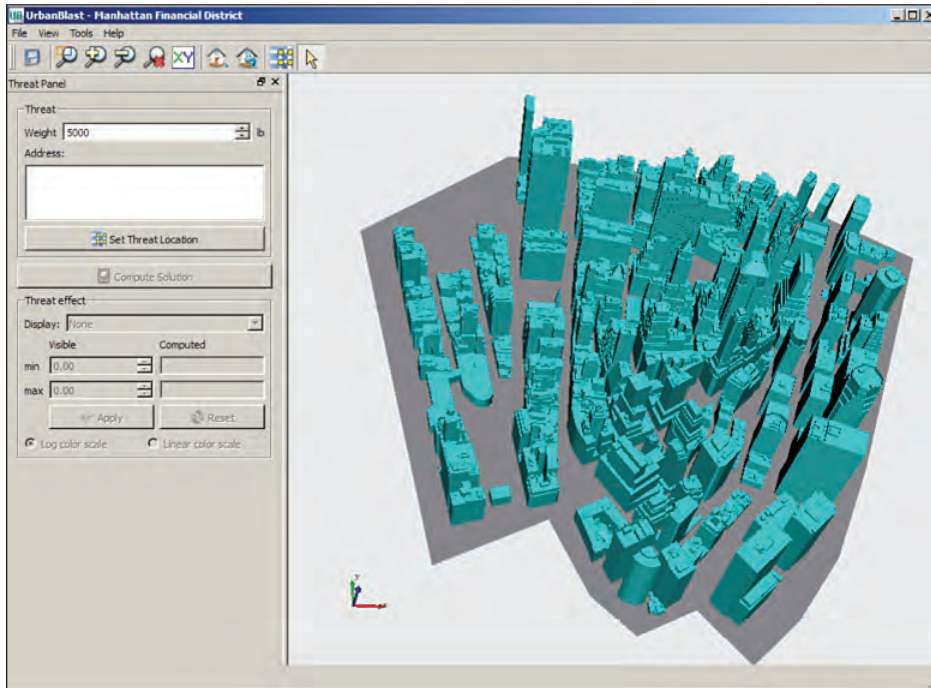


Figure 114:
UrbanBlast software for
Manhattan Financial District

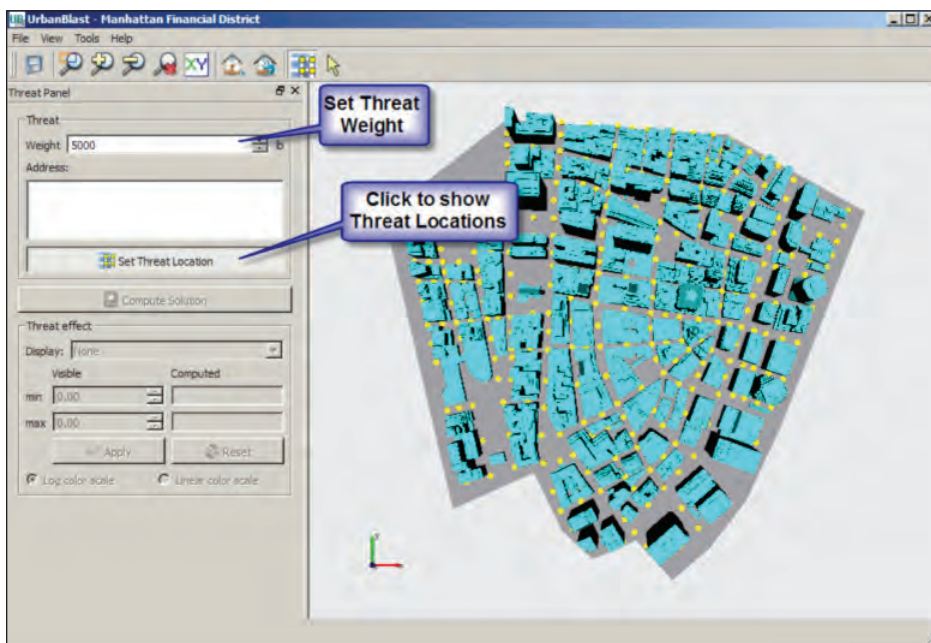
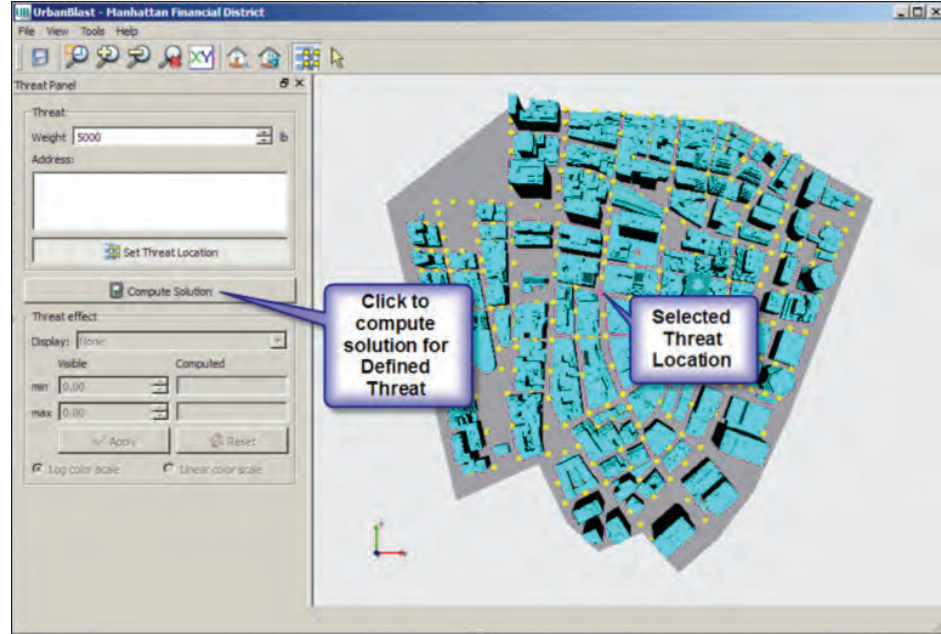


Figure 115:
Selectable threat locations
(shown in yellow)

The charge location points are displayed when the Set Threat Location button on the left side of the screen (or the Threat Location icon on the toolbar) is clicked. The user selects the location of the threat by clicking on one of the yellow location points. The selected charge location will turn magenta as shown in Figure 116.

Figure 116:
Select the threat location by clicking on one of the yellow Threat Location Points; the selected location is colored magenta



When the Compute Solution button on the left side of the screen is clicked, the UBT will automatically compute the airblast environment produced by the explosion, taking into account the presence of buildings, streets, alleyways, and other urban features. Once the airblast solution for the defined threat has been computed, the color of the threat location changes from magenta to red, and the other threat location points (yellow) are hidden from the display as shown in Figure 117. By default, the peak pressure distribution produced by the explosive blast within the urban setting is displayed. A description of the threat details and the type of results currently being displayed are shown in the upper right corner of the display screen as in Figure 117. (Note that the user can change the threat location point at any time by clicking on the Set Threat Location button and choosing a new location.)

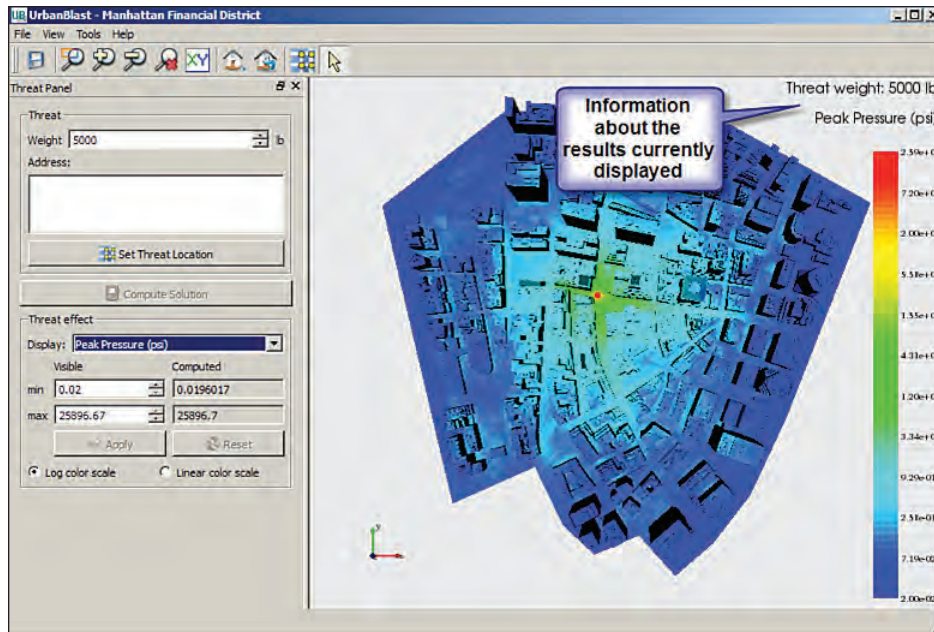


Figure 117:
Computed results are presented
in the display window

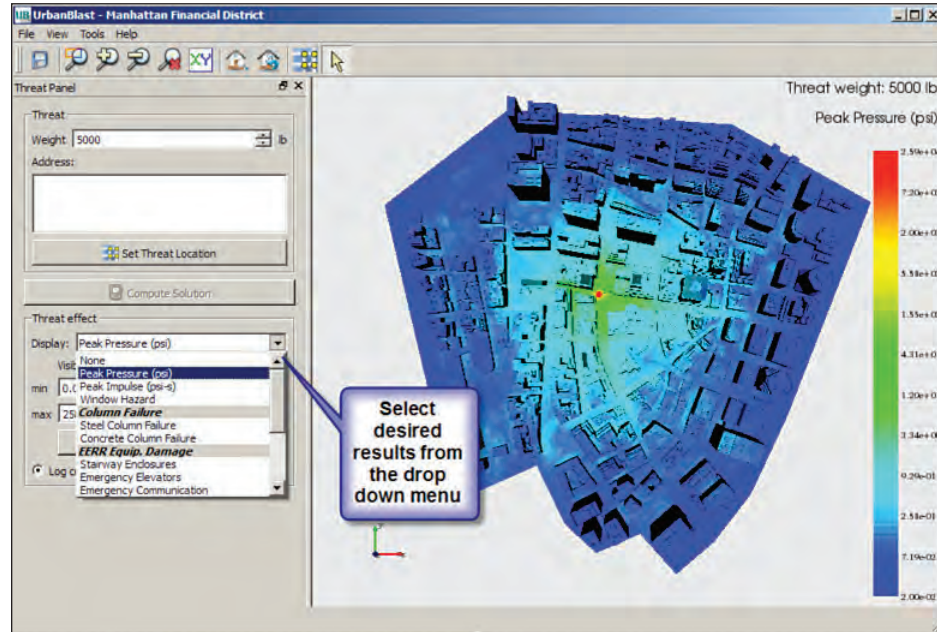
7.7.2 Results Display Functions

UrbanBlast currently provides four main categories of results:

1. airblast results: Maximum (peak) pressure and impulse fields produced by the blast are provided.
2. Window damage information: Both window breakage and window hazard regions, on the exterior of buildings, resulting from the blast are identified.
3. Column damage information: Potential column failure for nearby buildings, which may result from the blast, is provided for both concrete and steel column construction.
4. EERR damage information: Potential that EERR equipment located within a building may be compromised by a nearby explosive blast is provided for eleven different types of EERR equipment.

The user selects the results of interest to be displayed from the drop down menu list as shown in Figure 118.

Figure 118:
User can select seventeen
different types of results for
display



7.7.2.1 Airblast Results

Once the airblast solution has been computed, the UBT allows the user to display the distribution of peak pressure and peak impulse produced by the explosion, taking into account the complex effects of the presence of buildings within the urban scene. Figure 117 shows the peak pressure results for the selected threat location and explosive yield. The results for peak pressure and impulse are presented using a log scale by default. The user has controls at the left side of the screen to switch between log and linear scales and to change the minimum and maximum values of the data range to be displayed.

7.7.2.1.1 Airblast Evaluation Approach

A large database of results from high-fidelity CFD simulations for the MFD is used to compute the peak pressure and impulse airblast results displayed by the UBT. The database contains high-fidelity results for blast at each selectable threat location. High fidelity results were computed for two threat sizes (1000 lb and 30,000 lb) near the upper and lower bounds of the threat sizes of interest. Data at these two threat levels combined with the null condition (zero blast pressure for a zero weight charge) are used as the basis for determining scaling factors (assuming a quadratic fit) to compute the pressure and impulse values at each location within the model for the user's requested threat weight. This approach provides a good engineering estimate of the airblast pressures and distributions within the urban setting. Figure 119 through Figure 123 presents a representative set of approximate peak pressure and impulse values computed

using the fast running UBT (results were computed in several seconds) compared with the results from high-fidelity MAZ CFD simulations which required approximately one week of computer time. The results were evaluated for threat weights of 500 lb, 1000 lb, 4000 lb, 10,000 lb and 30,000 lb. The comparisons between the approximate results from UBT and the high-fidelity CFD results are quite good. This accuracy is sufficient for the current needs of the UrbanBlast software. Should future needs arise requiring even greater fidelity, the UrbanBlast approach can be enhanced by performing an additional set of MAZ CFD simulations representing the threat weight of 10,000 lb detonating at each of the predefined threat locations and adding these results to its database.

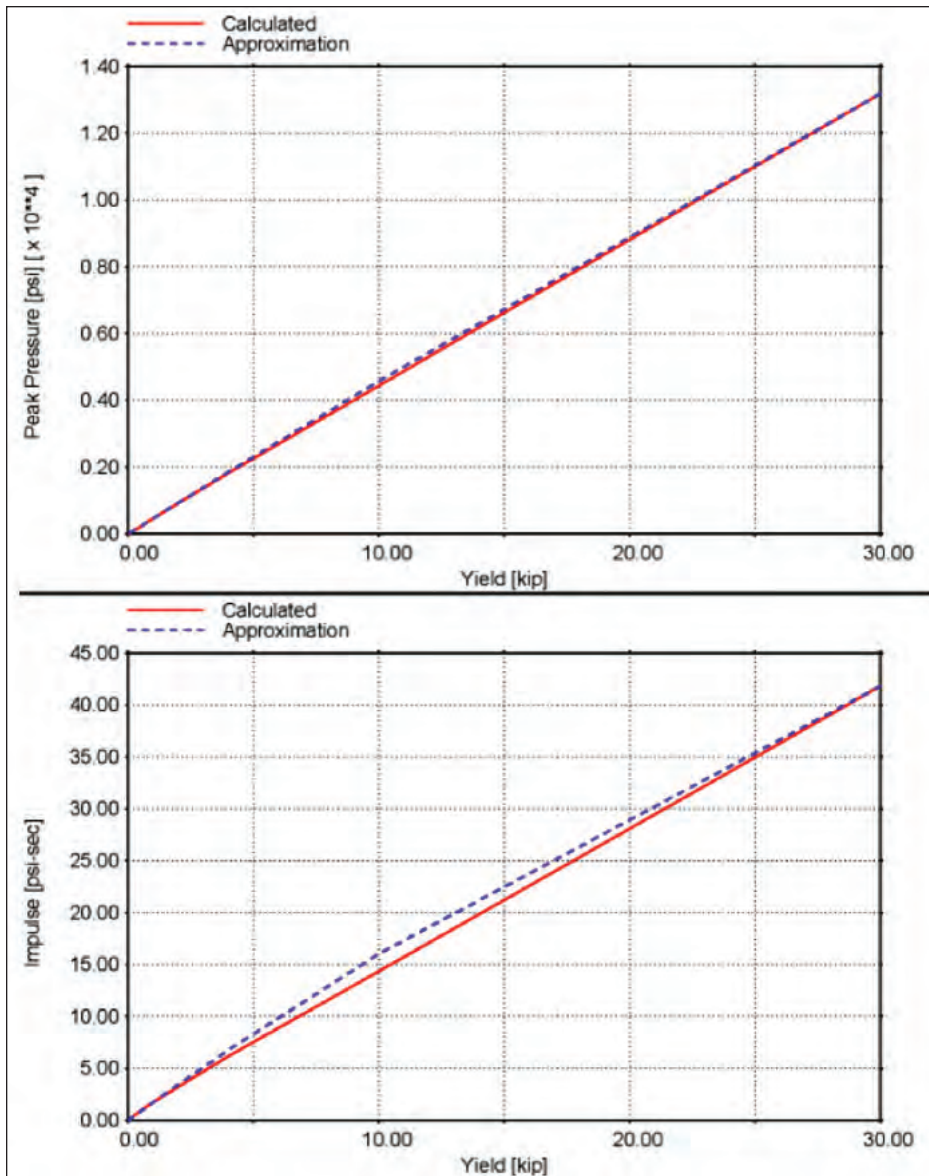
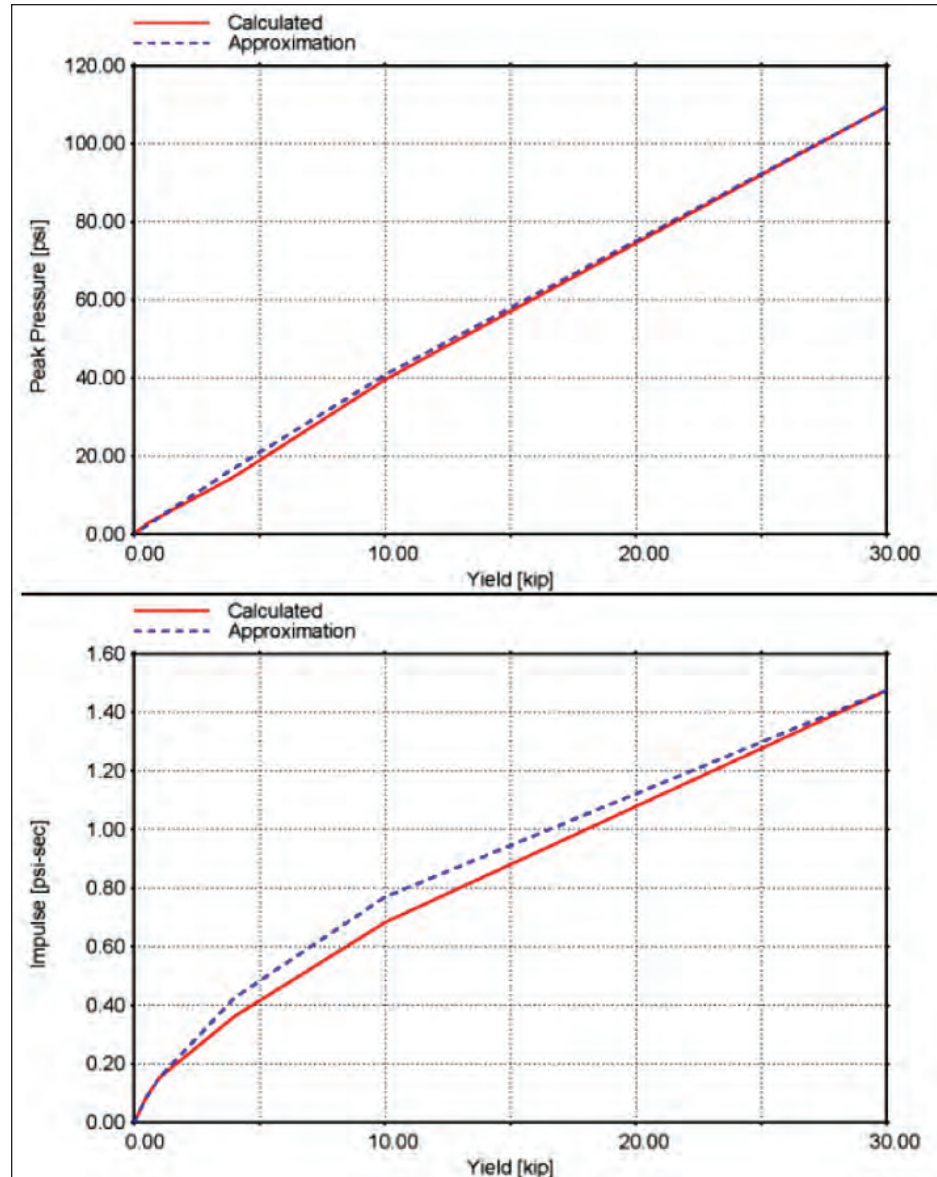


Figure 119: Comparison of approximated values of peak pressure and peak impulse from UrbanBlast with high-fidelity MAZ CFD calculated results

(high pressure location: pressure = ~13,000 psi for 30,000 lb threat)

Figure 120:
Comparison of approximated
values of peak pressure and
peak impulse from UrbanBlast
with high-fidelity MAZ CFD
calculated results



(medium pressure location: pressure = ~110 psi for 30,000 lb threat)

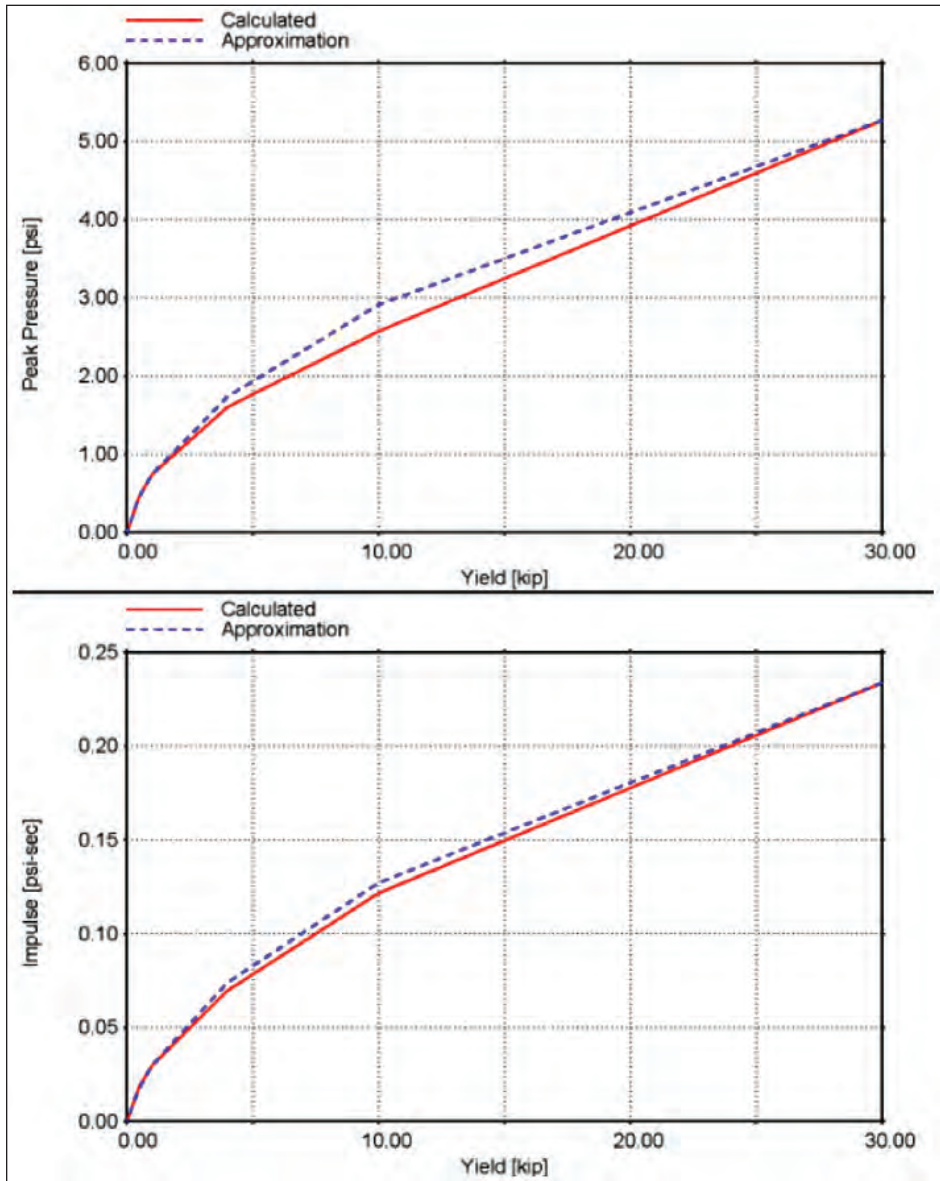
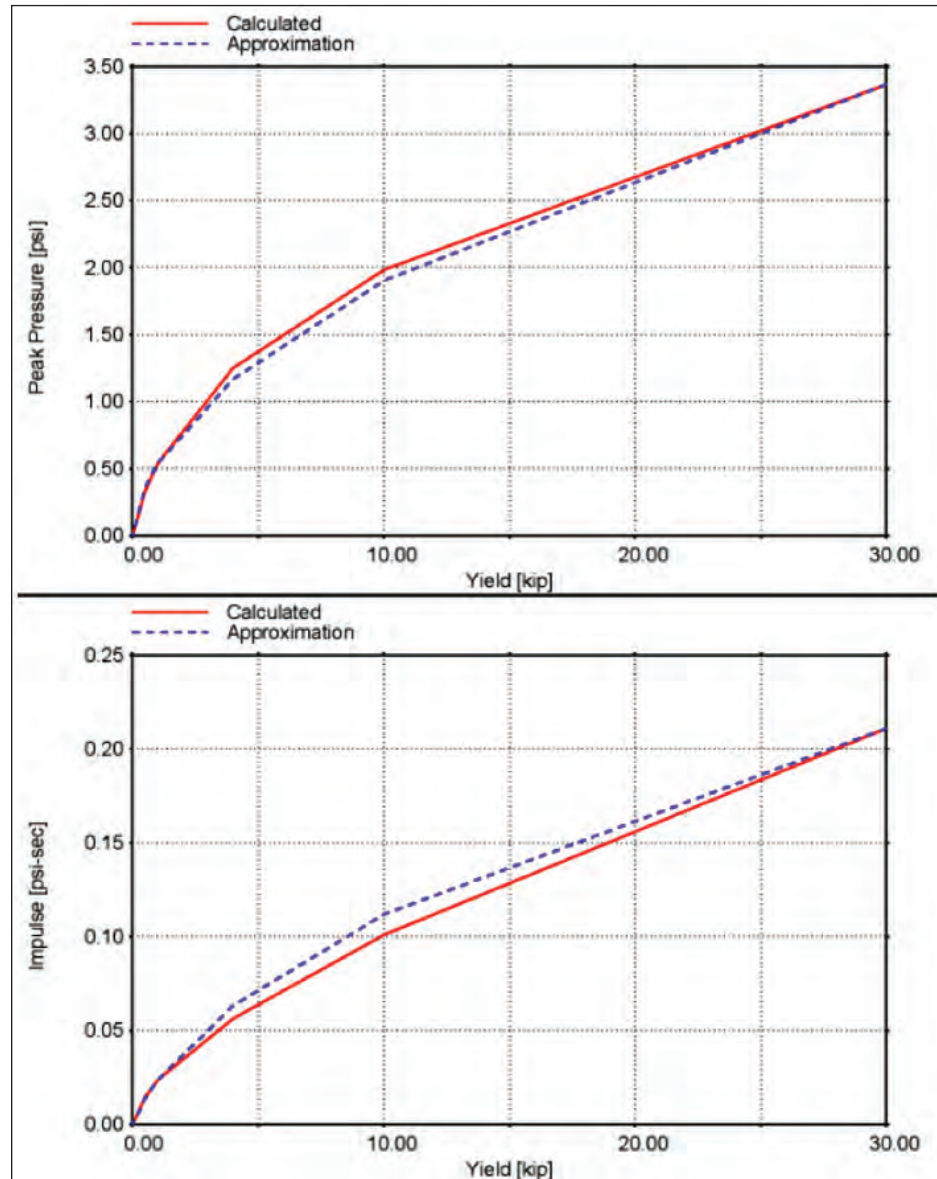


Figure 121: Comparison of approximated values of peak pressure and peak impulse from UrbanBlast with high-fidelity MAZ CFD calculated results

(low pressure location: pressure = ~5 psi for 30,000 lb threat)

Figure 122:
Comparison of approximated
values of peak pressure and
peak impulse from UrbanBlast
with high-fidelity MAZ CFD
calculated results



(low pressure location: pressure = ~3 psi for 30,000 lb threat)

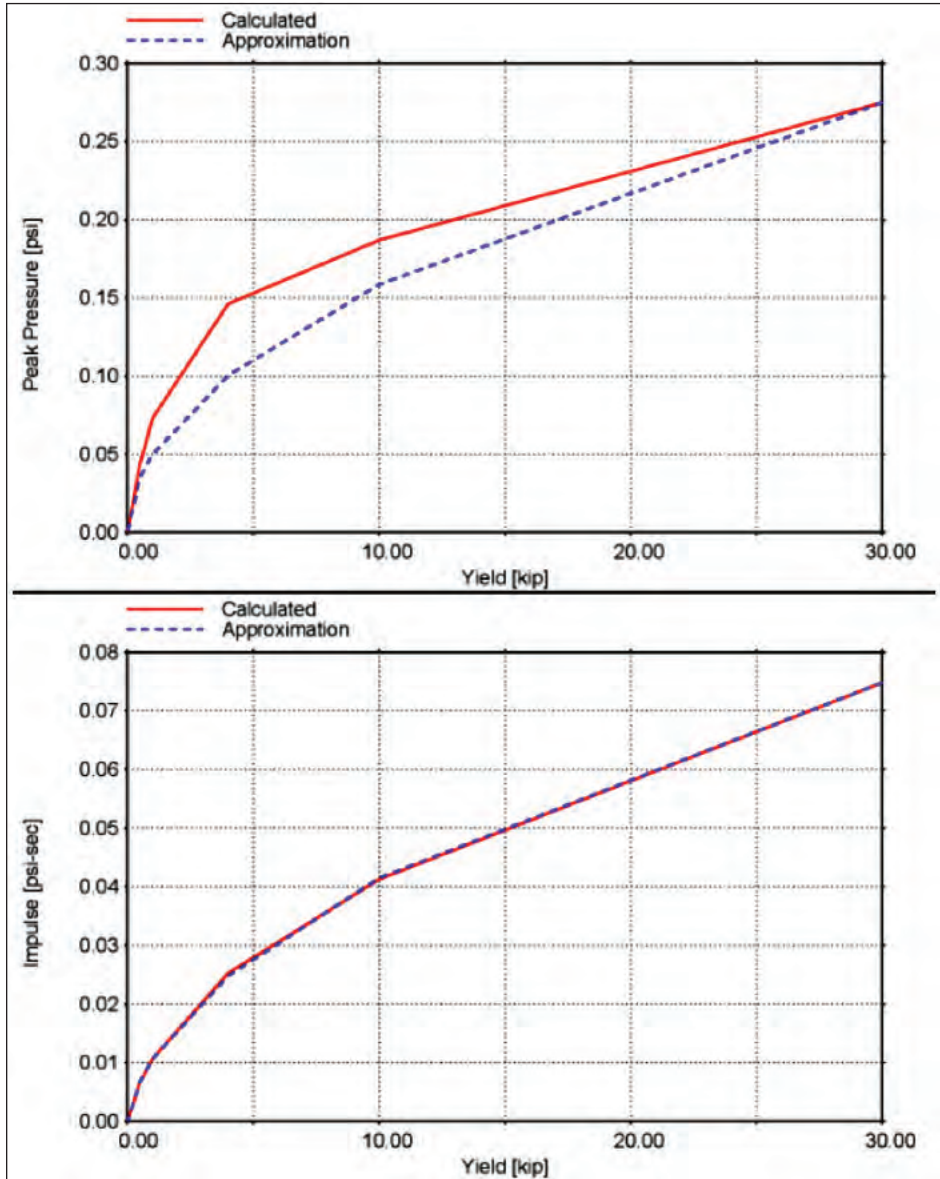


Figure 123: Comparison of approximated values of peak pressure and peak impulse from UrbanBlast with high-fidelity MAZ CFD calculated results

(very low pressure location: pressure = ~0.3 psi for 30,000 lb threat)

7.7.2.2 Window Damage Results

The user can select Window Hazard in the Threat Effect Display pull down menu at the left of the screen. This option evaluates the distribution of window breakage and window hazard information on the exterior envelop of each building in the urban setting.

In the UBT, window breakage means the breakage (failure) of glass windows under the blast pressure loading. Window hazard is a more severe condition. Herein, it represents the GSA Condition 4 or higher, indicating window glass will fly into the room at least 10 feet and strike a wall at that standoff from the window. Window hazard conditions can cause significant injury to building occupants.

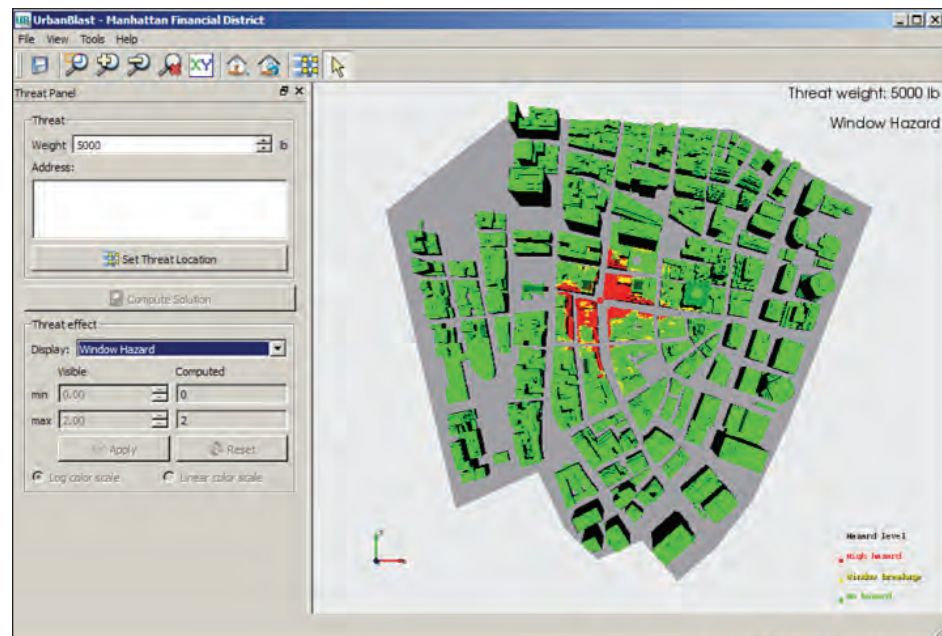
7.7.2.2.1 Window Damage Evaluation Approach

The peak pressure and impulse computed on the exterior of each building are compared with the window breakage and window hazard criteria shown in Table 18.

Table 18: Window damage criteria

| Window Damage | Peak Pressure Threshold | Peak Impulse Threshold |
|---------------|-------------------------|------------------------|
| Breakage | 1.0 psi | 0.015 psi-s |
| Hazard | 1.5 psi | 0.025 psi-s |

Figure 124:
Example of window breakage
and window hazard distribution
in urban setting



7.7.2.3 Column Damage Results

The user can select either steel or concrete column failure options in the Threat Effect Display pull down menu at the left of the screen. These options evaluate the likelihood of columns, of the chosen construction type, failing under the blast pressures caused by the explosion. If a column could fail under the blast pressure loading on any portion of a building, the entire building is painted with a color representing that result. This indicates the building could, potentially, experience some form of progressive collapse. Generally, the airblast pressures on the building section nearest the blast govern the column damage assessment for the building.

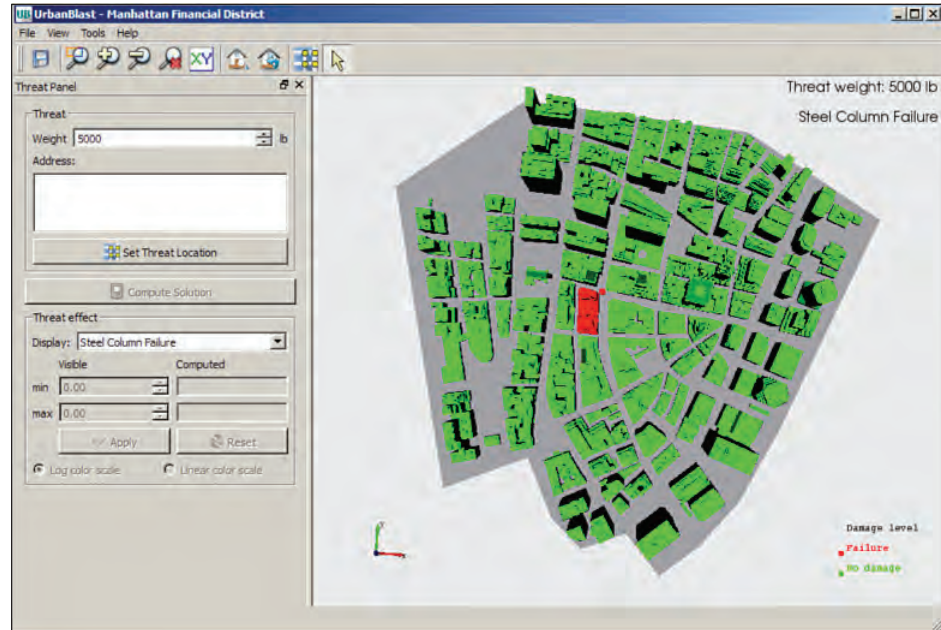
Because the CAD database representing the MFD does not include information classifying the type of construction (either steel or concrete), UBT is not able to automatically select between steel or concrete columns for each building. Hence, the current implementation allows the user to request damage estimates for either concrete or steel construction. When steel column damage is selected, each building is assumed to use steel construction, and the column damage assessment is performed. When the concrete column damage option is selected, each building is assumed to use concrete construction. In the future, it may be possible to survey and assign the actual construction type to each building.

7.7.2.3.1 Column Damage Evaluation Approach

The pressure and impulse generated by near proximity explosions can cause extensive damage to steel and concrete columns, as discussed in Section 2. The airblast pressure and impulse generated by the user defined explosive threat are used to determine the likelihood of column failure. The UBT first determines a typical ground floor column for each building, based on the height of the building. Then the worst case blast pressure on the building, caused by the user defined threat, is determined. Based on previous simulation studies of column damage from blast pressures, conservative estimates of combined pressure and impulse environments, required to cause blast failure of the column, were determined. These criteria are used to determine whether column failure would occur for a representative ground floor column for the building.

This approach could be refined in a follow-on phase of this effort by actually incorporating fast running models for blast response of steel and concrete columns within the UBT.

Figure 125:
Example of steel column failure
display



7.7.2.4 EERR Damage Results

The user can select one of eleven EERR equipment types to assess damage and failure in the Threat Effect Display pull down menu at the left of the screen. These options evaluate the likelihood of EERR equipment of the selected type failing under the blast pressures caused by the explosion.

The different types of EERR equipment that can be selected are:

1. Egress stairway enclosures
2. Elevator used during emergencies
3. Emergency communications
4. Emergency lighting
5. Conduit chases
6. Sprinkler pipe systems
7. Air ducts
8. Stair pressurization systems
9. Smoke detection systems
10. Emergency generators
11. Fire doors

7.7.2.4.1 EERR Damage Evaluation Approach

Section 6 of this report provides an in-depth discussion of the methodology developed in this effort to define the fragilities of EERR equipment. Most EERR equipment is located interior to a building. The UBT does not have a building specific database of EERR locations within each structure within the urban model. Therefore, the tool characterizes the worst case blast pressure environment inside the building, based on the exterior blast pressures the building will experience, and uses this information to evaluate damage to EERR equipment that are non-location specific. The UBT assumes that blast pressures penetrate into a building due to the breakage of exterior windows or from open vents. WAI's previous experience with the effects of 'blast through failing surfaces' provides empirical guidance on developing reasonable estimates of the reduction in exterior peak pressure and impulse that would be encountered in the interior of a building due to breakage of a building's windows. The UBT approximates the peak pressure within the building as being ~33% of the exterior pressure values and the peak impulse within the building to be ~50% of the exterior impulse values. This information combined with the EERR fragility data discussed above is used to assess the damage state of the specific EERR equipment item the user has requested.

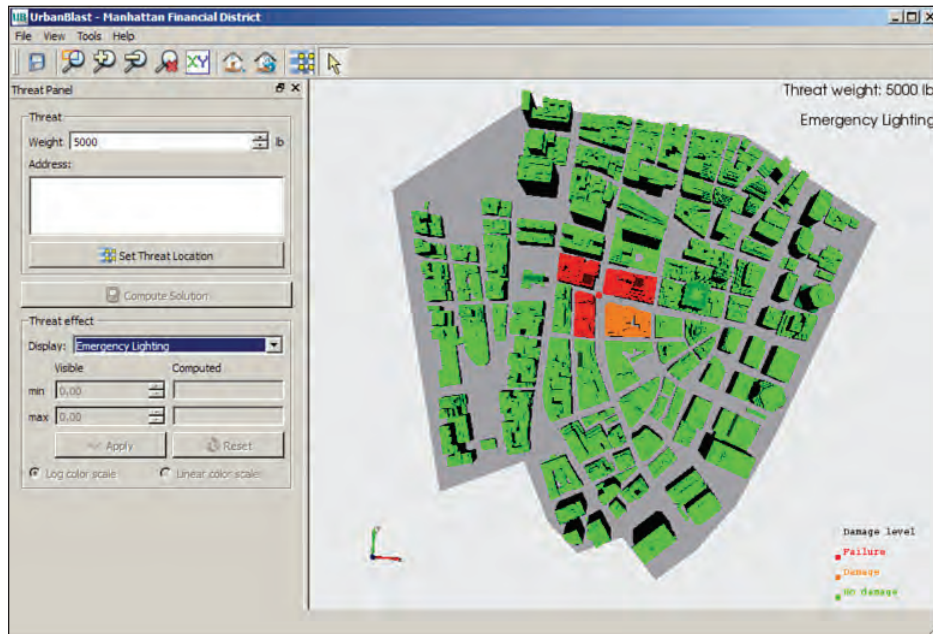


Figure 126:
Example of EERR equipment
damage display: emergency
lighting

The UBT considers all EERR items listed above to be subjected to interior blast pressures except for the stair pressurization systems and the emergency generators. These two items are assumed to be located near the roof of the building and are expected to be subjected to the exterior blast pressure loading experienced by the building at that location.

If the building's EERR equipment is assessed to fail under the blast pressure loading of any portion of the building, the entire building is painted with a color representing that result. This indicates the building may experience some amount of EERR equipment damage or failure. The specific color coding used is red for failure, orange for damage, and green for fully functioning.

7.7.2.5 Saving an Image of UrbanBlast Results

A user can save a graphic image of the results computed by the UBT by selecting the Save Image option located in the File menu.

7.7.3 Viewing the Model

By default, the UBT presents results in a plan view of the entire urban scene for the urban blast scenario of interest. There are several ways for a user to inspect the results in more detail by manipulating the 3D model of the urban scene.

7.7.3.1 Mouse Manipulation of the Scene

The user can interactively manipulate the urban scene by using the mouse. If the computer has a three button mouse:

1. Holding down the left button and moving the mouse will rotate the scene.
2. Holding down the right button and moving the mouse will zoom in or out on the scene.
3. Holding down the center button (or center wheel) and moving the mouse will pan the model.

An example display of a rotated and zoomed model is shown in Figure 127.

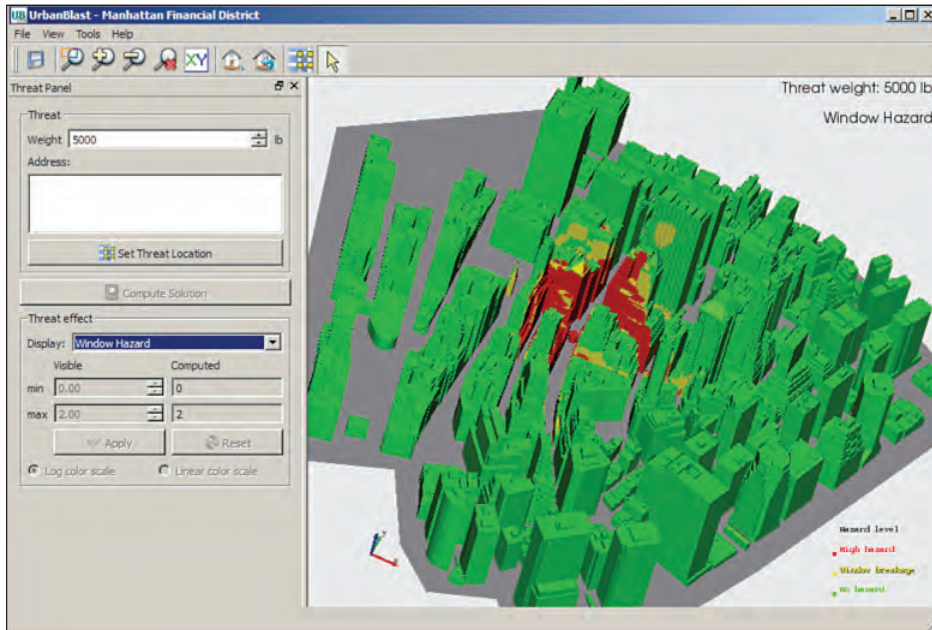


Figure 127:
Rotated and zoomed image of
the model

7.7.3.2 Controls Toolbar for Viewing the Model

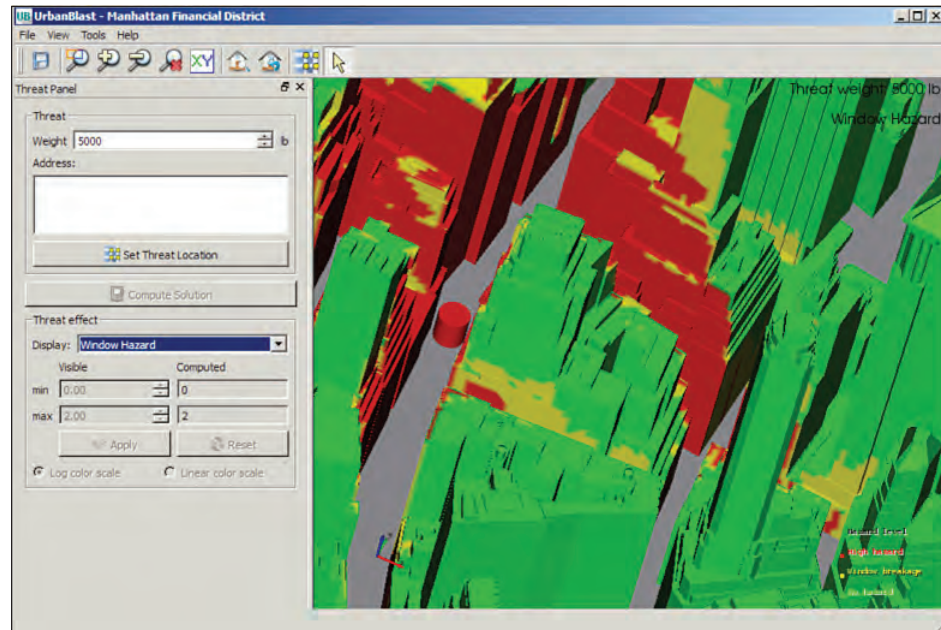
Several icons are provided in the Display Controls toolbar to aid in visualizing the model results as shown in Figure 128. These controls provide the option to zoom in or out on the urban scene by clicking on the + and – icons and to zoom into an area of interest by clicking and dragging a bounding box around that area. A control is also provided to reset the view to the plan view of the model, i.e., in the x-y plane.



Figure 129 shows an example of the model where the user has zoomed in on a local region of interest.

Figure 128:
Display control toolbar

Figure 129:
Close-in view of the blast
pressure provided by UBT



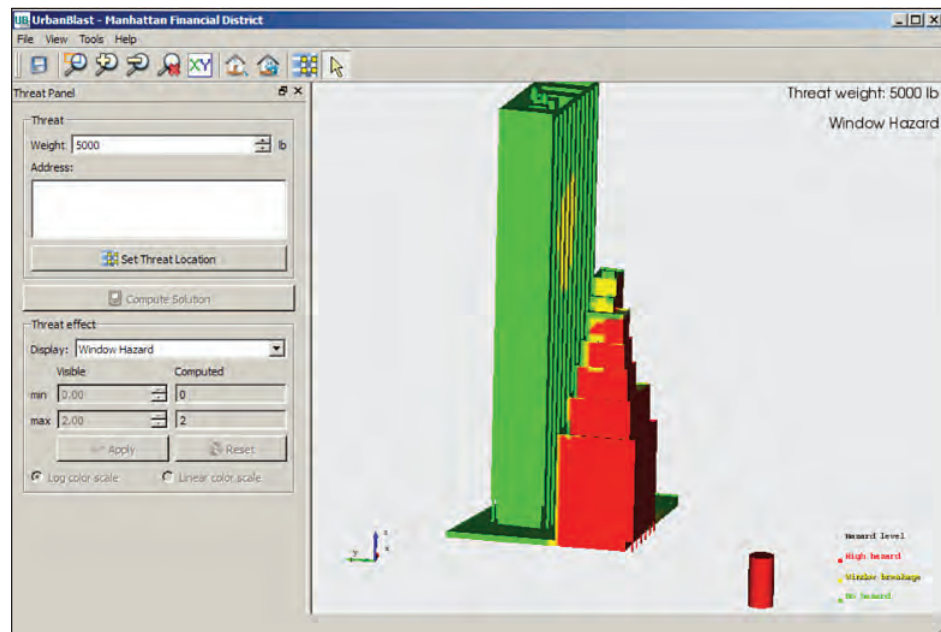
7.7.3.3 Controlling which Buildings are Displayed in the Scene



Figure 130:
Building display toolbar

Two icons are provided in the Building Display toolbar, as shown in Figure 130, to aid in visualizing the results for a single building or a small group of buildings. When the left icon is clicked, the user can click on a single building of interest or drag a bounding box around a group of buildings of interest. These building will be selected for display and all other buildings in the urban scene will be hidden as Figure 131 shows. The user can reset the display to show all buildings by clicking on the Building Display toolbar right icon.

Figure 131:
Specific buildings can be
elected for display




7.8 Initial Release of UrbanBlast

UrbanBlast Manhattan Financial District, version 1.2.00, is the initial release of the UBT. A significant amount of blast assessment technology has been implemented within the tool, and a strong emphasis has been placed on constructing the software interface to make UBT easy to use. Comments and feedback from initial users of the software will be addressed in later releases of the tool.

WAI anticipates making further refinements and enhancements to the software in future phases of this effort.

7.8.1 Installation of the Software

The UBT is provided for installation on a DVD. The supporting database for UBT is large. Installation from a DVD requires copying about 3 gigabyte of data onto a user's CPU or laptop; this can take some minutes to complete. The installation process will install the UrbanBlast shortcut Icon, , on the user's desktop.

7.8.2 Software Registration

UBT software requires a computer specific registration key to run on the computer. When a new user installs the software and runs it for the first time, UBT will provide instructions for emailing a request for a registration key to UB_help@wai.com. Once the request has been made, the user should close the application and wait for the official registration key to be provided. Once the registration key arrives, the user can rerun UrbanBlast and enter the registration key. Once the correct registration key is provided, UrbanBlast can be successfully run on the computer.

Guidelines on How to Apply the UBT to Protect Structures to Resist IED Attacks

The design of buildings to resist the effects of explosive detonations requires an accurate determination of blast loading. While conventional weapons (CONWEP) software that are based on the Kingery-Bulmash relationships provide accurate blast loading information for structures that are not subjected to multiple reflections from neighboring buildings and BlastX software that are based on ray-tracing algorithms provide reasonable approximations for the effects of neighboring buildings, there is little available guidance regarding the effects of explosions in dense urban streetscapes. Although the effects of multiple reloading may be conservatively approximated using amplification factors to the CONWEP calculated impulses, the diffusion of the blast wave over buildings, between buildings, and around corners is not so easily approximated. The estimate of collateral damage and the corresponding design to limit the extent of collateral damage as the result of an attack on a nearby iconic structure, therefore, requires detailed computational fluid dynamics (CFD) analysis to accurately determine the intensity of blast loading. The UrbanBlast Tool (UBT) catalogs the results of

The design of buildings to resist the effects of explosive detonations requires an accurate determination of blast loading.

detailed CFD analyses of a family of detonations in the lower Manhattan Financial District and provides the user a simplified means of interpolating to determine the blast loading for a specific explosive detonation. The results of the UBT may be used to evaluate or design buildings that are either the target of an explosive detonation and surrounded by multiple reflecting surfaces or are exposed to the collateral effects of an explosion in the vicinity. This blast loading information includes cumulative effects of the primary positive phase shock wave, the subsequent negative phase, and the multiple reflections that may reload the surface of the building. Therefore, once the size of the potential blast is specified, the first step is to determine the corresponding blast loads that may be applied to the building surface. These loads are used to determine the performance of the different building components and systems that may be damaged by the blast effects.

The desired/specified level of protection (LOP) determines the extent to which the building is to be protected and the corresponding hazard to which the occupants will be exposed. While advanced numerical analyses will determine the likely failure mechanisms and the extent of damage in response to the calculated blast loads, these models require very accurate information regarding the structural details and material properties. Although such detailed analyses are warranted for high consequence buildings and structural components,



The desired/specified level of protection (LOP) determines the extent to which the building is to be protected and the corresponding hazard to which the occupants will be exposed.

they are rarely performed for more conventional buildings and less critical components. Instead, simplified dynamic nonlinear analyses of single degree of freedom (SDOF) systems or semi-empirical data may be used to determine the extent of damage in response to the calculated blast loads. The results of these simplified models are often compared to the cataloged damage thresholds that were determined for a wide range of primary and secondary structural components by

the Department of Defense (DOD) in order to define the corresponding levels of protection. These damage thresholds may be specified in terms of ductility or deformation or may be presented as iso-damage curves on a pressure-impulse (P-I) chart. A series of calculations must therefore be conducted in order to evaluate the building performance in response to the calculated loading. These dynamic nonlinear calculations may consider individual building components, one at a time, as fixed-base models in which the resulting reaction forces are applied to the supporting members in addition to any blast loads that may be directly applied to these supporting members. In this fashion, the structural and non-structural building components may be evaluated, one at a time, to determine the extent of damage. Because the sequential

analysis of building components does not account for the beneficial effects of compliant supports or phased loading, dynamic nonlinear analyses of more detailed multiple degrees of freedom (MDOF) models, or finite element analyses (FEA), are required to account for these interactive effects. Regardless of the choice of analytical method, the accuracy of the approach will depend on the accurate representation of the loading, the building details, and the material properties. These analyses will be performed for all building columns, beams, and slabs that are exposed to the exterior vehicle-borne explosive loading and all interior structural elements that may be exposed to infill pressures that may enter through the damaged façade. The extent of blast loading that may infill the building following façade damage may be estimated based on the calculated resistance of the façade and the intensity of the exterior blast loading. In addition to structural and façade components, the performance of internal partitions, ducts, and mechanical systems will determine the effectiveness of the emergency evacuation, rescue and recovery (EERR) systems that first responders rely upon for the life safety of the occupants. An evaluation of the EERR systems in response to the specified explosive threats will determine the adequacy of such systems and whether they will likely provide for the safe evacuation of the building.

Not all hazards can be related to the calculated response to the blast loading. In addition to the evaluation of structures to the calculated intensity of blast loading and the design of components to minimize the hazard of collapse or debris impact, structural systems require additional robustness to protect against threat independent events that may locally damage primary load bearing elements. The DOD's threat independent design requirements, as documented in the January 2010 UFC 4-023-03, were evaluated for three different classes of buildings; in all cases the structures were able to redistribute the gravity loads following the instantaneous removal of a single exterior column. These threat independent design requirements, known as the alternate path method (APM), provide a level of fault tolerance that enables a damaged structure to remain stable and to enable the safe evacuation of the occupants. While this approach cannot be considered comprehensive of all possible threat independent damage states that may precipitate a collapse, it provides a significant degree of robustness and ductile detailing that may otherwise not be required by blast resistant design and detailing. This combination of threat specific and threat independent design is the preferred design approach for buildings that may either be considered primary targets or in close proximity to buildings that may be considered primary targets. The American Society of Civil Engineers Disproportionate Collapse Standards and Guidance Committee is currently developing a consensus based approach for the design of both government and commercial

buildings to prevent progressive collapse. The centerpiece of the proposed standards and guidance are the threat independent methods presented in the UFC 4-023-03 and demonstrated to be effective through detailed finite element analysis for the three different structural systems considered in this report. While the UrbanBlast Tool (UBT) provides an accurate representation of the blast loads and a rational evaluation of generic buildings in proximity to explosive events, it is no substitute for a detailed analysis and a building specific design to resist the calculated intensity of blast loading.

Many options exist for upgrading buildings to resist blast loading. Concrete columns may be wrapped with steel or composite jackets; steel columns may be encased in concrete and their connections to the beams or girders upgraded. Façades may include window systems, masonry, or concrete panels. The window systems can be upgraded with films or with the glazing replaced with laminated glass. The framing and connections would also be upgraded to carry the new loads that a laminated glazing system would put on the system. Both masonry and concrete panels can be backed with liners that can upgrade the resistance to blast loads. Progressive collapse upgrades can include the options for upgrading the columns listed above and adding composite toppings to floor slabs to resist uplift. In addition, spandrel beams may require stronger connections.

References

1. “Fast Running Urban Airblast Assessment Tool for NYC Financial District”, Prepared by WAI for the Department of Homeland Security, June 18, 2010.
2. Vaughan, D. K., "FLEX User's Guide," Report UG8298, Weidlinger Associates, Mountain View, CA, May 1983 plus updates through 2010.
3. Lawver Darell, Raymond Daddazio, Michael Stanley, Darren Tennant and David Rubin, “FLEX FE Models and Full Scale Tests of Blast Loaded Reinforced Concrete Columns”, DDESB 33rd Explosives Safety Seminar, Palm Springs, August 2008.
4. Hassig, P., Tennant, D., Weeks, J. and Levine, H. “The Effects of Airblast Clearing on Structural Loads.” Proceedings of the 13th International Symposium on the Interaction of the Effects of Munitions with Structures, Brühl, Germany, May 2009.
5. D. Lawver, R. Daddazio, G. J. Oh, C. K. B. Lee, A. Pifko and M. Stanley, “Simulating The Response of Composite Reinforced Floor Slabs Subjected To Blast Loading,” 2003 ASME International Mechanical Engineering Congress and RD&D Expo, November 2003.
6. Tunnel Target Defeat ACTD, Weidlinger Associates Simulation Capability Documentation”, Report submitted to DTRA Modeling Assessment Group, 24 May 2004, Distribution C.

7. "Updated Model/Simulation Description for the Flex code used by Weidlinger Associates for TTD ACTD", Report submitted to DTRA Modeling Assessment Group, 28 Feb. 2006, Distribution C.
8. Tennant, D., Levine, H., Lawver, D. and Smilowitz, R 'Analysis of a Multi-Story Flat Slab Building Subjected to an External Detonation Using A First Principles Finite Element Code, 70th Shock and Vibrations Symposium, Nov. 15-19, 1999.
9. Schlamp, R. J., Hassig, P. J., Nguyen, C. T., Hatfield, D. W., Hookham, P. A., "MAZ User's Manual," Defense Nuclear Agency Contract Report, Contract No. DNA001-91-C-0153, March, 1995.
10. A. Harten, High Resolution Schemes for Hyperbolic Conservation Laws, *J. Comput. Phys.*49, 357 (1983).
11. UFC 4-023-03, dated 1 Oct. 2008 (steel Frame and 25 ft bay concrete moment frame) or dated 14 July 2009.
12. Berning, W.W., 1948: Investigation of the Propagation of Blast Waves Over Relatively Large Distances and the Damaging Possibilities of Such Propagation. BRL-675.
13. Catalog of Atmospheric Acoustic Prediction Models, 1995, U.S. Army White Sands Missile Range, Document 383-95.
14. U.S. Standard Atmosphere, 1976, U.S. Government Printing Office, Washington, D.C., 1976.
15. Landolt, S. D., R. Tardif and P. H. Herzegh, 2006: A comparison of atmospheric profiles using a twelve channel microwave profiling radiometer and radiosondes during low ceiling events. 12th Conference on Aviation, Range and Aerospace Meteorology, Atlanta, GA
16. American Society of Civil Engineers (ASCE), "Minimum Design Loads for Buildings and Other Structures," ASCE STANDARD ASCE/SEI 7-05, 2006.
17. Anagnos, T., "Development of an Electrical Substation Equipment Performance Database for Evaluation of Equipment Fragilities," Pacific Gas and Electric and the Pacific Earthquake Engineering Center Report, April 1999.
18. Applied Research Associates, Inc., "Integrated Munitions Effects Assessment Software, Module for Buildings and Bunkers, Version 4.1," Methodology Report, Prepared for Defense Threat Reduction Agency (DTRA), December 2001.
19. Applied Technology Council, "Interim Testing Protocols for Determining the Seismic Performance Characteristics of Structural and Non-Structural Components," FEMA 461, June 2007.

20. Applied Technology Council, "Guidelines for Seismic Performance Assessment of Buildings, ATC-58 50% Draft," Prepared for U.S. Dept. of Homeland Security and Federal Emergency Management Agency, April 15, 2009.
21. Applied Technology Council (ATC), "ATC-3-06 Tentative Provisions for the Development of Seismic Regulations for Buildings," including the 1982 "Amendments to ATC-3-06 Tentative Provisions for the Development of Seismic Regulations for Buildings for Use in Trial Designs," 1982.
22. American Lifelines Alliance, "Seismic Fragility Formulations for Water Systems," Sponsored by ASCE and FEMA, April 2001.
23. Badillo-Almaraz, H., Whittaker, A.S., Reinhorn, A., "Seismic Fragility of Suspended Ceiling Systems," *Earthquake Spectra*, Volume 23, No. 1, February 2007.
24. Bley, D.C., Perla, H.F., Wakefield, D.J., Smith, B.D., "Enhanced Seismic Risk Assessment of Diablo Canyon Power Plant," 10th International Conference on Structural Mechanics in Reactor Technology, Anaheim, CA, 1989.
25. Burningham, C., Mosqueda G., Saavedra, R.R., Comparison of Seismic Fragility of Free Standing Equipment Using Current Testing Protocols and Recorded Building Floor Vibrations," Network for Earthquake Engineering Simulation (NEES) Research Experiences for Undergraduates Program Summer 2007.
26. Choun, Y.S., Choi, I.K., "Effect of the Seismic Capacity of Equipment on the Core Damage Frequency in Nuclear Power Plants," 18th International Conference on Structural Mechanics in Reactor Technology (SMiRT 18), Beijing, China, August 2005.
27. Ellingwood, B., "Validation of Seismic Probabilistic Risk Assessment of Nuclear Power Plants," Dept. of Civil Engineering: The John Hopkins University, U.S. Nuclear Regulatory Commission Report NUREG/GR-0008, January 1994.
28. Ghiotto, A., Penrose, J.D., "Investigating the Acoustic Properties of the Underwater Implosion of Light Globes and Evacuated Spheres," Australian Acoustical Society Conference, Joondalup, Australia, November 2000.
29. Giovinazzi, S., King, A., "Estimating Seismic Impacts on Lifelines: An International Review of RiskScape," Proceedings: 2009 New Zealand Society for Earthquake Engineering Conference.

30. Heard, G.J., McDonald, M., Chapman, N.R., Jashke, L., "Underwater Light Bulb Implosions – A Useful Acoustic Source," Proceedings: IEEE Oceans Conference, 1997.
31. Kuwata, Y., Takada, S., "Seismic Risk Assessment of Lifeline Considering Hospital Functions," Dept. of Civ. Eng. Kobe Univ., Japan, Asian Journal of Civil Engineering (Building and Housing) Vol. 8, No. 3, 2007.
32. Lin, L., Adams, J., "Lessons for the Fragility of Canadian Hydropower Components Under Seismic Loading," Ninth Canadian Conference of Earthquake Engineering, Ottawa, Canada, June 2007.
33. Lupoi, G., "Fragility Analysis of the Seismic Response of Freestanding Equipment," European School for Advanced Studies in Reduction of Seismic Risk, Rose School, August 2005.
34. Merkle, D. H., Rochefort, M. A., Tuan, C. Y., "Equipment Shock Tolerance," Applied Research Associates, Inc., U.S. Air Force Civil Engineering Support Agency Report Number ESL-TR-92-65, April 1993.
35. Porter, K., "Fragility of Hydraulic Elevators for Use in Performance-Based Earthquake Engineering," Earthquake Research Institute, Earthquake Spectra, Volume 23, No. 2, May 2007.
36. Porter, K., Kennedy, R., Bachman, R. "Creating Fragility Functions for Performance-Based Earthquake Engineering," Earthquake Research Institute, Earthquake Spectra, Volume 23, No. 2, May 2007.
37. Ravindra, M. K., "Seismic Probabilistic Safety Assessment of Nuclear Power Plants," ABSG Consulting, Inc., International Atomic Energy Agency Report: IAEA-TECDOC-1478, February 2006.
38. Shinozuka, M., "Advances in Seismic Performance Evaluation of Power Networks," University of California, Irvine: Seminar on Earthquake Disaster Management Of Energy Supply Systems, September 3, 2003.
39. Sonnenburg, P., "Fragility Data Analysis and Testing Guidelines for Essential Equipment Used in Critical Facilities," Construction Engineering Research Laboratories Special Report CERL-SR-M-209: Seismic Design Criteria for Interior Utility and Lifeline Systems, March 1977.
40. Soong, T.T., Yao, G.C., Lin, C.C., "Near-Fault Seismic Vulnerability of Non-Structural Components and Retrofit Strategies," Earthquake Engineering and Engineering Seismology, Vol. 2, No. 2, September 2000.

41. Whitehouse, S.R., Kilijanski, M.S., "Fragility Data for C3I Equipment Subjected to Conventional Weapon Effects," Applied Research Associates, Inc., Naval Surface Warfare Center, Dahlgren Division Report: ARA-5209, February 1996.
42. Wilcoski, J., Gambill, J. B., Smith, S. J., "The CERL Equipment Fragility and Protection Procedure (CEFAPP): Experimental Definition of Equipment Vulnerability to Transient Support Motions," US Army Corp of Engineers Construction Engineering Research Laboratories Technical Report 97/58, March 1997
43. U.S. Army Corps of Engineers, Protective Design Center, "Component Explosive Damage Assessment Workbook: CEDAW," Version 1.0, April 23, 2005
44. U.S. Army Corps of Engineers. PDC-TR 06-08 Rev 1: "Single Degree of Freedom Structural Response Limits for Antiterrorism Design," September 2008
45. Porter, K., Johnson, G., Sheppard, R., Bachman, R., "Fragility of Mechanical, Electrical, and Plumbing Equipment," Earthquake Spectra Volume 26, Issue 2, May 2010.
46. National Institute of Standards and Technology, NISTIR 5339, 1994 at <http://www.usfa.dhs.gov/downloads/pdf/publications/fa-150.pdf>
47. United States Office of Compliance Safety and Health, "FAST FACTS: Proper Fire Doors and Improper Fire Door Openings," September 2004.
48. United States Office of Compliance Safety and Health, "FAST FACTS: Fire Sprinkler System: A Life Saver and Building Protector," October 2009.
49. U.S. Department of Labor, Occupational Safety and Health Administration, "Fire Service Features of Buildings and Fire Protection Systems," 2006.
50. Steel Door Institute, "American National Standard SDI-100: Recommendations for Standard Steel Doors and Frames," American National Standards Institute, Ref: A250.8-2003, November 2003.
51. Advanced Technology Systems, LLC., "Center Opening Installation Manual for Car and Hoistway Doors Using ATS Track & Hangers," Manual Number 13.0, Revision Number 1.0, October 2008.
52. Schindler Elevator Corporation, "QKS Door Operators," (Brochure), DBS-6002a, B0110, 2001.
53. The National Elevator industry Inc., "Standard Elevator Layouts: Elevator Engineering Standards," New York, 1975.

54. Honeywell International, Inc., “MS-9600LS(E)/MS-9600UDLS(E): Intelligent Addressable FACP with Optional 2nd Loop,” df-60334:A4, A1-100, December 2009.
55. Siemens Switzerland Ltd, “FC2020 Fire control panel,” Document No. 009383_b_en_-, 2006.
56. Grinnell Corporation, “Fire Control Panel for Releasing Device Service,” PFC Series 2000RC, TD275, June 1992.



Acronyms

| | |
|------|---|
| 1D | one-dimensional |
| 2D | two-dimensional |
| 3D | three-dimensional |
| A/E | Architecture and Engineering |
| ABNC | airblast near concrete |
| ACEC | American Council of Engineering Companies |
| ACI | American Concrete Institute |
| ABD | airblast database |
| AISC | American Institute of Steel Construction |
| ALE | Arbitrary Lagrangian-Eulerian |
| ANFO | ammonium nitrate and fuel oil |
| APM | alternative path method |
| ASCE | American Society of Civil Engineers |
| ATC | Applied Technology Council |
| AZ | adaptive zoning |
| BIPS | Building and Infrastructure Series |
| CAD | computer-aided design |



ACRONYMS

| | |
|----------------|--|
| CEDAW | Component Explosive Damage Assessment Workbook |
| CEFAPP | CERL Equipment Fragility and Protection Procedure |
| CERL | USACE Construction Engineering Research Laboratory |
| CFD | computational fluid dynamics |
| CIA | Central Intelligence Agency |
| CMU | concrete masonry unit |
| COB | center of blast |
| CONWEP | conventional weapon |
| CPU | central processing unit |
| CPVC | chlorinated polyvinyl chloride |
| DHS | Department of Homeland Security |
| DNA | Defense Nuclear Agency |
| DOD | Department of Defense |
| DTRA | Defense Threat Reduction Agency |
| EERR | Emergency Evacuation, Rescue and Recovery |
| EMRTC | Energetic Materials Research and Testing Center |
| ERDC | USACE Engineer Research and Development Center |
| FACEDAP | Facility and Component Explosive Damage Assessment Program |
| FEA | finite element analysis |
| FEMA | Federal Emergency Management Agency |
| FRM | fast running model. (See fast-running software tool) |
| ft | foot |
| GSA | General Services Administration |
| GUI | graphical user interface |
| HE | highly explosive |
| HFPB | high-fidelity physics-based |
| HPC | high performance concrete |
| HS | heat strengthened (glass) |
| HVAC | heating, ventilation, and air conditioning |



| | |
|--------|--|
| IAEA | International Atomic Energy Agency |
| IBC | International Building Code |
| ID | identification |
| IDD | Infrastructure Protection and Disaster Management Division |
| IED | improvised explosive device |
| IGU | insulated glazing unit |
| IMEA | Integrated Munitions Effects Assessment |
| IMF | intermediate moment frame |
| in | inch |
| JWL | Jones-Wilkins-Lee |
| K/km | change in atmospheric temperature (degrees Kelvin) per kilometer of altitude |
| km | kilometer |
| ksi | Kips per square inch (unit of pressure). 1 Kip = 1000 lbs |
| lb | pound |
| LOP | level of protection |
| m/s | meters per second (velocity units) |
| MAZ | multiphase adaptive zoning |
| MDOF | multiple degrees of freedom |
| MEVA | Modular Effectiveness/Vulnerability Assessment |
| MFD | Manhattan Financial District |
| mph | miles per hour |
| Msec | milliseconds (unit of time, 1000th of a second) |
| NE | nuclear explosive |
| NY | New York |
| NYC | New York City |
| PB | polybutylene |
| PDC | Protective Design Center |
| P-I | pressure-impulse |
| ProCAT | Progressive Collapse Assessment Tool |



ACRONYMS

| | |
|-----------------|--|
| psf | pound per square foot |
| psi | pound per square inch |
| RAM | random access memory |
| S&T | Science and Technology |
| SBIR | Small Business and Innovation Research |
| SDOF | single degree of freedom |
| SMP | symmetric multi-processing |
| TNT | trinitrotoluene |
| TT | thermally tempered (glass) |
| TTD-ACTD | Tunnel Target Defeat Advanced Concept Technology Demonstration |
| TVD | total variation decreasing |
| U.S. | United States |
| UBT | UrbanBlast Tool |
| UFC | Unified Facilities Criteria |
| USACE | U.S. Army Corps of Engineers |
| VAPO | Vulnerability Assessment Protection Option |
| VBIED | vehicle-borne improvised explosive device |
| VTK | Visualization Toolkit |
| WAI | Weidlinger Associates Incorporated |

Glossary

Adaptive zoning (AZ). A numerical simulation scheme in which the computational mesh is changed as needed during a simulation to provide an accurate solution for a problem.

ALE finite element techniques/methods. Arbitrary Lagrangian-Eulerian finite element method. ALE is an advanced numerical analysis scheme for solving physical problems using mesh based methods.

Column failure. The inability of a structural column to continue to perform its design function, i.e., no longer able to support the weight of the building for which it has been designed. Column failure may be caused by damage from blast or impact.

Euler equations. The set of fundamental scientific equations that govern inviscid (non-viscous) fluid flow. Euler equations represent a subset of the general Navier-Stokes equations.

E-TABS software. A commercial software package commonly used by structural engineers to analyze buildings and aid in their design. www.csiberkeley.com/etabs.

Fast-running software tool. A software tool that provides rapid answers to complex problems, often based on precomputed results from more computationally intensive high-fidelity analyses.

Fixites. Points in a model of a building that are fixed, i.e., restrained and not permitted to move. Fixities are commonly used in models to approximate connections to foundations or other well-anchored supports.

Hardening. Making a structure stronger or more resistant to failure.

Moment frame action. The behavior of a moment frame, a commonly used building design method that enables a structure to withstand lateral loads, such as wind forces acting on the building.

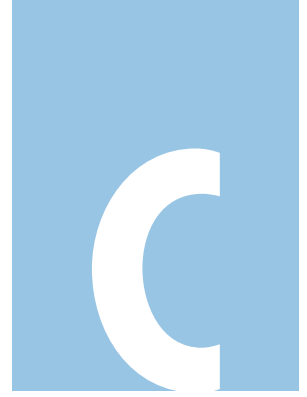
Navier-Stokes equations. Fundamental scientific equations governing the general motion of fluids including air.

NLFlex software. State-of-the-art finite element modeling software for calculating structural performance in response to blast and impact loads.
<http://www.wai.com/nlflex.aspx>

P-Delta. The secondary effect on shears and moments of structural members due to the combined action of axial loads and transverse displacement resulting from various loading conditions. The secondary shears and moments produced by the P-Delta effect contribute to the destabilization of the structure.

Riemann scheme. A numerical approach often used to solve the Euler equations in the field of computational fluid dynamics.

SAFE software. A commercial software package commonly used by structural engineers for designing concrete floor and foundation systems.
www.bentley.com/en-US/Products/STAAD.Pro.



Appendix C: Methodologies Used in Developing the UrbanBlast Tool for NYC Financial District

C.1 Overview

Weidlinger Associates, Inc. (WAI) developed the UrbanBlast Tool for the Department of Homeland Security (DHS). UrbanBlast is a fast running software tool designed to quantify the extent of propagating blast pressures and potential structural damage caused within the New York City Financial District by a conventional explosive threat detonated on a city street. The purpose of the tool is to provide security planners and first responders with helpful information for assessing the potential threat posed by explosions in urban settings. The NYC Financial District was chosen as the initial proof-of-principle for the development approach adopted for the effort. The UrbanBlast methodology was specifically developed to be extensible to other urban settings as needed in the future.

Detonations in urban settings are complex events. The interaction of propagating blast pressures with large buildings will channel the airblast down streets and alleys, amplifying the blast pressures compared to those produced in unobstructed settings. The potential for explosions (a) to damage primary structural members of a building potentially leading to progressive collapse of a structure, (b) to blow out windows, and (c) to damage Emergency Evacuation, Rescue and Recovery (EERR) systems needs to be better understood. An effective methodology that accurately addresses the complex phenomena associated with blast in urban settings requires the application of advanced high-fidelity modeling tools and an in-depth understanding of the problem.

This appendix briefly summarizes WAI's background in relevant areas of research provides background information on the high-fidelity physics based modeling software that provide the foundation on which the fast running assessment results are based.

C.2 Weidlinger Associates' Background

Weidlinger Associates, Inc. Consulting Engineers has served clients worldwide since 1949 in the fields of structural and civil engineering, transportation/infrastructure, and advanced analysis for applied science research. A pioneer in the design of high rise, long span, fabric, blast resistant, and other special structures, the firm is also known for innovative bridge rehabilitation, blast and seismic design and retrofit, and development of software for government and private industry.

WAI's Applied Science Division engages in research, development, and testing for U.S. government agencies and private industry. Activities cover a wide range of subjects within the broad areas of applied mechanics, applied mathematics, materials science, and computational methods. A significant part of WAI's business involves writing and maintaining computational software for modeling blast, shock, and impact loadings of military and civilian structures subjected to terrorist and conventional weapons loadings. WAI has a strong team of engineers and computer scientists with expertise in non-linear dynamic structural analysis, three dimensional airblast computations, development of advanced engineering analysis techniques, and assessment of structures under blast loads.

Weidlinger Associates has extensive experience and capabilities in all technical disciplines needed to meet the goals of the current DHS project including:

1. Developing and applying high-fidelity physics based modeling software for airblast and structural response simulations.
2. Understanding of buildings, their design and construction, and their behavior in progressive collapse scenarios.
3. Simulating the degradation effects of bomb blast pressures and fragments on structural components and the progressive collapse response of buildings.
4. Performing first principle's Computation Fluid Dynamics (CFD) simulations to simulate blast pressures propagating from detonating explosives.
5. Developing Fast Running Models (FRMs) in general and specifically for progressive collapse applications and airblast loading.
6. Developing and maintaining software tools for Government agencies, private industry, and universities worldwide.

C.3 Development of Fast Running Assessment Tool for Blast in Urban Environments

High Fidelity Physics Based (HFPB) tools such as Multiphase Adaptive Zoning (MAZ) [1] for airblast simulations and NLFlex [2] for simulations of structural response are effective at modeling explosive detonations and the behavior of structures responding to blast pressures. However, the computational resources required for these analyses far exceed what can practically be brought to bear by most users.

MAZ CFD calculations of urban blast scenarios can take weeks to run. NLFlex progressive collapse simulations can require months of computer time. First responders, city planners, military, and other government agencies have a need for fast running tools which rapidly provide high-fidelity simulation results. WAI designed an approach to provide HFPB results in a reasonable time frame for use by these organizations. The approach uses CFD simulations to pre-compute an extensive database of airblast results for specific urban sites. This database can be adapted to the needs of a fast running tool for quickly presenting blast pressure data and structural damage estimates for specific explosive threats, accounting for their explosive yield and location within a city.

WAI is currently using this approach to develop the fast running UrbanBlast Tool (UBT) that will provide good predictions of airblast loadings and structural damage for the dense urban environment of the

Financial District in Lower Manhattan. This tool accesses a database of airblast solutions generated by MAZ to provide input to embedded fast running structural response tools. It provides an end-to-end evaluation of the damage caused by an improvised explosive device (IED) detonated in the dense urban environment within a few seconds running on a desktop or laptop computer.

It is not practical to use HFPB models to simulate all potential explosive threats that might occur in the NYC Financial District. WAI calculated several different threat levels at each of 268 physical locations uniformly distributed on streets throughout the Financial District. Scaling methods are used to interpolate between pre-calculated yields to allow the user to specify any weight of the explosive charge ranging up to 30,000 lbs. The number of threat yields that are pre-computed for the database at each threat location can be expanded in the future, as desired, in order to satisfy the level of accuracy required of the tool. Because a large number of CFD simulations were required to develop the fast running model, WAI purchased approximately \$100,000 of supplementary computing hardware, at corporate expense, to provide the computing resources needed to meet the goals of the project and fit within DHS's timeline.

C.3.1 WAI Experience Developing Fast Running Engineering Models

WAI has extensive experience developing FRMs for structural response and airblast applications. Several of these tools have been or are being incorporated into primary DOD software environments such as the Integrated Munitions Effects Assessment (IMEA) and Vulnerability Assessment Protection Option (VAPO) programs developed by Defense Threat Reduction Agency (DTRA) and the MEVA software developed by the Air Force. WAI developed FRMs include, but are not limited to:

- **WABEAM, WABEAMST, and WASLAB** were developed by WAI to implement single degree of freedom (SDOF) modeling of reinforced concrete beams, steel beams, and reinforced concrete or steel slabs. These codes transform single structural components into equivalent SDOF models based on the methods found in *Structural Dynamics* by John Biggs [3]. WAI has used these programs on several hundred vulnerability assessments of airport, embassy, courthouse, military, infrastructure, office, and other facilities.
- **ABNC:** WAI's AirblastNearContact (ABNC) tool was developed to provide accurate blast pressure loading on structural components from near contact detonations. More traditional airblast prediction tools, such as the CONWEP code developed by the U.S. Army, are not accurate for close proximity detonations. WAI developed the

ABNC code to rapidly define the blast pressure loading from near contact satchel charges that cannot be adequately addressed with CONWEP or other simplified blast load tools. WAI used the MAZ CFD code to generate a large database of airblast simulations which provides the quantitative results on which the FRM is based.

- **ProCAT:** WAI developed the Progressive Collapse Assessment Tool (ProCAT) to provide an efficient tool that could quickly build and perform progressive collapse assessments of blast damaged buildings. The ProCAT tool performs advanced multi-degree of freedom (MDOF) analyses using advanced nonlinear resistance functions for each structural component in the model. These resistance functions are developed using NLFlex high-fidelity finite element models. The tool can evaluate the progressive collapse response of steel and concrete frame buildings that are exposed to exterior vehicle-borne explosive devices.

C.4 High Fidelity Physics Based Modeling

Urban environments provide a complicated setting for determining the airblast loads that result from explosive detonations and the structural damage they may produce. Tall buildings focus and channel airblast, resulting in significant enhancement of loads at range from the detonation. Buildings reflect pressures that increase loading at some locations and shield other areas thus mitigating the loads. The pressure loads acting on a building can damage key structural members and, potentially, cause a progressive collapse of the damaged structure. Even when primary structural components are not damaged, window breakage and/or damage to key emergency equipment can lead to significant human injury and potential loss of life.

HFPB simulation models are required to accurately address the challenges of defining airblast behavior and structural response in urban settings. The complex airblast interaction with buildings, streets, and alley ways is best predicted using high-fidelity CFD simulations. WAI uses the MAZ CFD code for simulating blast pressure propagation in urban environments. MAZ has a long track record of accurate simulation of airblast pressures and WAI continues to advance its capabilities for airblast modeling. Additionally, WAI uses the NLFlex software for computing the structural response of buildings subjected to blast and fragment loads and other extreme events. NLFlex has over twenty years of application to modeling structural response to nuclear, terrorist, and conventional weapons effects. It is also a leader in the field of simulating progressive collapse of blast damaged buildings.

Because the MAZ and NLFlex software provide the technical foundation upon which the fast running UBT is being developed, the following discussion briefly describes these tools and provides an overview of validation of these software programs for computing the airblast response of structures in urban settings.

C.4.1 The MAZ Software for CFD Simulations

Multiphase Adaptive Zoning (MAZ) is one of several CFD codes that have been developed with a specific focus on modeling blast wave propagation and has a history of verification and validation within the DOD airblast modeling community. The MAZ [1] code is a state-of-the-art CFD code specifically designed for the prediction of explosive events. MAZ was developed by Titan Research & Technology Division of Titan Corporation (previously known as California Research & Technology) under sponsorship from the Defense Nuclear Agency (DNA). MAZ development began in 1990 as a replacement for the 2D/3D DICE code, which had been in use since the early 1970s for high explosive (HE) and nuclear explosive (NE) multiphase airblast and dust cloud simulations. MAZ is used to solve a variety of blast related problems that include HE detonations, NE detonations, structure loading, thermal effects on airblast, cloud rise, conventional munitions blast and fragmentation, shock tube phenomenology, dust and debris dispersion, and atmospheric shock propagation. Some of the models included in the code are: non-responding and responding structures, non-interactive and interactive particles with two-phase flow, several atmosphere models, multi-materials, a large material library, an HE detonation model with a large library of ideal and non-ideal (aluminized) explosives, a non-ideal explosive particulate and gaseous after-burn model, a second-order closure turbulence model, a surface heating model, and water and dust vaporization.

MAZ is a 2D and 3D CFD code that solves the Reynolds-averaged, unsteady Navier-Stokes equations. It employs a second-order accurate linearized Riemann scheme for the 2D/3D Euler equations with the total variation decreasing (TVD) flux limiting method of Harten [4]. A general finite-volume formulation is implemented to accommodate the underlying grid methodology, which includes adaptive zoning (AZ) and arbitrary Lagrangian-Eulerian (ALE) grid motion and geometries. Adaptive zoning of individual cells (3D hexahedrals, 2D quadrilaterals) allows spatial resolution to be concentrated automatically where numerical detail is most needed. ALE enables the tracking of a moving physical interface between different type materials as well as defining the boundaries of arbitrarily-shaped physical elements. All grid/variable data is stored in memory within an unstructured topology, which lends itself to efficient use of vectorizing CPU architectures. WAI implemented

symmetric multi-processing (SMP) directives in MAZ in order to take advantage of the multiple CPU/multiple core processors available in today's computers.

MAZ uses an unsteady adaptive zoning/grid feature to capture all the shock physics of the flow accurately and efficiently, from the initial detonation to the long-range blast decay. Adaptive zoning allows spatial resolution to be concentrated where pressure gradients are highest. This capability is particularly important when performing 3D calculations, when computational resources are a concern. WAI recently implemented multi-block grid techniques in MAZ. This capability simplifies initial grid generation and permits more generalized grid configurations. For example, an arbitrarily configured ventilation system embedded in a multi-room structure can be easily incorporated.

MAZ accurately captures the important airblast features, including all shocks and their reflections, and the interface between pure air and explosive products. The generalized equation-of-state (EOS) capability of MAZ is used to model the effects of the gaseous products of the explosion; currently the Jones-Wilkins-Lee (JWL) equation-of-state is used. A high temperature air model is used for the shocked ambient. This separation of EOS is accomplished by tracking the mass fraction of HE products. With this method any new/advanced energetic material can be modeled. Another important feature of the MAZ code in charge effectiveness/directionality optimization is the ability to consider a variety of exotic charge shapes. MAZ airblast predictive capability has been validated through comparisons with multiple field tests and verified against other airblast codes. It is currently being used by WAI for predictions of environments produced by terrorist explosive devices.

The primary funding for the original MAZ software development came from DOD's Defense Threat Reduction Agency (DTRA). DTRA provided the MAZ code to WAI in 1997. Paul Hassig, one of the original authors of the MAZ software, joined WAI's staff in 2004. WAI has applied MAZ to a wide range of airblast applications including blast in urban environments and internal detonations and relies heavily on this code for generating high-fidelity blast pressure loads for computing the response of structural models.

C.4.2 Verification and Validation of the MAZ CFD Code

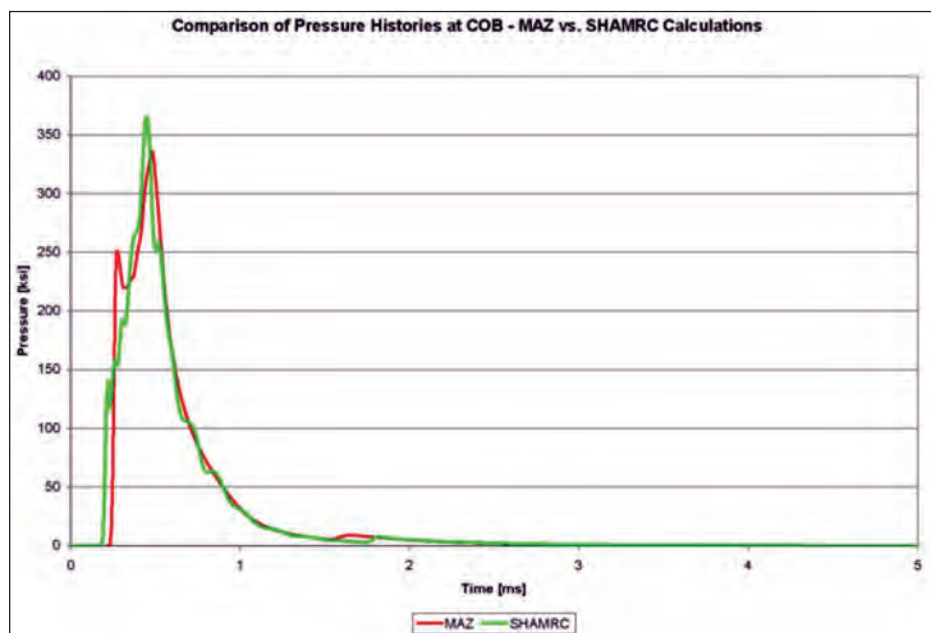
WAI has extensive experience predicting the response of structures subjected to blast loading. An important part of accurately determining the response of structures to blast loading is the accurate prediction of the airblast environment. WAI has used the MAZ CFD code extensively to

predict the airblast loads on structures. MAZ has been compared to field tests and other CFD codes of comparable fidelity. It is well recognized among verification and validation organizations that knowledgeable, experienced analysts are at least as important as the software. These calculations were performed by a CFD code author and expert in airblast simulations with decades of experience in airblast simulations.

C.4.2.1 U.S. Army Corps of Engineers – Bridge Project

WAI under contract to the USACE performed detailed airblast and structural analysis to support design of retrofits to mitigate the impact of vehicle-borne improvised explosive devices. The design effort was not supported by field testing. However, to insure the accuracy of the analysis, comparison between different computational tools was made to provide code verification. Figures 132 and 133 show comparison of airblast response opposite the explosive for calculations performed by WAI using MAZ and those performed by the ERDC using the SHAMRC code [5], another validated airblast modeling code well regarded within the DOD airblast community.

Figure 132:
Pressure comparison between
MAZ and SHAMRC



C.4.2.2 TSWG/EMRTC Steel and Concrete Column Tests

WAI, under contract to EMRTC, provided computational support for a series of explosive tests of steel and concrete columns to generate a fast running structural evaluation and design tool. Tests of column response were conducted using “flake TNT” as the explosive. WAI supported these

tests with pretest and post-test calculations of airblast loading and structural response. As part of the effort, WAI generated a JWL EOS for flake TNT. An example comparison with test data is shown in Figure 134. The results of both airblast and structural response calculations have been documented. [6]

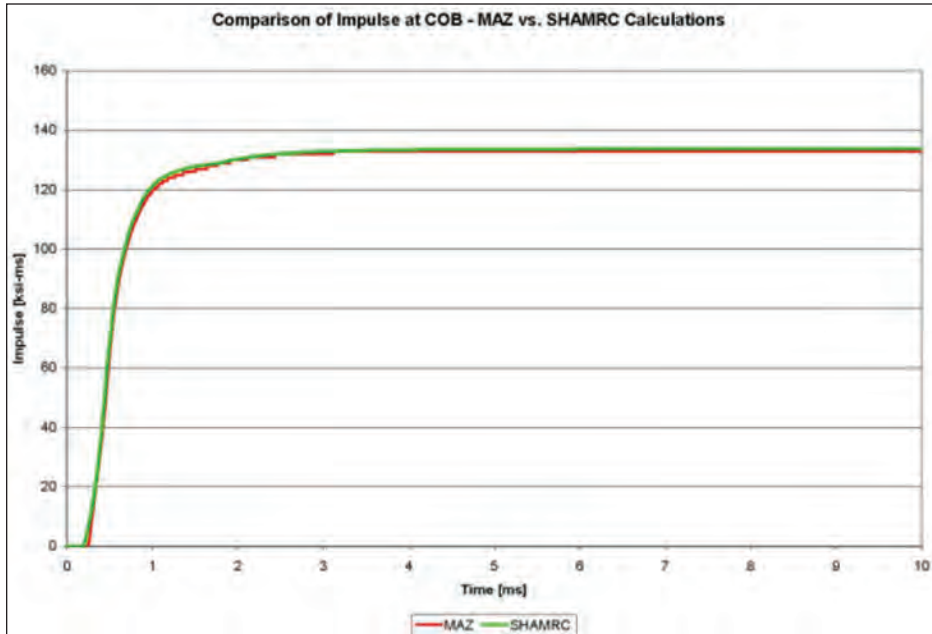


Figure 133:
Impulse comparison between
MAZ and SHAMRC

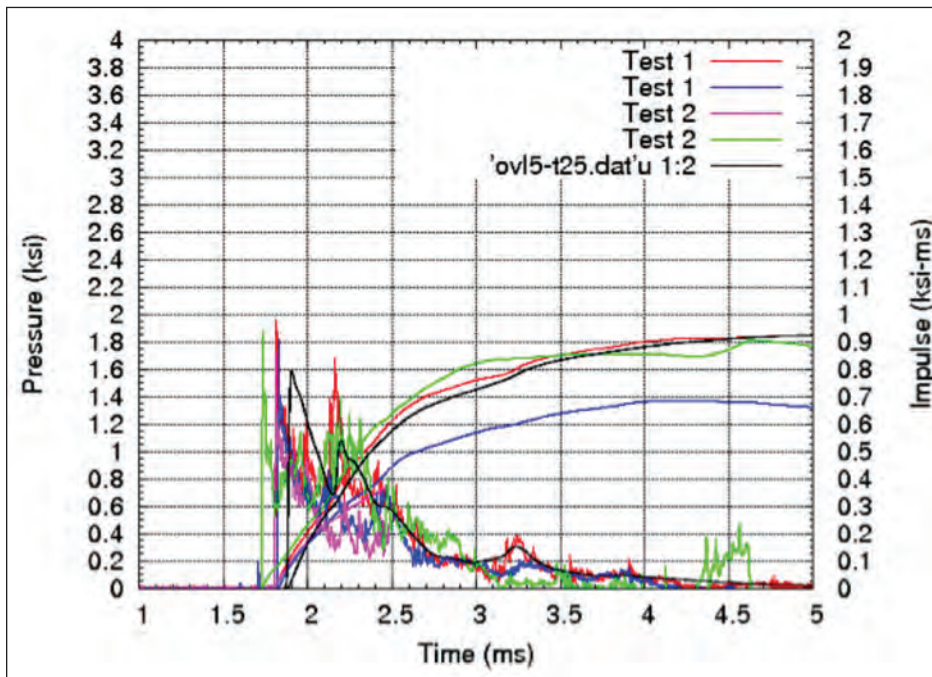


Figure 134:
Comparison of measured and
calculated Airblast

C.4.2.3 Curtain Wall Test

WAI provided planning and integration services for a test of a curtain wall system designed to resist explosive loading. Key to demonstrating the performance of the curtain wall design is accurately characterizing the airblast load. WAI supported the test series with pretest predictions of the full test and calibration tests to insure the load delivered to the structure met the test requirements. [7] Shown in Figure 135 are comparisons of predicted and measured loads on the test structure. Loads are normalized due to security concerns.

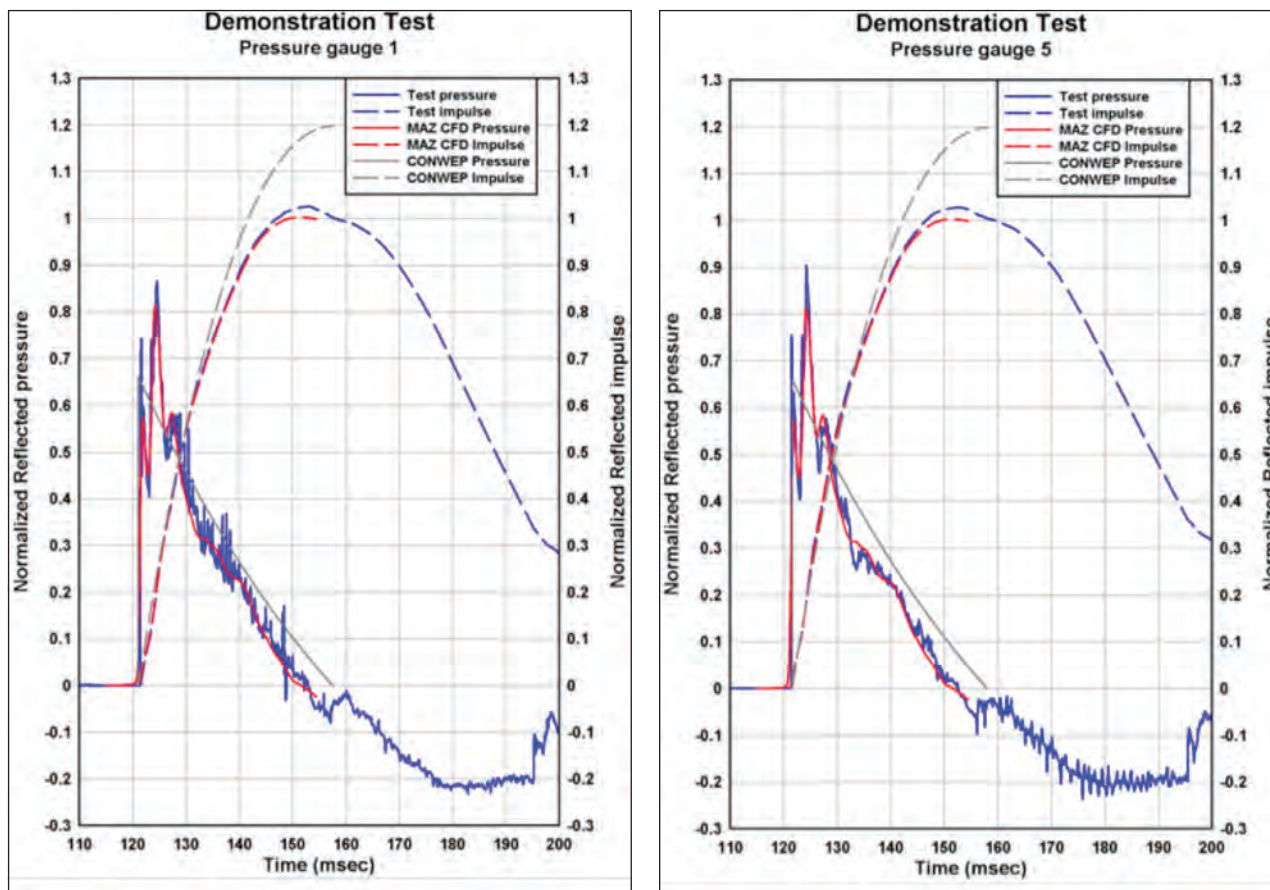


Figure 135: Comparison of measured and predicted blast pressures

C.4.2.4 TSWG/EMRTC CORESlab Loading Dock Tool Development

WAI conducted pretest MAZ calculations of the explosive loading produced on the underside of the loading dock floor slab test structure shown in Figure 136a. A snapshot of the propagating blast pressure from the MAZ simulation is shown in Figure 136b. Figures 137 and 138 show comparisons of predicted and measured airblast pressure and impulse.

The loads generated using the MAZ CFD code were used to load NLFlex models of the mitigated and unmitigated structures. Results of the airblast and structural calculations were used to generate the results data base used in the CORESlab FRM. [8]



Figure 136a: Loading dock test structure.

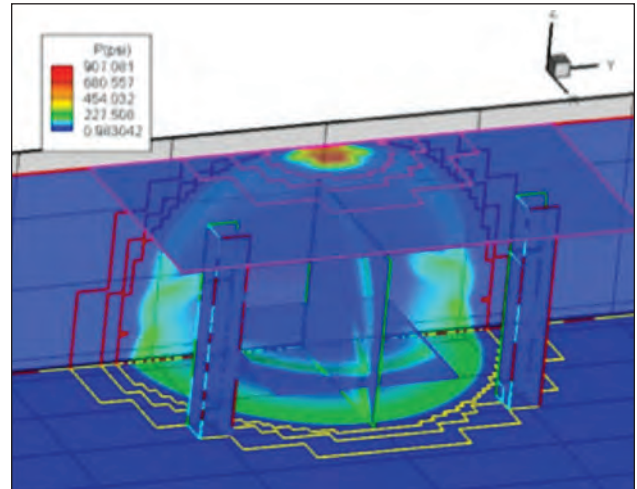


Figure 136b: Propagating Airblast pressures explosive test simulation from MAZ

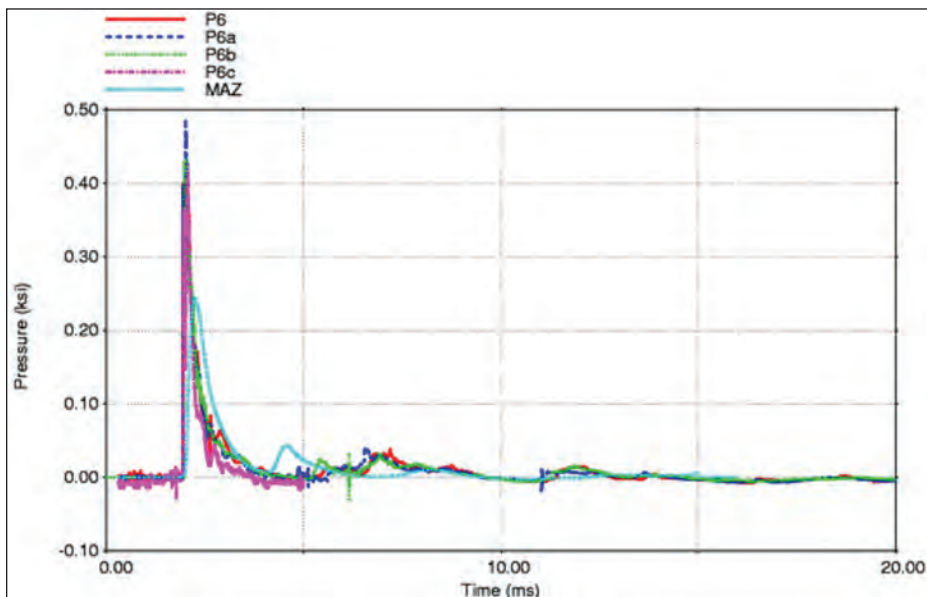
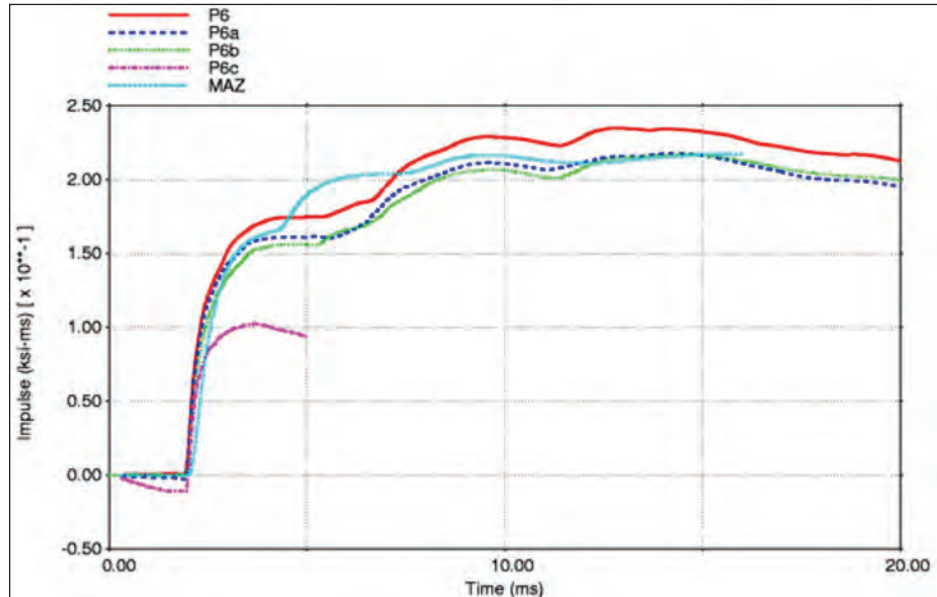


Figure 137: Comparison of measured and predicted pressure time history for loading dock test

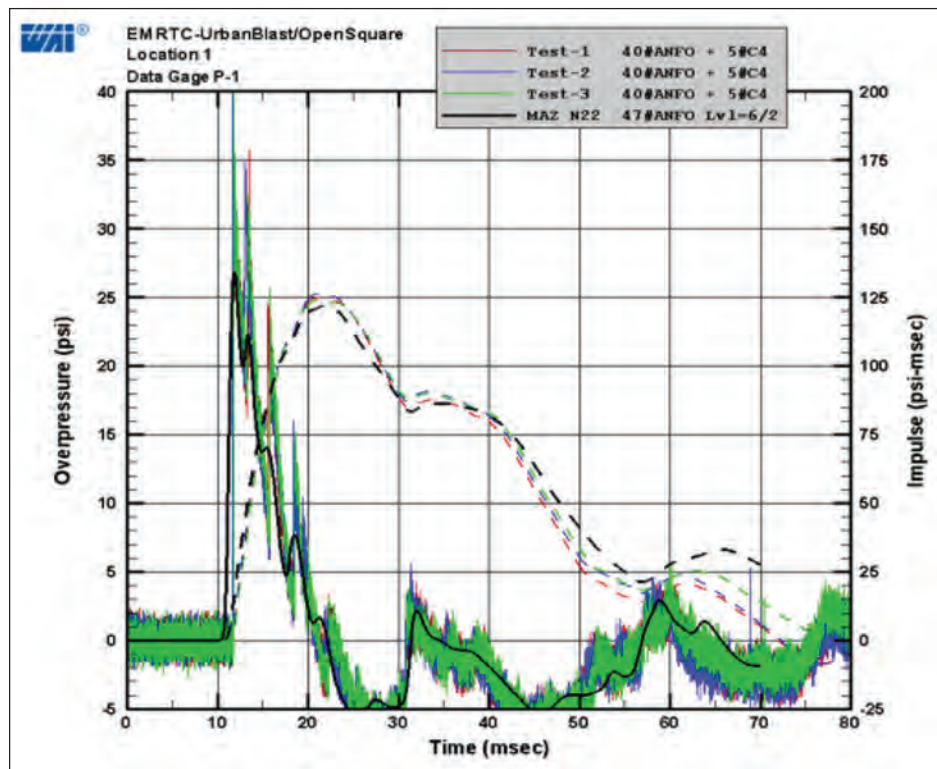
Figure 138:
Comparison of measured and predicted impulse time history for loading dock test



C.4.2.5 TSWG/EMRTC Urban Canyon Testing

WAI, under contract to New Mexico Tech EMRTC, is participating in urban canyon testing. These tests will provide additional validation of MAZ in complex urban blast settings. Figures 139 and 140 show comparisons between measured and predicted response for tests conducted using ANFO.

Figure 139:
Comparison with measured and predicted blast pressures



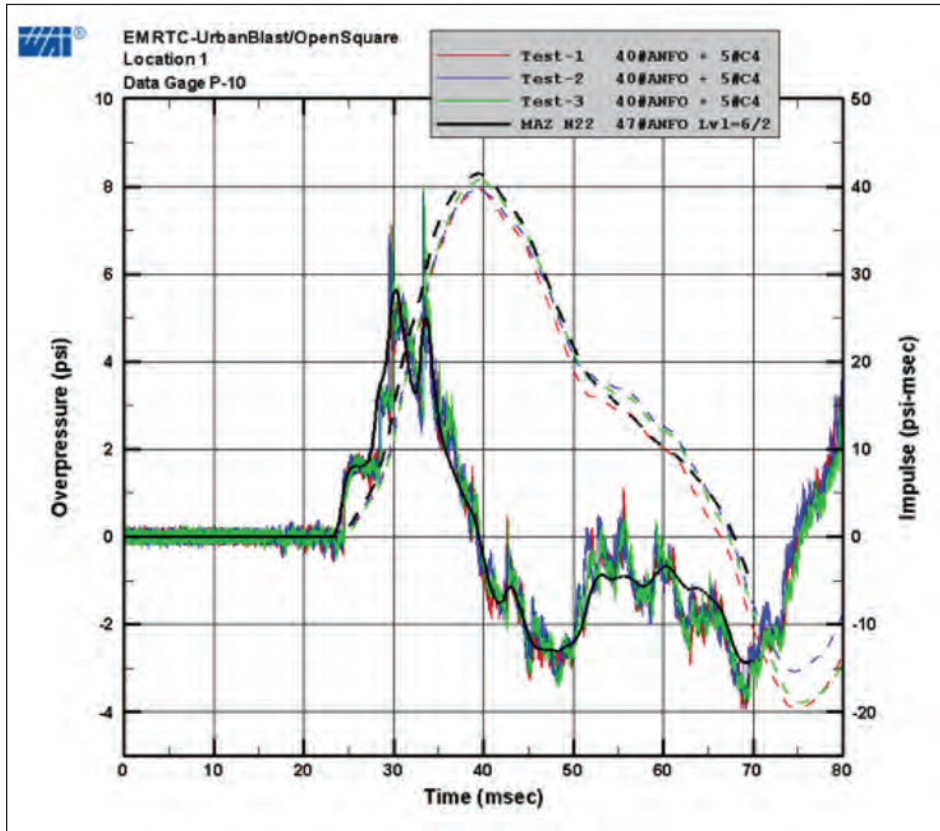


Figure 140: Comparison with measured and predicted blast pressures

C.4.3 The NLFlex Software for Structural Response Simulations

NLFlex [2] is an explicit, nonlinear, large deformation transient analysis finite element code for the analysis of structures subjected to airblast, fragment, impact, and ground shock loadings. It was developed by WAI. Development of the NLFlex software has been funded by a wide range of DOD and other U.S. Government organizations including the Defense Threat Reduction Agency (DTRA), the U.S. Air Force, the U.S. Army, and the CIA. NLFlex has a library of finite elements and constitutive models that are tailored to the solution of large, transient nonlinear problems through failure. Its primary emphasis is dynamic analysis, but static solution options are also available for combined gravitational, impact, and blast loading of buildings and shelters. Theoretically sound constitutive models for ductile and brittle materials and for pressure dependent and rate sensitive materials have been developed during the past 30 years [6 through 11] and are available so that buildings, building components, and hardened structures and equipment that are constructed from metals, masonry, ceramics, fiber reinforced composites, rock, and reinforced concrete are readily analyzed through failure. An extensive validation effort, involving comparison with blast, ground shock, and impact tests, is

documented in a report submitted to DTRA as part of the Tunnel Target Defeat Advanced Concept Technology Demonstration, TTD-ACTD program. [9 and 10]

C.4.4 Validation of the NLFlex Software for Structural Response Simulations

WAI has extensive experience predicting the response of structures subjected to blast loading and continues to be at the forefront of modeling and evaluating structures for blast, impact, and progressive collapse. NLFlex has been applied to a wide range of blast, impact, ground shock, and progressive collapse applications.

C.4.4.1 Hard Target Defeat

Under DTRA, ERDC, and Air Force sponsorship, WAI has used its expertise in nonlinear dynamic analysis to design and predict the vulnerability of hard targets such as buried reinforced concrete bunkers, missile silos, and deeply buried tunnels subjected to conventional and nuclear weapons attacks. First principles computations have been performed for complex three dimensional facilities subjected to internal and external airblast and fragment loads and penetrating weapons. Simplified models have been developed using these computations and test results as the vulnerability database. The results were validated through extensive comparisons of pretest predictions and post-test analyses with full scale and small-scale tests (Figure 141).

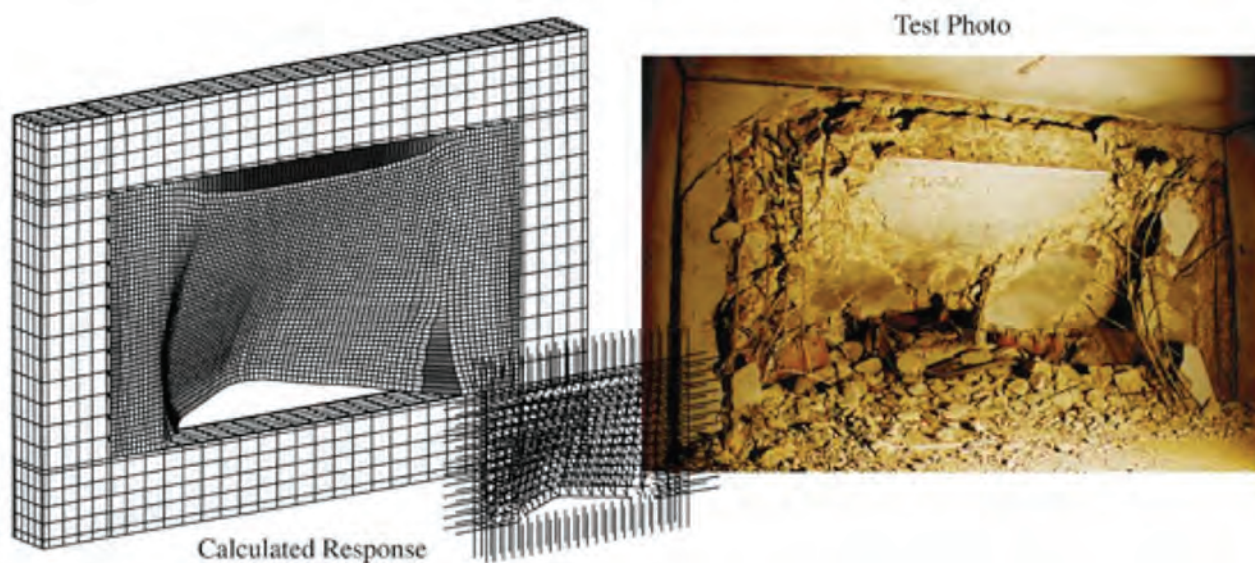


Figure 141: Comparison of experimental and computed response for internal wall

C.4.4.2 Blast Response of Conventional Structures

WAI has been at the forefront of design and evaluation of conventional structures subjected to blast. An example of the application of NLFlex to modeling structures subjected to blast loading is the CTS1 test conducted by DTRA. [11] Figure 142 shows pretest NLFlex results compared with the actual blast damage produced by the test. WAI provided pretest planning support to define the standoff range required for this test to produce significant column damage but not collapse the structure.



Figure 142: Photos of CTS1 test vs. pretest NLFlex simulation results

C.4.4.3 ACEC Grand Conceptor Award

In 2004, WAI won the American Council of Engineering Companies (ACEC) Grand Conceptor Award for its study of the 9/11 attack on the World Trade Center, Figure 143. In support of this study, the NLFlex software was used to model both aircraft impacts into the twin towers as well as the collapse failure of the damaged structures.

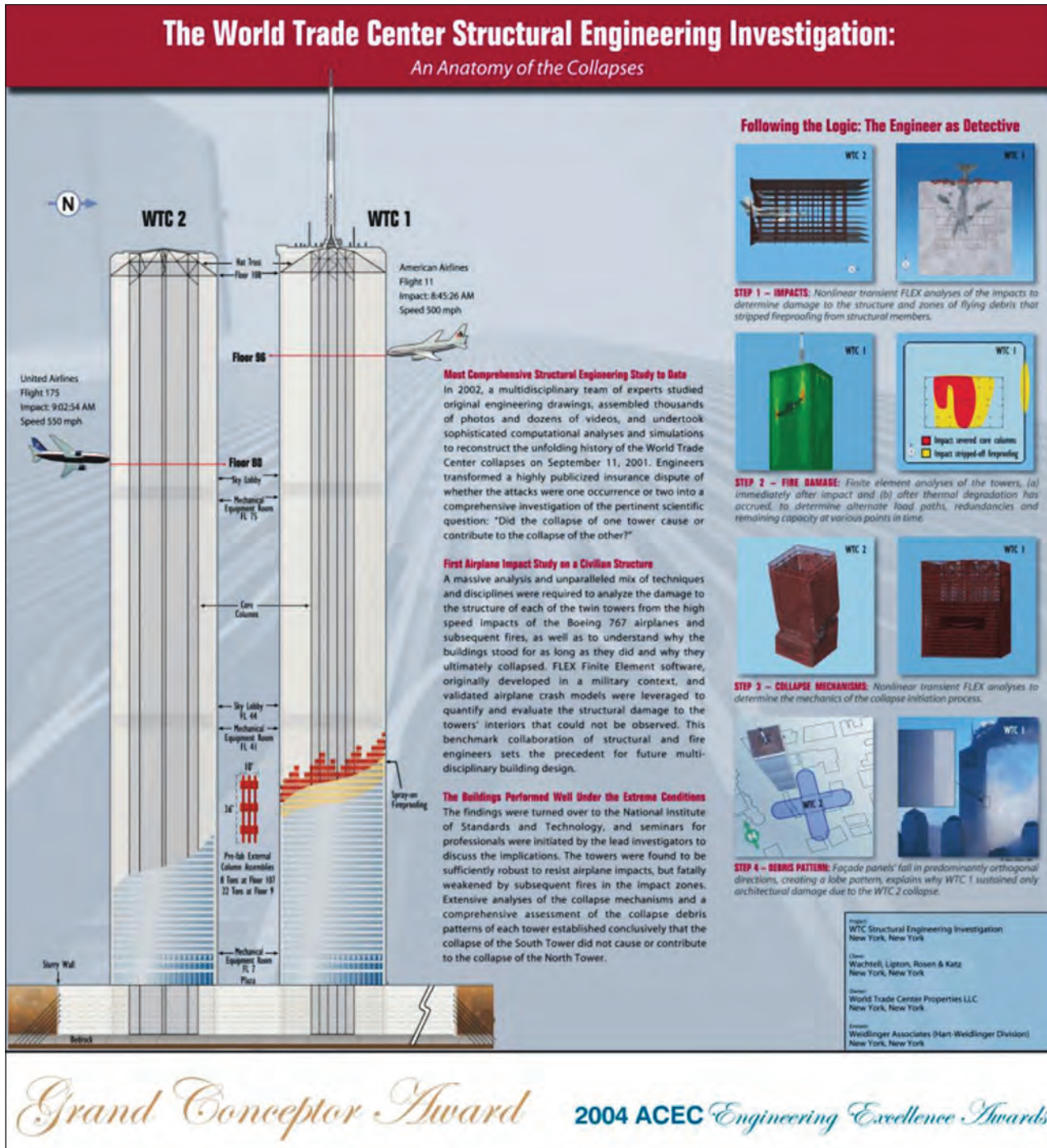


Figure 143: ACEC Grand Conceptor Award to WAI

C.4.4.4 Progressive Collapse

Under a Phase II SBIR effort WAI was able to validate the NLFlex software with pretest prediction of a series of subscale structural collapse tests conducted in a centrifuge. Figure 144 compares predicted response with observed collapse. WAI is currently working on a Phase II SBIR to develop methodology for performing rapid high-fidelity computations to evaluate structures for progressive collapse.

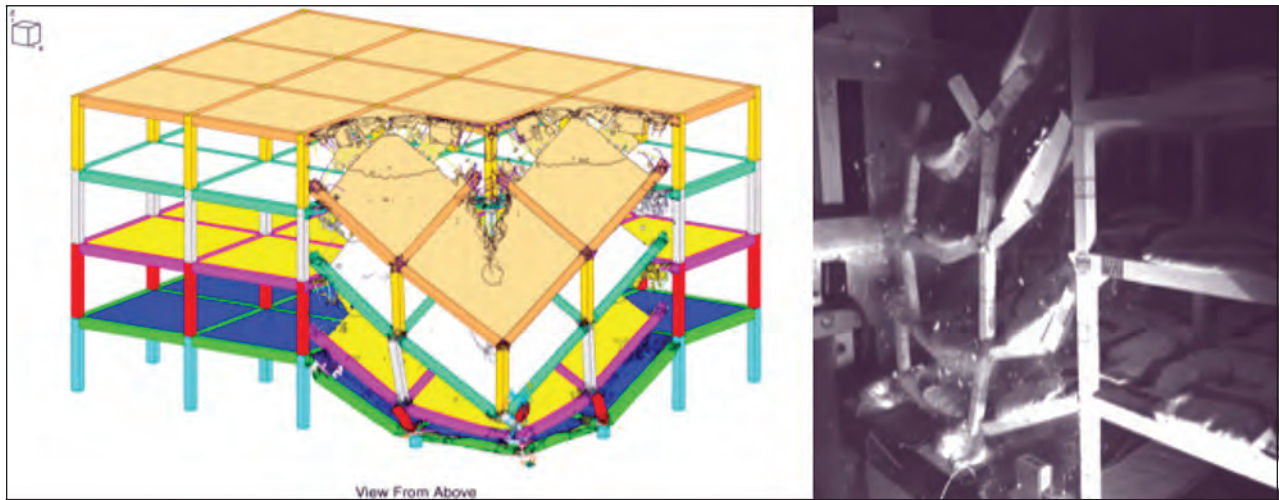


Figure 144. Comparison of progressive collapse analysis with test

C.5 References

1. Schlamp, R. J., Hassig, P. J., Nguyen, C. T., Hatfield, D. W., Hookham, P. A., "MAZ User's Manual," Defense Nuclear Agency Contract Report, Contract No. DNA001-91-C-0153, March, 1995.
2. Vaughan, D. K., "FLEX User's Guide," Report UG8298, Weidlinger Associates, Mountain View, CA, May 1983 plus updates through 2010.
3. Biggs, J., "Introduction to Structural Dynamics," McGraw-Hill, 1964.
4. Harten, High Resolution Schemes for Hyperbolic Conservation Laws, J. Comput. Phys. 49, 357 (1983).
5. NYCDOT Hazard Mitigation for East River Bridges: Brooklyn Bridge. 10% Concept Design Report Submittal. WAI Project No. 25-362. July 3, 2006.

6. Darell L., Daddazio, R., Stanley, M., Tennant, D., and Rubin D., “FLEX FE Models and Full Scale Tests of Blast Loaded Reinforced Concrete Columns”, DDESB 33rd Explosives Safety Seminar, Palm Springs, August 2008.
7. Hassig, P., Tennant, D., Weeks, J., and Levine, H., “The Effects of airblast Clearing on Structural Loads.” Proceedings of the 13th International Symposium on the Interaction of the Effects of Munitions with Structures, Brühl, Germany, May 2009.
8. D. Lawver, R. Daddazio, G. J. Oh, C. K. B. Lee, A. Pifko and M. Stanley, “Simulating The Response of Composite Reinforced Floor Slabs Subjected To Blast Loading,” 2003 ASME International Mechanical Engineering Congress and RD&D Expo, November 2003.
9. Tunnel Target Defeat ACTD, Weidlinger Associates Simulation Capability Documentation”, Report submitted to DTRA Modeling Assessment Group, 24 May 2004, Distribution C.
10. “Updated Model/Simulation Description for the Flex code used by Weidlinger Associates for TTD ACTD”, Report submitted to DTRA Modeling Assessment Group, 28 Feb. 2006, Distribution C.
11. Tennant, D., Levine, H., Lawver, D. and Smilowitz, R. ‘Analysis of a Multi-Story Flat Slab Building Subjected to an External Detonation Using A First Principles Finite Element Code, 70th Shock and Vibrations Symposium, Nov. 15-19, 1999.

